TR-AP-71-3

An Evaluation Of

LOX/HYDROGEN ENGINE TECHNOLOGY

For Advanced Missions

JUNE 1, 1971

SPACE DIVISION CHRYSLER CORPORATION

TECHNICAL REPORT

TR - AP - 71 - 3

AN EVALUATION OF LOX/HYDROGEN ENGINE TECHNOLOGY FOR ADVANCED MISSIONS

June 1, 1971

Approved by: G. M. Joseph

G. M. Joseph
Study Manager

Approved by: J. G. Swider

J. G. Swider, Manager
Flight Mechanics Section

Preparaed for

The National Aeronautics and Space Administration,
Office of Advanced Research and Technology,
Washington, D. C., under Contract NAS7 - 790

CHRYSLER CORPORATION SPACE DIVISION, P. O. BOX 29200
NEW ORLEANS, LOUISIANA 70129

FOREWORD

This report was prepared by the Chrysler Corporation Space Division, New Orleans, Louisiana, and contains the results of a study performed for the National Aeronautics and Space Administration, Office of Advanced Research and Technology, under contract NAS7-790, "An Evaluation of LOX/ Hydrogen Engine Technology for Advanced Missions".

ACKNOWLEDGEMENTS

An Evaluation of LOX/Hydrogen Engine Technology for Advanced Missions was performed under the direction of Frank Stephenson, NASA Headquarters, telephone (202) 962-1703.

Propulsion company support was provided by Rocketdyne Division, North American Rockwell Corporation. Specific contributions included parametric performance, size, and weight data for various oxygen-hydrogen engine cycles. This support was valuable to the study and was much appreciated.

Chrysler Corporation Space Division personnel responsible for major contributions to the study included:

G. M. Joseph - Study Manager, telephone (504) 255-2307

P. D. Thompson - Principal Investigator, telephone (504) 255-2308

TABLE OF CONTENTS

TABLE OF CONTENTS (continued)

LIST OF ILLUSTRATIONS

LIST OF ILLUSTRATIONS (continued)

LIST OF TABLES

Section 1

INTRODUCTION

Hydrogen and oxygen are at this time the leading candidate propellant combination for use in NASA's advanced missions - particularly the Space Tug or Orbit to Orbit Shuttle, OOS. The objective of this study was to develop and provide the National Aeronautics and Space Administration with information which would aid in assessing LOX/hydrogen engine and stage technology requirements for future missions. The results of this study quantitatively define the importance of engine and stage design criteria on the sizing requirements of the complete stage. They include engine parameter (i.e. chamber pressure, area ratio and mixture ratio) optimization analyses for two engine cycles as a function of stage size and mission profile. Also, sensitivity studies were undertaken to develop influence coefficients on factors such as engine weight, number of engines, Isp efficiency, coast times, initial departure orbit inclination, and design constraints, etc.

Five missions were investigated: a) earth orbit to synchronous orbit and return; b) earth orbit to lunar orbit and return; c) lunar orbit to lunar surface and return to lunar orbit; d) retro of a scientific payload into a Martian orbit; and e) a two-burn Mars mission in which the stage provided the interplanetary transfer velocity increment as well as the planetary orbit insertion.

These studies have been accomplished utilizing "Chrysler's Upper Stage Sizing and Evaluation Routine computer program described in Section 2. Use of this program enables rapid and accurate optimization studies to be performed on chemical upper stages requiring "n" burns and "n" different payloads.

Section 2

STUDY APPROACH

2.1 GENERAL

To meet the objectives of this study it was necessary to size a very large number of stages corresponding to a wide range of missions, payloads, design constraints and design alternatives (e.g., selected materials of construction). To facilitate the handling of this large number of variables, a digital computer program was used. The program has the capability to accomplish stage optimization for a specified mission considering the following major variables or constraints and their interdependent relationships:

1. Engine chamber pressure, area ratio, mixture ratio and thrust.
2. Number of coast periods and time duration of each.
3. Payload requirements for each burn. (A different payload can be used for each burn).
4. Thermal control and meteoroid protection requirements.
5. Jettisonable weights (size internal to program) and jettison time.
6. Power system requirements and weights.
7. Propulsion system weights (including pressurization, propellant residual, reaction control system and propellant orientation systems, etc.)
8. Astrionics weights.
9. Miscellaneous weights.
10. Payload weights.
11. Dimensional constraints (e.g., maximum diameter).
12. Design constraints (e.g., minimum skin gauges).
13. Structural design (e.g., semi-monocoque, honeycomb, etc.).

The following paragraphs describe the computer program and illustrate the manner in which it was used for this study.

2.2 SIZING COMPUTER PROGRAM DESCRIPTION

2.2.1 General

The sizing computer program which was used in this study is comprised of numerous smaller subprograms and subroutines that are used to analyze the requirements for the various systems which make up an upper stage. Table 2-1 provides a listing of the more important subroutines included in the program.

Table 2-1 Upper Stage Sizing Program Subroutine Listing Summary

CUSSER	-	is the main subroutine which handles the program control, determines the stage geometry and size, computes propellant load requirements and selects the optimum stage for each mission. This subroutine is predicated upon a specified stage gross weight. The payload is computed as the dependent variable.
WCREEP	-	is an alternate routine to CUSSER and differs only in that this routine is used for cases where payload is specified as the independent parameter, and the stage weight is the dependent variable.
THERM	-	which is comprised of several other subroutines, optimizes the thermal control system on the basis of minimum thermal mass penalty. It determines the optimum combination of insulation thickness and tank pressure. The subroutine also determines the initial ullage volume requirements, tank weights, pressurization system weights, and the amount venting (if desired).
METEOR	-	establishes meteoroid protection requirements and determines the optimum shield geometry and weight.
STRUCT	-	computes the weight of the shell and interstage.
THRST	-	determines the thrust cone and spider beam weight.
RCS3	-	determines the weight of reaction control propellant required and the entire subsystem weight on the basis of a limit cycle analysis.

The program is designed to permit the determination of either: 1) the optimum size upper stage and corresponding payload for a specified mission and specified booster, or 2) the required stage size for a specified mission and specified payload(s). For either of these options the engine parameter optimization is accomplished in the same fashion, i.e., by means of a series of do-loops within the program which vary the engine parameters one at a time and determine the corresponding payloads or stage size. For example, if 5 values were assumed for each of the 3 parameters (Pc, ϵ and MR) then 125 (5 x 5 x 5) payloads (and their corresponding stages)would be determined.

The program has the capability of finding the optimum by means of a search technique; however, in general these data are manually cross plotted to find the optimum engine parameters. This permits sensitivities to off-optimum selections to be identified.

If the option is selected which accomplished stage sizing for a specified booster and mission, the approach used is as follows: Stage gross weight (sum payload, total stage weight and interstage weight) is assumed as the independent variable and stage size, payload, interstage weight and propellant load are all computed as dependent variables. This is done to allow the velocity split between the booster and the upper stage to be determined in a straight forward manner. Figure 2.1 shows a typical launch vehicle performance capability plot; i.e., payload (or gross weight above the booster) versus velocity. The total mission velocity is defined as:

$$\Delta V_{\text{Mission}} = \Delta V_{\text{Booster}} + \sum_{i=1}^{\eta} \Delta V_{\text{Upper Stage Burns}_i}$$

where n is the total number of burns.

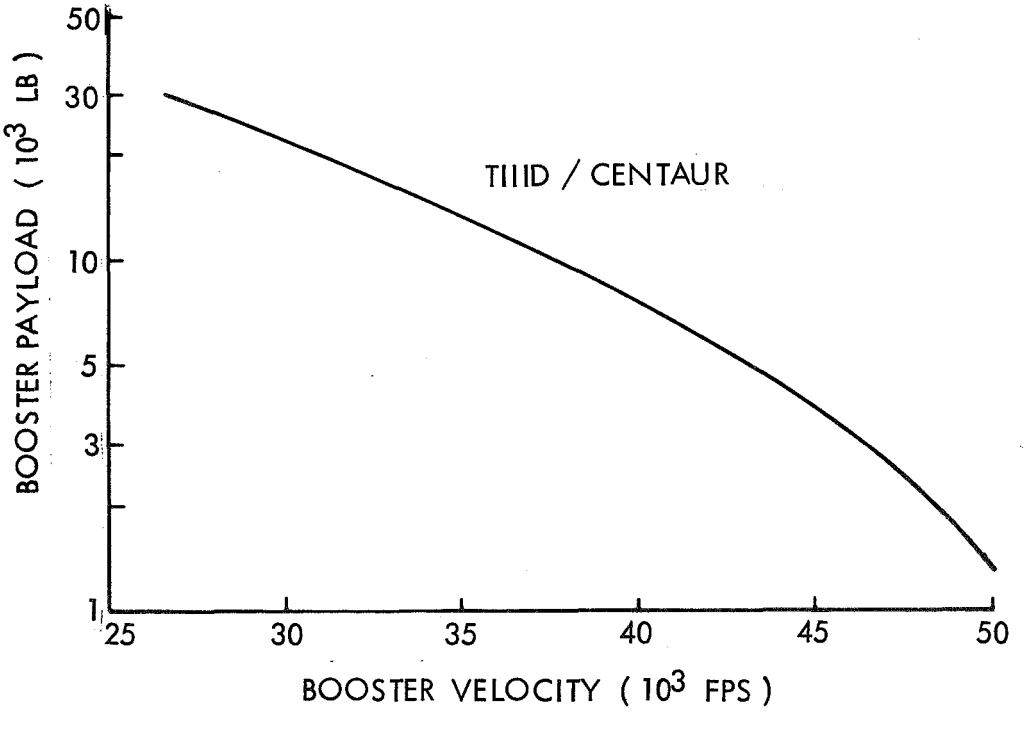

Figure 2- 1 Typical Launch Vehicle Performance Capability Plot

Thus, if the upper stage gross weight is specified then the velocity which can be obtained from the booster can be determined from figure 2-1 and the total velocity requirement of the upper stage can be determined from this equation. Knowing the specific impulse (corresponding to a particular combination of engine parameters) and the velocity requirements, the upper stage propellant load requirements can be computed as follows:

$$\mu_i = \exp \frac{\Delta V_{\text{UPPER STAGE}}}{g\, I_{sp}} \qquad i = 1,2,3,\ldots\ \eta \text{ burns}$$

and

$$\mu_i = \frac{W_{GROSS} - \sum_{i=1}^{\eta}\left(W_{VENT_i^i} + W_{STARTUP_i}\right) - \sum_{i=1}^{\eta}\left(W_{SHUTDOWN_{i-1}} + W_{PROP_{i-1}}\right) - W_{JET_i}}{W_{GROSS} - \sum_{i}^{\eta}\left(W_{VENT_i} + W_{STARTUP_i} + W_{PROP_i}\right) \sum_{i=1}^{\eta}\left(W_{SHUTDOWN_{i-1}}\right) - W_{JET_i}}$$

where

$$W_{JET} = [1 - (\text{PAYLOAD FRACTION})] \times [\text{REFERENCE PAYLOAD}]$$

Solving for the propellant consumed during each burn

$$W_{PROP} = \left[\frac{\mu_i - 1}{\mu_i}\right] \times \left[W_{GROSS} - W_{JET} - \sum_{i=1}^{\eta}\left(W_{VENT_i} + W_{STARTUP_i}\right) - \sum_{i=1}^{\eta} W_{SHUTDOWN_{i-1}}\right]$$

hence the total propellant load becomes

$$W_{PROP\ TOTAL} = \phi \sum_{i=1}^{\eta} W_{PROP_i}$$

where ϕ accounts for residuals.

Based on the total calculated propellant load, various geometries are considered for trade-off within the program. For each of these geometries, the inert weights are determined and the geometry which yields maximum payload is selected. Payload is determined by subtracting, from the assumed gross weight, the propellant load and all the inert weights. The remainder is payload which, if the mission requirements are too severe, may be computed as less than zero. The optimum gross weight and, hence, stage size and propellant load are determined by varying assumed gross weights until a critical point (e.g., maximum) is obtained in a plot of payload versus gross weight.

If the option is selected which determines stage size as a function of input payload requirements, the calculation procedure is similar except that gross stage weight is initially estimated and then iterated upon until the computed gross weight agrees to within a specified tolerance. Figure 2.2 presents a simplified diagram showing the manner in which propellant loads and subsystem weights are calculated.

The following paragraphs discuss the various geometries which are incorporated in the program and the structural, thermal protection, meteoroid protection, reaction control system, and other subroutines which are used.

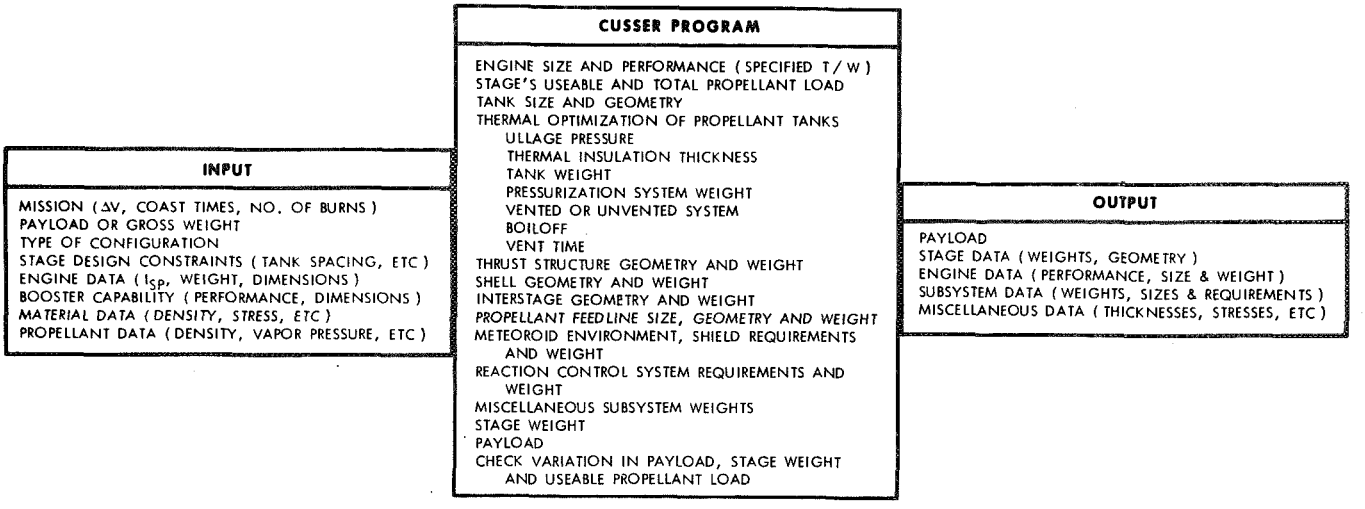

Figure 2- 2 Simplified Program Logic Diagram

2.2.2 Stage Configurations

Chrysler's Upper Stage Sizing and Evaluation Routine (CUSSER) has the capability of analyzing 64 separate stage configurations. The program computes the required propellant load required to perform the desired mission; and sizes each stage to carry the necessary propellant while adhering to certain geometric constraints. The stages which are evaluated by the program are "designed" by specifying the type of tankage arrangement, the type of bulkhead on each set of tanks, and the type and location of the thrust structure.

The five general tankage arrangements which can be evaluated are shown in figure 2.3. Four of these consist of stages which have one large propellant tank and one to four smaller tanks for the other propellant. Another geometry is based on two tanks for each propellant.

The tandem tank version, figure 2.3(1), has the smaller propellant tank located directly above the larger tank. The program determines the tank radii and the necessity of cylindrical sections in each set of tankage, on the basis of required tank volume and geometric constraints imposed on the stages' maximum diameter.

The next three tankage arrangements, figures 2.3(2), 2.3(3) and 2.3(4), depict two, three and four small tanks, respectively, located below a single large tank. The small tanks of these three configurations are located as far from the stages' longitudinal axis as possible, without extending past the periphery of the larger tank. The angular displacement of the small tanks is such that the stage's center of gravity (at ignition) lies along the vehicle's centerline. The program assumes that the large tank is used for the propellant having the largest total volume requirement (hydrogen in this case). The smaller tank(s) are used for the other propellant (oxygen).

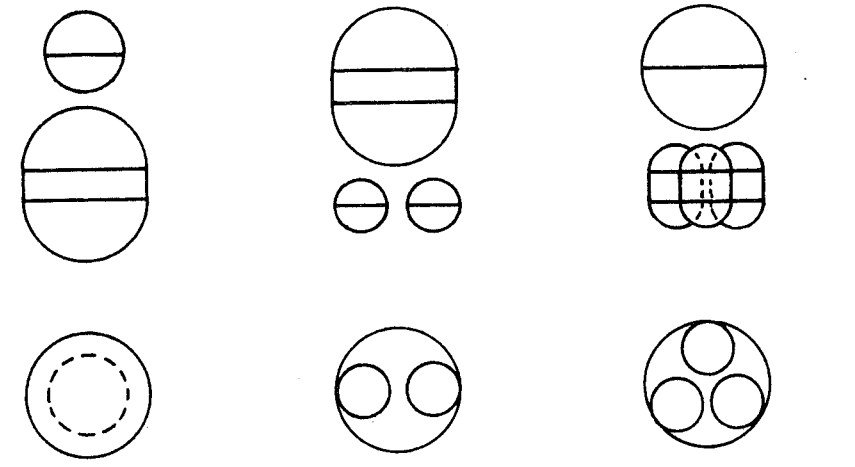

Figure 2- 3 Basic Tankage Arrangements

Figure 2.3(5) shows the last tankage arrangement around which the stage can be "designed". This geometry uses two tanks for each propellant. As with the other geometries, the program determines the tank radii and the necessity of cylindrical sections on the basis of required tank volume and the geometric constraints imposed on the stage.

Another specified criteria is the type of bulkhead on each set of tanks. Although the tanks illustrated in figure 2.3 all have hemispherical domes, it is possible to specify elliptical bulkheads for either the larger or smaller tank(s), or both.

The remaining item which must be defined in order for the program to "design" a stage, is the type and location of the thrust structure. Figure 2.4 shows the basic types -- thrust cone and spider beam, and the three possible locations of the spider beam. The program logic places the thrust cone, figure 2.4(1), directly below the larger tank. This permits the single smaller tank on the tandem tank arrangement, figure 2.3(1), to be placed above the larger tank; and the small tanks on the multiple tank versions, figures 2.3(2) thru 2.3(4), to be located directly below the thrust cone. The cone type thrust structure cannot be utilized on the transtage version, figure 2.3(5)

A program option permits various locations of the spider beam. The first, figure 2.4(2), locates the spider beam directly below the multiple tanks. The second, figure 2.4(3), locates the spider beam at the center of the multiple tanks. The last, figure 2.4(4), positions the spider beam so that the exit plane of the engine is at the bottom of the tanks. The program checks each spider beam location to insure that the gimbal point of the engine is not above the top of the tanks and that the engine's exit plane is below the bottom of the tank. If either of these constraints is violated, the program repositions the spider beam. A tandem tank-spider beam combination cannot be considered, because of the excessive shell length associated with this configuration would make the stage weight undesirably high.

The geometry of the basic configurations previously discussed are influenced by one or more geometric constraints. The constraints used in the program are listed in table 2.2. The one which has the largest impact on all the configurations is the maximum allowable stage diameter.

The maximum stage diameter is a constraint which permits the entire stage, payload and interstage, to be shrouded or carried internally when desired. If an unshrouded stage is to be considered, the diameter of the booster is used as the maximum stage diameter. Depending upon the total propellant load and mixture ratio, this constraint determines whether or not the single large propellant tank has a cylindrical section. This influences the length of the larger tank which determines, to a large extent, the overall stage length. The maximum engine expansion ratio is also limited by the stage diameter because during stage separation, the engine nozzle must pass through the upper interstage opening, the diameter of which is determined by the stage's diameter.

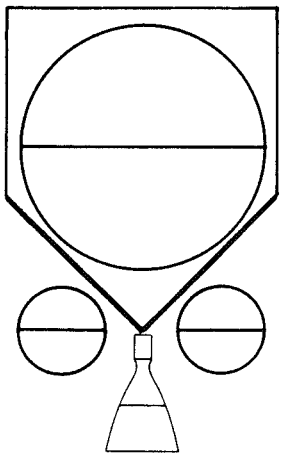

(1) THRUST CONE

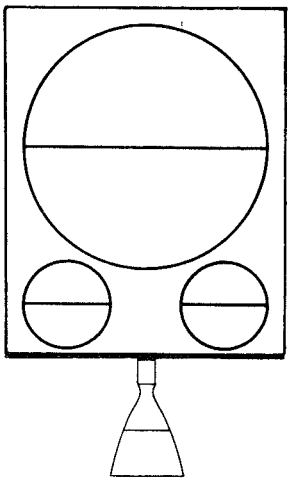

(2) SPIDER BEAM (A)

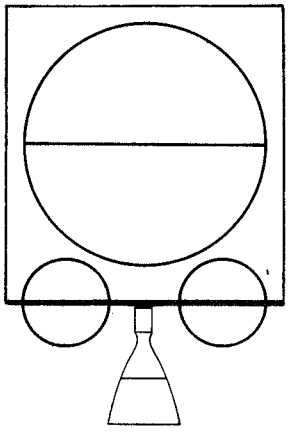

(3) SPIDER BEAM (B)

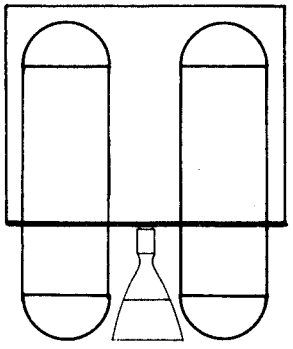

(4) SPIDER BEAM (C)

Figure 2- 4 Basic Thrust Structures

Table 2-2 Constraints on Stage Geometries

CONSTRAINT	MAJOR AREA AFFECTED
MAXIMUM STAGE DIAMETER	SIZE AND TYPE OF LARGE PROPELLANT TANKS LENGTH OF THE STAGE MAXIMUM ENGINE EXPANSION RATIO INTERSTAGE SIZE
SHELL TO TANK SPACING	SIZE AND TYPE OF PROPELLANT TANKS
TANK TO TANK SPACING	SIZE AND TYPE OF MULTIPLE TANKS
ENGINE TO TANK SPACING	SIZE AND TYPE OF MULTIPLE TANKS STAGE CONFIGURATION
ENGINE EXIT TO BOOSTER SPACING	INTERSTAGE SIZE

The shape of the larger tank is also affected to a small extent by the various spacing constraints used in the program. Figure 2.5 shows the constraints used in defining the configuration geometry. The shell-to-tank spacing criteria ensures that the thermal insulation and meteoroid shields will fit between the shell and the larger tank. Similarly, the tank-to-tank spacing is used to make the necessary clearances for the thermal and meteoroid protection systems on the tanks, and to ensure adequate room for the propellant feedlines.

Two engine-to-tank clearance criteria are used to ensure engine submergibility on those configurations having multiple tanks. Basically, these are constant coefficients, which when multiplied by the engine's throat diameter and exit diameter, establish the maximum diameter required for accommodating the upper portion of the engine (thrust chamber, turbopumps, etc.) and the engine's nozzle (including gimbal swing), respectively. The program computes the maximum allowable diameter of the multiple tanks from this criteria and the maximum stage diameter.

The engine exit-to-booster spacing establishes the clearance between the engine exit plane and the uppermost part of the launch vehicle. Using this spacing constraint it is possible to establish the correct interstage length for configurations where the booster's upper tank dome extends beyond the forward skirt on the launch vehicle.

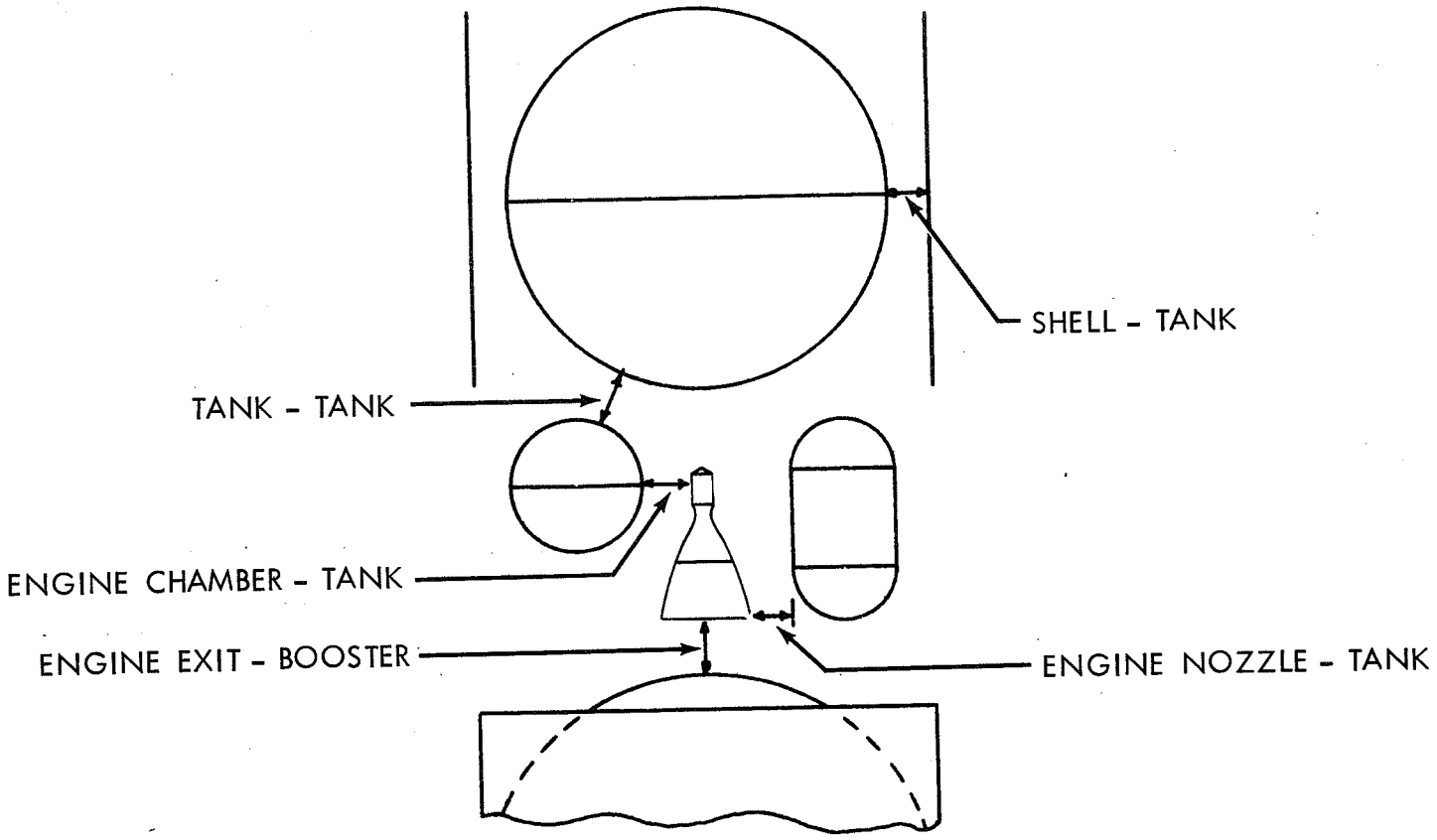

Figure 2- 5 Stage Geometry Constraints

2.2.3 Structural Systems

Five basic structural components were analyzed to determine their respective weights for each stage configuration evaluated by the program. They are: 1) propellant tankage, 2) shell, 3) interstage, 4) thrust structure, and 5) tank supports. Propellant tank weights were computed in accordance with geometric dictates using internal pressure as the design criteria and adhering to minimum allowable skin gauge constraints.

Weights for the shell, thrust cone type thrust structure, and interstage are computed by first determining what a monocoque design would weigh, and then applying a manually derived complex-to-monocoque structure weight ratio factor to the monocoque weight. The monocoque weights are computed using dimensional data calculated in the geometry subroutines as outlined in paragraph 2.2.2; and design criteria (i.e., loads) based on a simplified mass distribution model for each configuration and the inputed axial and lateral accelerations. The complex-to-monocoque weight ratios and the accelerations, were inputed to the program as a function of diameter and limit load and booster, respectively.

This approach has several advantages over the use of trend curves (e.g., interstage weight vs propellant load) to estimate structure weights. These are as follows:

1) Weight variation may be determined for alternate arrangements which have different dimensions, even though the propellant loads may be the same. This permits a more accurate and reliable optimization of parameters such as engine mixture ratio which may not change propellant load significantly, but which can alter the stage dimensions.

2) Any desired degree of accuracy can be achieved simply by re-evaluating the input monocoque-to-complex structure weight ratio factors and rerunning the cases of interest.

3) Various structural design concepts can be examined (e.g., sheet-stringer, honeycomb, truss) since the weight ratio factor is manually determined.

4) A minimum of "hand" analyses are required since it is rarely necessary to manually determine weight factors for more than one typical stage in the size range of interest, whereas, as many as 750 stages may be sized with the program to obtain a complete optimization.

Weights for the tank supports are determined for each propellant tank as a function of the weight being supported. The determination of the proper relationship was accomplished in a separate side study in which several concepts were considered. These included monocoque skirts, scalloped skirts, semi-monocoque skirts, and truss-to-ring structure, which are depicted in figure 2.6.

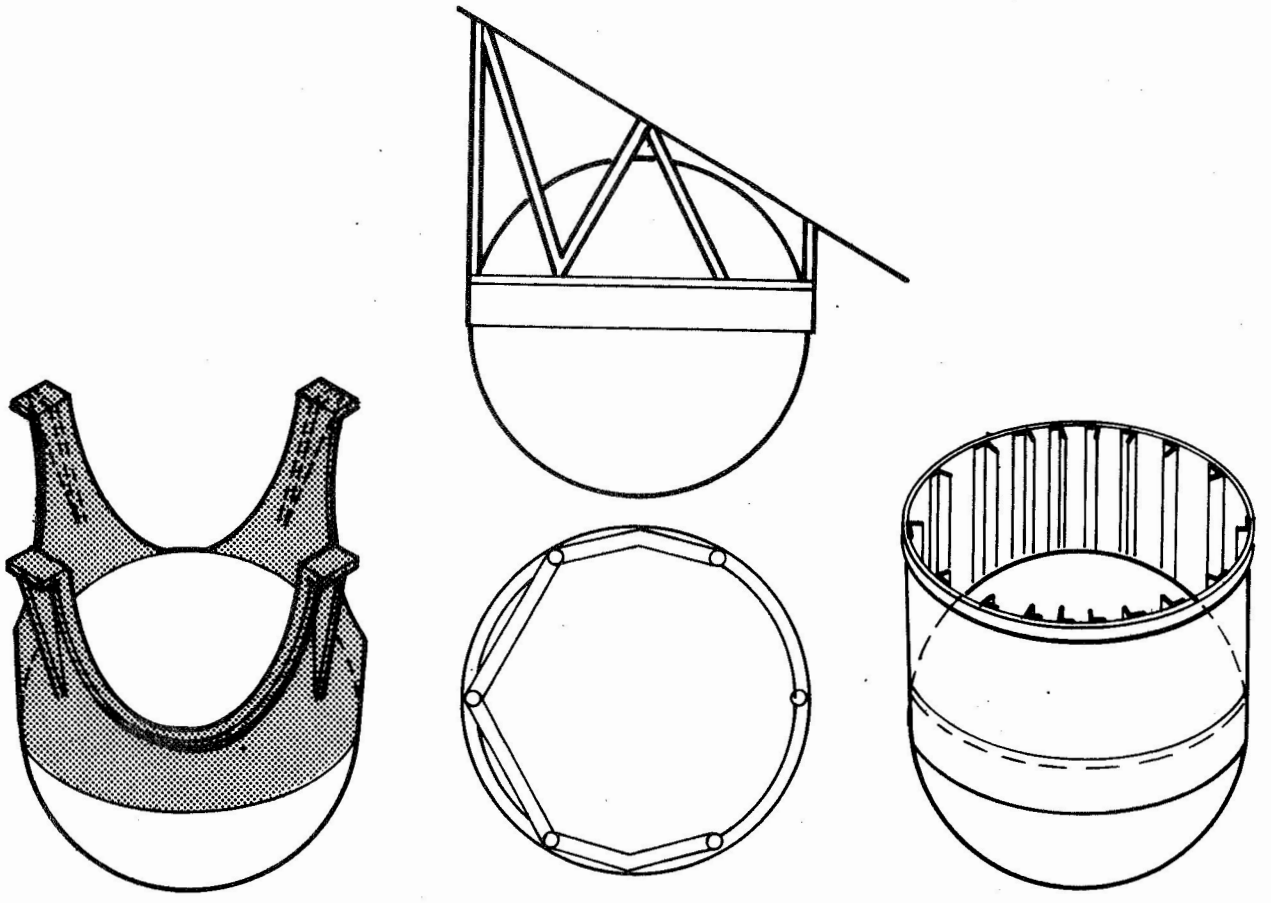

Figure 2- 6 Tank Support Concepts

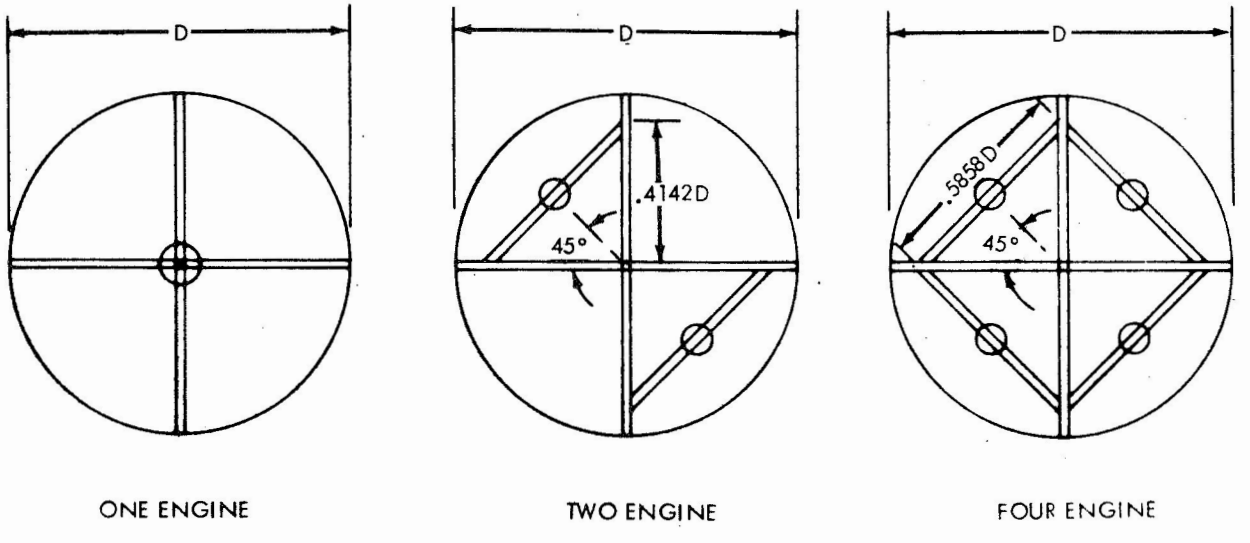

Figure 2- 7 Spider Beam Thrust Structure Concepts

A number of the configurations which can be considered in the program employ a beam type thrust structure. The concept for this thrust structure is assumed to be a conventional spider beam, ring frame and/or cross beam structural arrangement where the engine mount is assumed to be a conventional gimbal fitting. The particular structural arrangement was assumed, dependent upon the number of engines considered for the stage. The concepts assumed for each number-of-engines case is shown in figure 2-7. The weight equations for each concept were developed for the computer program with the following assumptions: 1) geometry of beams is as shown in figure 2-7, 2) beam sections are rectangular, 3) section is stable so material yield controls, and 4) engine attach points are located at the centerline of maximum inscribed circle for all engine sizes.

Weight equations for other shapes (i.e., rectangular tube, square tube) were developed and sufficient cases were analyzed to plot conversion coefficients as functions of required thrust level. These conversion coefficients are used as inputs to the program. The rectangular tube weight would equal the conversion coefficient times the rectangular block weight computed by the program.

2.2.4 Thermal Analysis

The approach used in determining thermal protection requirements is based on the criteria of minimizing the thermal mass penalty (TMP). The following equations show the development of the analytical definition of thermal mass penalty as used in this program:

1. $$\Delta V_n = g\, I_{sp} \ln \frac{W_{IGNITION_n}}{W_{BURN\,OUT_n}}$$

2. $$\mu_n = \exp\left[\frac{\Delta V_n}{g\, I_{sp}}\right] = \frac{W_{PL} + W_{INERT} + W_{PROP} - \sum_{i=1}^{n} W_{LIQ.\ VENT_i} - \sum_{i=1}^{n} W_{OTHER\ VENT_i} - \sum_{i=1}^{n-1} W_{BURN_i}}{W_{PL} + W_{INERT} + W_{PROP} - \sum_{i=1}^{n} W_{LIQ.\ VENT_i} - \sum_{i=1}^{n} W_{OTHER\ VENT_i} - \sum_{i=1}^{n} W_{BURN_i}}$$

OR

3. $$W_{PL} = -W_{INERT} - W_{PROP} + \sum_{i=1}^{n} LIQ.\ VENT_i + \sum_{i=1}^{n} W_{OTHER\ VENT_i} + \sum_{i=1}^{n-1} W_{BURN_i} + \frac{\mu_n}{\mu_n - 1} W_{BURN_n}$$

BUT

4. $$W_{PROP} = \sum_{i=1}^{n} W_{LIQ.\ VENT_i} + \sum_{i=1}^{n} W_{BURN_i}$$ (ASSUMING ZERO RESIDUAL); AND

5. $$W_{INERT} = W_{TANKS} + W_{ULLAGE\ GASES} + W_{PRESS.\ HDW.}$$

$\therefore$ SINCE THERMAL MASS PENALTY IS EQUIVALENT TO $-W_{PL}$

6. $$TMP = W_{TANKS} + W_{ULLAGE\ GASES} + W_{PRESS.\ HDW.} + \frac{\sum_{i=1}^{n} W_{LIQ.\ VENT_i}}{\mu_n - 1} - \sum_{i=1}^{n} W_{OTHER\ VENT};$$

Assumptions made in deriving the above equations are: 1) the weight of structure other than tankage is constant, and 2) the total weight of propellant initially loaded (including boil-off) is constant. The derivation itself is straightforward and shows that the thermal mass penalty is a function of:

1. Tank weight, which varies with the selected tank design pressure and the propellant tank volume.

2. The inert weight of the pressurization system, which is computed as a linear function of the total weight of pressurization gas used.

3. The weight of the insulation.

4. Vented propellant weight divided by $(\mu_n - 1)$, where μ_n is the mass ratio of the last burn.

5. The weight of vented inert gases and pressurization gases (non-propellant vapor.

6. The weight of propellant, pressurant and inert gas vapors present in the ullage at the end of the last burn.

The thermal analysis routine solves for the thermal mass penalty parametrically as a function of insulation thickness and tank vent pressure and selects the optimum combination of thickness and pressure. An illustration is given in figure 2-8.

The thermal subprogram is comprised of five subroutines plus numerous small subroutines which perform interpolation and other frequently encountered calculations. Figure 2-9 is a greatly simplified flow chart which illustrates the computation procedure. Each block contains the name of a subroutines which is described below.

THERM

This is the master thermal control subprogram. It manipulates the pressures and insulation thicknesses, determines the thermal mass penalty, selects the optimum operating conditions and executes the available options (e.g. selection of a vented case can be precluded). In addition, this routine sets up the data in the proper format for use in the other subroutines.

HEAT

This subroutine performs the heating analyses during each coast and determines: 1) temperature and pressure changes; 2) fraction of slush which is melted; 3) the amount of propellant boiled off into the ullage; 4) amount of inert gas, pressurization gas and propellant vapor vented; 5) amount of inert gas loaded prior to the first ignition which is necessary to satisfy the initial pressure requirements (i.e., $P_{inert} = P_{load} - P_{propellant\ vapor}$); and 6) propellant and ullage volumes at the end of each coast.

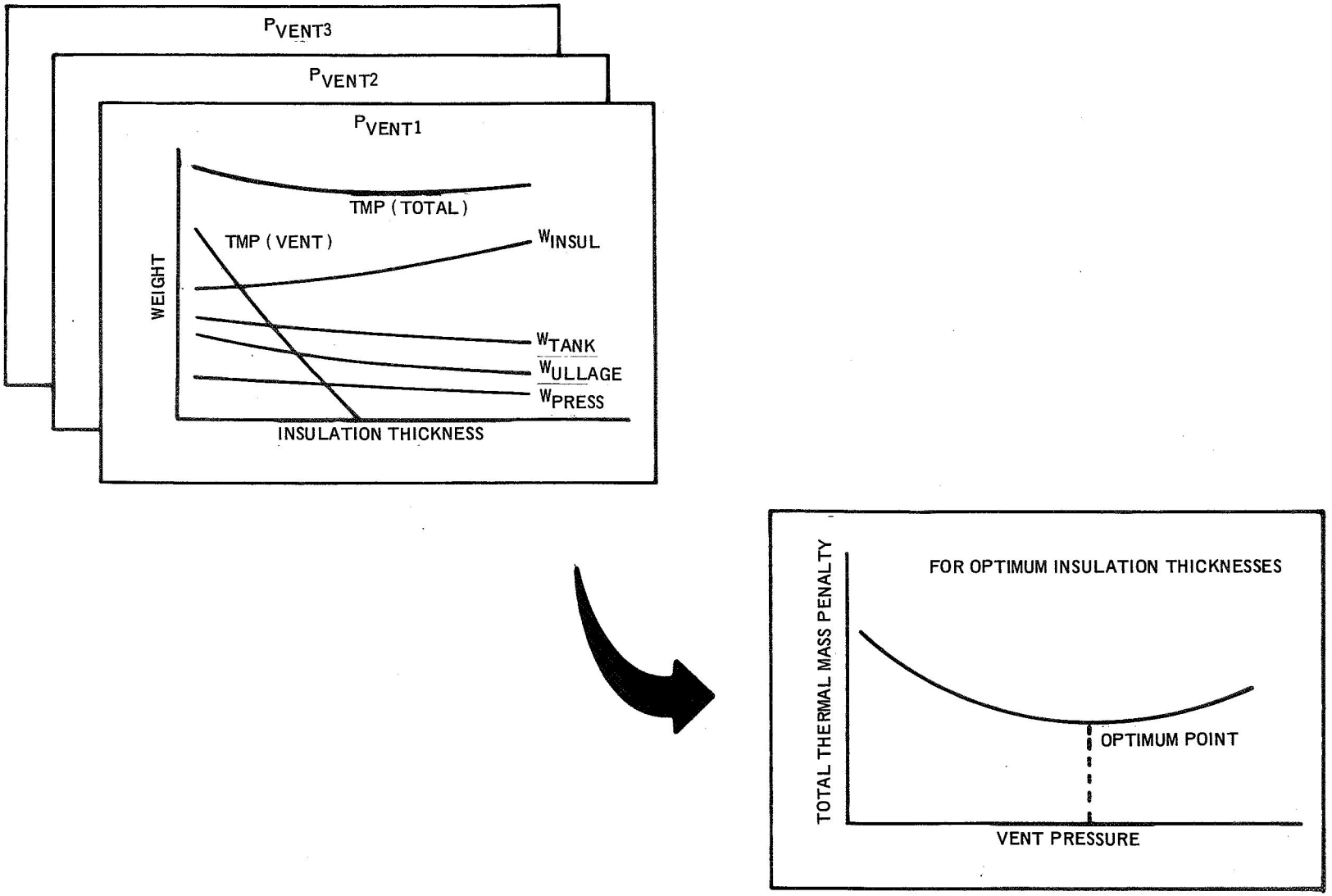

Figure 2- 8 A Typical Thermal Optimization

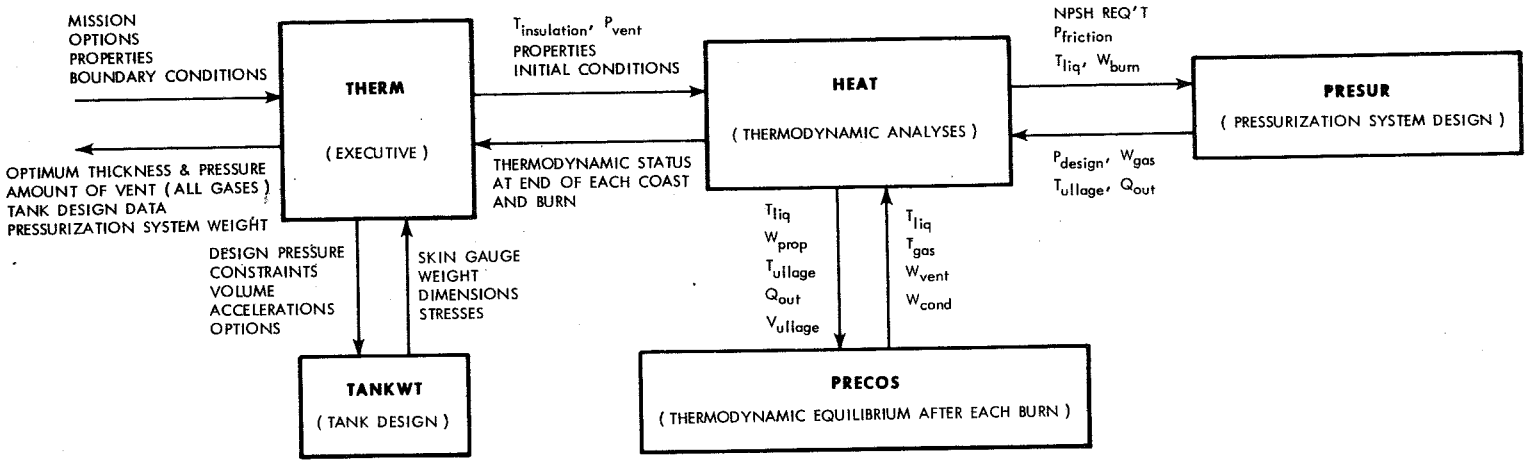

Figure 2- 9 Simplified Thermal Program Diagram

This routine also controls PRESUR and PRECOS discussed in the subsequent paragraphs.

HEAT may be considered as consisting of two parts for illustrative purposes. The first part may be viewed as performing the computations discussed above. To accomplish this, various estimates are required to "initialize" each pass through the subroutine. For example, to perform the necessary computations it is necessary to know tank volumes, surface areas and initial ullage volumes of the tanks. These cannot be known with accuracy until completion of the thermal-analysis which determines the condition of the propellant at the end of each coast. The second part of HEAT may be conisdered as controlling the various iterations required - i.e., updating the estimates and determining convergence (actually this latter function if not discernable as a separate entity in the program and is presented in this fashion as a matter of convenience only).

PRESUR

This subroutine estimates the amount of pressurization and gas required to satisfy NPSH requirements of the engine. The method of analysis is predicated on a non-dimensional analysis which enables computation of a collapse factor as a function of a modified gas Stanton number and a modified tank wall Stanton number. The complete analysis technique is described in "Pressurization Systems Design Guide, Volume 1, Systems Analysis and Selection", Report No. 2736, Aerojet General, Contract NAS7-169.

Based on the collapse factor obtained, the weight of pressure needed is computed and the final ullage gas temperature is determined. The subroutine then computes a hypothetical final temperature based on an adiabatic pressurization. The difference between the final ullage gas temperature and the hypothetical final temperature is assumed to be the result of a heat loss to the walls and propellant during outflow. This heat loss is determined from:

$$Q_{LOSS} = W_{GAS} \cdot C_{P_{GAS}} \cdot (T_{FINAL} - T_{HYPOTHETICAL})$$

PRECOS

This subroutine performs an analysis to determine the conditions which will exist when equilibrium has been reestablished after a burn. This subroutine considers as initial conditions: 1) the temperature of "hot" ullage gases; 2) the quantity of heat lost from pressurization gases to the liquid and walls; and 3) the temperature of the liquid at the end of the last burn (which is assumed equal to the temperature at the end of the last coast). A thermodynamic balance is used to establish the following: 1) equilibrium temperature and tank pressure, 2) quantity of slush remaining, 3) ullage gas composition, 4) quantity of liquid boil off or condensed, and 5) amount of each constituent of the ullage gas vented.

TANKWT

This routine configures the tanks in accordance with the type of bulkhead shape (hemispherical or elliptical) selected and the maximum tank radius constraint. It then determines the stresses, considering the ullage design pressure and propellant dynamic head. Two conditions are checked to obtain the design conditions. These are boost (i.e. high dynamic head and low ullage pressure) and upper stage flight (lower dynamic head but higher ullage pressures). The design pressure used is the greater of:

1) $P_{VENT} \cdot MEOP$

or

2) $(P_{SAT} + P_{FRICT} + P_{NPSH}) \cdot MEOP,$

where MEOP is a factor to obtain maximum expected operating pressure from nominal conditions.

Tank weights are obtained by multiplying the theoretical monocoque weight of each bulkhead and the cylindrical section by the corresponding land factor to account for bulkhead penetrations and weld lands. A safety factor is also used in addition to the MEOP and land factors.

PROP

This is a small subroutine which computes the capacitance and transport properties of the mixture of the ullage gases. It is called upon by all the other subroutines except for TANKWT.

The input requirements for the thermal analysis are summarized in table 2.3. Table 2.4 summarizes the main variables computed during this analysis. Those noted with an asterisk (*) are printed out. The others may be obtained when desired for special cases.

2.2.5 Meteoroid Protection

Space vehicles on long duration missions are subjected to encounters with meteoroids that could cause considerable damage to vital parts of the vehicle. To ensure adequate mission reliability, it is necessary to provide some type of protection against this hazard.

The most promising technique for protecting vital components and structures is to erect a thin bumper shield a short distance from the item to be protected. The shield serves to disintegrate the incoming meteoroid, allowing only a relatively diffuse debris cloud to strike the component. With the bumper shield, the rear wall need only withstand the impact of a cloud instead of a solid incoming meteoroid. The meteoroid environment and shield models used, the method of analysis, and typical results obtained are described in the remainder of this section.

2.2.5.1 Meteoroid Environment

The meteoroid flux varies considerably during the course of a year. The total activity comprises two components: 1) a fairly constant although sporadic component, and 2) the stream flux that has well defined recurring

Table 2-3 Summary of Input to Thermal Subprogram

A. Property Data
- Critical Temperature and Pressure of Propellant
- Heat of Fusion of Propellant
- Triple Point Temperature of Propellant
- Molecular Weights of Propellant, Pressurant and Inert Gas
- Density of Propellant as a Function of Temperature and Fraction of Slush
- Propellant Vapor Pressure as a Function of Temperature
- Heat Capacity of Propellant as a Function of Temperature
- Heat of Vaporization of Propellant as a Function of Temperature
- C_p of Propellant Vapor, Pressurant and Inert Gas as a Function of Temperature
- Thermal Conductivity of Propellant Vapor, Pressurant and Inert Gas as a Function of Temperature
- Viscosity of Propellant Vapor, Pressurant and Inert Gas as a Function of Temperature
- C_V of Propellant Vapor, Pressurant and Inert Gas as a Function of Temperature
- Density of Thermal Insulation
- Thermal Conductivity of Insulation as a Function of Temperature and Thickness
- Density of Tank Material
- Allowable Stress of Tank Material
- Minimum Skin Gauges of Tank Material
- Specific Heat of Tank Material as a Function of Temperature

B. Boundary Conditions
- The Propellant
- Total Propellant Load
- Initial Propellant Temperature
- Initial Propellant Pressure
- Initial Slush Fraction of Propellant
- Number of Burns
- Stage Mass Ratio for Each Burn
- Weight of Propellant Consumed During Each Burn
- Temperature of Pressurant Entering Tank for Each Burn
- Duration of Each Coast
- Refrigeration Provided During Each Coast
- Propellant Flow Rate from Tank
- Stage Acceleration
- External Temperature of Thermal Insulation

C. Constraints
- Options
- Minimum Ullage Fraction
- Residual Propellant Fraction
- Engine NPSH Requirements
- Factor for Maximum Exected Operating Pressure (MEOP)
- Propellant Feedline Pressure Drop
- Type of Tank Bulkheads
- Maximum Allowable Tank Radius

D. Other Data
- Heat Leak Factor as a Function of Propellant Load
- Coefficients for Inert Weight of Pressurization System
- Tank Land Factors

Table 2-4 Summary of Output from Thermal Subprogram

* Optimum Insulation Thickness
* Optimum Vent Pressure
* Tank Design Pressure
* Total Weight of Tank
* Thermal Insulation Weight
* Total Weight of Pressurization System
* Total Weight of Pressurant
* Total Weight of Propellant Vapor, Pressurant and Inert Gas Vented
* Total Tank Volume Required
* Major and Minor Axes of Tank Bulkheads
* Length of Cylindrical Section in Tank

Weight of Propellant Vapor, Pressurant and Inert Gas Vented During Each Coast
Final Weight of Propellant Vapor, Pressurant and Inert Gas Remaining in Tank Ullage
Weight of Upper Bulkhead, Cylindrical Section and Lower Bulkhead of Tank
Skin Gauges for Upper Bulkhead, Cylindrical Section and Lower Bulkhead of Tank
Stresses in Upper Bulkhead, Cylindrical Section and Lower Bulkhead of Tank
Temperature at the Beginning of Each Coast
Slush Fraction at the Beginning of Each Burn
Weight of Pressurant Required for Each Burn

peaks associated with the individual meteoroid streams. The intensity of these streams can vary up to 20 times that of the background, or sporadic flux.

It is a simple matter to use a sporadic environment model, which is time-invariant, to determine the shielding requirements. However, computation of the meteoroid design mass for the stream fluxes is more difficult since they vary from day to day and stream to stream. Since the exact mission times (day or month) were not known the stream flux parameters were time-averaged.

The meteoroid environment selected for this study was the average accumulative total meteoroid flux-mass model proposed by Cour-Palais, et al.[1]* Mathematically the unshielded, focused 1 A.U. meteoroid flux-mass relationship can be expressed as follows:

$$\log_{10}N_t = -14.339 - 1.584\log_{10}M - 0.063(\log_{10}M)^2 \text{ for } 10^{-12} \leq M\ 10^{-6}$$

and

$$\log_{10}N_t = -14.37 - 1.213\log_{10}M \text{ for } 10^{-6} \leq M \leq 10^{o}$$

where

N_t is the average unshielded, focused accumulative total flux (number of particles of mass, M, or greater per square meter per second)

and

M is the meteoroid mass (grams).

Figure 2.10 depicts this meteoroid flux-mass relationship graphically. Other pertinent data used in conjunction with this model are listed below:

Average Velocity	20Km/sec
Average Density	0.50 g/cc
Shape	Spherical

The actual number of meteoroid impacts received by a vehicle in cis-lunar space depends upon the vehicles altitude above the earth or moon. This dependence on altitude results from two phenomena: 1) gravity focusing and 2) body shielding. The gravitational attraction of the earth or moon will tend to enhance the meteoroid flux near the planet's surface. The gravitational focusing will decrease with distance from the earth. To correct for this phenomena, the average cumulative total meteoroid flux given in figure 2.10 must be corrected by multiplying a defocusing factor G_e. The defocusing factor used in the study is illustrated in figure 2.11.[2] These data assume the gravitational effect influences only the lower velocity, sporadic meteoroids, and hence the effect on the flux of the stream meteoroids has been omitted.

*All references listed in Appendix A

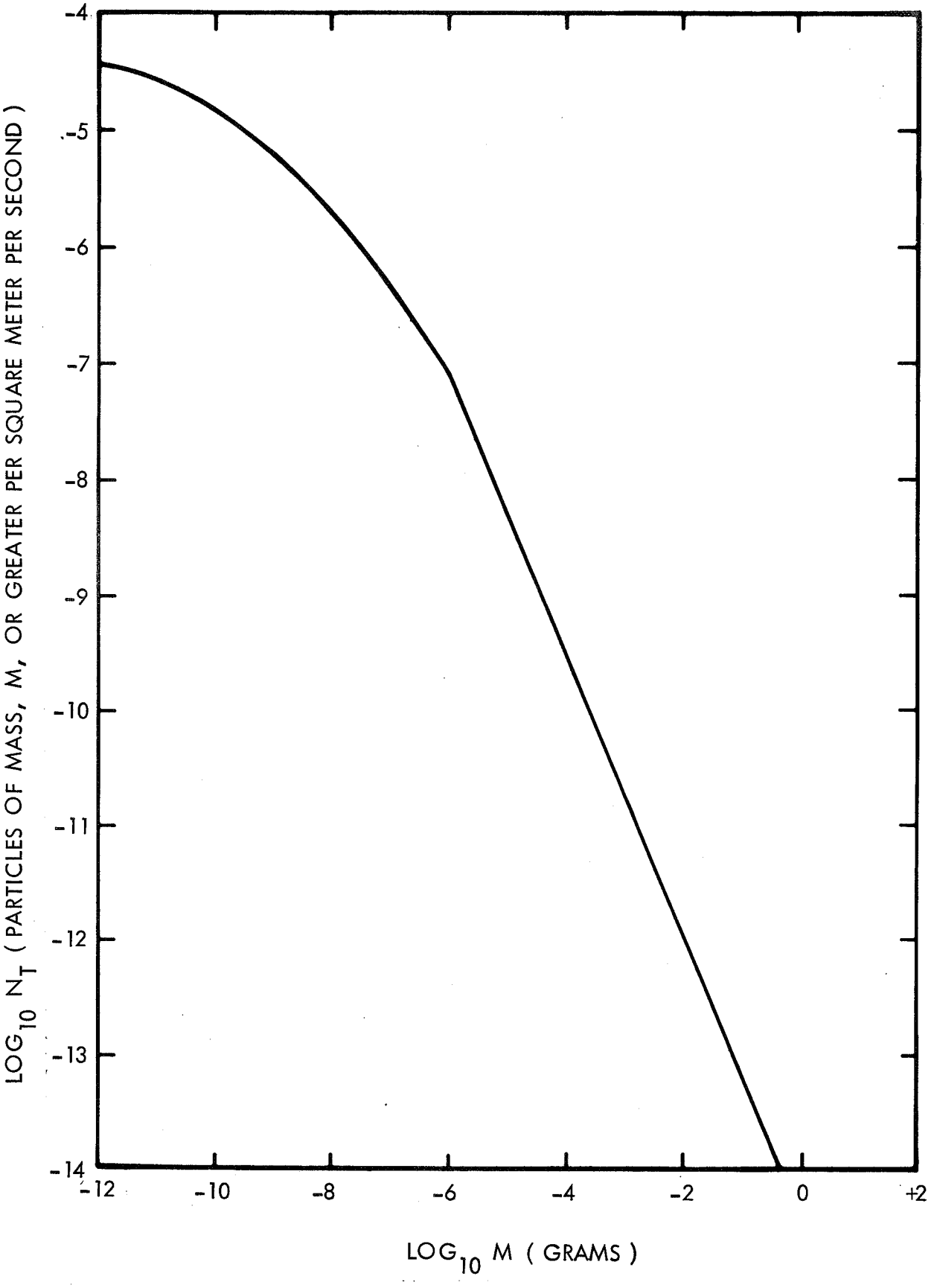

Figure 2-10 Average Unshielded-Focused Cumulative Total Meteoroid Flux - Mass Model for 1 a.u.

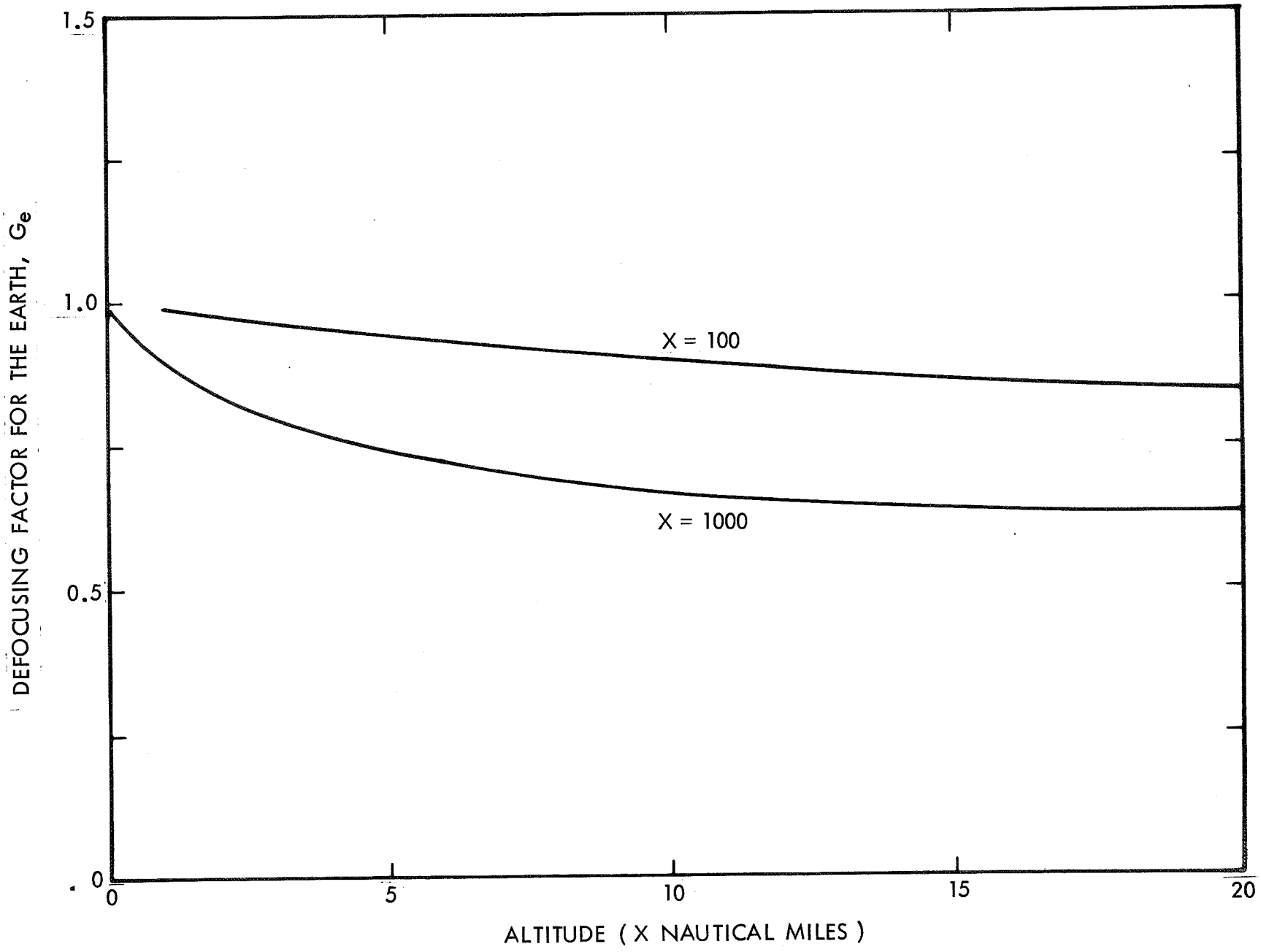

Figure 2-11 Defocusing Factor for Earth

The other altitude correction which must be applied to the flux accounts for shielding provided by the earth or moon. This occurs not only when the planet shields the vehicle from the impacts of sporadic meteoroids but also when the spacecraft, planet, and meteoroid stream are aligned so as to block the impacts of the stream meteoroids. The shielding factor, ζ, used in this study were computed from the following equations: (3)

$$\zeta = \frac{1 + \cos\theta}{2}$$

$$\sin\theta = \frac{R}{R + H}$$

where

R is the radius of the shielding body

H is the altitude of the spacecraft above the surface.

In developing these equations it was assumed that the space vehicle was spherical and randomly oriented. The shielding factor for the earth is presented as a function of altitude in figure 2-12. This shielding factor will yield only a small error in the total flux impacting on any shaped, randomly oriented, space vehicle, when multiplied by the unshielded defocused flux. Hence the total corrected flux can be found by multiplying the unshielded, focused flux by the defocusing factor, G_e, and the body shielding factor, , that is

$$N_{TC} = G_e \cdot \zeta \cdot N_T$$

where

N_{TC} is the average corrected accumulative total flux (number of particles of mass, M, or greater per square meter per second).

2.2.5.2 Meteoroid Design Mass

The present method of protecting a space vehicle from meteoroid damage is to ensure that the meteoroids do not impact directly on vital components. This is accomplished by designing the protective shield so that the largest meteoroid which would probably be encountered during the mission will not penetrate the shield.

The probability of encountering a meteoroid having a specific design mass is a function of the meteoroid flux, the area exposed and the time spent in the environment. Mathematically this can be expressed as,

$$P_o = \exp(-N_{TC}AT)$$

where

P_o is the probability of not being hit

A is area (square meters)

and T is the time (seconds).

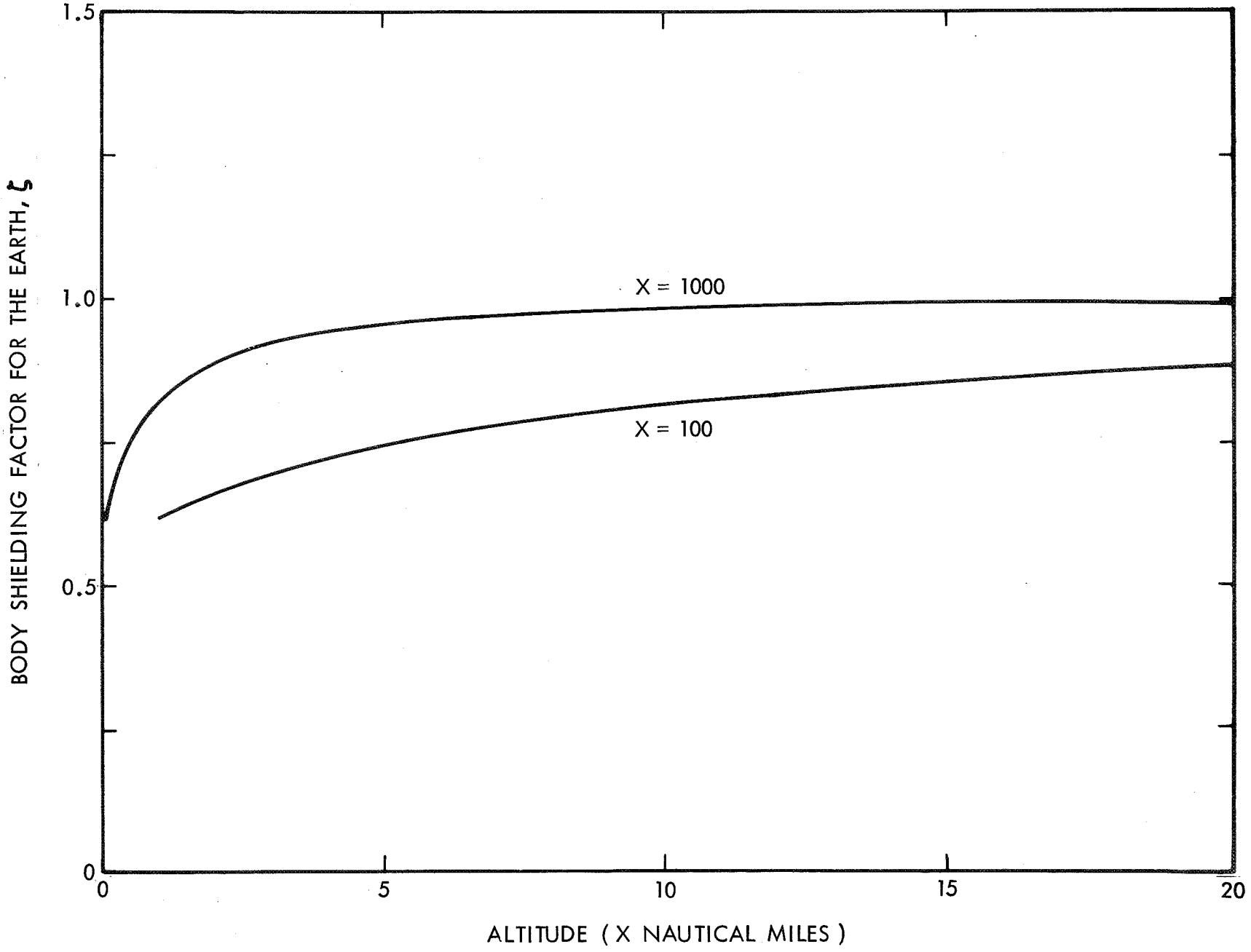

Figure 2-12 Shielding Factor for Earth

Substituting for the corrected flux, and then solving for the defocused - unshielded total average accumulated flux,

$$N_T = \frac{\log_e Po}{- G_e A T,}$$

it is possible to determine the corresponding meteoroid mass from the environment (see figure 2-10).

2.2.5.3 Meteoroid Shield Model

Whipple's bumper shield concept was used as a means of protecting the stages from meteoroid damage, since it is the most promising technique. Basically, this concept consists of a thin outer bumper and a primary or backup structure. The thin shield which surrounds the space vehicle, see figure 2-13, fragments the incoming meteoroid into a relatively diffuse cloud of smaller particles. The debris then impinges on a second backup wall or sheet. Since the backup wall is impacted by the diffuse debris cloud, the damage done to the spacecraft itself is much less than if it had been struck directly by the meteoroid.

The most important element in this type of meteoroid protection system is the shield or bumper, because it controls the physical state of the debris in the cloud. The cloud consists not only of the disintegrated meteoroid, but a significant amount of shield material. The debris, from both the shield and the meteoroid, can take the form of solid particles, liquid droplets, vapors, or some combination. Since it is evident that an all-gaseous debris would produce the least damage to the backup sheet, it is desirable to design the shield to vaporize the debris. In order to accomplish this it is necessary to look at the phenomena through which it can be achieved.

Cour-Palais[4] reasons that the impact of a hypervelocity meteoroid on a shield produces intense compressive shock waves which travel forward in the bumper and rearward in the particle. Because the shock waves are not isentropic, they increase the internal energies of both the shield and meteoroid. When the internal energy of debris exceeds its fusion energy or sublimation energy, the debris either becomes molten or vaporizes.

The maximum internal energy increase will occur when the unloading wave, which is reflected from the rear surface of the shield, overtakes the compressive wave in the meteoroid as the latter reaches the rear end of the particle. Therefore, the shield should be designed to a thickness which is proportional to the particle diameter. According to Cour-Palais[4] the optimum product of the bumper thickness and density falls between 0.1 and 0.2 of the product of the meteoroid diameter and density. However, he states that because there are more small particles in the meteoroid population than the size corresponding to this optimum ratio, a shield thickness-density product of the order of 0.3 of the meteoroid diameter-density product should be used. Mathematically, this can be expressed as:

$$t_s \simeq 0.3D \left(\frac{Pm}{Ps}\right)$$

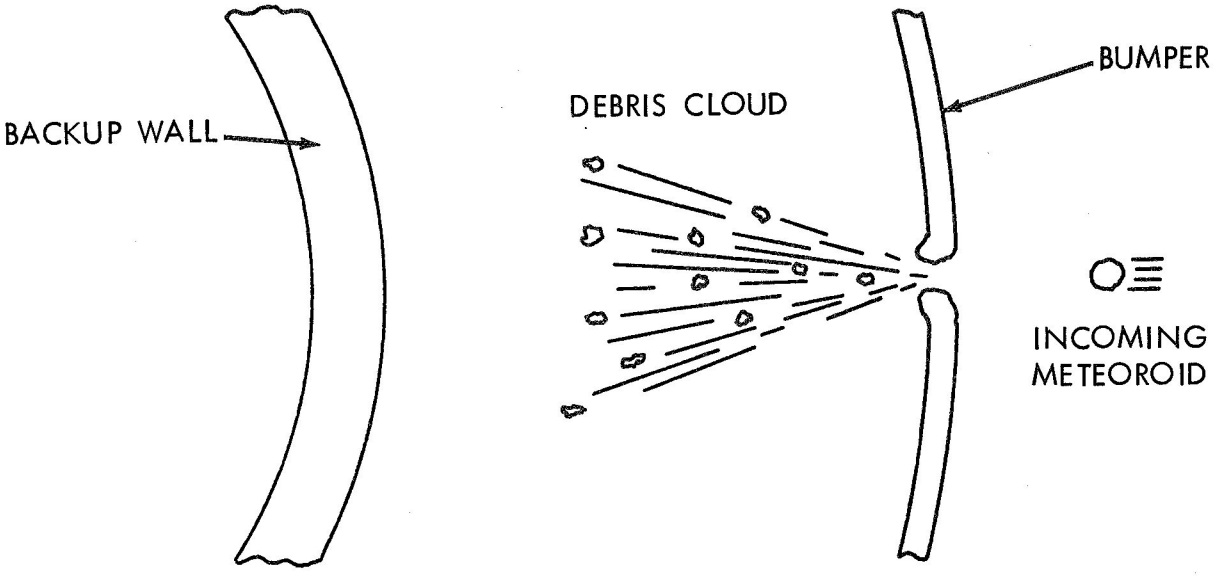

Figure 2-13 Whipple's "Bumper Shield" Concept

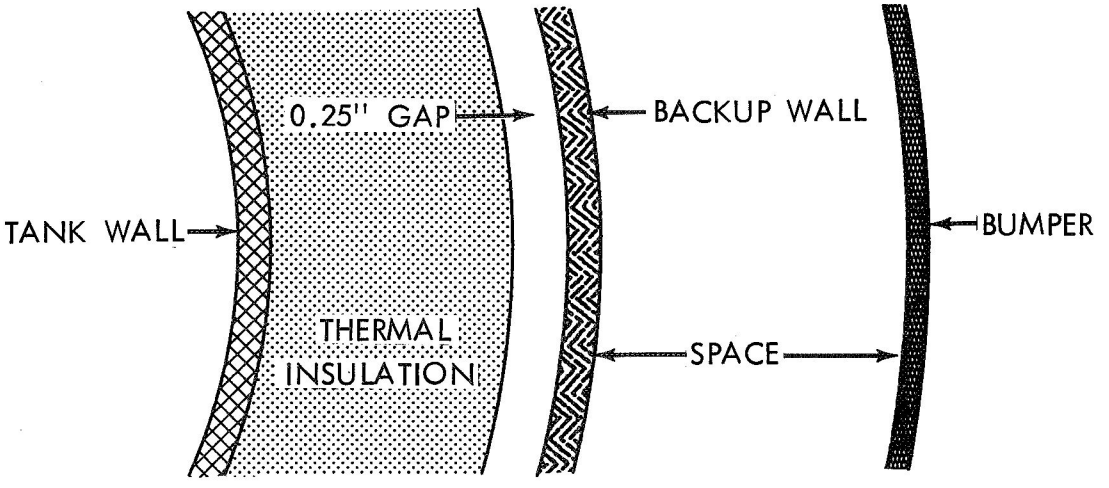

Figure 2-14 Meteoroid Shield Model

where

t_s is the thickness of the bumper or shield (centimeters),

D is the diameter of the meteoroid (centimeters),

Pm is the meteoroid density (grams per cubic centimeter), and

Ps is the shield density (grams per cubic centimeter).

When the bumper thickness falls outside the optimum region ($0.1 \leq P_s\ t_s/Pm\ D \leq 0.2$), the design of the backup sheet is governed by solid fragments in the debris cloud. The Manned Space Center's emperical formula for the non-optimum regions, which was used to calculate the backup wall requirements, is given by the following equation: (4)

$$t_b = \frac{0.055(P_s Pm)^{1/6}\ M^{1/3}\ V}{S^{1/2}} \left(\frac{70000}{\sigma}\right)^{1/2}$$

where

t_b is the thickness of the backup wall (centimeters),

m is the meteoroid mass (grams),

V is the meteoroid velocity (kilometers per second),

S is the spacing between the shield and backup wall (centimeters),

σ is the 0.2 percent yield stress for the backup wall material (pounds per square inch),

P_s is the density of the shield material (grams per cubic centimeter), and

P_m is the density of the meteoroid (grams per cubic centimeter).

Although the validity of the above expression has not been completely established, preliminary evidence suggests that it is valid for bumper-backup wall spacings between 10 and 30 particle diameters.(5)

2.2.5.4 Shield Design

Whipple's bumper shield concept previously discussed was used as a model for the meteoroid shield. As illustrated in figure 2-14, the backup wall was located between the thermal insulation and the shield. A computer routine was used to determine the meteoroid protection requirements and to optimize the shield weight on each stage evaluated. This was accomplished by selecting the shield spacing - the location of the shield relative to the backup wall - which yielded minimum weight, while maintaining several geometric constraints.

Several variations of Whipple's bumper shield concept were used for different missions during the study. For the symchronous orbit (baseline) and the alternate lunar missions (shuttle and lander), it was determined that the stage's shell and thrust structure were thick enough to permit their use as the bumper. This resulted in a substantial savings in stage weight. However, on the Mars missions (alternate) where the thermal considerations dictated the use of a truss type shell, a separate bumper was sized.

The backup wall thickness requirements for all the missions analyzed were computed using MSC's empirical relation. (See Section 2.2.5.3.) As depicted in figure 2-14, the backup wall was located 1/4 of an inch in front of the thermal insulation surrounding the tank. In cases where the spacing between the backup wall and the bumper exceeded 30 meteoroid diameters the backup sheet was designed for 30 diameters, although the spacing was larger.

For the Mars missions the required bumper thickness-density product was assumed to be 0.30 times the product of the diameter and density of the design meteoroid. Although this will not give the optimum thickness, it will yield results which are accurate enough for the preliminary designs conducted in this study. The reasons for this are twofold. First, as discussed in Paragraph 2.2.5.3, even though the optimum bumper product range is between 0.10 and 0.20 particle diameters, the bumper is usually designed to a slightly higher value; and second, even at a ratio of 0.30, a large number of bumper thickness requirements were found to fall below the minimum allowable skin gauges. The computer routine checked the skin gauge of each shield to ensure that the minimum gauges were satisfied.

The computer routine determined the spacing between the bumper and the backup sheet which yielded the minimum total weight (bumper + backup) and fitted within the specified configuration geometry. For the purpose of this study, the spacing was required to be at least equal to 10 times the meteoroid diameter, and was not permitted to exceed a distance which would locate the shield outside a maximum radius established by the restrictions placed on propellant tank spacing.

The complex relationships between the geometric, structural, and minimum weight requirements can best be illustrated by an example. The results of a typical meteoroid shield analysis are presented in figures 2-15 and 2-16. This shield was designed for a 0.995 probability of no impact by a meteoroid having the design mass or larger during a 5000 hour mission.

The analysis indicates (figure 2-15) that the required bumper thickness (0.004 inches) was less than minimum skin gauge (0.015 inches) and therefore it was necessary to make the bumper thicker and heavier than actually required for meteoroid protection. For this example, the 466 pound minimum total (see figure 2-16) occurred at a spacing of 2.417 inches.

The total weight begins to increase slowly for spacing to diameter ratios (S/D) greater than 30 because the constant thickness bumper's area increases as it is moved further away from the backup wall. Note that

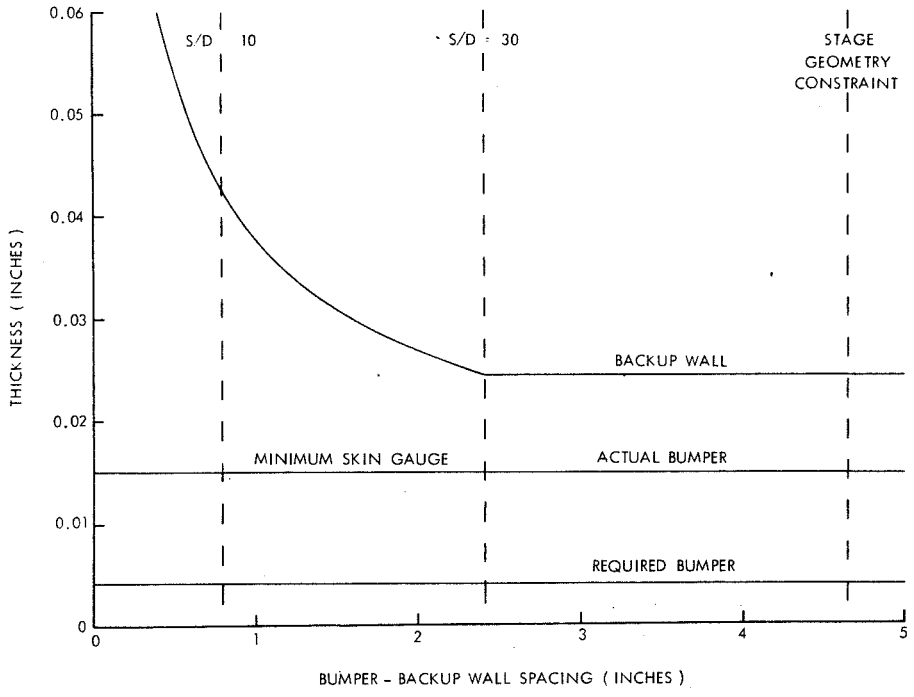

Figure 2-15 A Typical Meteoroid Shield Optimization

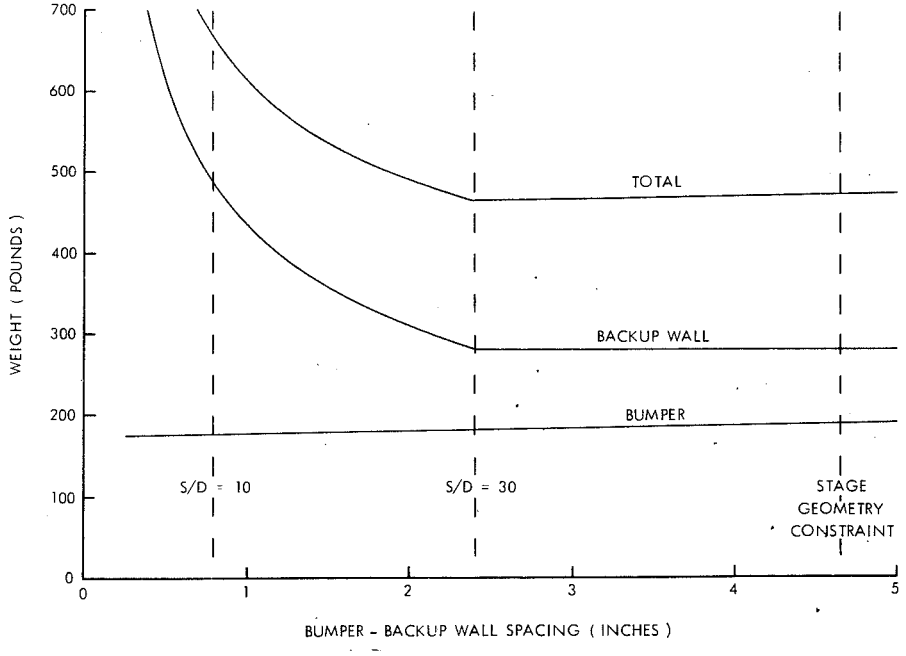

Figure 2-16 A Typical Meteoroid Shield Optimization Continued

the thickness and hence the weight of the backup sheet remains constant once a spacing ratio of 30 is reached. In this instance the optimum spacing (minimum weight) corresponds to a spacing to diameter ratio of 30. This need not be the case every time. Depending on the exposed area and the life expendency of the stage, it is possible for the required backup sheet thickness to be less than the allowable minimum skin gauge. In this instance the minimum weight would occur at the spacing where minimum skin gauge became the controlling criteria.

The computer program logic permits the use of insulation as a part of the backup wall. This is done by means of an input "collapse" factor which relates the actual insulation thickness to an effective backup wall thickness. For this study, however, the insulation was not used as an integral part of the backup wall. This was because it was felt that a meteoroid debris cloud could easily blow a hole in the insulation which, while not penetrating the tank wall, could result in a heat leak large enough to cause all the remaining propellant to boiloff and vent. Of course, whether all the propellant escapes through a puncture or through the vents is purely academic.

2.2.6 Reaction Control System (RCS)

The reaction control system (RCS) weights are based on a simple limit-cycle (pulse type thruster operation) where vehicle attitude and rates are sensed by inertial position and rate sensors. Deviations from the desired position or a rate of change of attitude produce error signals. When these signals exceed certain preset switching values, the appropriate thrusters are fired to provide a correcting impulse which drives the errors toward zero. The inertia of the vehicle, and the delays in thrust build-up and decay cause the vehicle to oscillate between the switching values, thereby requiring on-off thruster operation.

The size of the RCS was established using the following criteria:

1. Limit cycle of $\pm$ 5.00 degrees about all axes,
2. Angular velocity of 0.01 deg/sec about all axes,
3. Angular acceleration of 0.003 rad/sec about the axis having the minimum inertia, and
4. Monopropellant thrusters having a steady state specific impulse of 180 seconds.

The weight of propellant consumed during the mission is found from the following equation:(6)

$$W_P = \frac{\pi}{180}\left(\frac{\dot{\omega}^2}{\Theta I_{sp}}\right)\left[\left(\frac{I_{xx}}{r_{xx}}\right)+\left(\frac{I_{yy}}{r_{yy}}\right)+\left(\frac{I_{zz}}{r_{zz}}\right)\right]T$$

where

ω is the angular velocity (deg/sec),

θ is the limit cycle (degrees),

I_{sp} is average specific impulse (seconds),

T is the mission duration (seconds),

I is the moment of inertia (slug-ft^2),

and

xx, yy, and zz denote the pitch, yaw and roll axes, respectively. To facilitate calculation of the inertias, it was assumed that the payload was a uniform solid cone, and that the engine and stage were homogeneous solid cylinders. The basic geometry used, and the individual weights included in each section are depicted in figure 2-17.

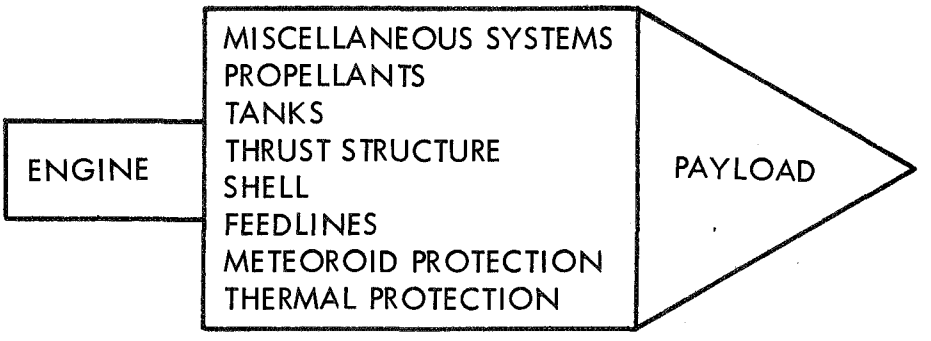

Figure 2-17 Reaction Control System Model

The total RCS weight was assumed to be directly proportional to the weight of propellant consumed during the mission.

Preliminary analyses indicated that the entire system would weigh approximately 25 to 30 percent more than the propellant. Therefore, the total RCS weight was computed from the following equation:

$$W_{RCS} = 1.30\ W_P$$

Any error introduced by the use of this technique would be small and would not affect the conclusions of the study.

2.2.7 Propellant Feedlines

The weight of individual propellant feedlines was computed on the basis of lengths and diameters, calculated to satisfy the stage geometry and propellant flow requirements, respectively. The diameter of each feedline was sized to provide the necessary flow rate at a specified feedline flow velocity.

Estimates of the length of the feedlines for the tandem tank stages were made using the geometry shown in figure 2-18. The lower tank feedline was assumed to run directly from the tank bottom to the engine gimbal point. The feedline length for the forward or smaller tank was estimated by assuming it ran along the stage's centerline from the bottom of the upper tank to the top dome of the lower tank, then along the lower tank's periphery to the stage's centerline at the lower tank bottom dome, and finally to the engine gimbal point along the stage's longitudinal axis.

The feedline lengths on the multiple tank configurations were computed in a similar manner except that the feedline geometry depended upon the number of tanks, and the type and location of the thrust structure being evaluated. The total line length required for each propellant on the multiple tank versions was assumed to be directly proportional to the number of tanks; that is, one feedline for each tank.

Estimates of the length of the feedlines on the configurations having a single large tank and multiple small tanks were made using the geometries shown in figures 2-19 and 2-20. The feedline from the large tank was assumed to be a straight line running directly from the bottom of the tank to the gimbal point on the engine.

When the bottom of the smaller multiple tanks were located above the thrust structure (thrust structure option 2), as depicted in figure 2-19, the feedlines were assumed to run horizontally from the bottom of the tanks to stage's centerline, and finally to the engine's gimbal point.

When the bottom of the multiple tanks were located in below the thrust structure (thrust structure options 1, 3 and 4), dip tubes were utilized in the propellant tanks. As illustrated in figure 2-20, these lines run from the bottom of each propellant tank to the top, then horizontally to the centerline of the stage, and finally to the engine's gimbal point.

The feedline geometries used for the "transtage" having multiple fuel and oxidizer tanks (tankage arrangement 5) are shown in figures 2-21 and 2-22. When the tankage is located above the spider beam, as shown in figure 2-21, the feedlines were assumed to run directly from the bottom of the tank to the stage's centerline and then to the engine's gimbal point.

When multiple fuel and oxidizer tanks were used in conjunction with thrust structure options 3 and 4 (tanks extend below spider beam) the feedline geometry illustrated in figure 2-22, was used. In these cases the feedlines ran from the bottom of the tanks along the periphery of the tank until it is directly across from the engine's gimbal point and finally horizontally to the gimbal point of the engine.

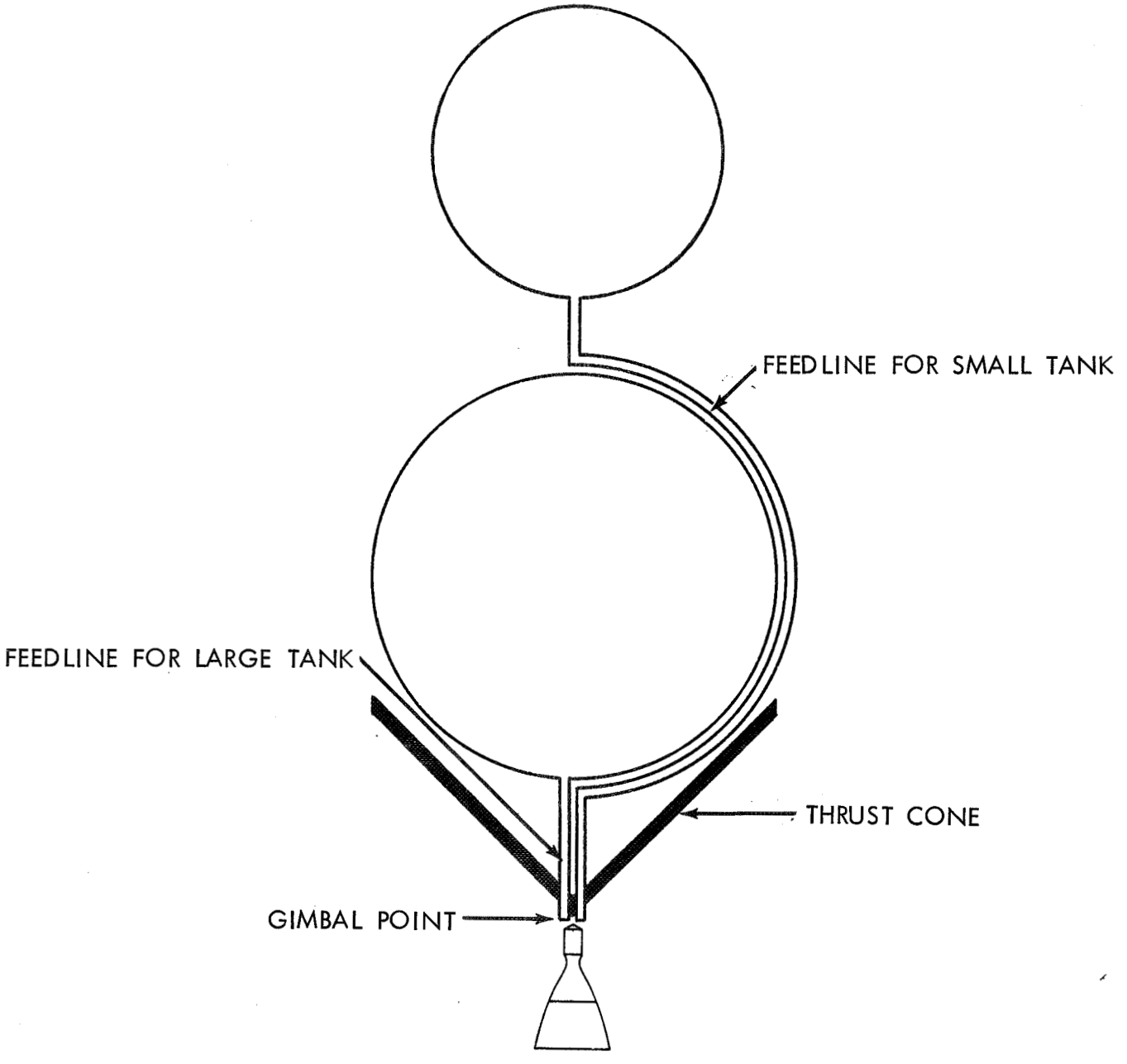

Figure 2-18 Feedline Geometries for Tandem Tank Stages

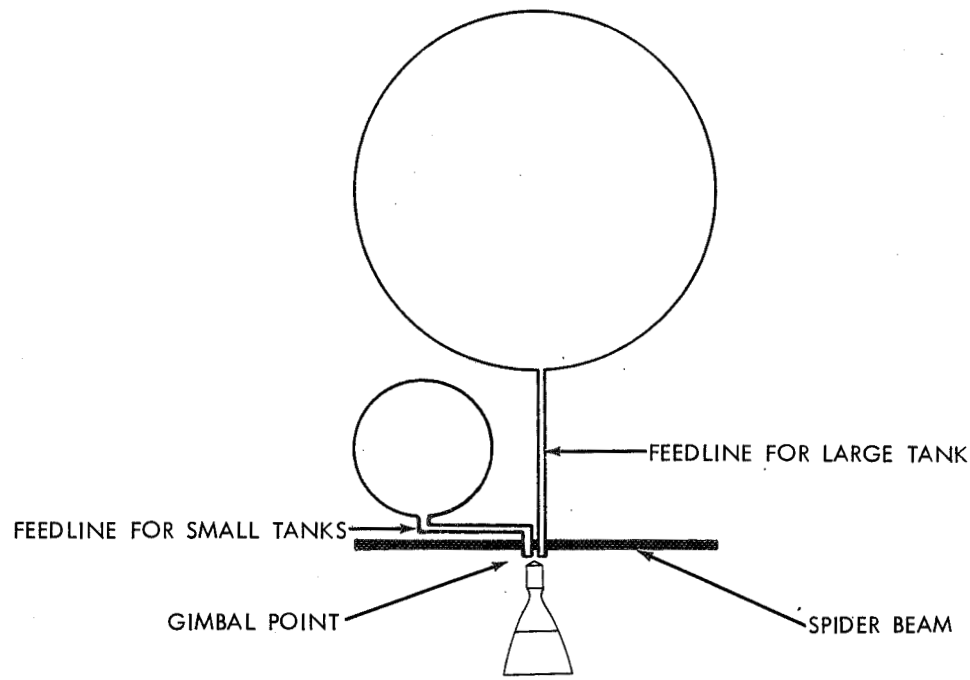

Figure 2-19 Feedline Geometries for Stages with Small Multiple Tanks Above the Thrust Structure

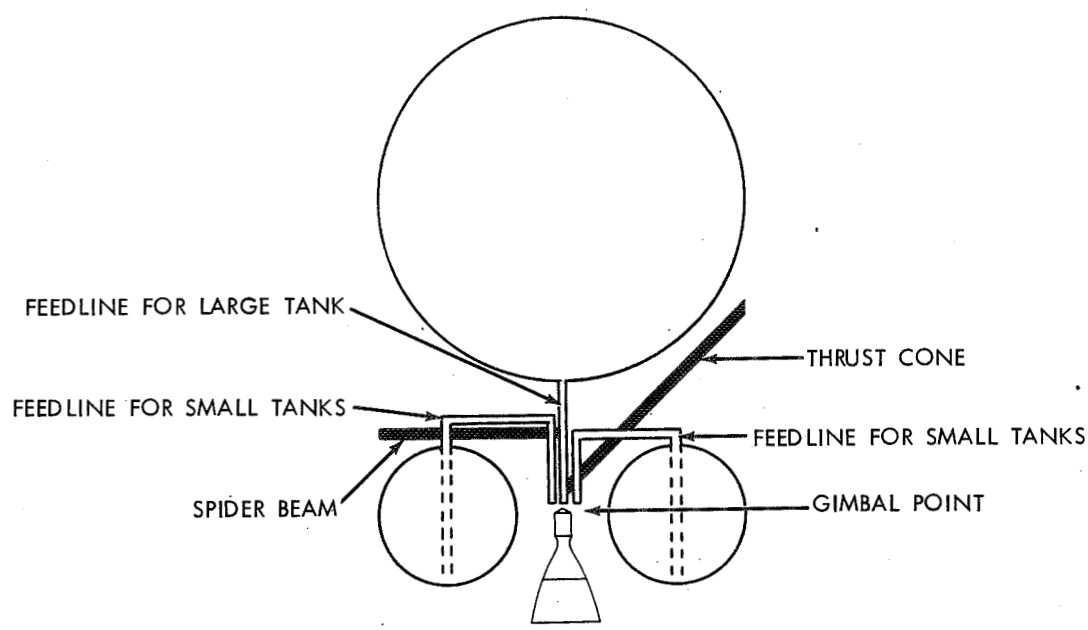

Figure 2-20 Feedline Geometries for Stages with Small Multiple Tanks Below the Thrust Structure

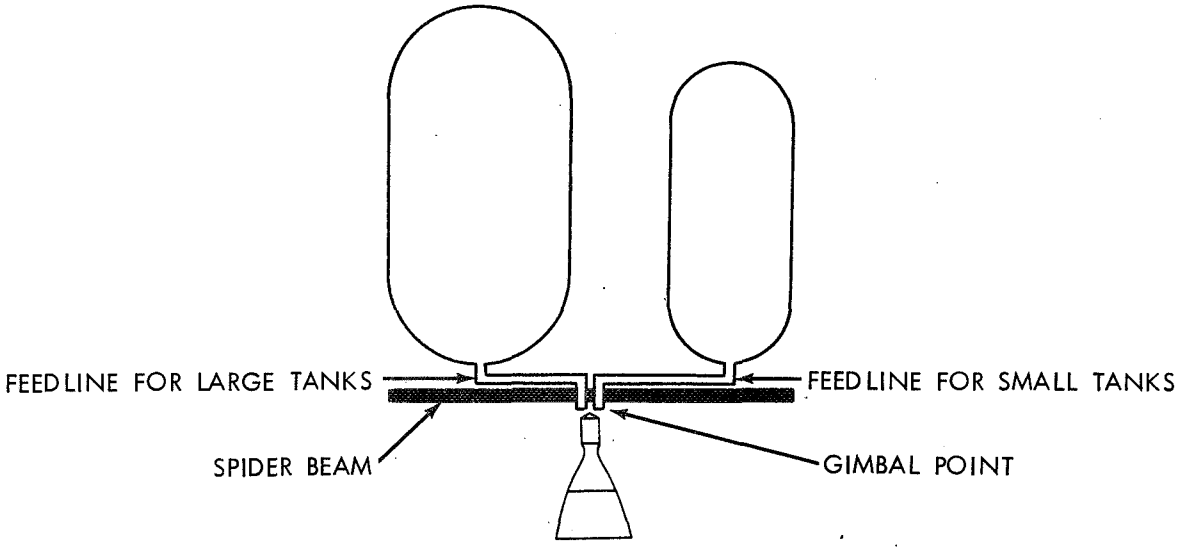

Figure 2-21 Transtage Feedline Geometries Having Tankage Above Spider Beam

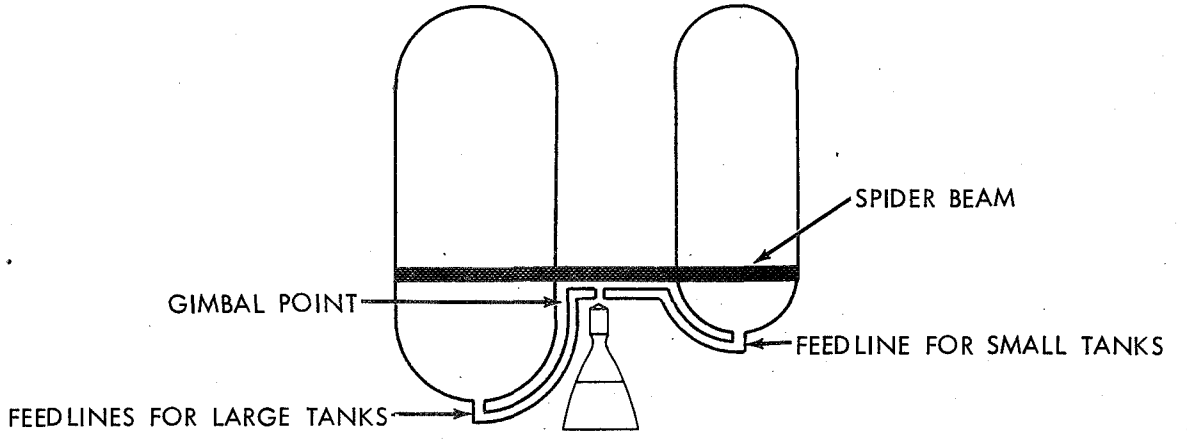

Figure 2-22 Transtage Feedline Geometries Having Tankage Below Spider Beam

Section 3

STUDY RESULTS

3.1 GENERAL

Five different missions were studied: 1) earth orbit to synchronous orbit and return; 2) earth orbit to lunar orbit and return; 3) lunar orbit to lunar surface and return to lunar orbit; 4) a single burn Mars planetary orbit insertion, and 5) a two burn Mars planetary mission. For the synchronous orbit mission, which was the study baseline, additional stage design sensitivity studies were conducted. The results of these analyses are presented in the subsequent sections according to mission.

3.2 DATA AND ASSUMPTIONS

Throughout the study, certain constraints, guidelines and pertinent design data were used. These are summarized in this section. Table 3-1 gives the design constraints used for each mission. Table 3-2 presents the prime structure data used in computing the weights of the shell, interstage, and thrust structures. Table 3-3 summarizes the assumed tankage design data including pertinent thermal and meteoroid protection data. These data are shown for each mission. It should be noted that for the lunar shuttle mission the density of the thermal insulation used was lower than for the other missions. This was done in an attempt to minimize the differences in assumptions between this study and those used in the Reusable Nuclear Shuttle studies. The weights assumed for the astrionics systems and for other miscellaneous systems are given in the weight summaries presented for each mission in the following sections.

Early in the study, parametric oxygen-hydrogen engine system performance, weight and geometry data used in optimizing the engine parameters and stage size, were obtained from Rocketdyne[7] for both the topping and expander cycles. This data covered engines having thrust between 15,000 and 120,000 pounds. As the study progressed, it was discovered that data covering lower thrust levels would be required, if the selected thrust to weight ratio were to be held throughout the study. This was particularly true for the analyses of the one burn Mars mission and multiple engine stages for the synchronous mission. Since low thrust engines utilizing a topping cycle (the baseline cycle) would be extremely difficult, if not impossible, to design; low thrust engine weight data was obtained from Rocketdyne[8] for the gas generator cycle engine used on the orbital maneuvering system. It was decided, with NASA approval,[9] to use the gas generator cycle weights and the topping cycle performance for those engines requiring thrust below 15,000 pounds. The parametric engine data supplied by Rocketdyne is presented in Appendix B.

Table 3- 1 Summary of Stage Design Constraints

CONSTRAINT / MISSION	SINGLE STAGE SYNCHRONOUS	TWO STAGE SYNCHRONOUS	SINGLE STAGE LUNAR SHUTTLE	TWO STAGE LUNAR SHUTTLE	LUNAR LANDER	INTERPLANETARY (MARS)
MAXIMUM STAGE DIAMETER (IN.)	270	180	396	396	192	270
SHELL - TANK SPACING (in	9.0	9.0	9.0	9.0	9.0	9.0
TANK - TANK SPACING (IN.)	5.0	5.0	5.0	5.0	9.0	9.0
ENGINE - TANK SPACING FACTOR (CHAMBER)	4.0	4.0	4.0	4.0	4.0	4.0
ENGINE - TANK SPACING FACTOR (EXIT)	0.8	0.8	0.8	0.8	0.8	0.8
ENGINE - BOOSTER SPACING (IN.)	0.0	0.0	0.0	0.0	0.0	0.0
ENGINE GIMBAL ANGLE (DEGREES)	3.0	3.0	3.0	3.0	5.0	3.0
THRUST - TO - WEIGHT RATIO	0.25	0.25	1.00	1.00	0.33	0.25
AXIAL ACCELERATION (G's)	1.00	1.00	1.00	1.00	1.00	1.00
LATERAL ACCELERATION (G's)	0.05	0.05	0.05	0.05	0.05	0.05
PAYLOAD DENSITY (LB / FT^3)	25.0	25.0	25.0	25.0	25.0	25.0
INERT WEIGHT CONTINGENCY FACTOR (%)	7.5	7.5	7.5	7.5	7.5	7.5

Table 3- 2 Summary of Structural Design Data

DATA \ STRUCTURE	SHELL	THRUST CONE	SPIDER BEAM	INTER-STAGE
MATERIAL	Aluminum	Aluminum	Aluminum	Aluminum
DENSITY (LB / FT^3)	183.0	183.0	183.0	183.0
MATERIAL STRENGTH (PSI)				
TENSION	67,000	67,000	67,000	67,000
COMPRESSION	46,000	46,000	46,000	46,000
MODULUS OF ELASTICITY (PSI)	10^7	10^7	10^7	10^7
SAFETY FACTORS				
TENSION	1.25	1.25	1.25	1.25
COMPRESSION	1.00	1.00	1.00	1.00
MONOCOQUE - TO - COMPLEX STRUCTURE WEIGHT RATIO	‡	‡	‡	N / A
SPIDER BEAM MULTIPLICATION FACTOR	N / A	N / A	‡	N / A

‡ A Function Of Diameter And Limit Load, See Appendix C.

Table 3- 3 Summary of Tankage Design Data

DATA / MISSION	SYNCHRONOUS	LUNAR SHUTTLE	LUNAR LANDER	INTERPLANETARY (MARS)
TANKAGE				
MATERIAL	Aluminum	Aluminum	Aluminum	Aluminum
DENSITY (LB / FT^3)	183.0	183.0	183.0	183.0
ALLOWABLE STRESS (PSI)	60,000	60,000	60,000	60,000
FACTOR OF SAFETY	1.10	1.10	1.10	1.10
MINIMUM SKIN GAUGE (IN.)	0.025	0.025	0.025	0.025
LAND FACTORS (BULKHEADS)	0.10	0.10	0.10	0.10
LAND FACTORS (CYLINDRICAL SECTION)	0.05	0.05	0.05	0.05
THERMAL PROTECTION				
INITIAL FUEL / OXIDIZER TEMPERATURE (°R)	36.0/162.6	36.0/162.6	36.0/162.6	36.0/162.6
INITIAL FUEL / OXIDIZER PRESSURE (PSI)	15.0/15.0	15.0/15.0	15.0/15.0	15.0/15.0
EXTERNAL INSULATION TEMPERATURE (°R)	450.0/470.0	415.0/425.0	470.0/500.0	400.0/420.0
INSULATION DENSITY (LB / FT^3)	4.5	2.5	4.5	4.5
INSULATION THERMAL CONDUCTIVITY (BTU/HR-FT-°R)	*	*	*	*
METEOROID PROTECTION				
PROBABILITY OF NO PUNCTURES	0.995	0.995	0.995	0.995
NOMINAL MISSION ALTIDTUE (N. M.)	200	200,000	200,000	500,000
SHIELD MATERIAL	Aluminum	Aluminum	Aluminum	Aluminum
MATERIAL DENSITY (LB / FT^3)	183.0	183.0	183.0	183.0
MATERIAL YIELD STRESS (PSI)	70,000	70,000	70,000	70,000
MINIMUM SKIN GAUGES (IN.)	0.015	0.015	0.015	0.015
MISCELLANEOUS				
MINIMUM FUEL / OXIDIZER ULLAGE VOLUME (%)	5.0/5.0	5.0/5.0	5.0/5.0	5.0/5.0
RESIDUAL FUEL / OXIDIZER FRACTION (%)	2.0/2.0	1.75/1.75	3.20/3.25	2.0/2.0
FEEDLINE FLOW VELOCITY (FPS)	20.0	20.0	20.0	20.0
TANK SUPPORT FACTOR	†	†	†	†

* A Function Of Temperature And Thickness, See Appendix C

† Dependent Upon Configuration, See Appendix C

3.3 SYNCHRONOUS ORBIT MISSION

3.3.1 Mission Profile

The baseline mission selected for this study was the transfer of payloads between a low inclination, low altitude earth (parking) orbit and a synchronous orbit. This mission would require the liquid hydrogen-liquid oxygen stage(s) to perform one of the following maneuvers:

1. Delivery of a payload from low earth orbit to synchronous orbit and return without a payload;

2. Transport a payload from the low-parking orbit to synchronous orbit and return with the same or a different payload; and

3. Fly empty from the parking orbit to the synchronous orbit, and return with a payload to the original departure orbit.

The use of both single stage and two stage vehicles for conducting the baseline synchronous mission were investigated. Figure 3-1 depicts the typical mission profile for the single stage vehicle. This involves a Hohmann type transfer maneuver from low earth orbit to snychronous altitude, a plane change and circularization at synchronous orbit, a return Hohmann transfer and plane change at synchronous orbit and circularization into the original low earth orbit.

The basic two stage mission profile is presented in figure 3-2. This mission profile consists of having the first stage impart part or all of the first velocity increment required for the Hohmann type transfer from low earth orbit to snychronous. After separating from the second stage, and coasting in an elliptical trajectory, the first stage provides the velocity necessary to recircularize itself in the original low earth orbit. Meanwhile, the second stage provides any additional impulse necessary to complete the outbound Hohmann type transfer, and then coasts to synchronous altitude where it supplies the velocity increment needed for the plane change and orbit circularization. The second stage also provides the two burns needed to return itself to the original low earth orbit.

An additional mission profile was examined for the two stage synchronous mission. The profile for this alternate two stage mission is presented in figure 3-3. Here the one stage performed four burns, just as a single stage vehicle would do; however, the fourth burn (or last burn) does not provide the total velocity increment needed to return and circularize the stage in the original low earth orbit. Instead, the stage is left in an elliptical orbit. The other stage then "flies up" from the original low earth orbit and rendezvous with the original stage. This stage provides the circularization impulse necessary to return both stages to the original low earth orbit.

The velocities used for the three synchronous missions assumed a Hohmann type transfer between 28 1/2° inclination, circular 100 nautical mile orbit, and an equatorial (0° inclination) synchronous orbit. The velocities were corrected to account for the effects of the stage's initial thrust-to-weight ratio and specific impulse. However, the effect

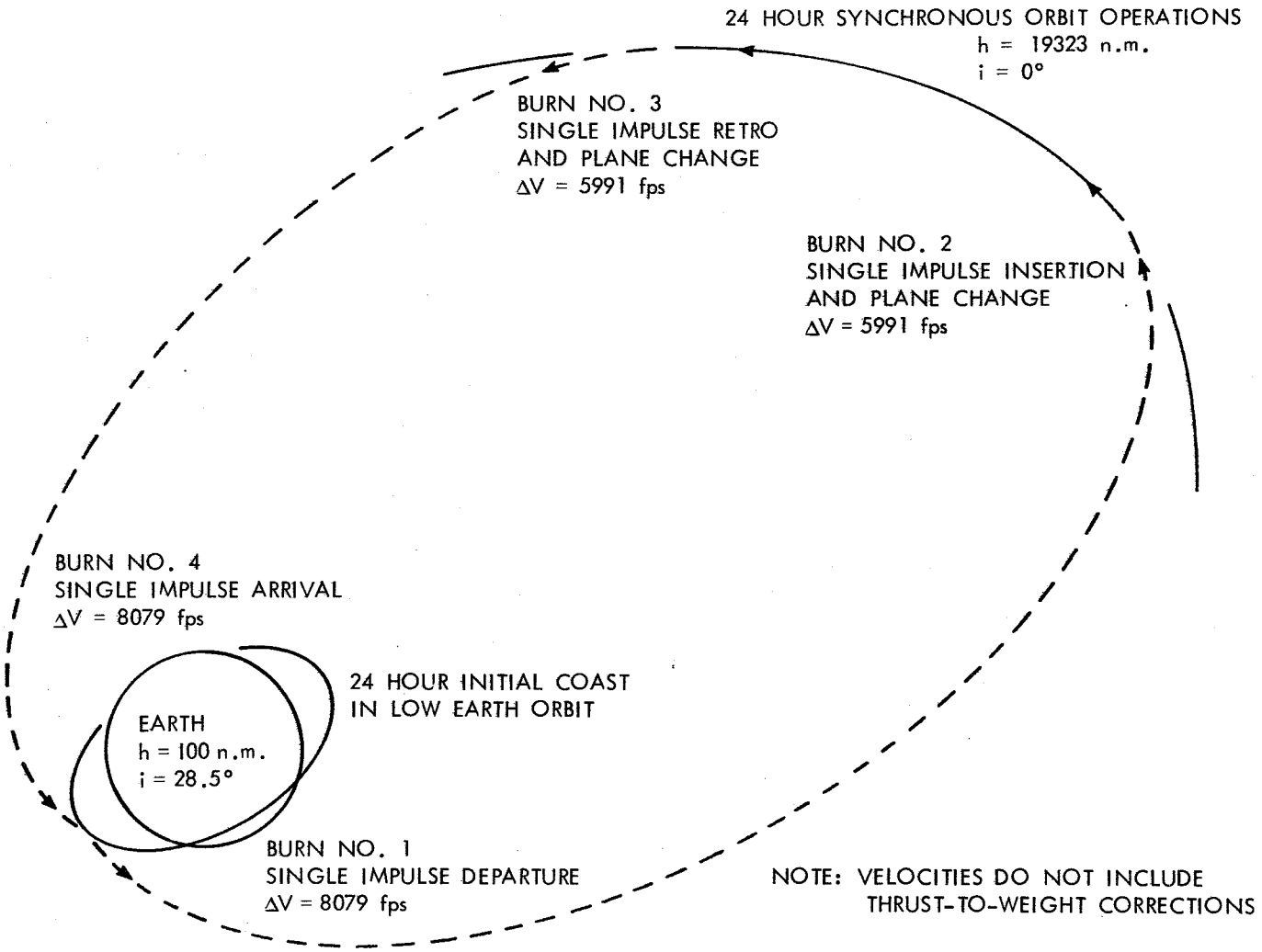

Figure 3- 1 Synchronous Orbit Mission Profile (Single Stage)

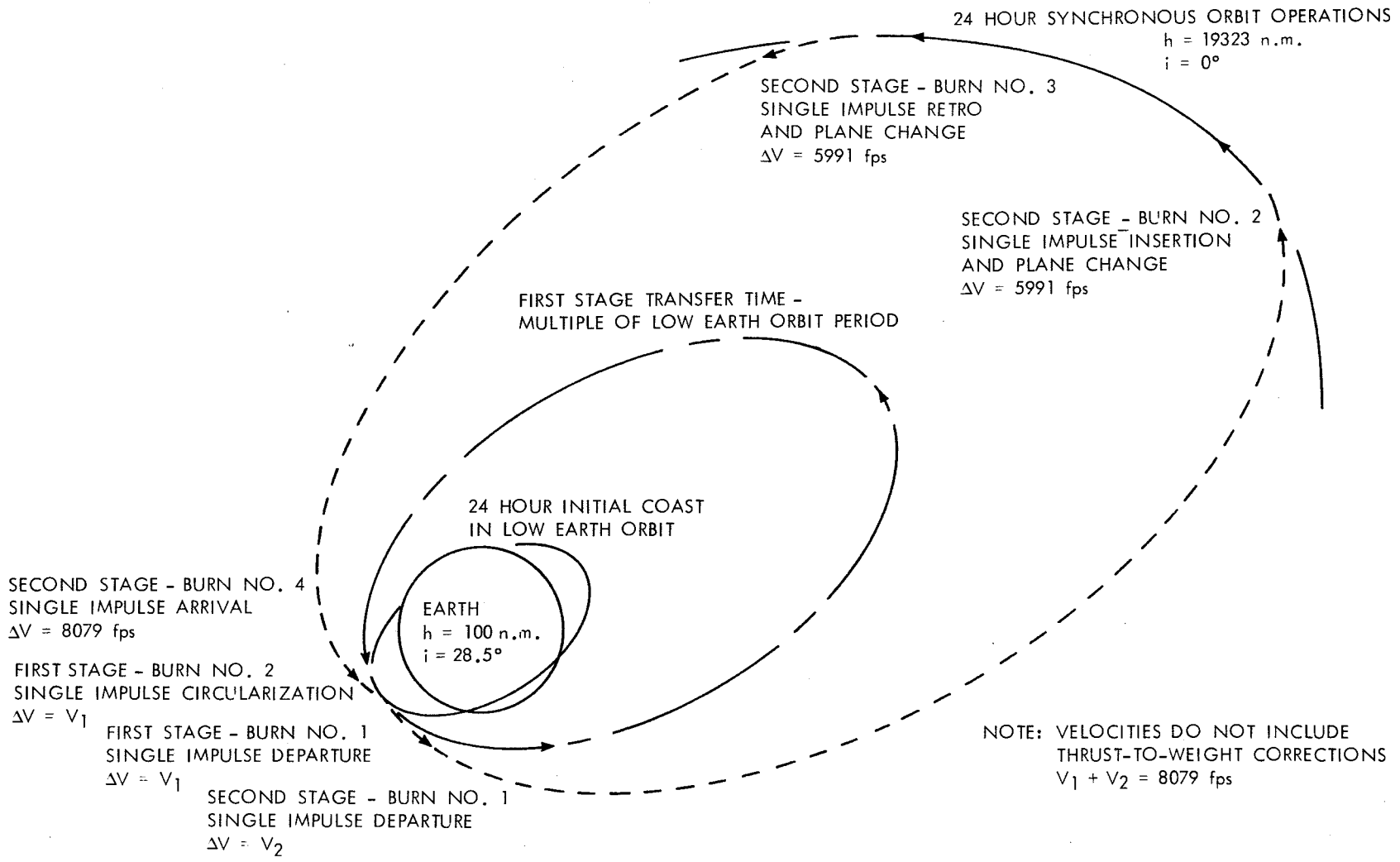

Figure 3- 2 Synchronous Orbit Mission Profile (Two Stage)

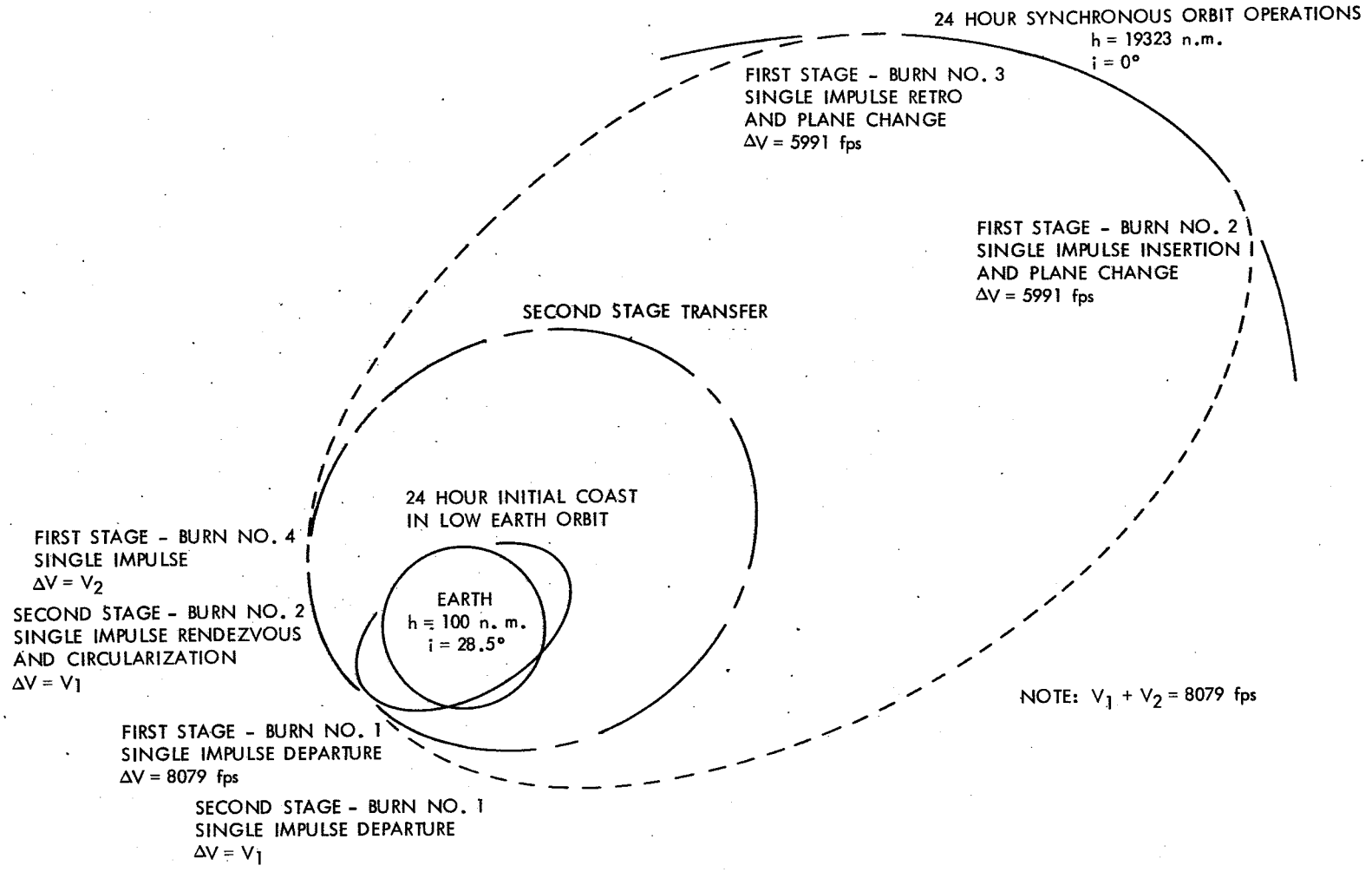

Figure 3- 3 Alternate Two Stage Synchronous Orbit Mission Profile

of orbital regression on the velocity requirements were not considered.

3.3.2 Engine Parameter Optimization

In order to reliably compare various stages, each had to be efficiently sized and its engine chamber pressure, mixture ratio and area ratio selected to ensure that maximum performance was attained for the particular mission of interest. Figures 3-4 through 3-6, which are discussed below, illustrate typical engine parameter optimization for an engine using a topping cycle. Figure 3-4 presents stage weight as a function of mixture ratio for three chamber pressures and three area ratios. These results have been cross plotted to give the curve showin in figure 3-5, which is the chamber pressure optimization. The optimum chamber pressure at each area ratio was then cross plotted to show the optimum area ratio as illustrated by figure 3-6. The data figures 3-4 through 3-6 are for stages with a thrust to weight ratio of 0.25, which were found to be optimum for a zero up/10K return payload requirement. Figures 3-7 to 3-9 show the results obtained for the same mission and a thrust to weight ratio of 0.7. The optimum engine parameters are similar in both cases. Although not shown herein, the results for other payload requirements were the same and indicate the optimum chamber pressure is 3000 psia or greater. The optimum mixture ratio is about 6.0:1 and the optimum area ratio is 400:1 or greater.

Similar optimization analyses were performed for stages using an engine predicated on an expander cycle. The results of the expander cycle optimization are shown on figures 3-10 to 3-12. It should be noted that the maximum chamber pressure attainable for this engine cycle is slightly less than 1000 psia (see Appendix B). Otherwise this cycle also would optimize at chamber pressures above 1000 psia.

3.3.3 Thrust to Weight Ratio Optimization

A better mass faction is obtainable as the stage's thrust to weight ratio is decreased because a smaller engine is required. However, gravity losses increase the total mission velocity requirements in accordance with the following equations:*

1. Velocity loss for transfer from 100 n.m. orbit to synchronous altitude with no plane change. (Reference impulsive velocity used is 8067.4 ft/sec).

$$V_{loss} = (Isp/445)^{.31}(Wo/T)^2 \left[11.2 - 1.13\ (Wo/T)^{.55} \right] \text{ fps}$$

2. Velocity gain at apogee for synchronous mission, that is, reduction in required circularization velocity due to high total burnout energy at perigee with no plane changes. (Reference impulsive velocity used is 4,851.8 ft/sec).

$$V_{gain} = (Isp/445)^{.27}\ (Wo/T)^2 \left[2.48 - .00072\ (Wo/T)^2 \right] \text{ fps}$$

*Private communication - Dr. Rex Finke (Institute for Defense Analysis) and D. L. Baradell (Chrysler).

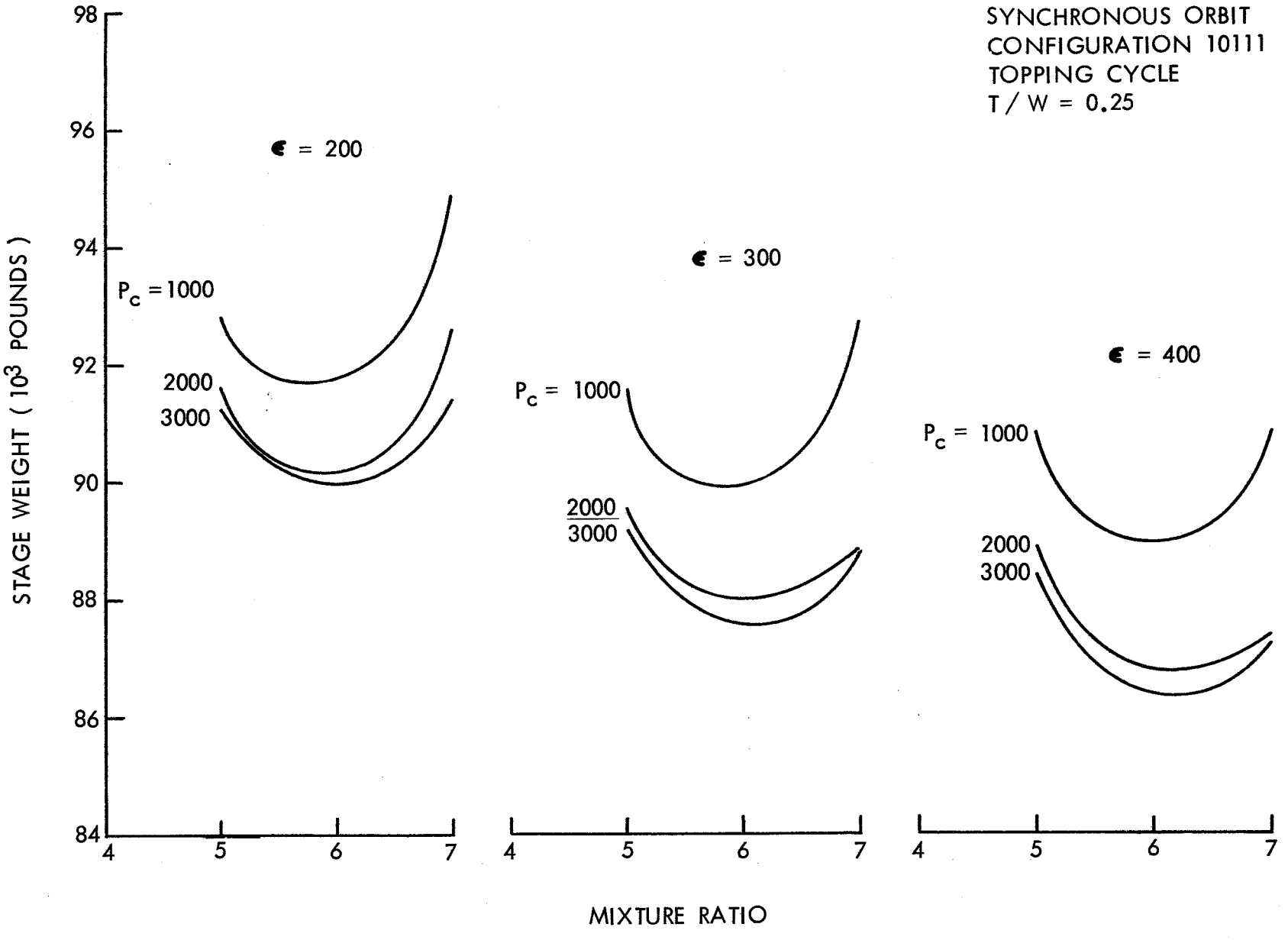

Figure 3- 4 Topping Cycle Engine Parameter Optimization (T/W = 0.25)

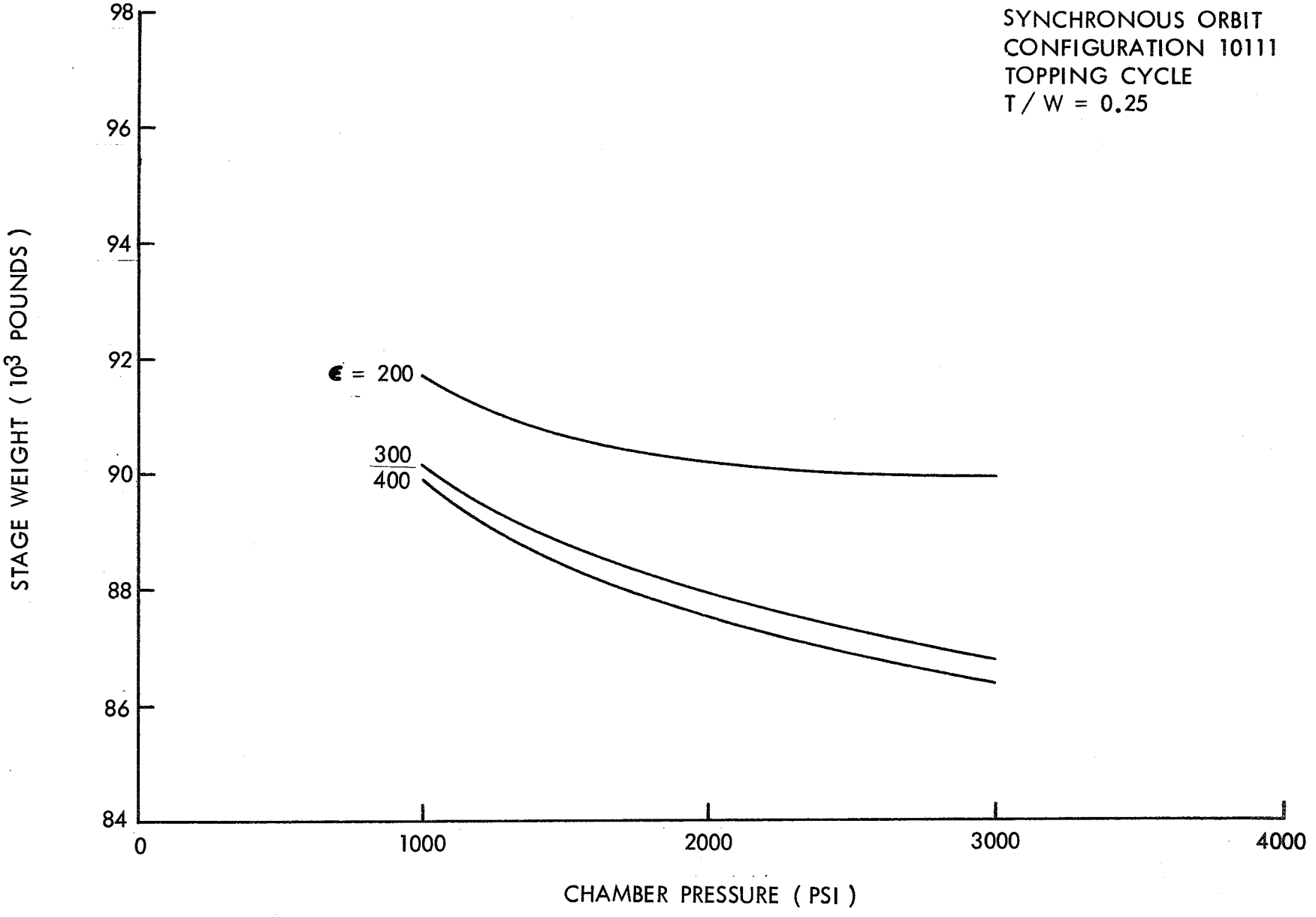

Figure 3- 5 Topping Cycle Chamber Pressure Optimization (T/W = 0.25)

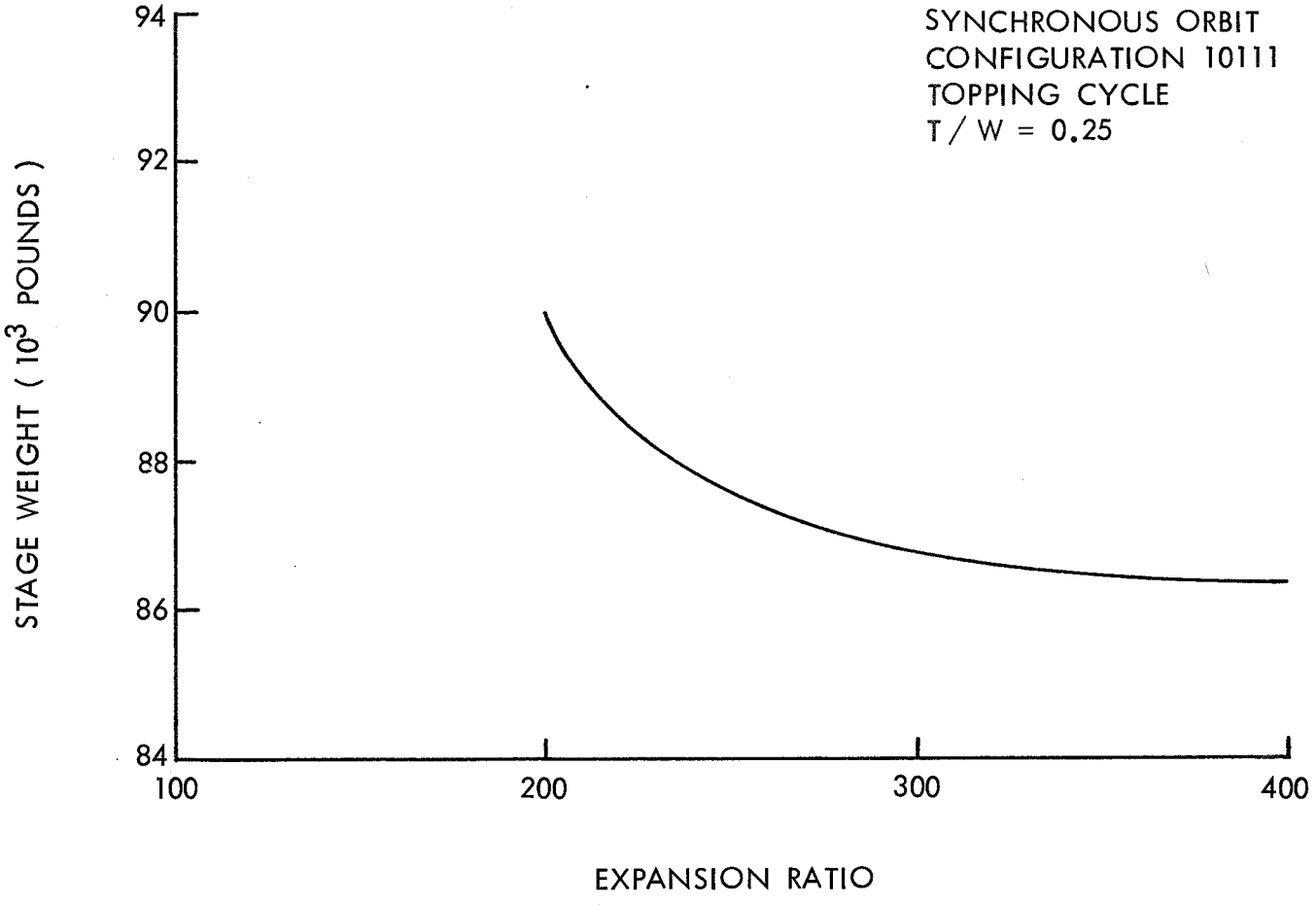

Figure 3- 6 Topping Cycle Expansion Ratio Optimization (T/W = 0.25)

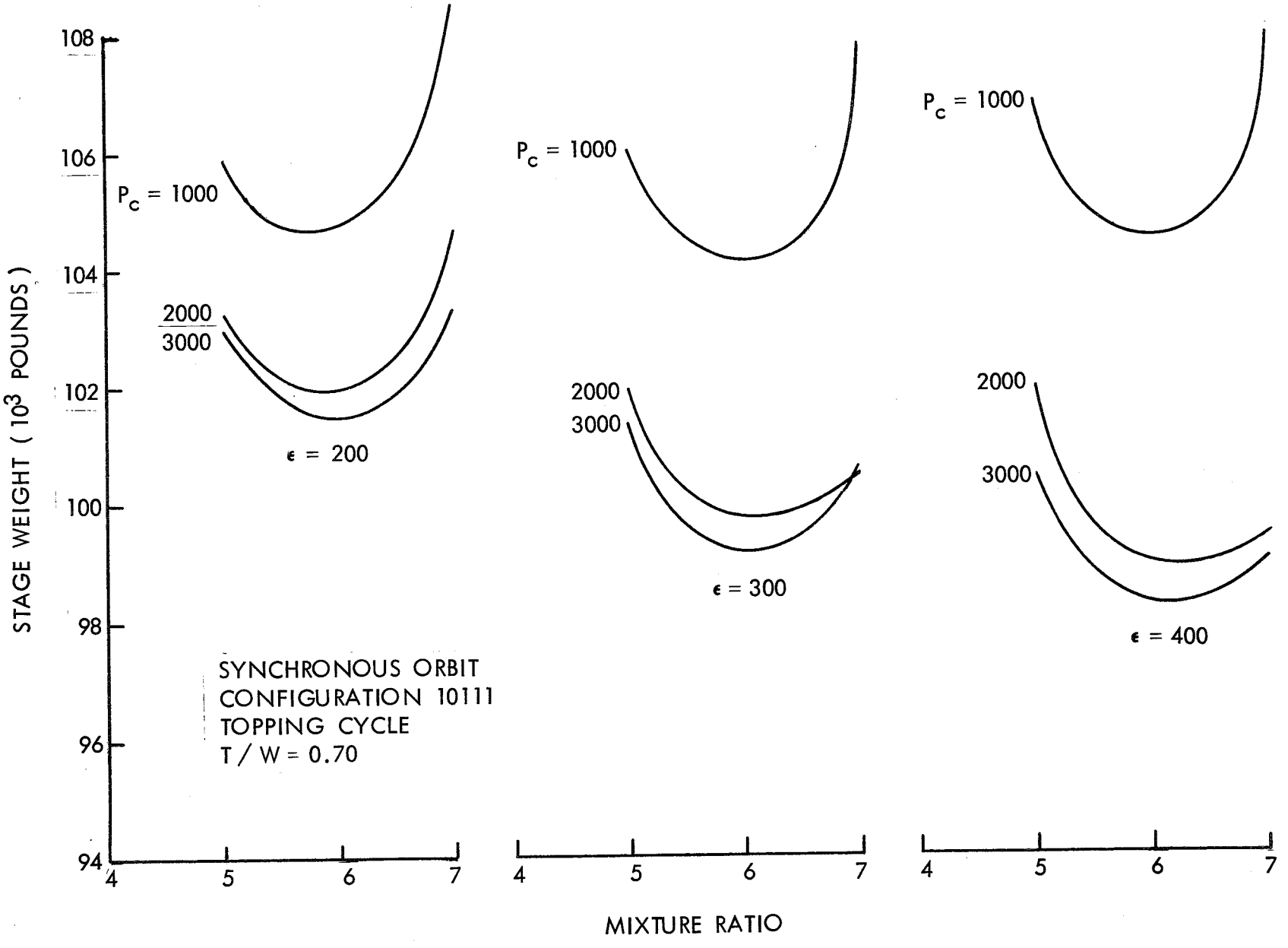

Figure 3- 7 Topping Cycle Engine Parameter Optimization Cycle (T/W = 0.70)

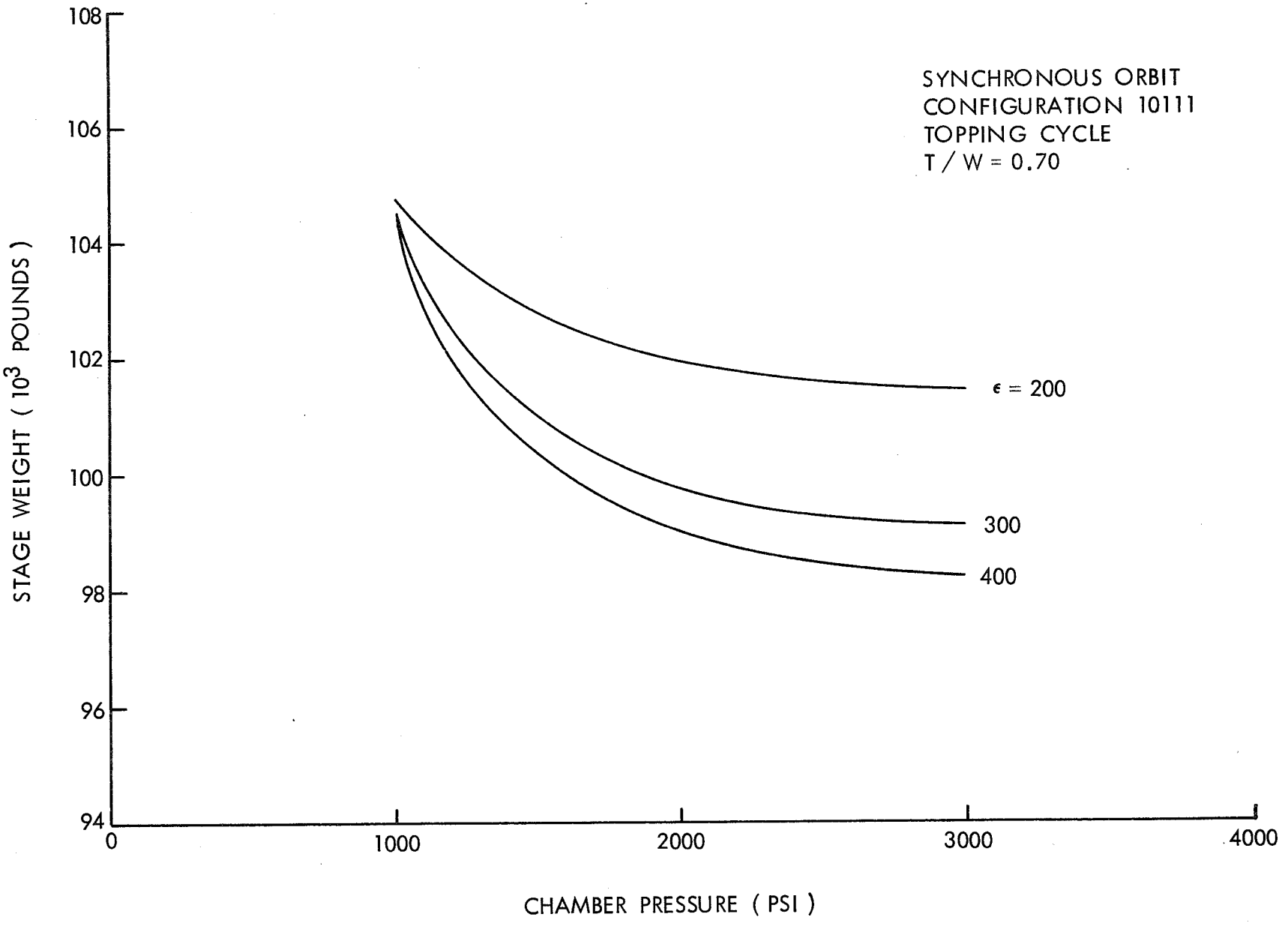

Figure 3- 8 Topping Cycle Chamber Pressure Optimization (T/W = 0.70)

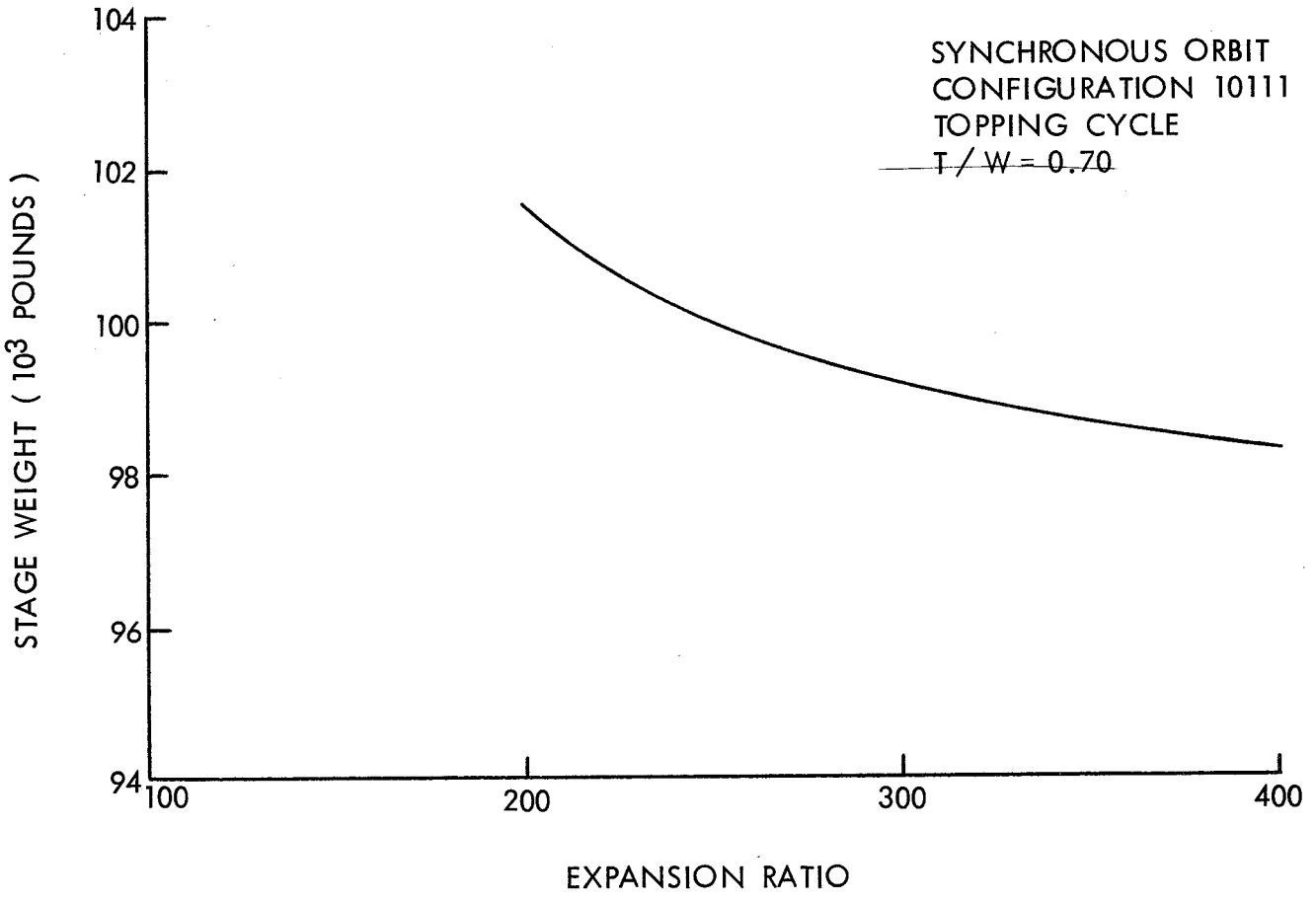

Figure 3- 9 Topping Cycle Expansion Ratio Optimization (T/W = 0.70)

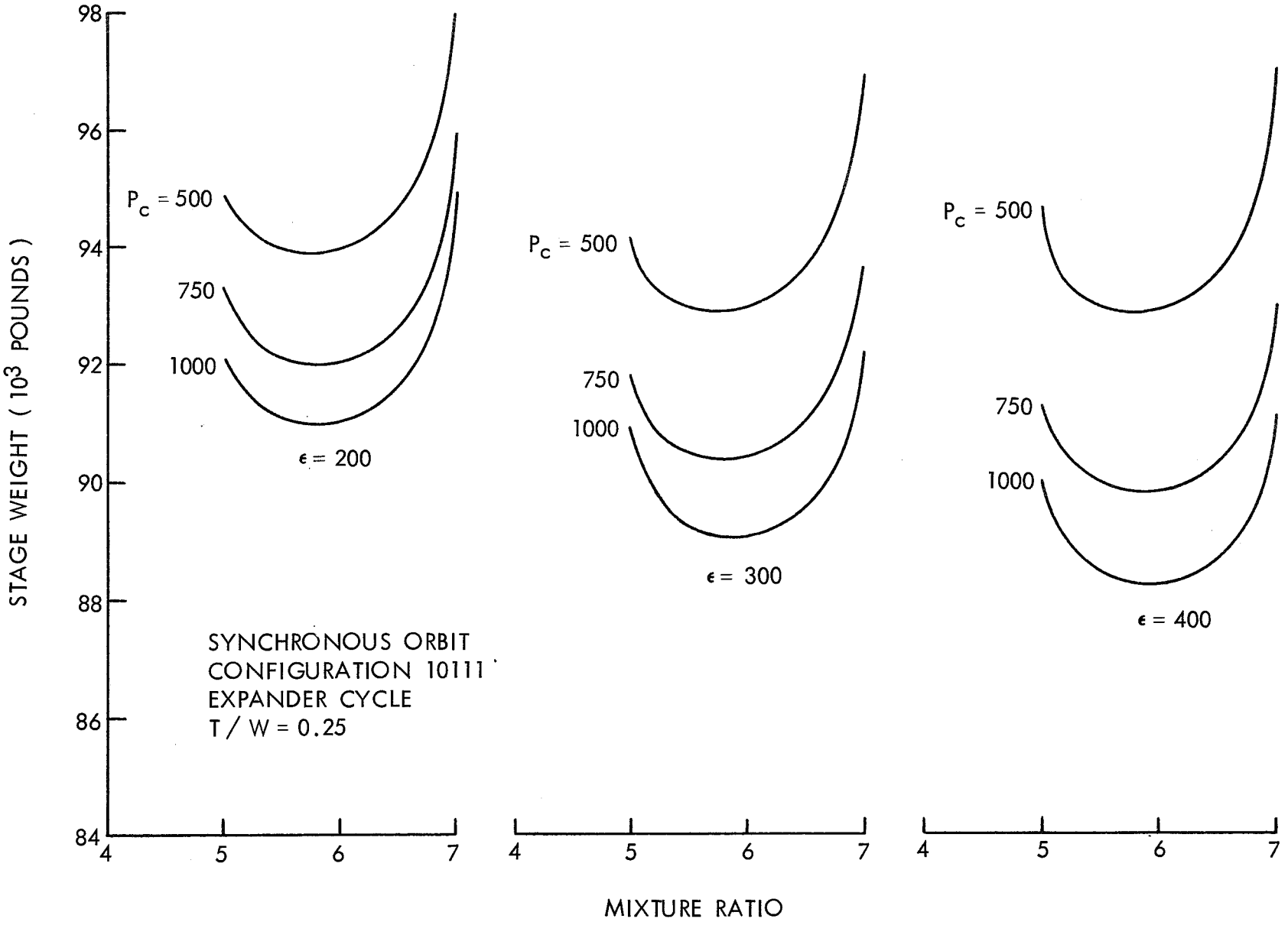

Figure 3-10 Expander Cycle Engine Parameter Optimization Cycle (T/W = 0.25)

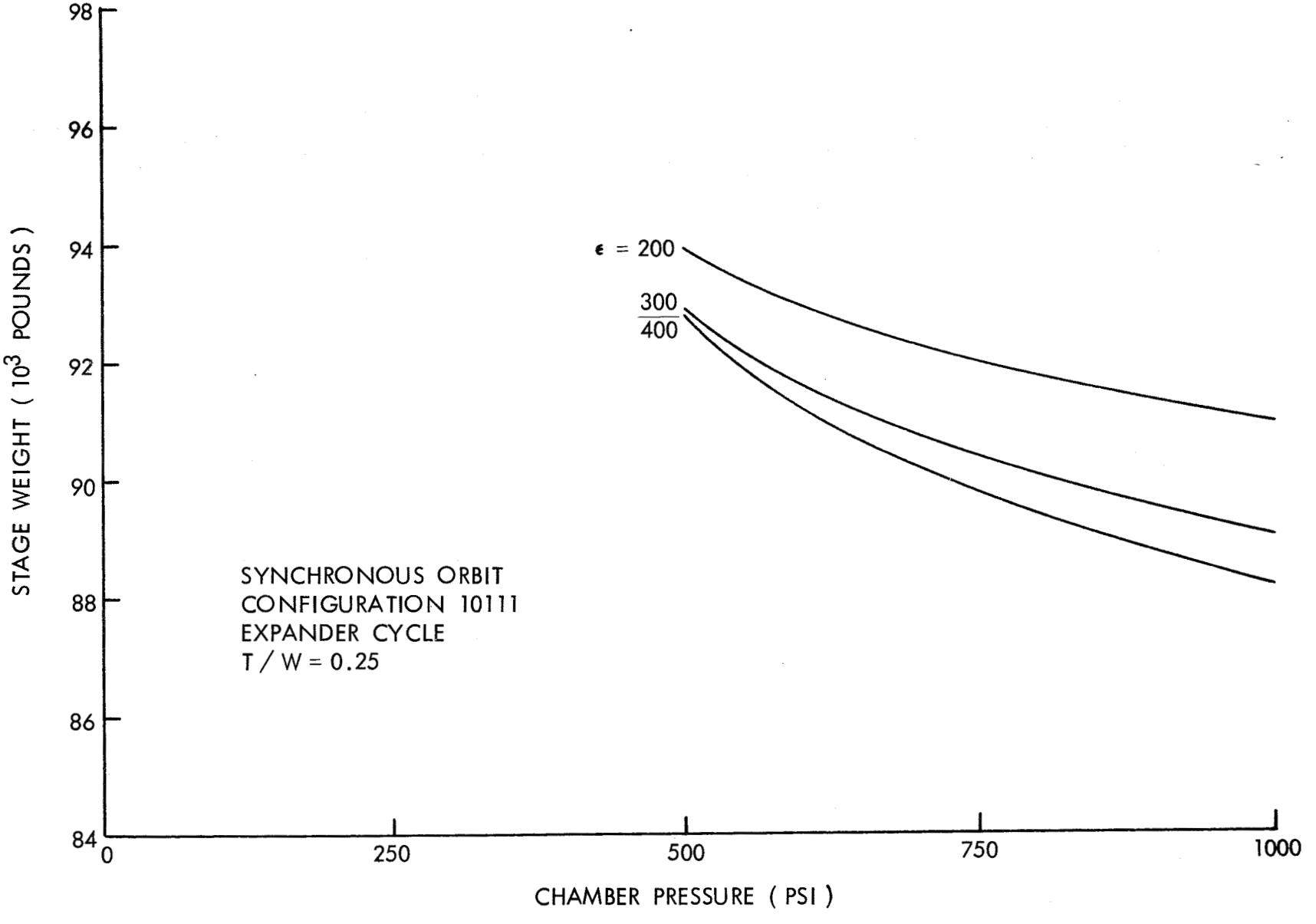

Figure 3-11 Expander Cycle Chamber Pressure Optimization (T/W = 0.25)

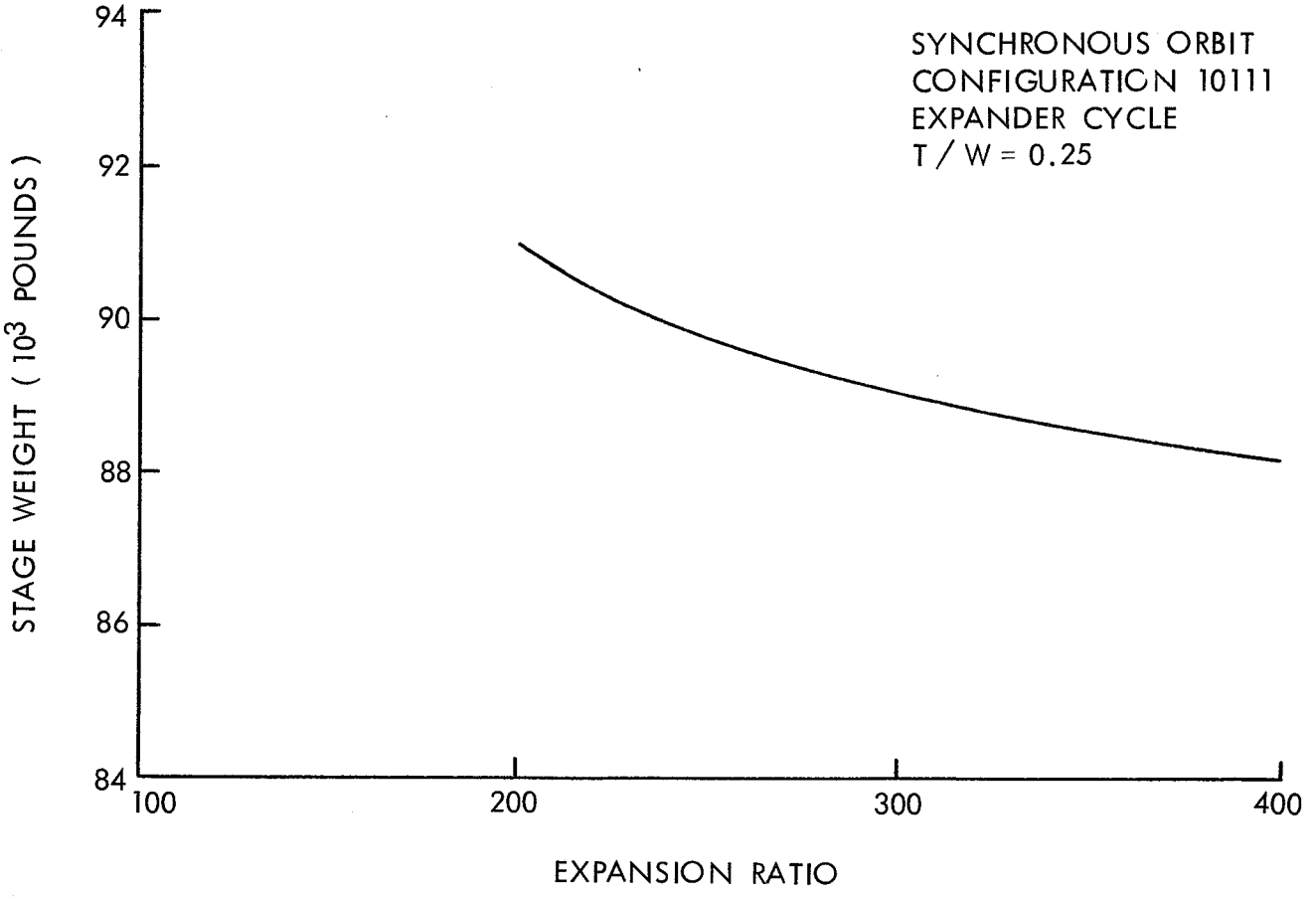

Figure 3-12 Expander Cycle Expansion Ratio Optimization (T/W = 0.25)

3. Velocity loss for escape velocity from 100 n.m. orbit with no plane changes. (Reference impulsive velocity used is 10,590.5 ft/sec).

$$V_{loss} = (Isp/445)^{.25} (Wo/T)^2 \left[76.1 - 50 (Wo/T)^{.1} \right] \text{ fps}$$

Figure 3-13 shows the results of a typical thrust to weight optimization. The optimum thrust to weight ratio occurs between 0.20 to 0.25. Figure 3-14 depicts the variation of propellant fraction, mission velocity and engine weight with the thrust-to-weight ratio. This data shows that the primary driver in determining the optimum thrust-to-weight ratio is the rapid increase in mission velocities which occur for thrust-to-weight ratios less than 0.20.

3.3.4 Single Stage Sizing and Engine Cycle Comparison

The single stage sizing requirements are presented in figure 3-15 as a function of outbound and return payloads, for stages using topping cycle engines. The corresponding propellant ratio for these stages is presented in figure 3-16.

Stages using an expender cycle engine were found to be 2.1 to 2.2% larger than the equivalent stages using the topping cycle engines. Refer to figure 3-17. The lower specific impulse and the larger engine weights (at the selected optimum engine parameters) of the expander cycle engines, result in the relatively higher stage weights. Table 3-4 presents a comparison of some of the major differences between the topping and expander stages having the same payload requirement.

Apart from weight, the expander cycle stage is also 40" longer in overall length. Of this, 38" is due to the difference in engine length. This results from the fact that the expander cycle engine must operate at lower chamber pressures.

It should be noted that the discussions in this and the previous two sections are all based on ideal engines. In specifying optimum parameters, no consideration was given to development risks and costs as they vary according to parameter selection. A review of the slopes of the 'optimization' curves shows that off-optimum penalties are generally small. Thus it may be expected that practicabilities such as engine cost, overall dimensions, availability, development risks, etc. could govern final selections.

3.3.5 Example Stage Weight Statement and Design Characteristic Summary

Table 3-5 presents a weight statement for a stage designed to deliver a zero payload to synchronous orbit and return to low earth orbit with 10,000 lbs. This example stage weighs 87,602 lbs. at liftoff and has a burnout weight of 7,307 lbs. and exhibits a propellant ratio of 0.911. Inert weight and Isp influence coefficients are also given to permit rapid adjustment in stage weight if desired. Table 3-6 summarizes some of the more salient features of this stage. It may be noted that an oxidizer vent occurs during the second and fourth coasts while the fuel does not vent at any time. These oxidizer vents actually occur immediately after the first and third burns while thermodynamic equilibrium is being re-estab-

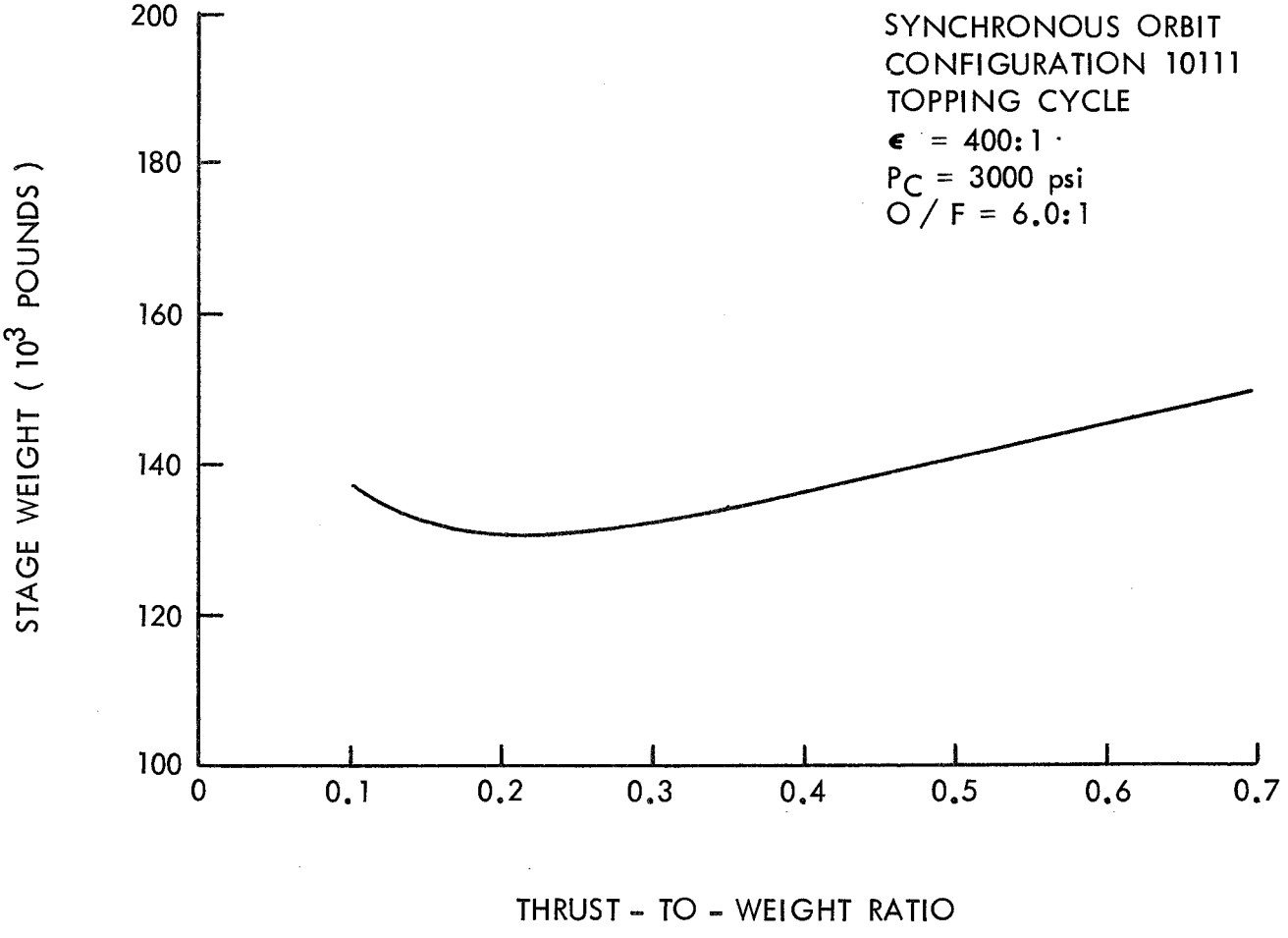

Figure 3-13 Thrust-to-Weight Ratio Optimization for the Synchronous Orbit Missions

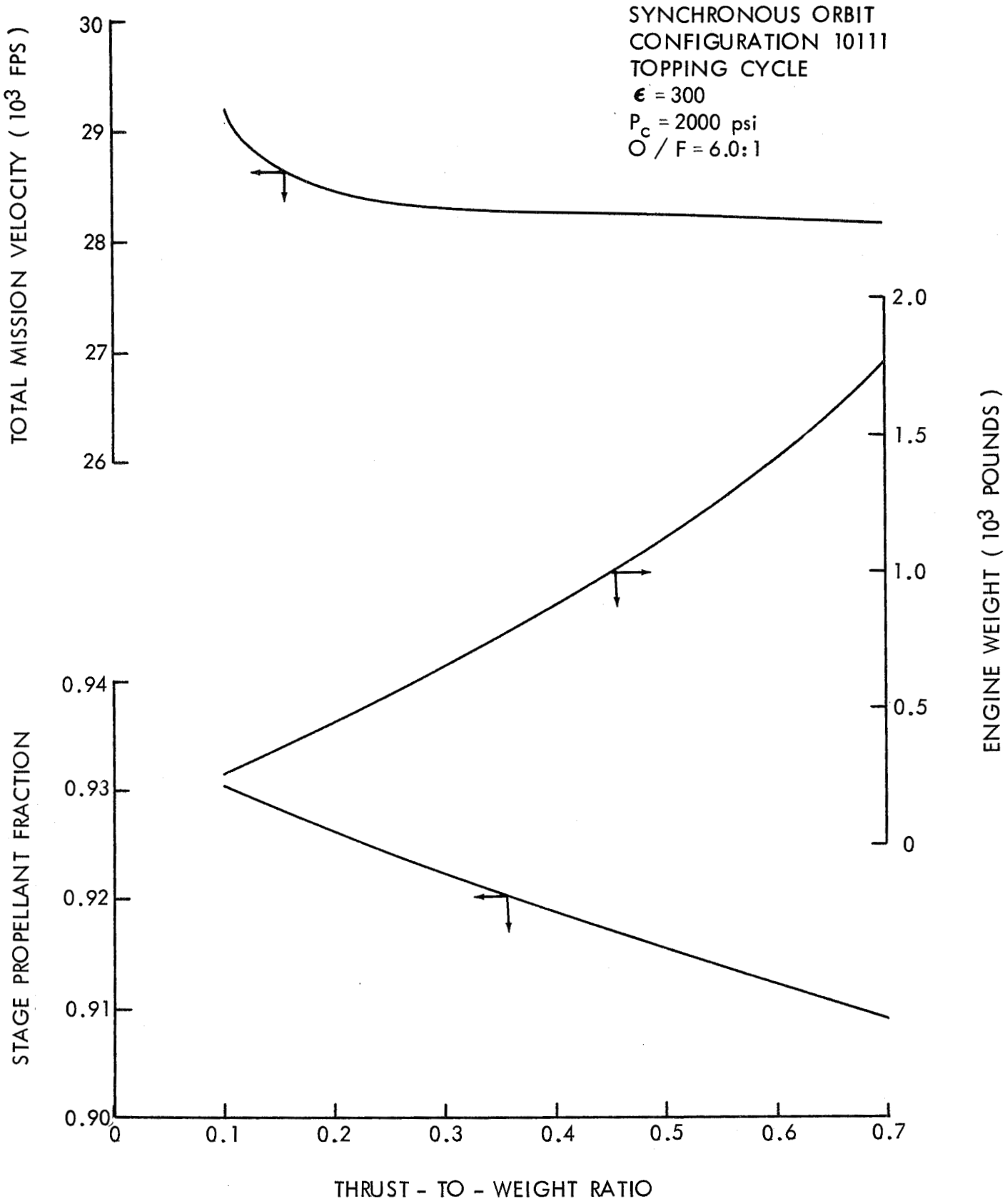

Figure 3-14 Factors Influencing the Thrust-to-Weight Ratio Optimization

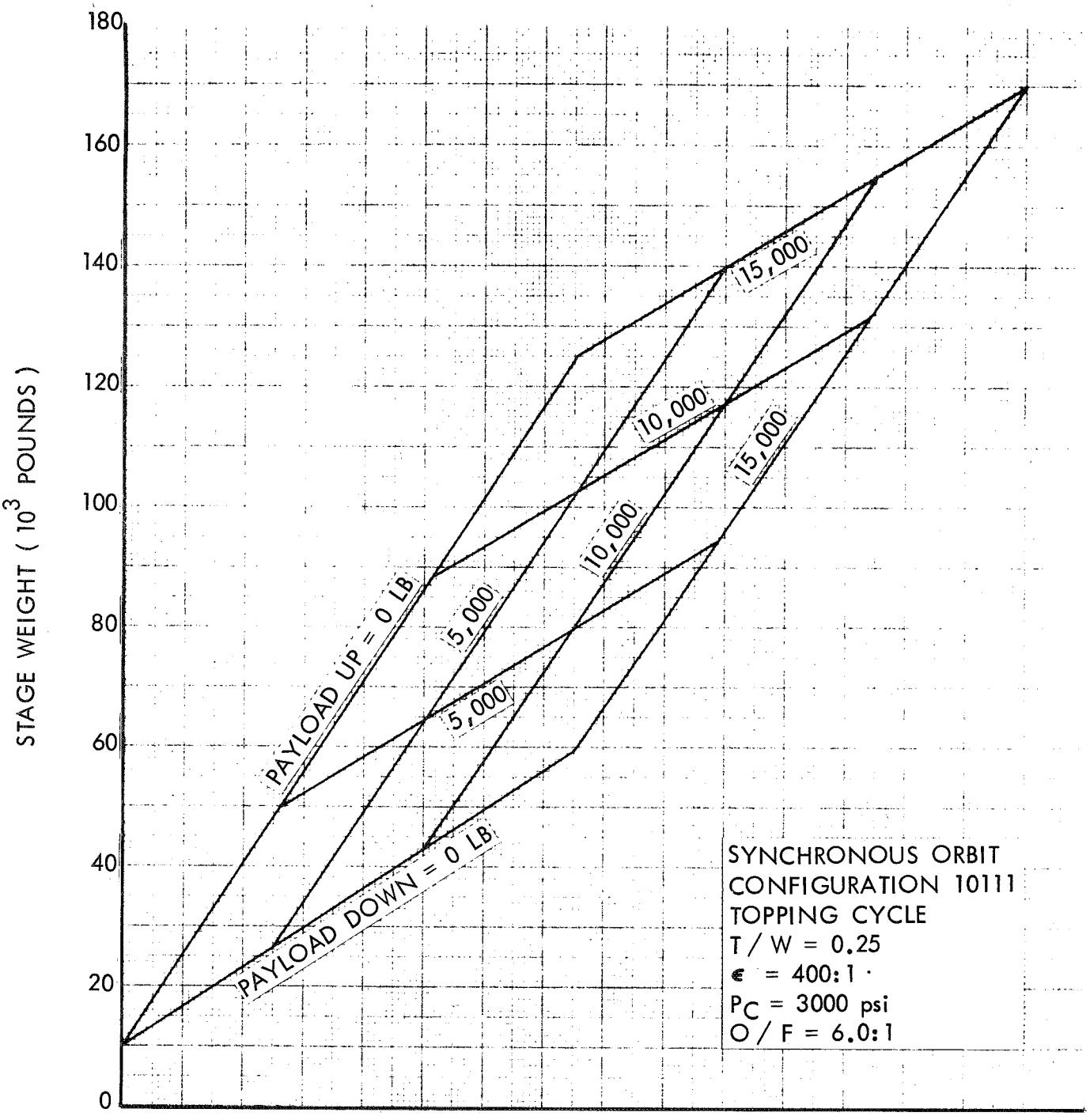

Figure 3-15 Single Stage Sizing Requirements for the Synchronous Orbit Missions

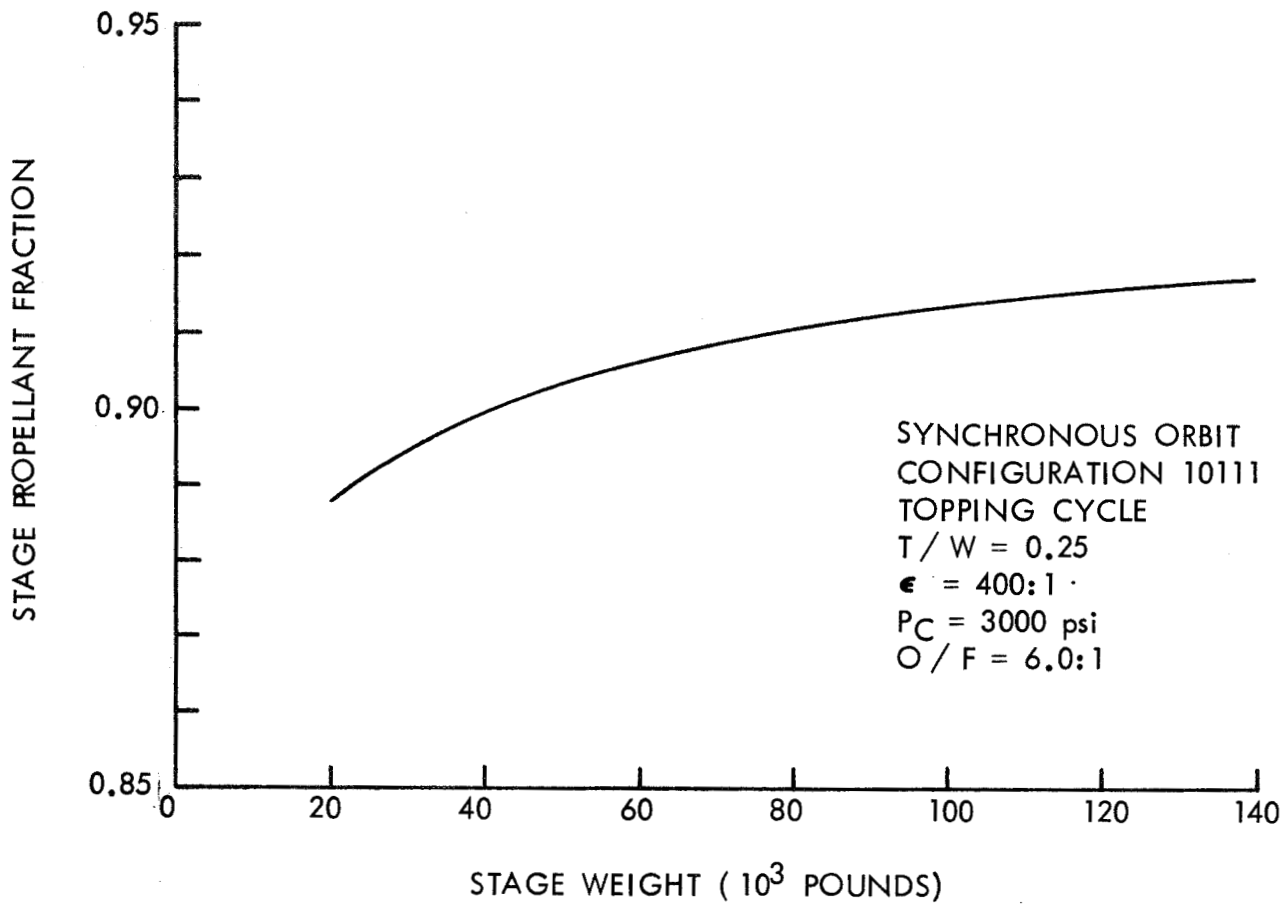

Figure 3-16 Stage Propellant Fraction for the Synchronous Orbit Mission

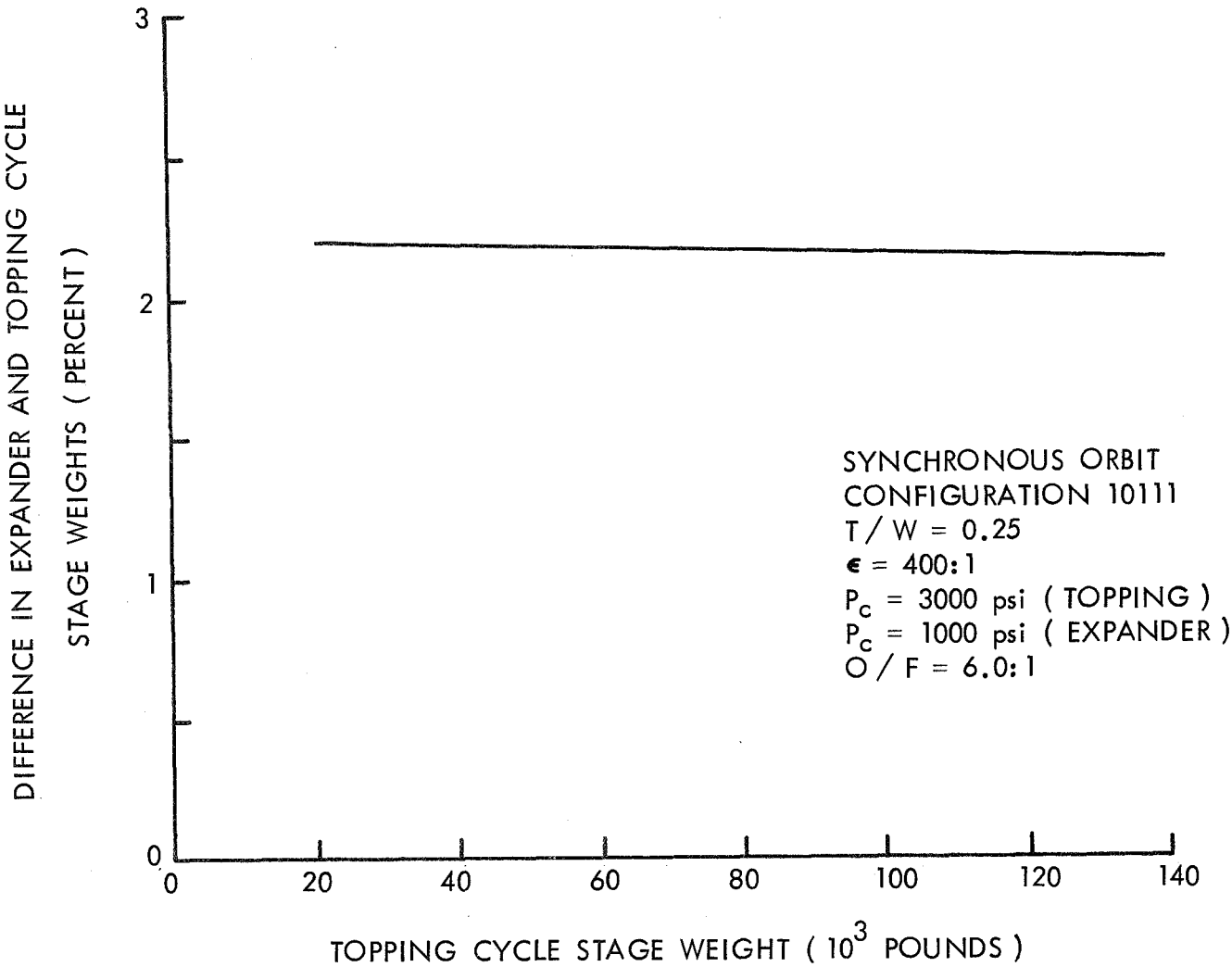

Figure 3-17 A Comparison of Stages Using Topping and Expander Cycles

Table 3- 4 A Comparison of Stages Utilizing Topping and Expander Cycles

CONFIGURATION 10111 (ENGINE CYCLE)	TOPPING	EXPANDER
STAGE WEIGHT (LB)	85990	88248
TOTAL PROPELLANT WEIGHT (LB)	80905	83003
SHELL WEIGHT (LB)	1064	1089
THRUST STRUCTURE WEIGHT (LB)	352	363
ENGINE SYSTEM WEIGHT (LB)	369	421
REACTION CONTROL SYSTEM WEIGHT (LB)	18	19
HYDROGEN SYSTEM WEIGHTS (LB)		
TANKAGE	428	439
INSULATION	79	80
PRESSURIZATION	40	41
FEEDLINES	25	25
TANK SUPPORTS	183	188
OXYGEN SYSTEM WEIGHTS (LB)		
TANKAGE	215	221
INSULATION	6	6
PRESSURIZATION	270	275
FEEDLINES	1041	1068
TANK SUPPORTS		

Table 3- 5 Weight Summary for a Synchronous Mission Stage with a Topping Cycle Engine

STRUCTURE			3449
TANKAGE		632	
Hydrogen	420		
Oxygen	212		
INTERSTAGE		0	
LANDING SYSTEMS		0	
SHELL		1080	
THRUST STRUCTURE		361	
OTHER(TANK SUPPORTS,FEED SYSTEMS)		1376	
METEOROID SHIELD		N/U	
INSULATION			148
FUEL TANK		116	
OXIDIZER TANK		32	
PROPULSION			682
ENGINE		375	
OTHER INERT(RCS,PRESS)		307	
ASTRIONICS			400
MISCELLANEOUS FIXED WEIGHTS			130
CONTINGENCY(@ 7.5 %)			361

PROPELLANT INVENTORY			82398
TOTAL FUEL LOAD		11914	
Useable	11399		
Residual	238		
Vented	0		
Final Ullage	224		
Startup/Shutdown	53		
TOTAL OXIDIZER LOAD		70484	
Useable	68397		
Residual	1410		
Vented	109		
Final Ullage	251		
Startup/Shutdown	317		
PRESSURIZATION & INERT GASES			20
TOTAL LOAD		20	
Vented	6		
Residual	14		
RCS PROPELLANT			14
TOTAL FLUIDS			82432
CONSUMED		80180	
VENTED		115	
RESIDUAL		2137	

BURN OUT WEIGHT	7307
TOTAL STAGE WEIGHT	87602
PROPELLANT FRACTION	0.911

$$\frac{\partial W_{STAGE}}{\partial I_{SP}} = -680 \ (LB / SEC)$$

$$\frac{\partial W_{STAGE}}{\partial W_{INERT}} = 12 \ (LB / LB)$$

Table 3- 6 Design Summary of a Synchronous Mission Stage with a Topping Cycle Engine

COAST AND BURN NUMBER		1	2	3	4
COAST TIME		24	5.3	5.3	24
PAYLOAD		0	0	10000	10000
VELOCITY INCREMENT(TOTAL= 28,346	fps)	8222.2	5950.8	5950.8	8222.2
PROPELLANT BURNED		36543	16458	14339	12456
FUEL VENT(incl. Press/Inert Gases)		0	0	0	0
OXID. VENT(incl. Press/Inert Gases)		0	73	0	42

ENGINE CHARACTERISTICS	
Thrust	21903
Specific Impulse	473.3
Area Ratio	400:1
Mixture Ratio	6.0:1
Chamber Pressure	3000

TANKAGE	FUEL	OXIDIZER
Vent Pressure	24.0	21.0
Design Pressure	26.4	30.5
Insulation Thickness	0.32	0.17
Additional Meteoroid Shield Thickness		
Bumper	N/U	N/U
Backup Wall	N/U	N/U
Volume	2815.9	1042.0

STAGE GEOMETRY	
Overall Length	532.8
Maximum Diameter	243.0
Stage L/D	2.19

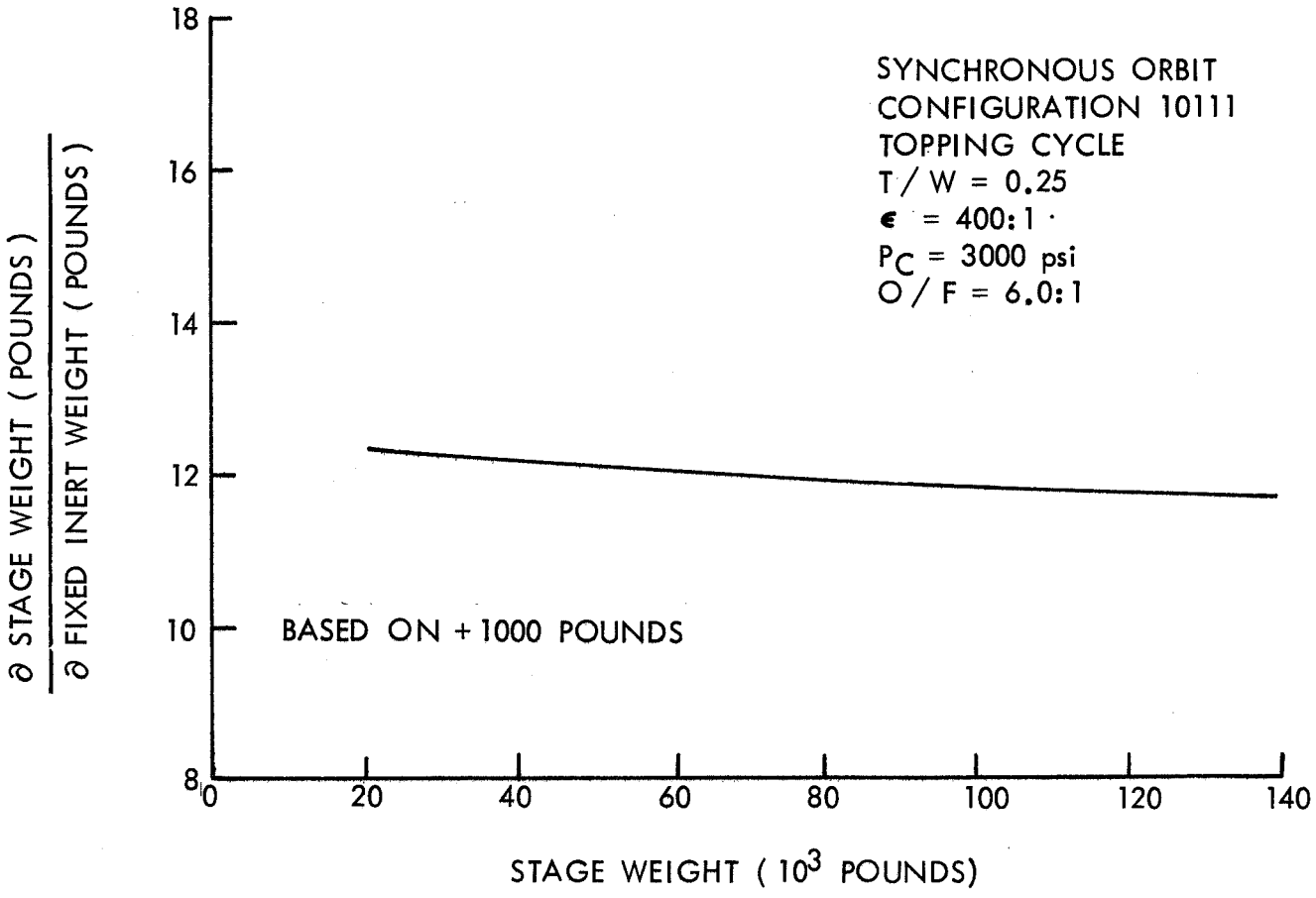

Figure 3-18 Sensitivity of Stage Size to Fixed Inert Weight

lished between the liquid and vapor states of the propellant. They result because it was necessary to 'lock up' the tank during each burn, at a pressure higher than the vent pressure, in order to satisfy the engine's NPSH requirement. Immediately after these burns, when the tank is 'restored' to the normal coast mode, a vent occurs. If pressurization had been accomplished with gaseous oxygen (GOX) instead of helium, these vents probably would not have occurred; nor would there have been as large a disparity between the vent pressure (21 psia) and the tank design pressure (30.5 psia).

3.3.6 Sensitivity Studies

3.3.6.1 General

Sensitivity studies were undertaken to show the influence of key parameters on stage design requirements. These results, which are presented in the following subparagraphs apply specifically to the synchronous orbit mission; however, they may be subjectively applied to other missions. They are intended not only to be used as a tool for sizing adjustments, but as an aid in the planning of resource allocations. For example, if a cost partial (dollars per pound of stage weight) can be developed for a stage, then the cost effectiveness of improving a technology, such as an increase in Isp efficiency, can be quantitatively assessed. That is, the cost of improving the technology can be weighed against the potential dollar savings in stage cost. These influence coefficients can also be used in future study task planning, to maximize the useful information return.

3.3.6.2 Fixed Inert Weights

Fixed inert weight, as used herein, referes to those inert weights (e.g., astrionics) which are presume to be invariant with stage size. Figure 3-18 presents the partial of stage weight with respect to fixed inert weight as a function of stage size. This partial varies from 11.2 to 12.5 pounds of stage weight per pound fixed inert weight over the range of stage weights investigated.

To illustrate how an increase in inert weight affects the total stage weight, the following example has been prepared:

> Consider a 1,000 lb.increase in the fixed inert weight of an 80,000 lb. stage. This would increase the stage weight by 12,000 lbs. including the original 1,000 lb. increase in inert weight. Of this 12,000 lb. increase about 84%, or 10,000 lbs., is usable propellant. Another 13%, or 1,600 lbs. is attributable to inert weight increases and the remaining 3%, or 400 lbs. results from increases in residual propellants and other fluids. The 13% increase in inert weight can be further broken down as follows:

SYSTEM AFFECTED	PERCENTAGE
ORIGINAL 1000 LB INCREASE	63
TANKAGE	16
TANK SUPPORTS	9
SHELL	6
THRUST STRUCTURE	3
ENGINE SYSTEMS	2
OTHER SUBSYSTEMS	1

3.3.6.3 Isp Efficiency

Figure 3-19 shows the effect a change in specific impulse efficiency would have on stage weight. To partially account for the non-linearity of this function, a separate curve is given for both an increase and a decrease in efficiency. Both curves are based on perturbing the Isp efficiency by 2% to generate the partial. As expected, this data indicates that a decrease in efficiency is relatively more costly than an increase is on savings.

3.3.6.4 Engine Weights

An analysis was performed to show the influence that engine weight has on stage size. This differs from the inert weight sensitivity in that changes in engine weight introduce additional second order effects; that is, a reduction in engine weight results in a smaller stage which requires in turn a smaller engine and again a lighter stage - hence the cycle continues. Figure 3-20 shows the influence of engine weight as a function of stage weight. The results show that there is little to be gained by attempting to lower the engine weights by small amounts.

3.3.6.5 Number of Engines

While a stage with a single engine will almost always be lighter than one with multiple engines, other criteria (such as, engine availability, engine out capability) may dictate the selection of two or more engines. Figure 3-21 depicts the influence that two and four engines have on stage weight. Depending on the size of the stage this effect can vary from less than 1% to over 10%. The larger sensitivity of the smaller stages can be attributed to the fact that for the smaller stages, a given change in inert (engine) weight represents a greater percent of the total stage weight. Table 3-7 was prepared to illustrate the manner in which an increase in the number of engines affects stage design for the same payload requirement. From this table it is evident that the largest increase occurs in the engine systems weights.

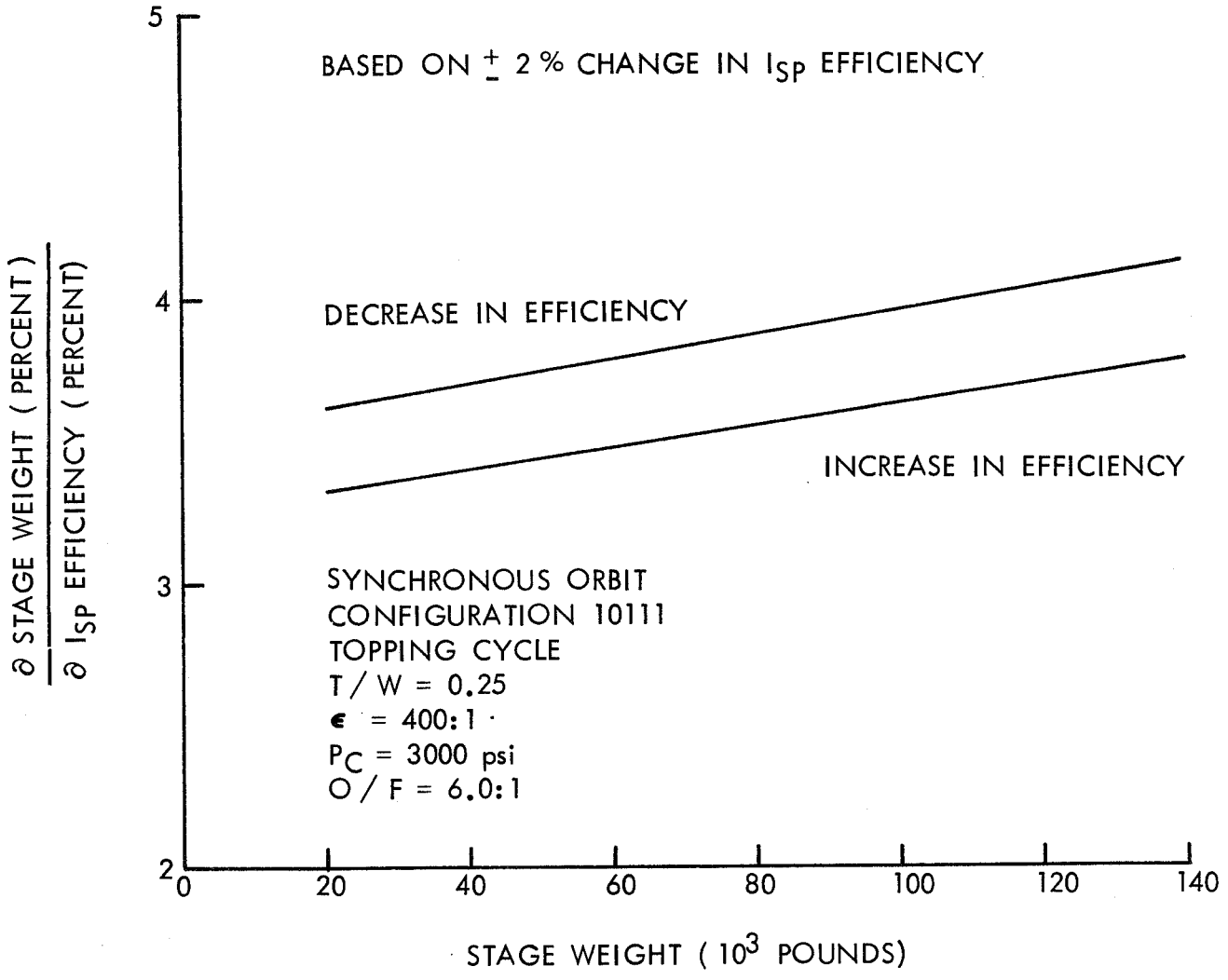

Figure 3-19 Sensitivity of Stage Size to Specific Impulse Efficiency

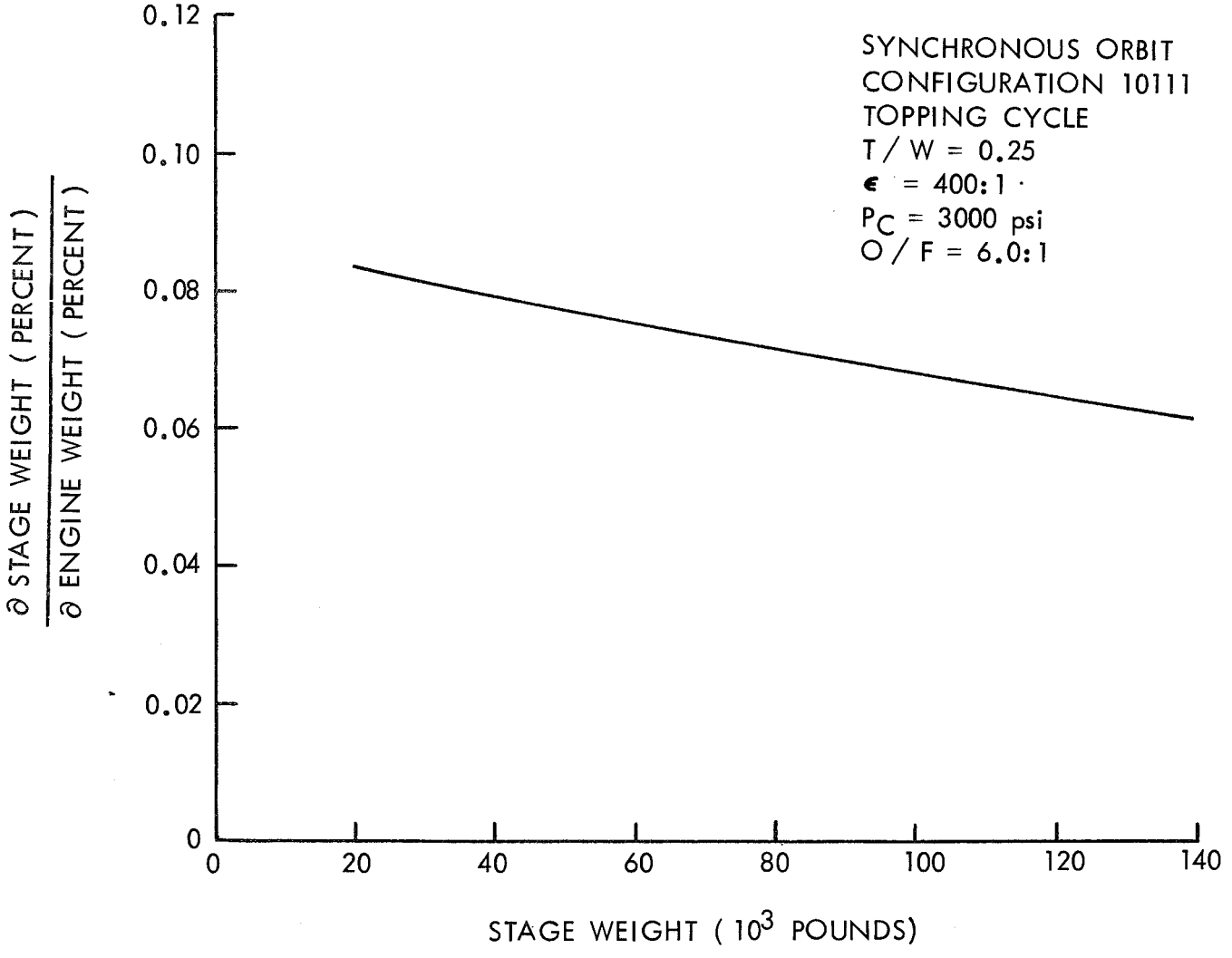

Figure 3-20 Sensitivity of Stage Size to Engine Weight

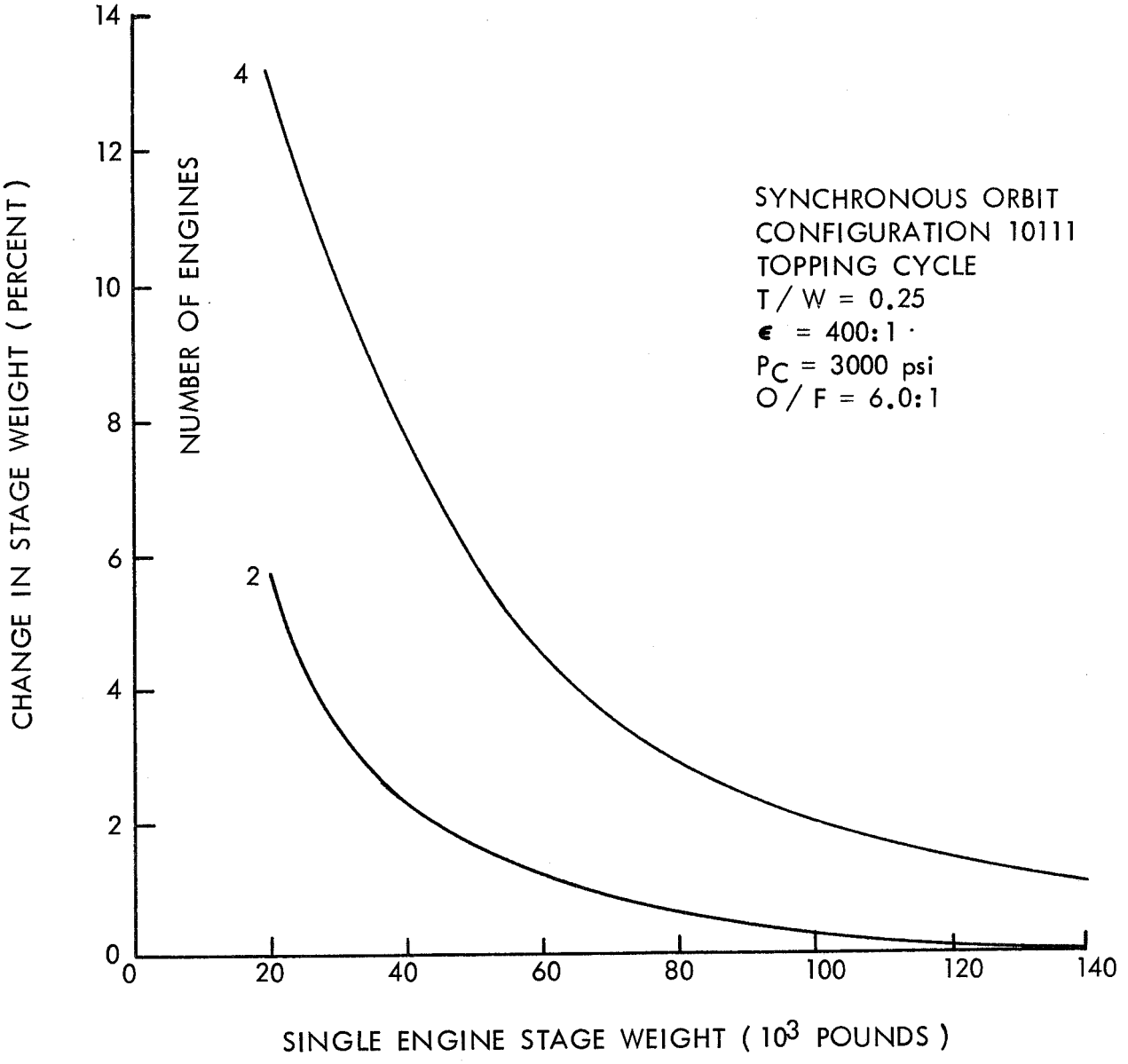

Figure 3-21 The Influence of Multiple Engines on Stage Size

Table 3- 7 A Comparison of Stages Having One, Two and Four Engines

NUMBER OF ENGINES	1	2	4
TOTAL STAGE THRUST (LB)	18241	18387	18903
STAGE WEIGHT (LB)	67966	68547	70612
PROPELLANT FRACTION	0.909	0.908	0.906
TOTAL PROPELLANT WEIGHT (LB)	63813	64320	66115
SHELL WEIGHT (LB)	802	805	821
THRUST STRUCTURE WEIGHT (LB)	283	289	294
TOTAL ENGINE WEIGHT (LB)	300	345	531
TANKAGE WEIGHT (LB)	533	537	550
THERMAL PROTECTION WEIGHT (LB)	73	73	74
PRESSURIZATION SYSTEM WEIGHT (LB)	240	240	240
FEEDLINE WEIGHT (LB)	121	121	123
TANK SUPPORT WEIGHT (LB)	966	973	1001

3.3.6.6 Configuration Selection

The stage geometry which was selected as a baseline to perform the majority of the analyses was the tandem tank configuration (10111). Refer to Section 2.2.2 for description of the various geometries which can be considered. The 10111 configuration was selected primarily as a matter of convenience since it was felt that the structural factors (monocoque/ complex structure weight ratios) were more accurate for this configuration than for the others.

To better understand the influence of tankage arrangement, and the type and location of the thrust structure, stages were sized for 19 additional configurations. A weight, length and diameter comparison of these stages if presented in table 3-8. Additional, more detailed comparisons of **six** of these are given in table 3-9.

Since the structural factors for the various configurations were not known to the same degree of accuracy, the exact weight difference between any two configurations cannot be stated with confidence. However, certain trends which are evident, can be used with confidence. In general, the configurations which look best from a performance standpoint are those which have multiple LOX tanks suspended below the thrust cone (i.e., 20111, 30111, and 40111). The reason that these geometries look more attractive, is that

Table 3- 8 A Summary of the Effects of Stage Configurations on Stage Size

CONFIGURATION	TANKAGE		TYPE OF T / S	STAGE WEIGHT	STAGE LENGTH	STAGE DIAMETER	Δ WEIGHT	Δ LENGTH	Δ DIAMETER
	FUEL	OXID							
10111	1S	1S	T / C	85990	520	241	0	0	0
20111	1S	2S	T / C	80586	346	223	-5404	-174	-18
20211	1S	2S	S / B	88394	457	229	+2404	-63	-12
20311	1S	2S	S / B	84870	373	226	-1120	-147	-15
20411	1S	2S	S / B	87000	346	228	+1010	-174	-13
30111	1S	3S	T / C	81203	347	223	-4787	-173	-18
30211	1S	3S	S / B	87681	427	228	+1691	-93	-13
30311	1S	3S	S / B	84647	354	226	-1343	-166	-15
30411	1S	3S	S / B	85038	357	226	-952	-163	-15
40111	1S	4S	T / C	81898	348	224	-4092	-172	-17
40211	1S	4S	S / B	87773	418	228	+1783	-102	-13
40311	1S	4S	S / B	85013	348	226	-977	-172	-15
40411	1S	4S	S / B	84286	331	226	-1704	-189	-15
50211	2S	2S	S / B	86618	358	258	+628	-162	+17
50311	2S	2S	S / B	83624	279	258	-2366	-241	+17
50411	2S	2S	S / B	87575	368	258	+1585	-152	+17
10122	1E	1E	T / C	89933	494	256	+3943	-260	+15
20121	1E	2S	T / C	84403	287	251	-1587	-233	+10
30221	1E	3S	S / B	91978	410	257	+5988	-110	+16
40312	1S	4E	S / B	84982	346	226	-1008	-174	-15

S = TANKS WITH SPHERICAL BULKHEADS, E = TANKS WITH ELLIPITICAL BULKHEADS
T / C = THRUST CONE TYPE THRUST STRUCTURE, S / B = SPIDER BEAM TYPE THRUST STRUCTURE

Table 3- 9 A Detailed Comparison of Selected Stage Configurations

CONFIGURATION	10111	20111	30111	30311	40111	40411	50311
STAGE WEIGHT (LB)	85990	80586	81203	84647	81898	84286	83624
TOTAL PROPELLANT WEIGHT (LB)	80905	76238	76768	79746	77898	79435	78862
SHELL WEIGHT (LB)	1064	563	568	1021	570	929	829
THRUST STRUCTURE WEIGHT (LB)	352	290	291	227	293	226	346
ENGINE SYSTEM WEIGHT (LB)	369	347	350	363	353	362	360
REACTION CONTROL SYSTEM WEIGHT (LB)	18	13	13	14	14	14	15
HYDROGEN SYSTEM WEIGHTS (LB)							
TANKAGE	428	403	406	421	409	420	607
INSULATION	79	76	76	78	76	78	135
PRESSURIZATION	40	39	39	39	39	39	55
FEEDLINES	25	23	24	26	24	16	86
TANK SUPPORTS	183	115	116	120	117	120	121
OXYGEN SYSTEM WEIGHTS (LB)							
TANKAGE	215	282	307	317	334	341	333
INSULATION	6	7	8	8	9	9	8
PRESSURIZATION	270	289	313	313	334	334	289
FEEDLINES	113	85	94	55	112	73	59
TANK SUPPORTS	1041	982	990	1028	1000	1024	678

shell size (and hence weight) is decreased since it no longer must enclose the LOX tanks (see figure 3-22). This decrease in shell weight more than offsets the increase in weight associated with tankage, pressurization and tank supports. (Note: Tank supports for the multiple LOX tank configurations may prove to be somewhat low, thus some of the 4,000 to 5,500 lb. weight savings may disappear upon further analysis).

These results apply to the relatively short duration synchronous orbit mission. For missions where meteoroid shielding is required, it may be possible to use the shell as both a load bearing structure and a meteoroid bumper. In these instances there is little or no advantage in eliminating any of the shell, since a meteoroid bumper would be needed on those tanks not enclosed by the shell.

Although it might be suspected that the use of elliptical tank domes would produce smaller stages, stages designed with elliptical bulkheads prove to be heavier (refer to table 3-10). The reason is, that in order for the tanks to contain the same volume, the tank's diameter must be enlarged or if constrained, the cylindrical section's length must be added or increased. This results in larger, heavier shells and thrust structures as well as heavier tank domes.

3.3.6.7 Diameter Constraint

Since the stages evaluated in this study might interface with the Earth Orbit Shuttle (EOS), an investigation was made to determine what influence a diameter constraint would have on the design of an Orbit to Orbit Shuttle (OOS) stage. Figure 3-23 presents the percent change in OOS stage weight as a function of stage size for diameter constraints of 120 and 180 inches. It is evident that a 120 inch restriction would severely penalize the OOS, regardless of stage size, while a 180 inch diameter would penalize only the very large stages. Figure 3-24 shows how diameter constraints affect stage length. Here the effect of the constraint is more demonstrable. (Note: The sharp drop off in the 180 inch diameter curve at approximately 60,000 pounds is due to a change from a frustum type shell to a frustrum cylinder shell geometry. This switch is internal to the computer program and results from the diameter of the hydrogen tank approaching its maximum allowable value.) In figure 3-23 it is seen that a diameter constraint affects a stage weight only for stages above a given size, hereinafter referred to as the 'break point'. Figure 3-25 shows how this break point varies with stage weight.

For reference purposes, figures 3-26 and 3-27, present maximum unconstrained stage diameter and length, and L/D respectively, as a function of stage weight. It is interesting that the unconstrained stage length-to-diameter ratio (L/D) remains fairly close to a value of 2.5 over a wide range of stage weights. (Note: The preceding analyses were based on topping cycle engines. However, had an expander cycle engine been used, the primary effect would be seen in stage length).

3.3.6.8 Orbital Inclination

The baseline orbital inclination for the 100 n.m. low earth orbit was 28 1/2°. Figure 3-28 depicts the effect that a change to a 55° inclination orbit would have on the results. In general, size of the stages

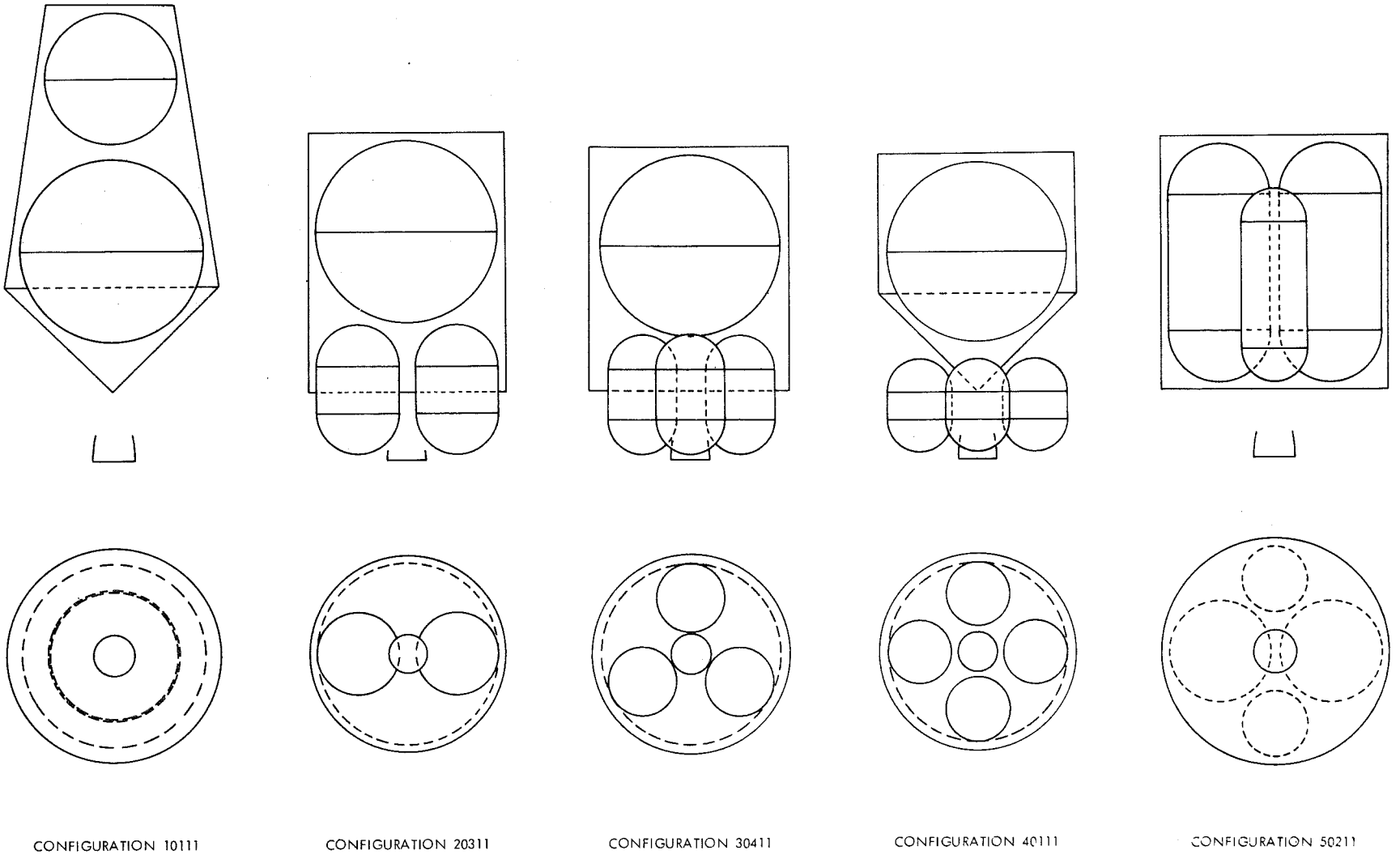

Figure 3-22. Several of the Stage Configurations Investigated

Table 3-10 Comparison of Hemispherical and Elliptical Bulkheads on a Tandem Tank Stage

CONFIGURATION	10111	10122
STAGE WEIGHT (LB)	85990	89933
TOTAL PROPELLANT WEIGHT (LB)	80905	84313
SHELL WEIGHT (LB)	1064	1044
THRUST STRUCTURE WEIGHT (LB)	352	406
ENGINE SYSTEM WEIGHT (LB)	369	384
REACTION CONTROL SYSTEM WEIGHT (LB)	18	19
HYDROGEN SYSTEM WEIGHTS (LB)		
TANKAGE	428	710
INSULATION	79	82
PRESSURIZATION	40	40
FEEDLINES	25	18
TANK SUPPORTS	183	195
OXYGEN SYSTEM WEIGHTS (LB)		
TANKAGE	215	329
INSULATION	6	6
PRESSURIZATION	270	270
FEEDLINES	113	110
TANK SUPPORTS	1041	1087

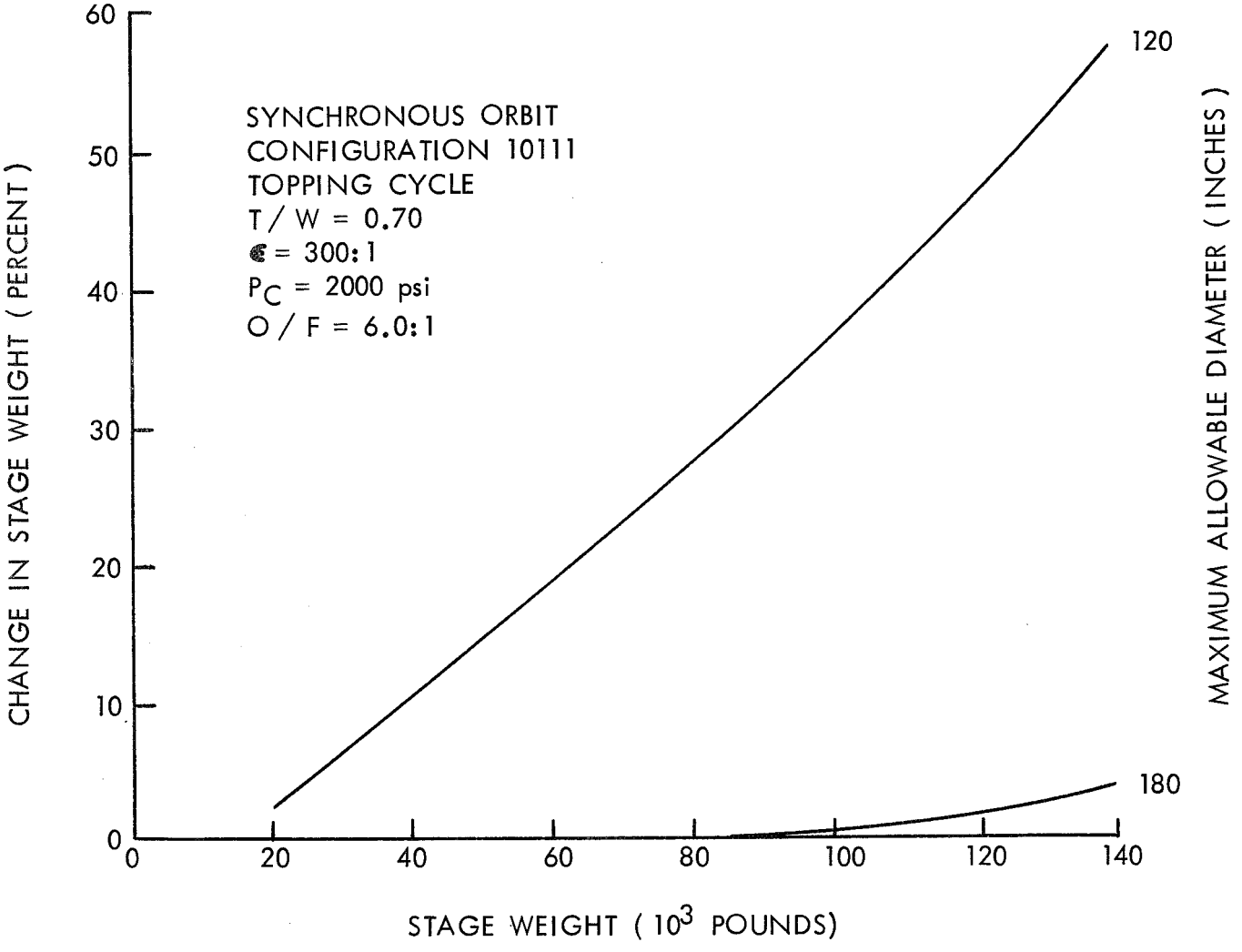

Figure 3-23 The Effect of Constraining Stage Diameter on Stage Weight

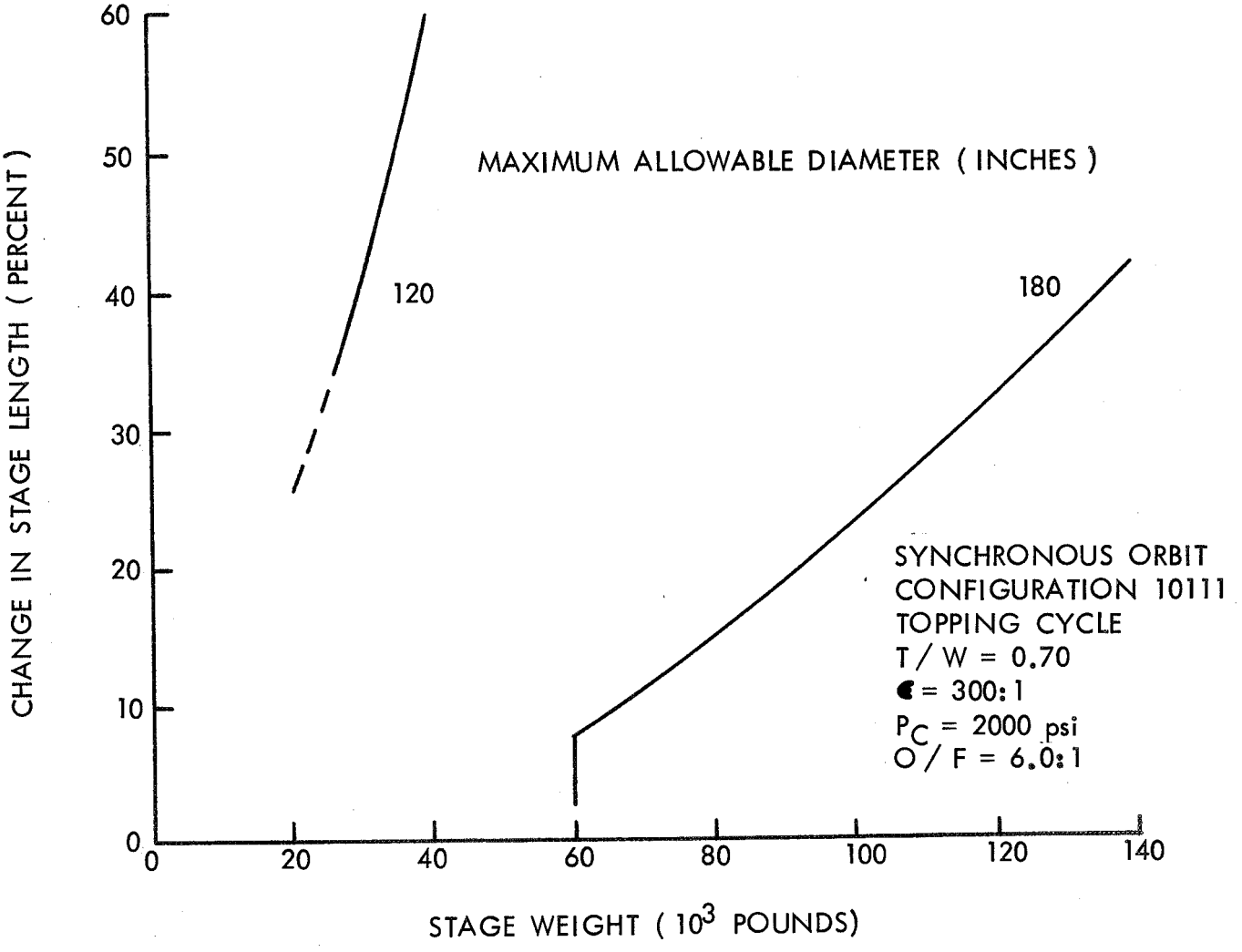

Figure 3-24 The Effect of Constraining Stage Diameter on Stage Length

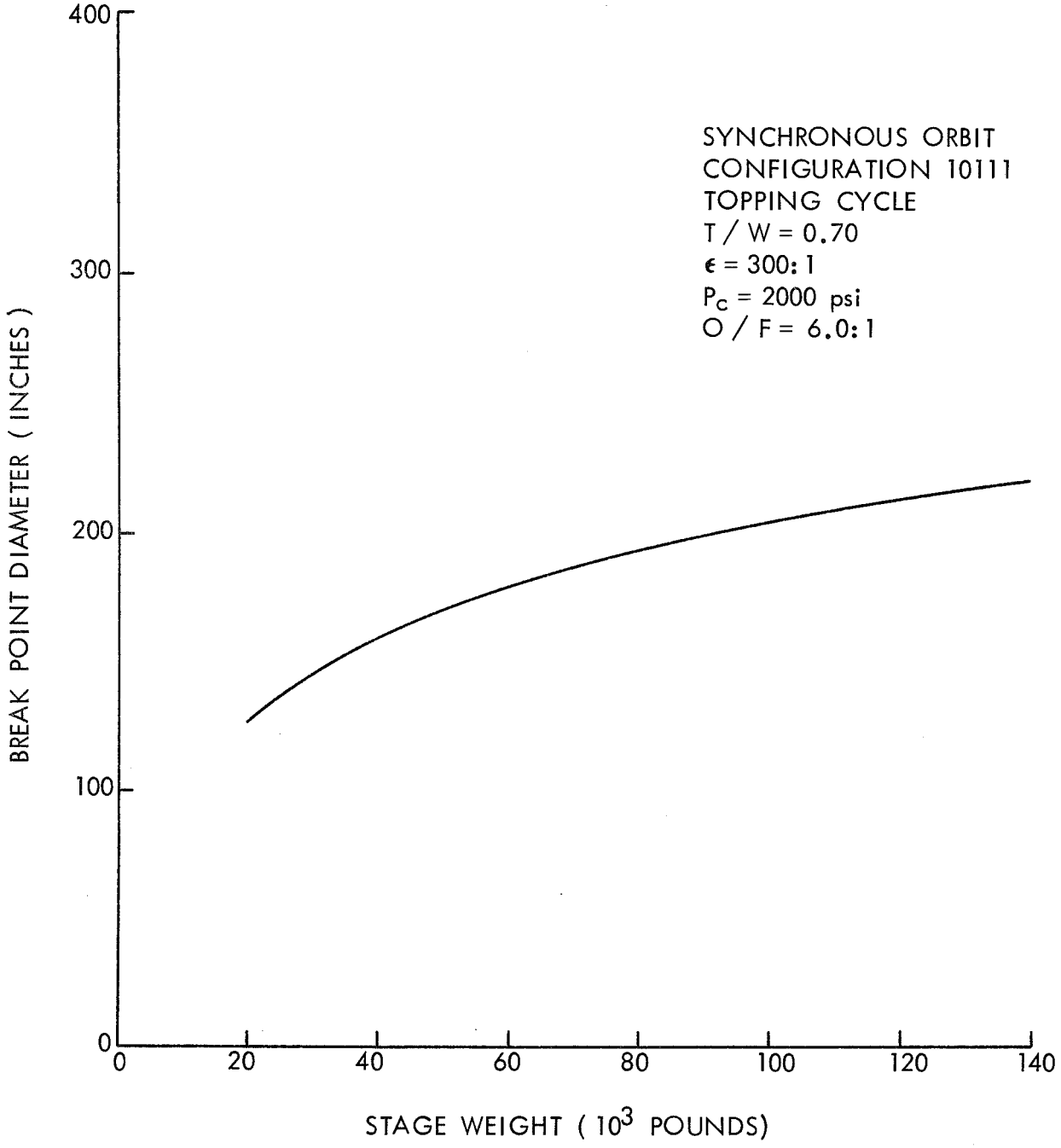

Figure 3-25 The "Break-Point" Diameter of Various Size Stages

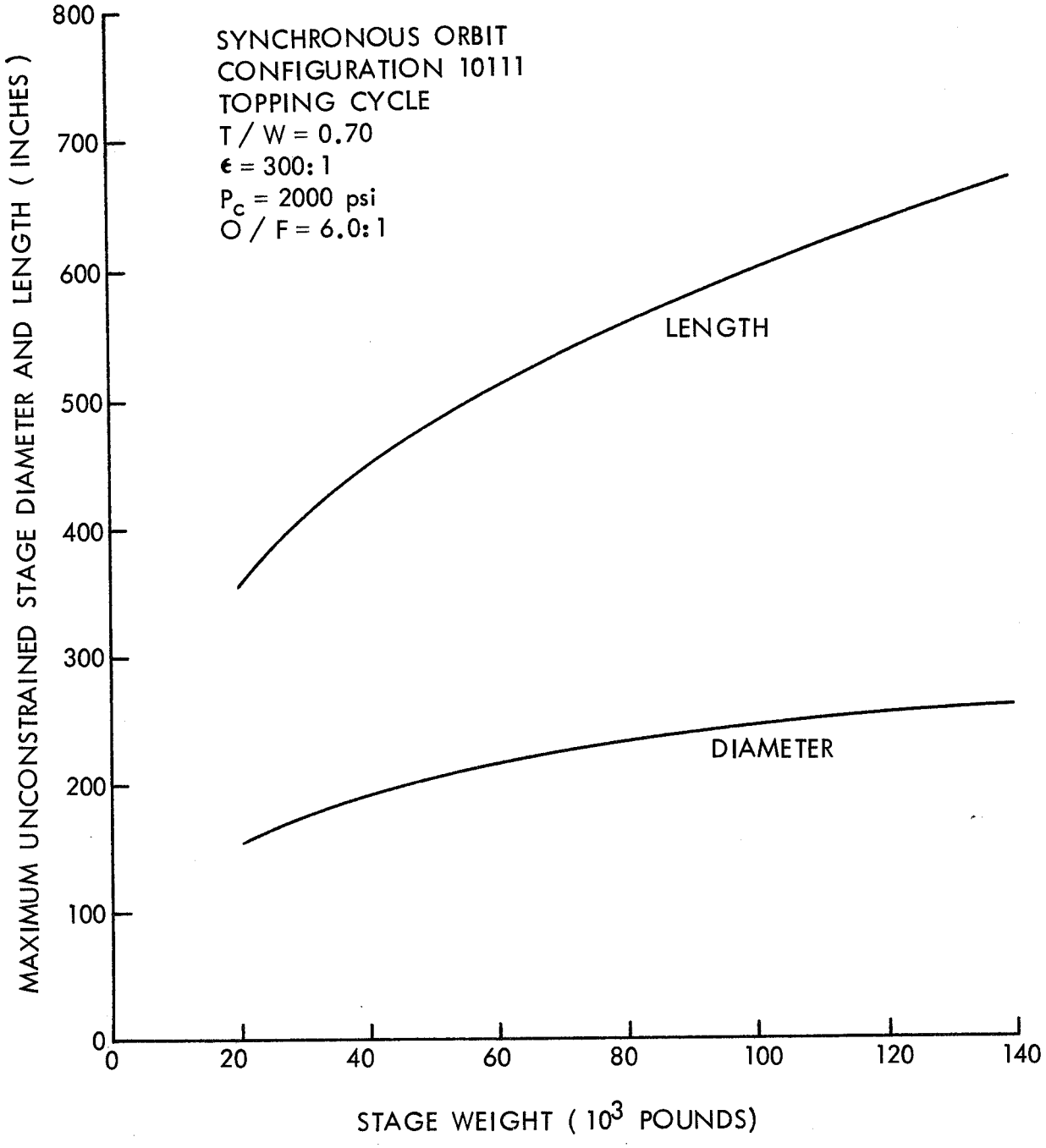

Figure 3-26 Maximum Unconstrained Stage Weight and Length

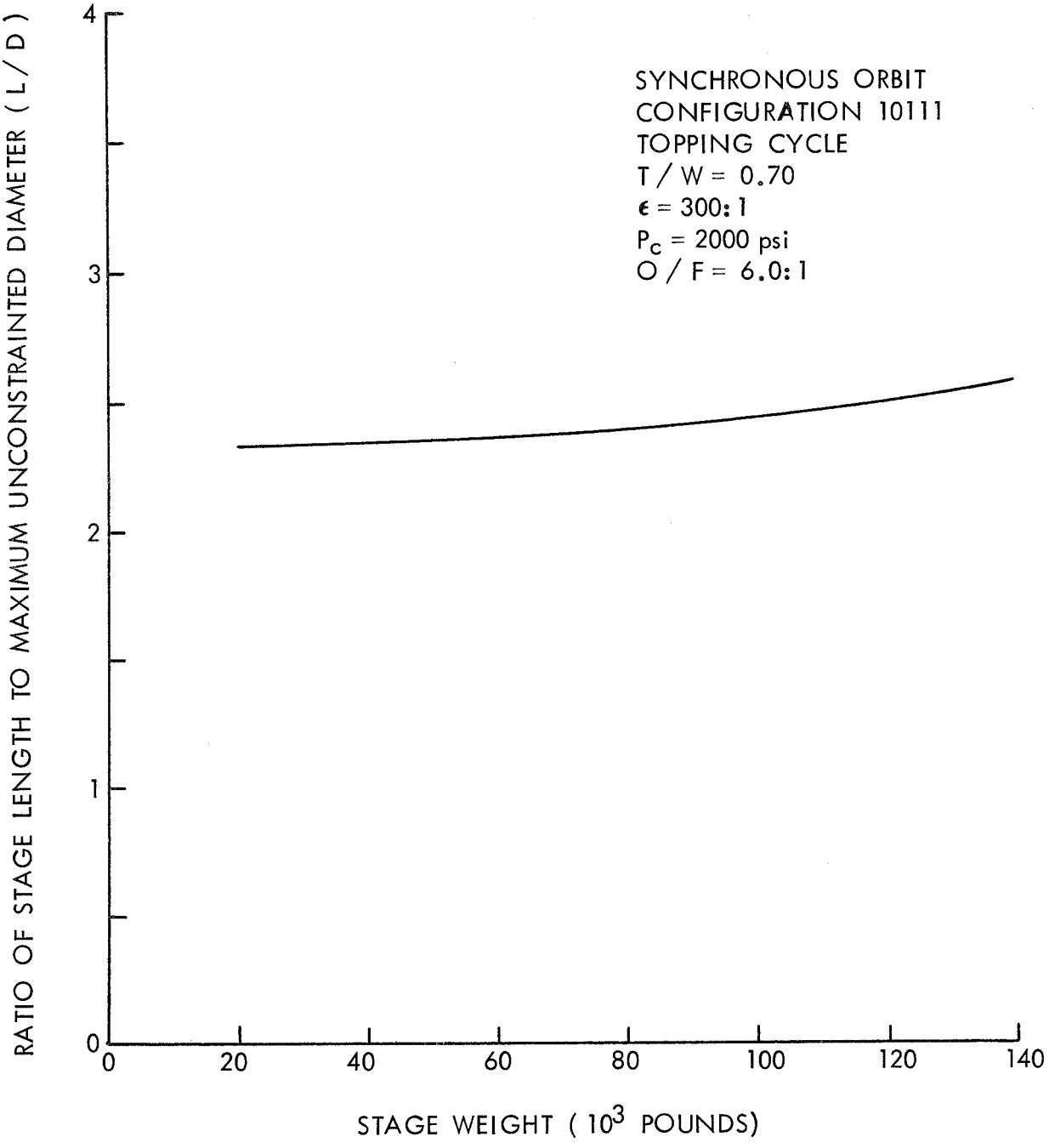

Figure 3-27 Length to Diameter Ratio (L/D) for Various Size Stages

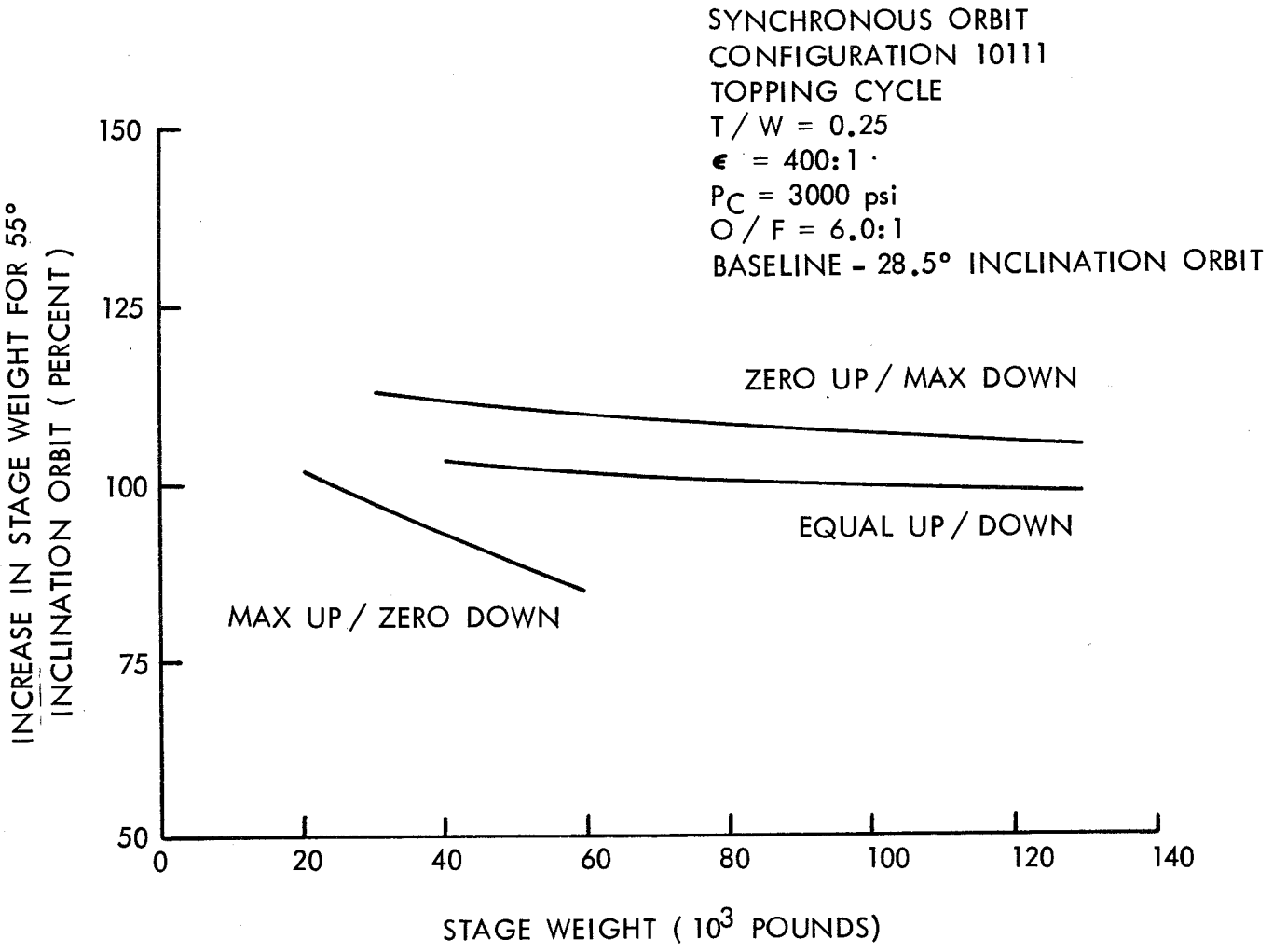

Figure 3-28 The Effect of Initial Orbit Inclination on Stage Size

just about doubles. Also, the effect not only varies with stage size, but depends upon the type of mission (that is, whether payload is taken up, brought back or both).

3.3.6.9 Initial Coast Time

For the baseline analyses it was assumed that the stages would be fully loaded and in the quiescent state for 24 hours prior to the first burn. Figure 3-29 shows how varying the initial coast to 7 and 30 days affects stage weight. Table 3-11 presents a summary of coast time effects on the thermal design characteristics of the stages. It is seen that at 30 days both fuel and oxidizer tanks optimize with a vent.

These results indicate that the penalty associated with initial hold time may be significant and should be considered in any operations anaysis for an Orbit to Orbit Shuttle, OOS.

3.3.6.10 Meteoroid Shielding Implications

It was assumed that the stages analyzed for the synchronous missions would be stored in a space hangar; thus, they would not require any special protection against meteoroids. Additional sensitivity analyses were performed to identify the penalty incurred by a stage which was required to provide its own meteoroid shield. Results are shown in figure 3-30, which presents the percent increase in stage weight, as a function of stage weight, for life expectancies of 6 months and 12 months. For these analyses the existing prime structure (i.e. shell and thrust cone) was used as the bumper since in every case thickness of the shell and thrust structure more than satisfied the required bumper thicknesses. A backup shield was placed around each tank to protect the tanks from the debris cloud which results when the bumper is impacted by a meteoroid. For the one year life expectancy, the thickness of the backup wall around the hydrogen tank varied from 0.025", for a 25,000 lb. stage, to 0.029" for a 135,000 lb. stage. If a separate bumper were used instead of utilizing the prime load bearing structure, the shielding weights would be much greater than indicated.

3.3.7 Synchronous Orbit Mission - Two Stage Sizing

Analyses were performed to determine the sizing requirements for accomplishing the synchronous mission with two stages (refer to Section 3.3.1 for a description of the mission profile). Three payload requirements were considered - 0 up/max down, maximum up/0 down, and equal outbound and return. For each case the absolute value of payload was selected to give combined stage weights of between 75,000 and 100,000 lbs. The results are shown in figures 3-31 through 3-33, which show first, second and combined stage weights as a function of the outbound velocity delivered by the first stage. (The second stage delivered the remainder of the outbound transfer velocity, which is about a total of 8200 fps, and then performed the three remaining burns). In each case, the first stage returned to the original low earth orbit with the interstage.

Noted on the figures are the velocity increments which the first stage can have that will put the first stage into a transfer orbit with a

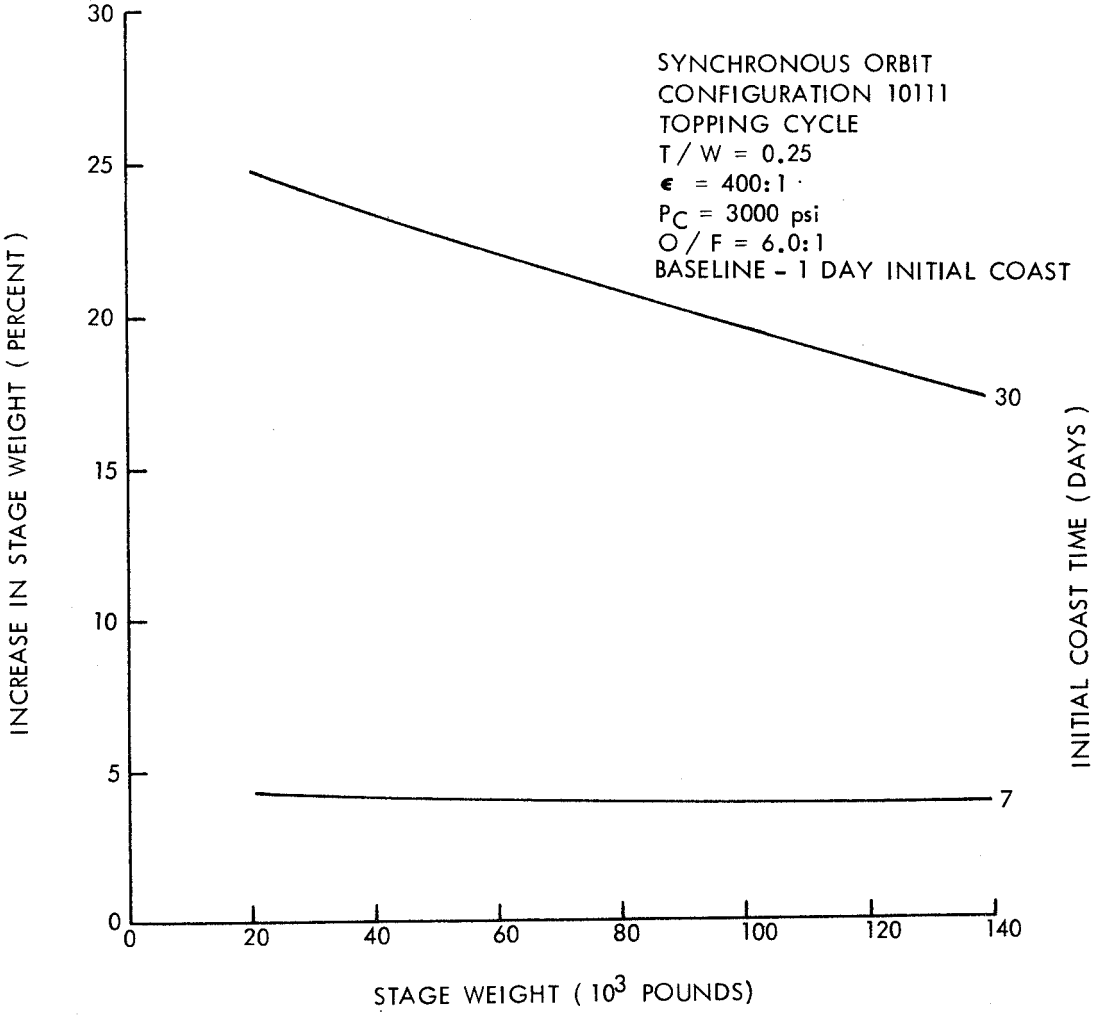

Figure 3-29 The Effect of Initial Coast Time on Stage Size

Table 3-11 The Effect of Initial Coast Duration on the Stages Thermal Design Criteria

INITIAL COAST TIME	W_{PROP} (TOTAL)	P_{VENT}/P_{DESIGN}	INSULATION THICKNESS	W_{TANK}	W_{INSUL}	W_{PRESS} (INERT)	W_{ULLAGE}	TMPBO	TMP
A. FUEL									
24 HOURS	11914	24.0 / 26.4	0.32	419.8	116.1	41.7	224.9	0	802.5
7 DAYS	12390	25.0 / 27.5	0.68	460.5	256.3	46.5	244.2	0	1007.5
30 DAYS	14570	38.0 / 45.9	0.76	942.7	329.7	79.7	507.7	223.8	2083.6
B. OXIDIZER									
24 HOURS	70484	21.0 / 30.5	0.17	211.8	31.8	250.8	263.8	135.9	894.1
7 DAYS	73336	22.0 / 31.8	0.22	228.8	42.4	270.9	295.3	238.7	1076.1
30 DAYS	83869	26.0 / 35.3	0.42	290.5	89.0	336.9	375.8	220.2	1311.4

Notes: Synchronous Orbit Mission
Coast Times: Initial, 8 Hours, 24 Hours, 8 Hours
Initial Fuel / Oxidizer Temperature: 36 / 162.6 °R
Initial Fuel / Oxidizer Pressure: 15 / 15 PSI
Fuel / Oxidizer NPSH Requirement: 2 / 10 PSI
Insulation Density: 4.5 Lb / Ft^3
Insulation Thermal Conductivity: Variable
Average Fuel / Oxidizer Value: 2.1×10^{-5} / 2.8×10^{-5} BTU / Ft - °R - Hr
External Fuel / Oxidizer Insulation Temperature: 450 / 470 °R
Fuel / Oxidizer Pressurant: H_2 / He

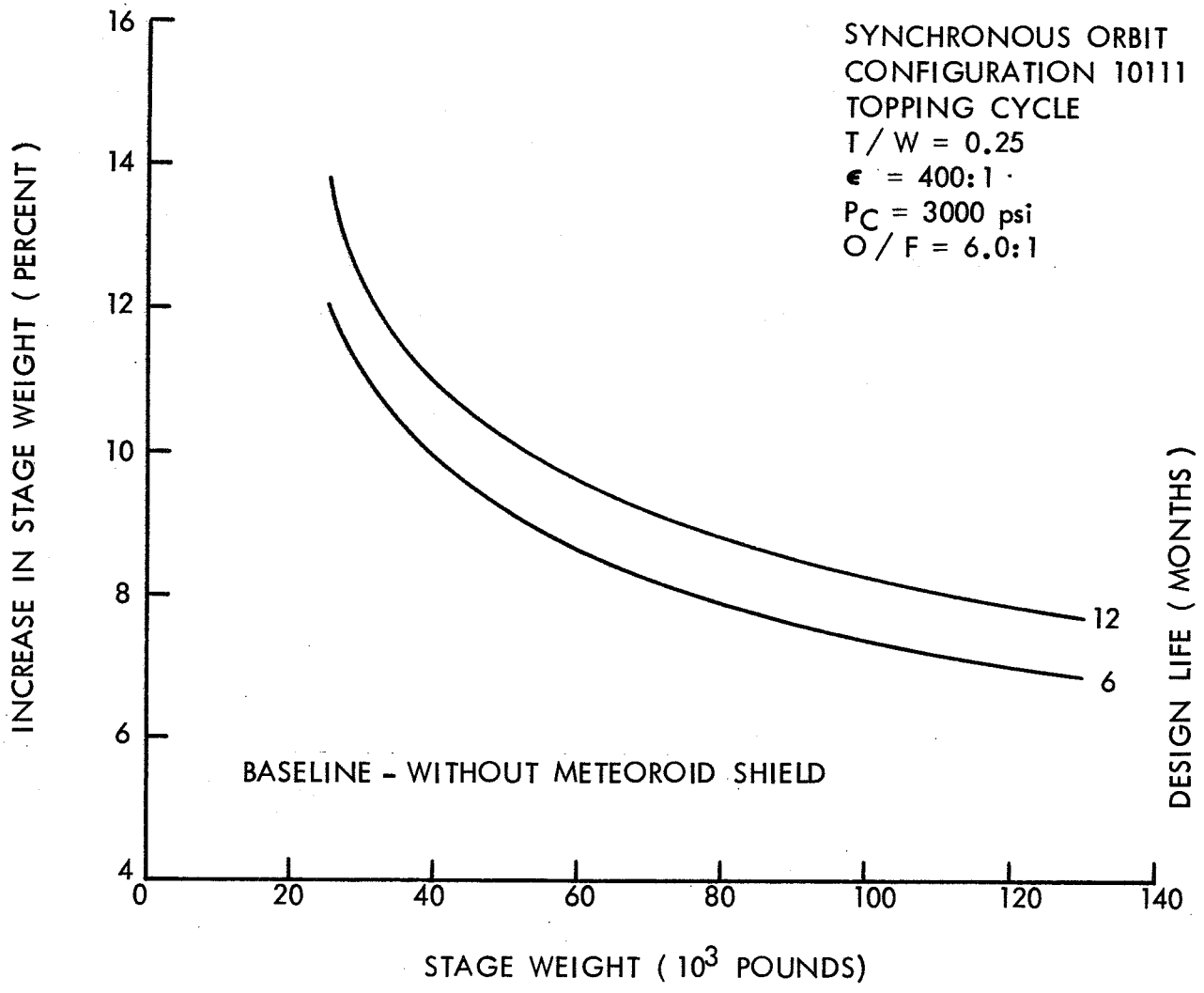

Figure 3-30 The Effect of Meteoroid Shielding on Stage Size

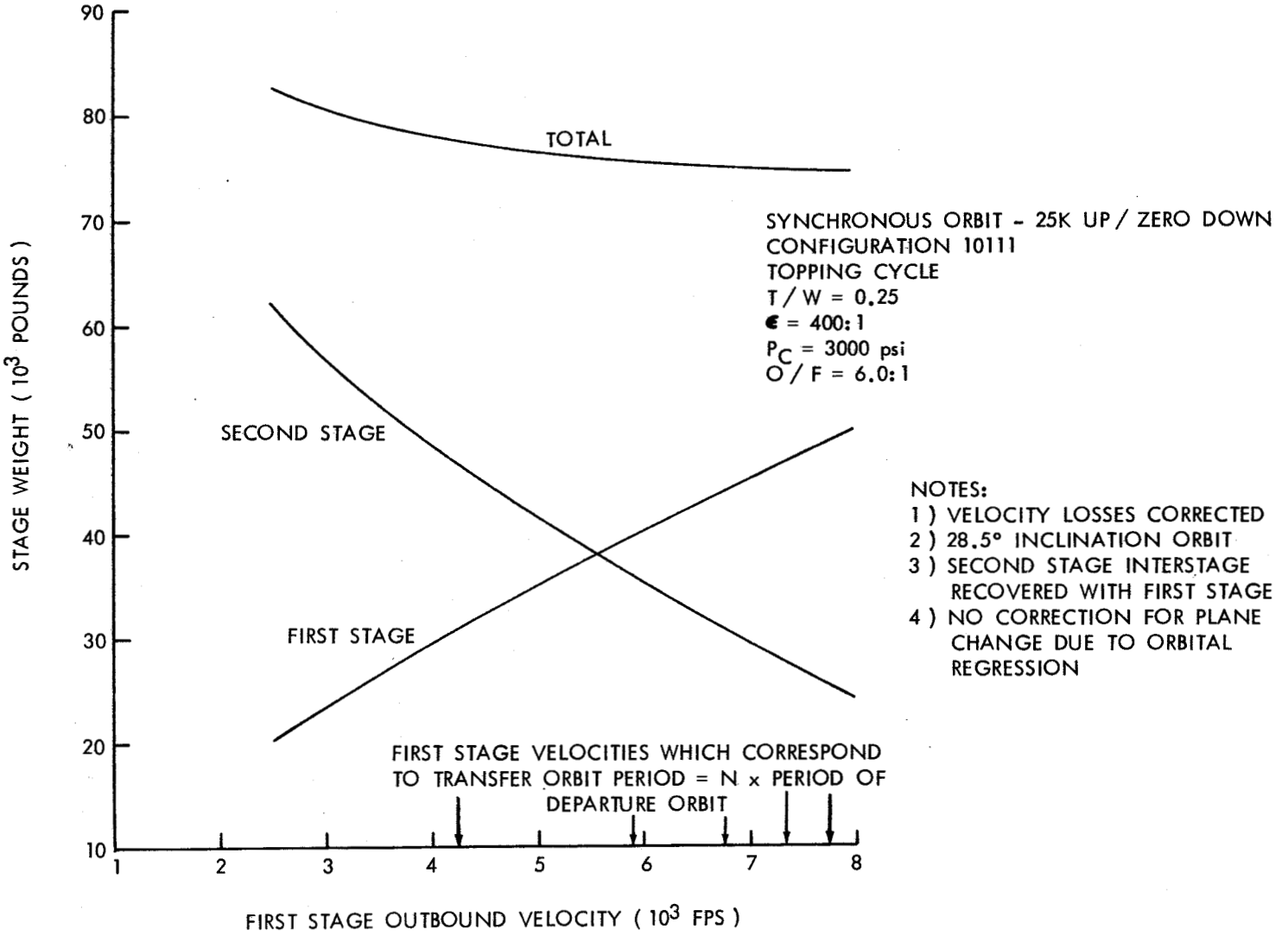

Figure 3-31 Two Stage Sizing Requirements for the Synchronous Orbit Mission (25,000 lbs. Outbound/Zero Return)

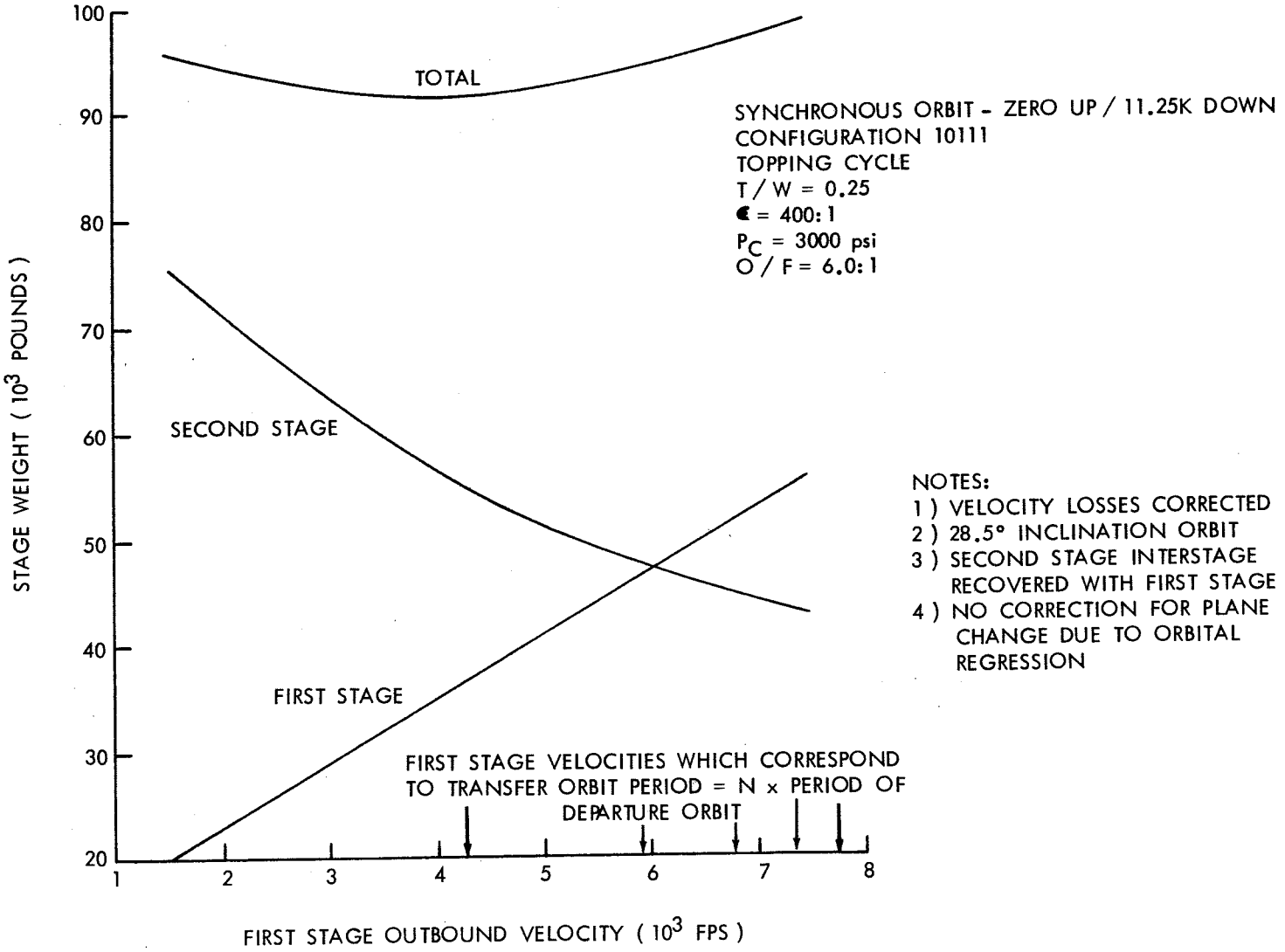

Figure 3-32 Two Stage Sizing Requirements for the Synchronous Orbit Mission (Zero Outbound/11,250 lbs. Return)

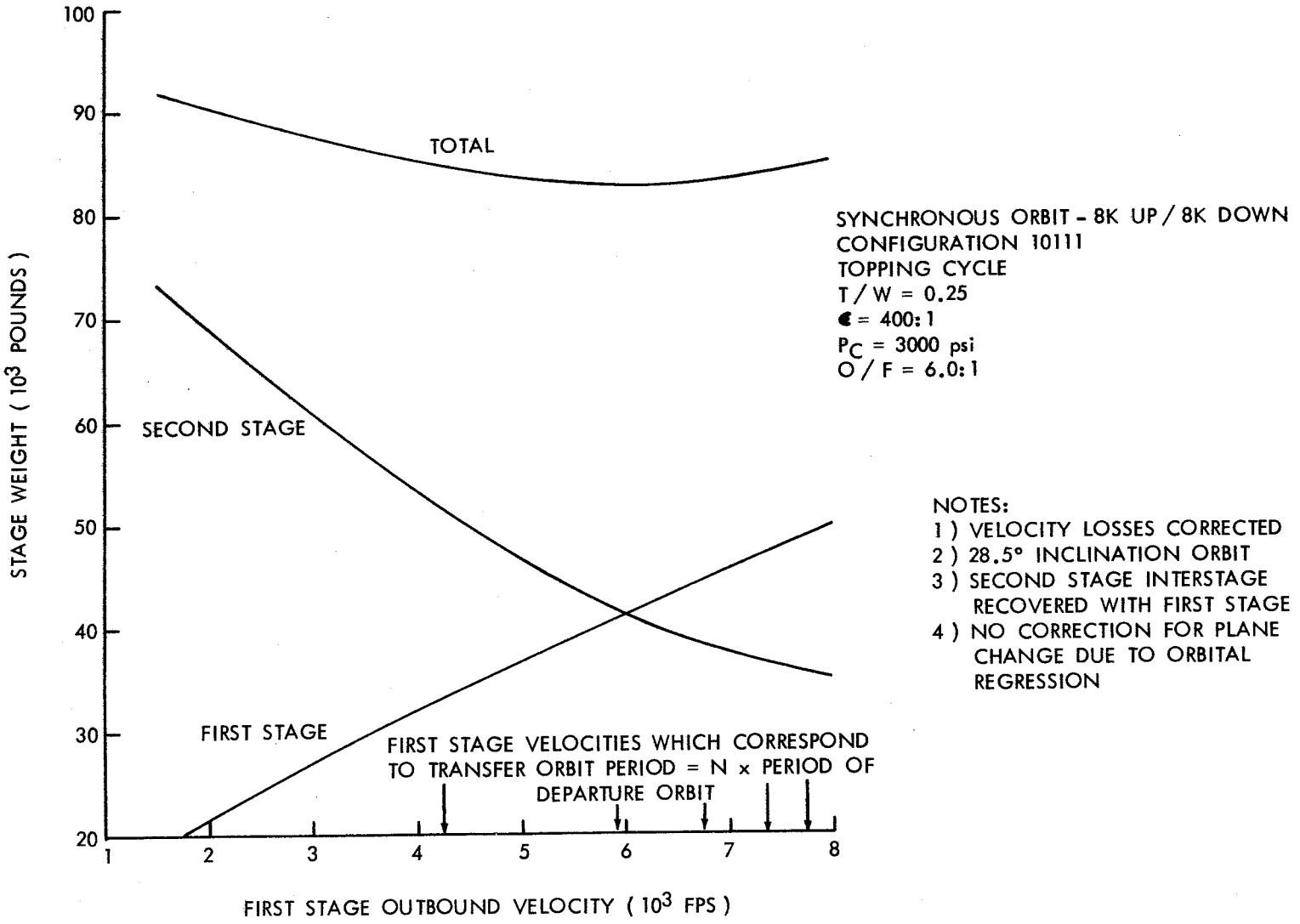

Figure 3-33 Two Stage Sizing Requirements for the Synchronous Orbit Mission (8,000 lbs. Outbound/8,000 lbs. Return)

period equal to an integral number of times the period of the departure orbit. These are the only velocities which permit the first stage to return to the same point in its original departure orbit without incurring any phasing problems.

Inspection of the results shows that the selection of either equal size stages or stages where the first stage performs the entire outbound transfer velocity, result in a total combined weight which is not far from the optimum weight point. In fact, for less than 10% penalty, a very wide range of stage size combinations can be used. This may prove to be significant in selecting a fleet of stages to perform a wide range of missions, using both single and multiple stages.

The results shown in figure 3-34 depict the sizing requirements for the alternate two stage mission profile discussed in section 3.3.1. For this profile a synchronous orbit shuttle (designated in figure 3-3 as the first stage) performs the first three burns and as much of the fourth burn as it can. This stage is then returned and circularized in its original low earth departure orbit using a smaller stage. It is evident that this is an attractive profile from a weight standpoint, however, the rendezvous problems may be significant.

Furthermore, when all the ΔV's are included to account for phasing and rendezvous, much or all of the weight advantage may disappear. A more detailed operation and mission profile analysis was beyond the scope of this study. Although the results shown are only for the equal outbound and return payload case, similar trends should occur for all the cases.

3.4 LUNAR SHUTTLE

3.4.1 Mission Profile

The mission profile selected for the lunar shuttle mission was taken from reference 10 and is the same as that used for the baseline Reusable Nuclear Shuttle (RNS) sizing. This profile is depicted in figure 3-35, where the velocity increments and associated coast times are shown. There are a total of six burns and the velocities shown include estimated gravity losses. A 90^{o} plane change capability in lunar orbit was included in the profile as a ground rule. The specified payloads of 120,000 lbs to the moon and 21,800 lbs. returned are the same as those used in sizing the RNS having 300,000 lbs. of hydrogen. Accomplishing the mission with two stages was also investigated. For this mission the first stage was used to provide part of the outbound velocity increment, and the second stage delivered the remainder of the outboard velocity increment as well as the remaining five velocities associated with the lunar shuttle mission. Both stages were recovered in the initial low earth orbit. This two stage lunar shuttle profile is shown in figure 3-36. From a weight standpoint the alternate two stage profile investigated for the synchronous orbit mission probably would have proven attractive here, but was not investigated.

3.4.2 Mixture Ratio Optimization

For the lunar shuttle mission, the thermal and meteoroid protection requirements are more severe than for the synchronous orbit mission. Since the system weights depend on tank sizes, a mixture ratio optimization was necessary to ensure that minimum weight stages were sized. A chamber

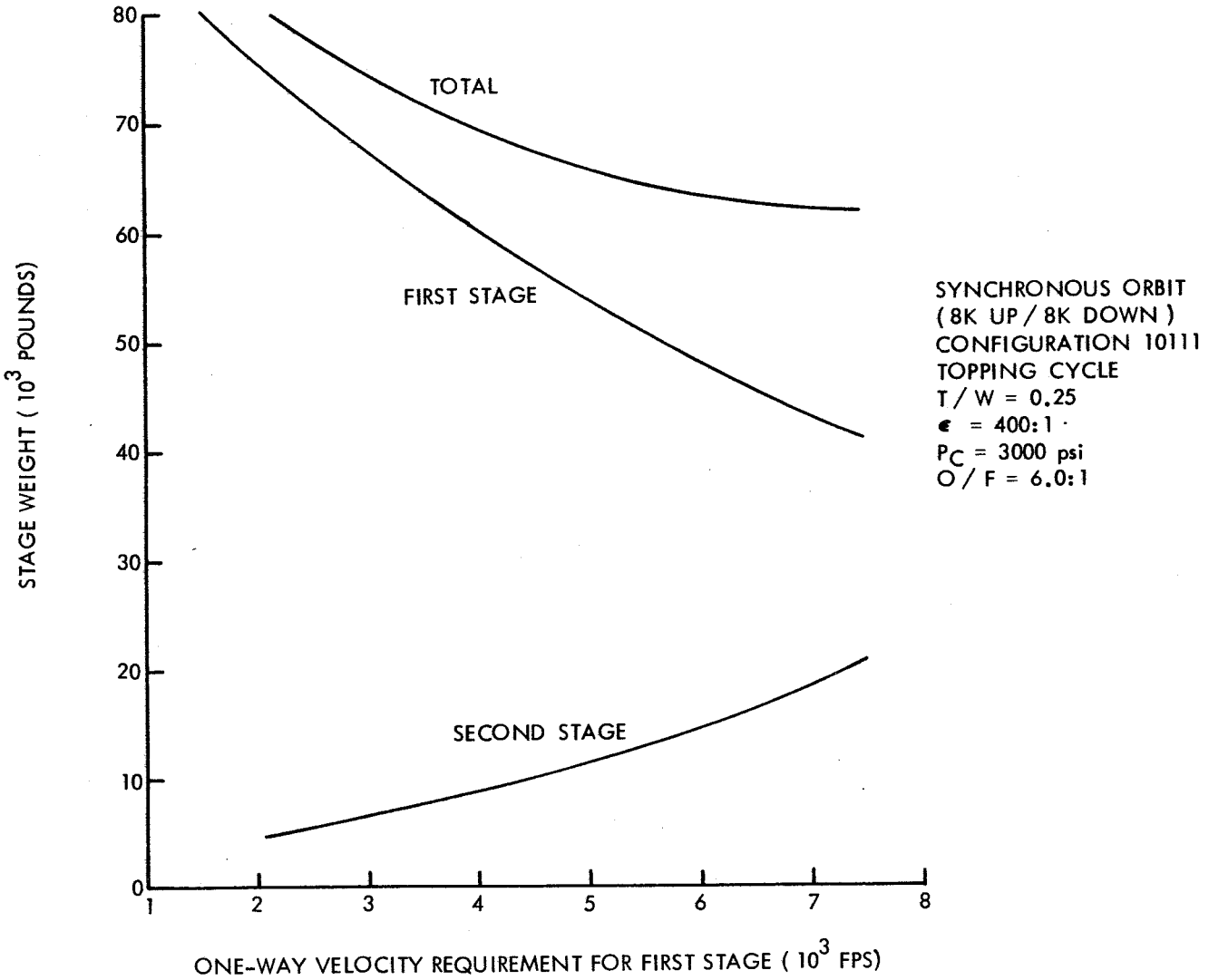

Figure 3-34 Two Stage Sizing Requirements for the Alternate Synchronous Orbit Mission

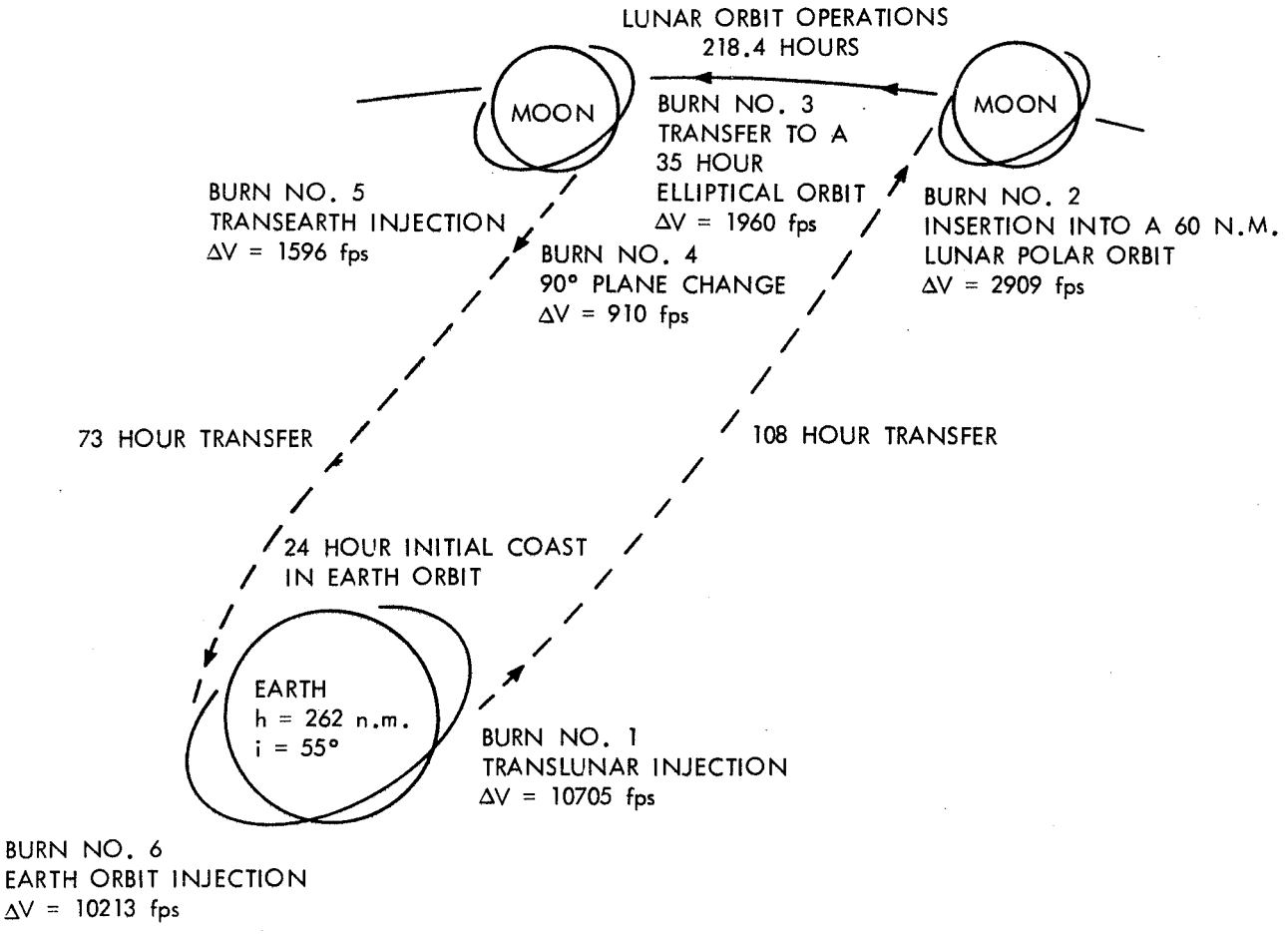

Figure 3-35 Single Stage Lunar Shuttle Mission Profile

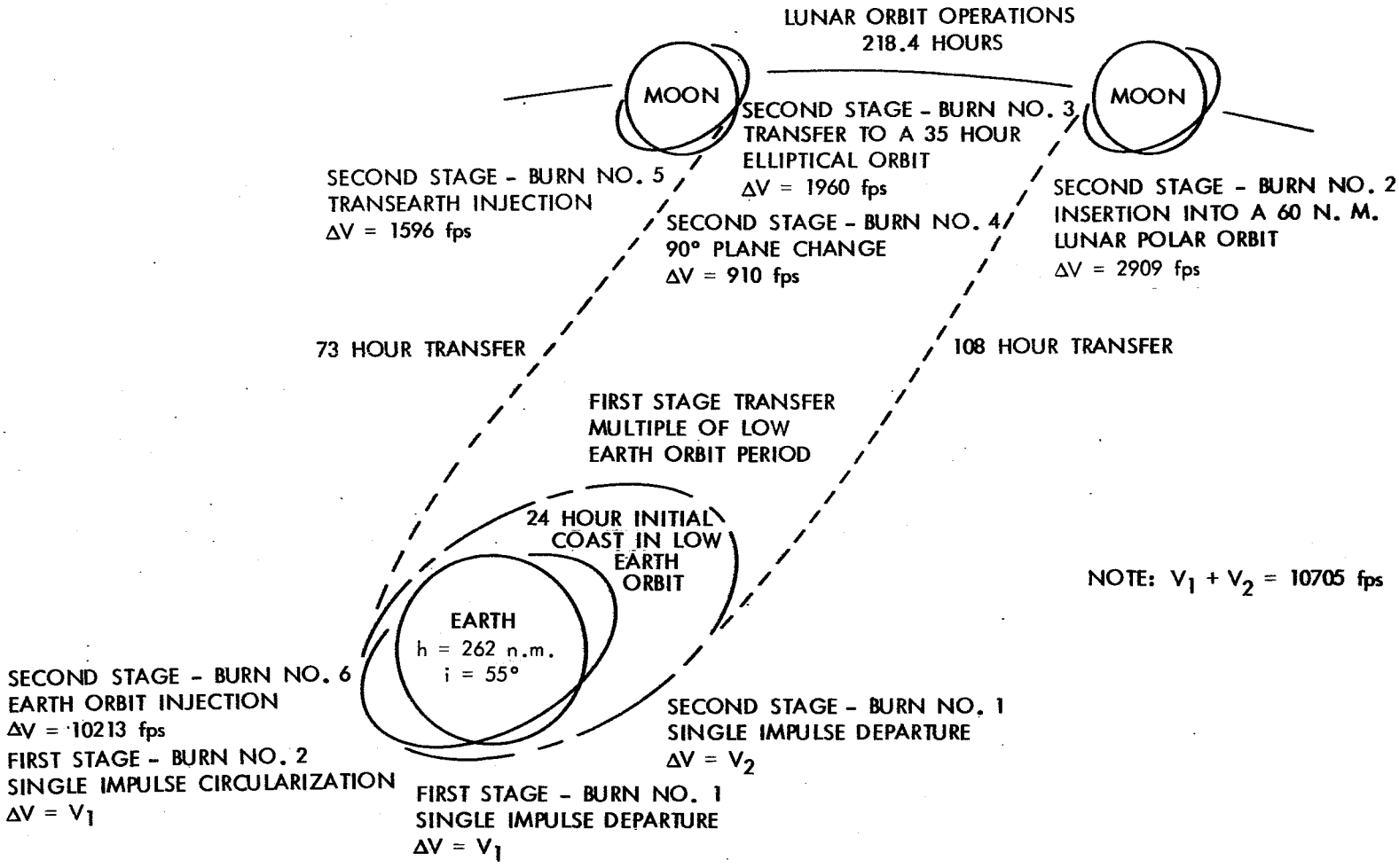

Figure 3-36 Two Stage Lunar Shuttle Mission Profile

pressure of 3,000 psia and an area ratio of 400:1 was used. The results, given in figure 3-37, show that the optimum mixture ratio lies between 6:1 and 7:1.

3.4.3 Stage Weights and Design Characteristics

A summary weight statement is given in table 3-12 for a stage with a mixture ratio of 6:1. This stage will deliver the specified payloads to and from the moon and is about equivalent (for this mission) to a Reusable Nuclear Shuttle having a 300,000 lb. hydrogen load. The salient design features of the stage are summarized in table 3-13. Special note should be paid to the thermal insulation densities assumed for this stage (refer to section 3.2). This insulation is less dense than that used for the other missions investigated during this study. For this mission, the selected densities were chosen to provide consistency with the RNS thermal protection.

The weights shown in table 3-12 for the meteoroid shield are the weights associated with only a backup wall around the tank. The prime load bearing structures (i.e., shell and thrust structure) were found to be adequate to serve as bumpers.

Influence coefficients which can be used to adjust the stage weights for changes in the inert weights (e.g. astrionic system) and engine performance have been included in table 3-12. They show that the lunar shuttle sizing requirements are extremely sensitive to inert weight and engine performance.

The data presented in tables 3-12 and 3-13 assume that almost 100% of the heat entering the tanks comes through the insulation. To determine the influence that the effectiveness of heat blocks has on stage size, an analysis was conducted assuming that only 50% of the heat entering the tanks came through the insulation. (The remainder entered through the skirts and attached points, plumbing, etc.) Table 3-14 provides a summary comparison which shows how this assumption affects the stage design. From these results it would appear that the development of effective heat blocks should prove to be a very cost effective endeavor.

3.4.4 Lunar Shuttle - Two Stage Sizing

Studies were accomplished to determine the optimum size stages necessary to perform the lunar shuttle mission with two stages. The mission profile was previously discussed in Section 3.4.1. Figure 3-38 illustrates the results of this analysis. Shown are first, second and total combined stage weights as a function of that portion of the outbound transfer velocity accomplished with the first stage. The optimum (minimum) total weight occurs with the first stage delivering around 7,000 feet per second. However, almost no penalty is incurred in reducing the first stage velocity to about 6,5000 feet per second where equal size stages are required.

If the first stage is required to perform the entire first burn, a slight penalty (about 5% in total weight) is incurred. However, the two stages vary greatly in size and may have advantages from the standpoint of

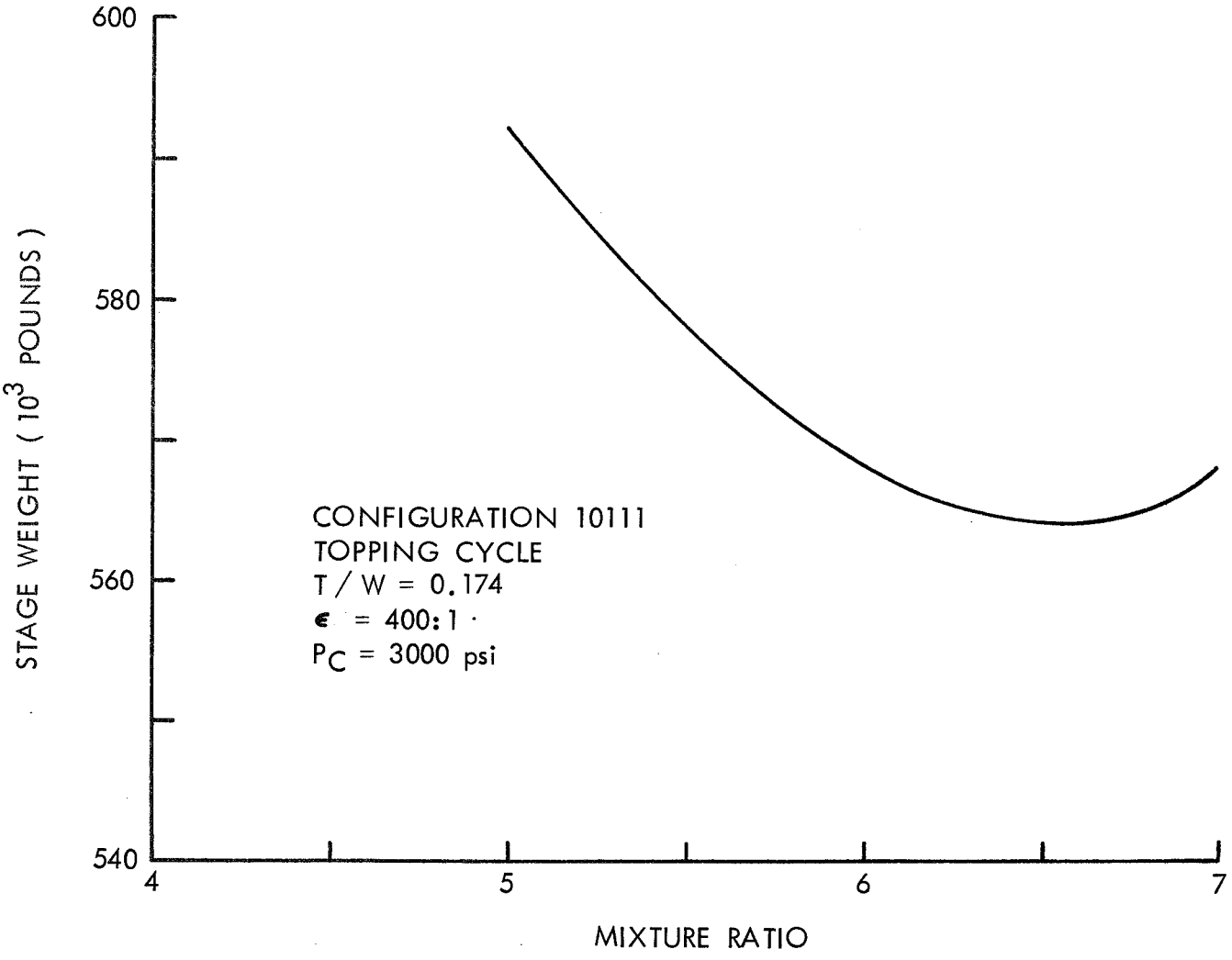

Figure 3-37 Single Stage Lunar Shuttle Mixture Ratio Optimization

Table 3-12 Weight Summary of a Single Stage Lunar Shuttle

STRUCTURE			19250
TANKAGE		4928	
Hydrogen	3076		
Oxygen	1852		
INTERSTAGE		0	
LANDING SYSTEMS		0	
SHELL		3693	
THRUST STRUCTURE		1900	
OTHER(TANK SUPPORTS, FEED SYSTEMS)		8729	
METEOROID SHIELD			2738
INSULATION			858
FUEL TANK		753	
OXIDIZER TANK		105	
PROPULSION			4024
ENGINE		1825	
OTHER INERT(RCS, PRESS)		2199	
ASTRIONICS			2530
MISCELLANEOUS FIXED WEIGHTS			
CONTINGENCY(@ 7.5 %)			2204

PROPELLANT INVENTORY			535195
TOTAL FUEL LOAD		77990	
Useable	73953		
Residual	1365		
Vented	504		
Final Ullage	1733		
Startup/Shutdown	435		
TOTAL OXIDIZER LOAD		457205	
Useable	443716		
Residual	8001		
Vented	1132		
Final Ullage	1744		
Startup/Shutdown	2612		
PRESSURIZATION & INERT GASES			167
TOTAL LOAD		167	
Vented	42		
Residual	125		
RCS PROPELLANT			1343
TOTAL FLUIDS			536705
CONSUMED		522059	
VENTED		1678	
RESIDUAL		12968	

BURN OUT WEIGHT	44572
TOTAL STAGE WEIGHT	568309
PROPELLANT FRACTION	0.911

$$\frac{\partial W_{STAGE}}{\partial I_{SP}} = -4143 \text{ (LB / SEC)}$$

$$\frac{\partial W_{STAGE}}{\partial W_{INERT}} = 15.7 \text{ (LB / LB)}$$

Table 3-13 Design Data Summary of a Single Stage Lunar Shuttle

COAST AND BURN NUMBER			1	2	3	4	5	6
COAST TIME			24.0	108.0	218.4	35.0	0.5	73.0
PAYLOAD			120000	120000	21800	21800	21800	21800
VELOCITY INCREMENT(TOTAL	28,293	fps)	10705	2909	1960	910	1596	10213
PROPELLANT BURNED			347728	59158	21851	9190	14780	64962
FUEL VENT(incl. Press/Inert Gases)			0	0	0	116	160	230
OXID. VENT(incl. Press/Inert Gases)			0	0	1172	0	0	0

ENGINE CHARACTERISTICS	
Thrust	120000
Specific Impulse	472.5
Area Ratio	400:1
Mixture Ratio	6.0:1
Chamber Pressure	3000

TANKAGE	FUEL	OXIDIZER
Vent Pressure	21.0	26.0
Design Pressure	27.4	33.8
Insulation Thickness	1.06	0.29
Additional Meteoroid Shield Thickness		
Bumper	*	*
Backup Wall	0.035	0.030
Volume	18407.8	6759.4

STAGE GEOMETRY	
Overall Length	984.2
Maximum Diameter	384.0
Stage L/D	2.56

* SHELL USED AS BUMPER

Table 3-14 The Effect of Heat Blocks on Stage Design

ITEM	BASELINE	LESS EFFECTIVE HEAT BLOCKS
STAGE WEIGHT (LB)	568309	599664
TOTAL PROPELLANT WEIGHT (LB)	535195	563701
TANKAGE WEIGHT (LB)		
HYDROGEN	3076	3863
OXYGEN	1852	1986
INSULATION WEIGHT (LB)		
HYDROGEN	753	776
OXYGEN	105	228
VAPOR VENTED (LB)		
HYDROGEN TANK	506	1471
OXYGEN TANK	1172	0
TANK DESIGN PRESSURE (PSI)		
HYDROGEN	27.41	31.97
OXYGEN	33.79	35.68
TANK VENT PRESSURE (PSI)		
HYDROGEN	21.00	25.00
OXYGEN	26.00	30.00
INSULATION THICKNESS (IN.)		
HYDROGEN	1.06	1.04
OXYGEN	0.29	0.61

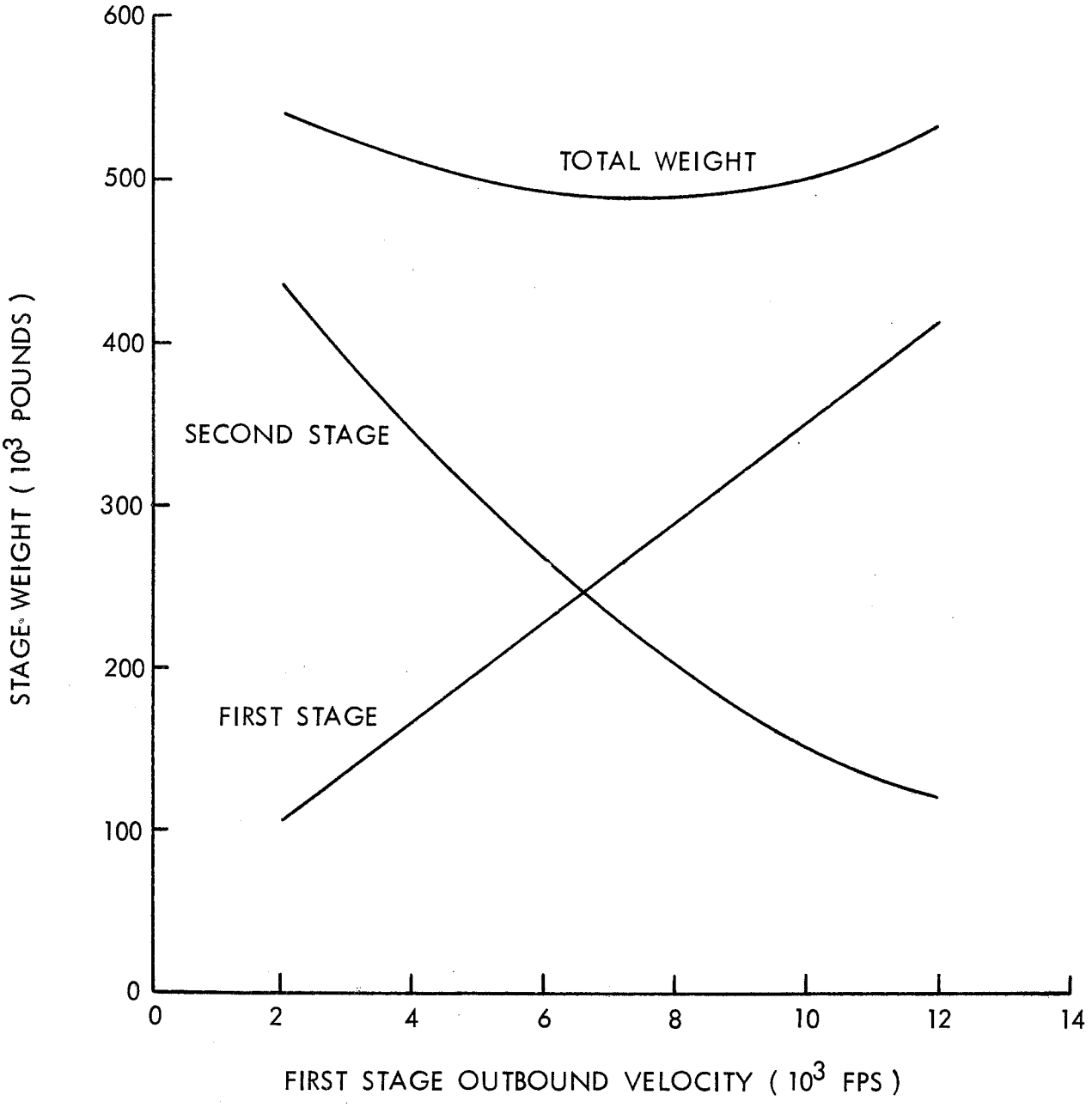

Figure 3-38 Two Stage Lunar Shuttle Sizing Requirements

fleet versatility. For example, the first stage could also be used (slightly modified) as a lunar lander or orbit-to-orbit shuttle.

As a matter of interest, the use of the Earth Orbit Shuttle Orbiter as the first stage of two stage Orbit-to-Orbit Shuttle was examined. The unmodified orbiter selected for this investigation was assumed to have a propellant load of 471,000 pounds, and a total weight of 735,000 pounds. The results of this analysis, which are shown in figure 3-39, present solutions for four different total orbiter weights. The total orbiter weights given reflect the removable of various amounts of inert weight (e.g. aerodynamic farings, landing gear, etc.) from the orbiter. For reference, an orbiter having a liftoff weight of 555,000 pounds would correspond to a propellant fraction of 0.85. The intersection of the second stage curve with the four orbiter performance curves are solutions which will satisfy the mission criteria. Two of these points are of some interest. First, the unmodified orbiter (735,000 pound orbiter) could apparently serve as a backup first stage. This could have significance from a logistics or safety standpoint. Second, if unneeded inert weight is stripped out of the orbiter until it has a liftoff weight of 555,000 lbs., then the second stage size requirement is reduced to just a little over 100,000 lbs. This raises the possibility of using the second stage as both the lunar shuttle and the lunar lander (see section 3.5). Although this might require some modification of the payload requirements, a significant programmatic advantage would occur - only one completely new stage need be developed instead of two or three. Furthermore, it would be a relatively smaller stage than an RNS or comparable single stage chemical shuttle. Of course, the amount of propellant used per flight would be greater - thus annual recurring costs would be sacrificed to attain a significant reduction in development costs.

Study funding would not permit more than this cursory examination of the use of the EOS Orbiter as an orbit-to-orbit stage. It is recommended, however, that this possibility be re-examined in any future chemical shuttle studies.

3.4.5 Comparison with Reusable Nuclear Shuttle

A detailed comparison between a chemical and nuclear lunar shuttle would require a considerably larger effort than the funding available in this study would allow. However, a preliminary evaluation shows that use of a chemical shuttle instead of a nuclear shuttle could easily prove to be the least costly way to accomplish the lunar shuttle mission. A summary comparison of the chemical nuclear shuttles is presented in table 3-15.

From an operational standpoint, a major cost factor in a lunar shuttle program would be the cost to deliver the necessary propellants to the lunar shuttle. The first part of the table shows the number of Earth Orbit Shuttle, EOS, trips necessary to deliver the propellant needed for both the chemical and nuclear lunar shuttles. The presently planned EOS is volume limited rather than weight limited for the delivery of hydrogen to earth orbit. Thus, even though the RNS requires only 300,000 pounds of propellant as compared to 535,000 pounds of propellant for the chemical shuttle, the same number of supply trips are required to deliver the propellant required for both types of stages. From a propellant logistics

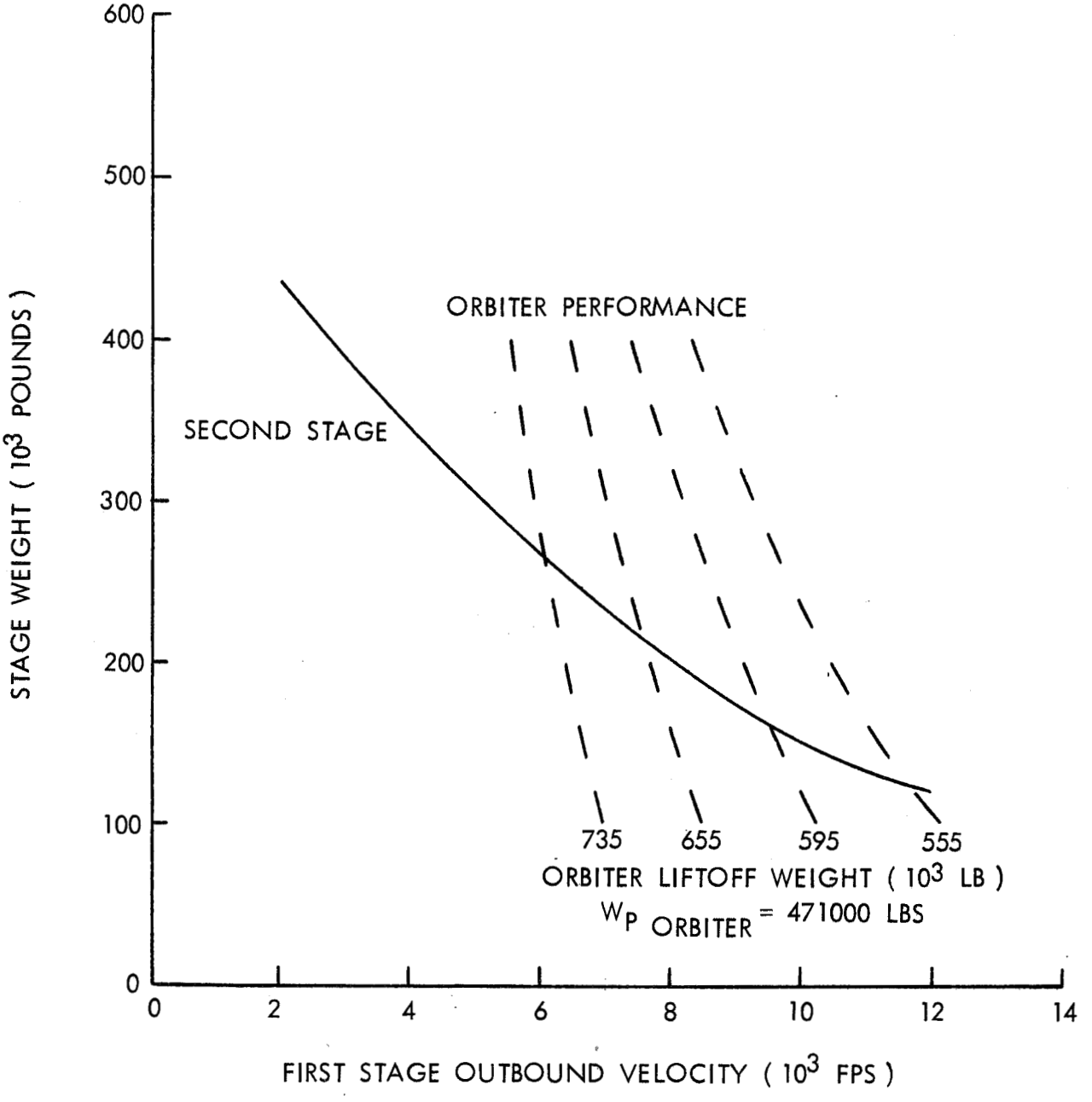

Figure 3-39 Two Stage Lunar Shuttle Sizing, Using the Orbit-to-Orbit Orbiter as a First Stage

Table 3-15 A Comparison of Chemical and Nuclear Lunar Shuttles

- PROPELLANT LOGISTICS

Configuration	Propellant Weight		No. Of EOS Trips		Total No. Of Trips	Advantage
	H_2	O_2	H_2	O_2		
Nuclear	300K	---	8	-	8	Neither
Chemical (Single Stage)	78K	457K	2.07	5.72	8	

Note: Maximum LH_2 Weight Per EOS Trip = 37,600 Lb (Volume Limited)
Maximum LO_2 Weight Per EOS Trip = 80,000 Lb

	ADVANTAGE	
	CHEMICAL	NUCLEAR
• DEVELOPMENT & PRODUCTION COST	√	
• SUPPORT SYSTEM REQUIREMENTS (PDP, Shields, Storage, Manipulators)	√	
• SAFETY & OPERATIONS (Disposal, Rendezvous, Docking, Manned)	√	
• ADVANCEMENT OF TECHNOLOGY		√
• USE FOR MANNED INTERPLANETARY EXPLORATION		√

standpoint neither stage has a significant advantage. This assumes that the added cost of handling two propellants will be offset by the higher cost of hydrogen as compared to oxygen.

The chart also provides a subjective evaluation of the relative merits of the two stages in terms of cost requirements, advancement of technology, operational safety, and versatility. It is believed that the nuclear stage is to be preferred only in terms of advancing technology and for use in manned interplanetary exploration. Of course these latter factors may in themselves be sufficient to outweigh all other considerations and the RNS could be the most cost effective stage from the standpoint of long range planning.

3.5 LUNAR LANDER

3.5.1 Mission Profile

The payload requirements and mission profile for the sizing of a lunar lander are identical to those given in Reference 11. Figure 3-40 depicts the flight profile used for the lander. The 7,200 fps velocity increment budget for each leg of the trip between a 60 nm lunar orbit and the lunar surface and the return to a 60 nm lunar orbit is considered to be a conservative value. This velocity increment includes contingencies for hovering, rendezvous, etc. but does not include plane change velocities. The 20,000 lb. payload was assumed to be comprised of a 10,000 lb. crew capsule, 5,000 lbs. of mobility aids and 5,000 lbs. of scientific equipment. The thermal protection requirements were based on the criteria that the stage remain fully loaded in the quiescent state for 180 days (in lunar orbit) and a 42-day stay time on the lunar surface. The 180-day initial 'coast' is based on a requirement for a rescue vehicle.

3.5.2 Mixture Ratio Optimization

As with the lunar shuttle, a mixture ratio optimization was conducted to ensure that minimum weight stages were sized. The results, given in figure 3-41, indicate that the theoretical optimum occurs at a value greater than 7 to 1. However, the slope of the curve is very slight and there is little to be gained in going beyond a mixture ratio of 6 to 1.

3.5.3 Sample Stage Weight Statement and Design Characteristics Summary

A summary of the weights and design characteristics of this stage is given in tables 3-16 and 3-17, respectively. The example stage selected used a mixture ratio of 6 to 1, which is somewhat less than the theoretical optimum.

It should be noted that a considerable amount of insulation is required on both the fuel and oxidizer tanks - and these were obtained using very effective heat blocks in the tank supports and plumbing. If the amount of heat entering through the supports and plumbing were allowed to increase to half of that entering the insulation, the insulation thickness of the fuel and oxidizer tanks would increase to 7.60 and 3.85 inches, respectively. And the stage weight would increase from 74,854 lbs. to 83,539 lbs. However, there is some question as to whether super insulations can be used

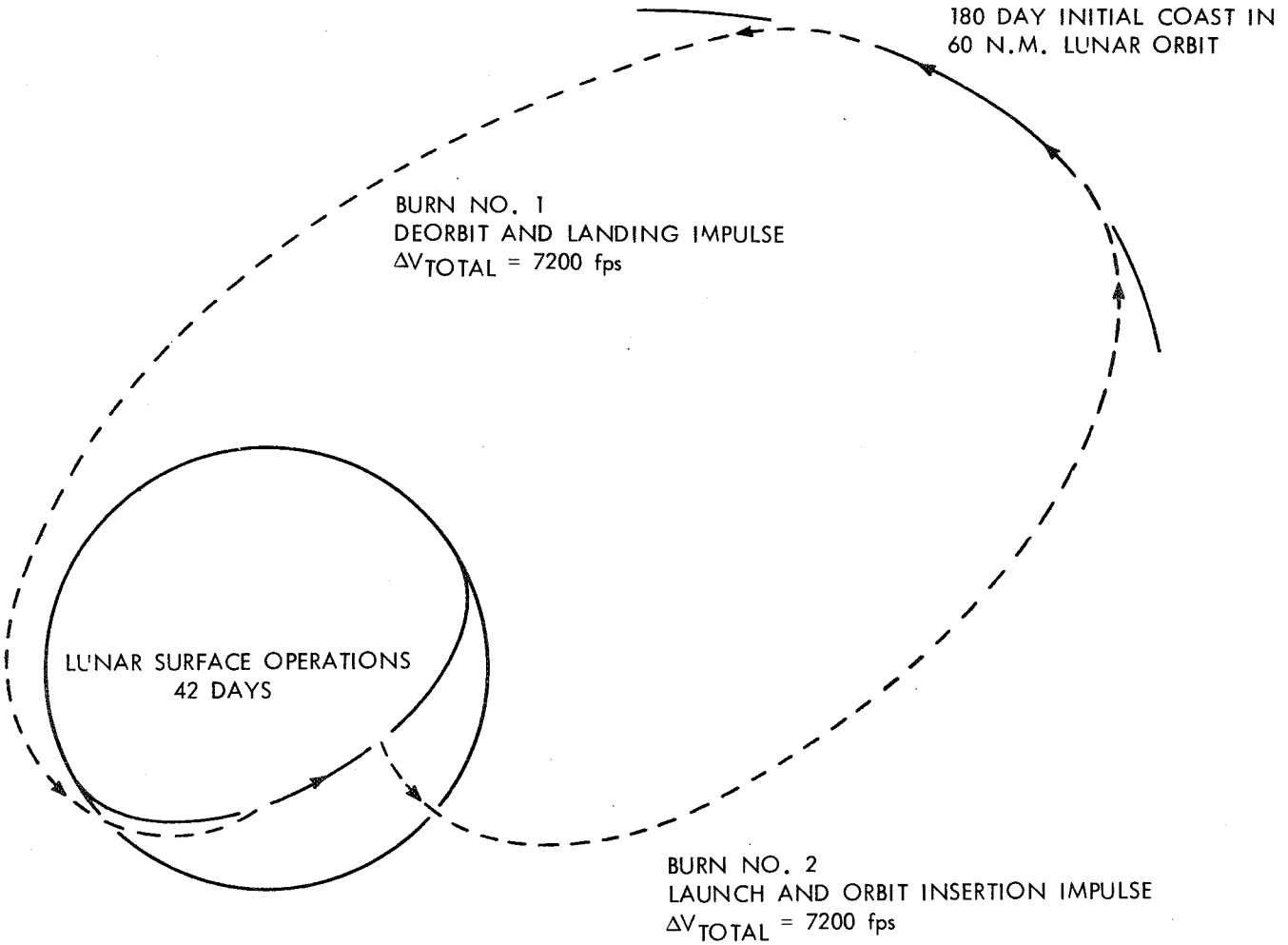

Figure 3-40 Lunar Lander Mission Profile

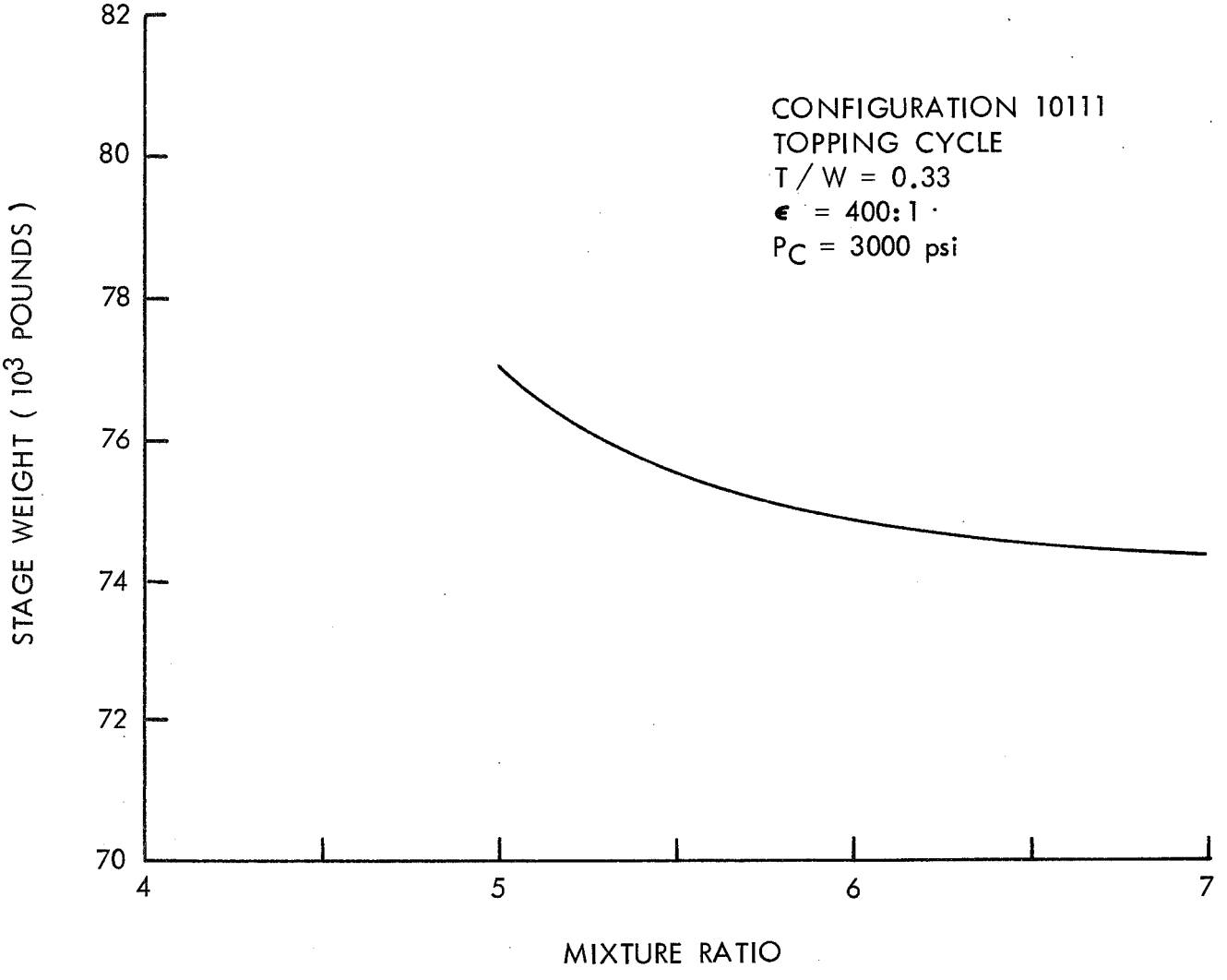

Figure 3-41 Lunar Lander Mixture Ratio Optimization

Table 3-16 Weight Summary of a Lunar Lander

STRUCTURE			6560
TANKAGE		901	
Hydrogen	687		
Oxygen	214		
INTERSTAGE		0	
LANDING SYSTEMS		3100	
SHELL		1213	
THRUST STRUCTURE		213	
OTHER(TANK SUPPORTS, FEED SYSTEMS)		1133	
METEOROID SHIELD			574
INSULATION			2066
FUEL TANK		1758	
OXIDIZER TANK		308	
PROPULSION			1202
ENGINE		518	
OTHER INERT(RCS, PRESS)		684	
ASTRIONICS			1355
MISCELLANEOUS FIXED WEIGHTS			
CONTINGENCY(@ 7.5 %)			883

PROPELLANT INVENTORY			60978
TOTAL FUEL LOAD		9378	
Useable	8244		
Residual	300		
Vented	527		
Final Ullage	269		
Startup/Shutdown	38		
TOTAL OXIDIZER LOAD		51600	
Useable	49462		
Residual	1677		
Vented	0		
Final Ullage	234		
Startup/Shutdown	227		
PRESSURIZATION & INERT GASES			26
TOTAL LOAD		26	
Vented	1		
Residual	25		
RCS PROPELLANT			1210
TOTAL FLUIDS			62214
CONSUMED		59181	
VENTED		528	
RESIDUAL		2505	

BURN OUT WEIGHT	15145
TOTAL STAGE WEIGHT	74854
PROPELLANT FRACTION	0.771

Table 3-17 Design Data Summary of a Lunar Lander

COAST AND BURN NUMBER	1		2
COAST TIME	4320		1056
PAYLOAD	20000		20000
VELOCITY INCREMENT(TOTAL 14,400 fps)	7200		7200
PROPELLANT BURNED	35664		22042
FUEL VENT(incl. Press/Inert Gases)	169		359
OXID. VENT(incl. Press/Inert Gases)	0		0
ENGINE CHARACTERISTICS			
Thrust		31304	
Specific Impulse		473.3	
Area Ratio		400:1	
Mixture Ratio		6.0:1	
Chamber Pressure		3000	
TANKAGE	FUEL		OXIDIZER
Vent Pressure	38.5		41.5
Design Pressure	41.1		68.4
Insulation Thickness	5.05		1.95
Additional Meteoroid Shield Thickness			
Bumper	*		*
Backup Wall	0.027		0.024
Volume	2331.4		776.7
STAGE GEOMETRY			
Overall Length		563.9	
Maximum Diameter		180.0	
Stage L/D		3.13	

* SHELL USED AS BUMPER

effectively at these large thicknesses.

Table 3-18 shows the effect of restricting the thermal insulation thicknesses to 1 inch on both the fuel and oxidizer tanks. Surprisingly, the penalty is not as severe as might be suspected. The thermal mass penalty attendant with the significant increase in boil-off was largely offset by the reduced weight of insulation.

Since vented hydrogen has a significant thermal capacity for cooling the oxygen tank, a special sizing run was made to show the effect of venting the hydrogen through coils in the LOX tank. Table 3-19 provides a comparison between this stage and the baseline stage in which the hydrogen vent was not used for cooling. It appears that the additional complexity of a cooling system may be worthwhile and this type system should be considered in future design studies of stages requiring extensive thermal protection.

3.6 PLANETARY MISSIONS

3.6.1 Mission Profile

The two planetary missions represented the last general type of mission studied. The first corresponded to a mission in which a relatively small stage circularized a scientific payload into an orbit about the planet after a long interplanetary coast. The stage was assumed to be placed on a Mars trajectory by another stage or booster. The mission profile for this single burn case is shown in figure 3-42. For illustrative purposes, the selected coast times and ΔV's correspond roughly to a typical Mars mission.

The second planetary mission required a single stage to perform two major burns. The first burn provided the transfer velocity to place the stage on an interplanetary Mars trajectory. The second burn performed the same function as discussed for the previous stage - i.e., circularization at Mars. The mission profile for this two-burn Mars stage is shown in figure 3-43. Again, velocities and coast times were selected to approximate a Mars mission.

Hereinafter, the two cases are referred to as the single-burn and two-burn Mars missions, respectively. The 7,000 pound payloads selected for these missions were felt to be typical for a Mars mission.

3.6.2 Engine Parameter Optimization

The results of mixture ratio optimization for the single-burn Mars missions are presented in figure 3-44. The single-burn Mars stage optimized at a mixture ratio between 6.0:1 and 7.0:1. This shift to higher mixture ratios is typical for missions having severe thermal protection requirements. For reasons discussed in section 3-2, it was necessary to use both gas generator and topping engine cycle data for the small single-burn Mars stage. Hence, it was not possible to do a complete engine parameter optimization for this case. The assumed thrust-to-weight, area ratio, and chamber pressure were 0.25, 200:1 and 1,000 psi, respectively.

Because the two-burn Mars stage was larger, it was possible to use a consistent set of engine (topping) cycle data and perform a complete engine parameter optimization. The results of this analysis are presented

Table 3-18 Effect of Restricting the Thermal Insulation Thickness on Stage Size

ITEM	BASELINE	LIMITED THICKNESS
STAGE WEIGHT (LB)	74854	75588
TOTAL PROPELLANT WEIGHT (LB)	60978	62835
TANKAGE WEIGHT (LB)		
HYDROGEN	687	830
OXYGEN	214	188
INSULATION WEIGHT (LB)		
HYDROGEN	1758	398
OXYGEN	308	154
VAPOR VENTED (LB)		
HYDROGEN TANK	528	3029
OXYGEN TANK	0	435
TANK DESIGN PRESSURE (PSI)		
HYDROGEN	47.05	44.32
OXYGEN	45.65	40.05
TANK VENT PRESSURE (PSI)		
HYDROGEN	38.50	36.50
OXYGEN	41.50	26.50
INSULATION THICKNESS (IN.)		
HYDROGEN	5.05	1.00
OXYGEN	1.95	1.00

Table 3-19 Effect of LOX Tank Cooling on Stage Size

ITEM	BASELINE	COOLED LOX TANK
STAGE WEIGHT (LB)	74854	72892
TOTAL PROPELLANT WEIGHT (LB)	60978	59713
TANKAGE WEIGHT (LB)		
HYDROGEN	687	514
OXYGEN	214	186
INSULATION WEIGHT (LB)		
HYDROGEN	1758	1628
OXYGEN	308	200
VAPOR VENTED (LB)		
HYDROGEN TANK	528	845
OXYGEN TANK	0	0
TANK DESIGN PRESSURE (PSI)		
HYDROGEN	47.05	36.37
OXYGEN	45.65	40.15
TANK VENT PRESSURE (PSI)		
HYDROGEN	38.50	29.00
OXYGEN	41.50	36.50
INSULATION THICKNESS (IN.)		
HYDROGEN	5.05	4.80
OXYGEN	1.95	1.30

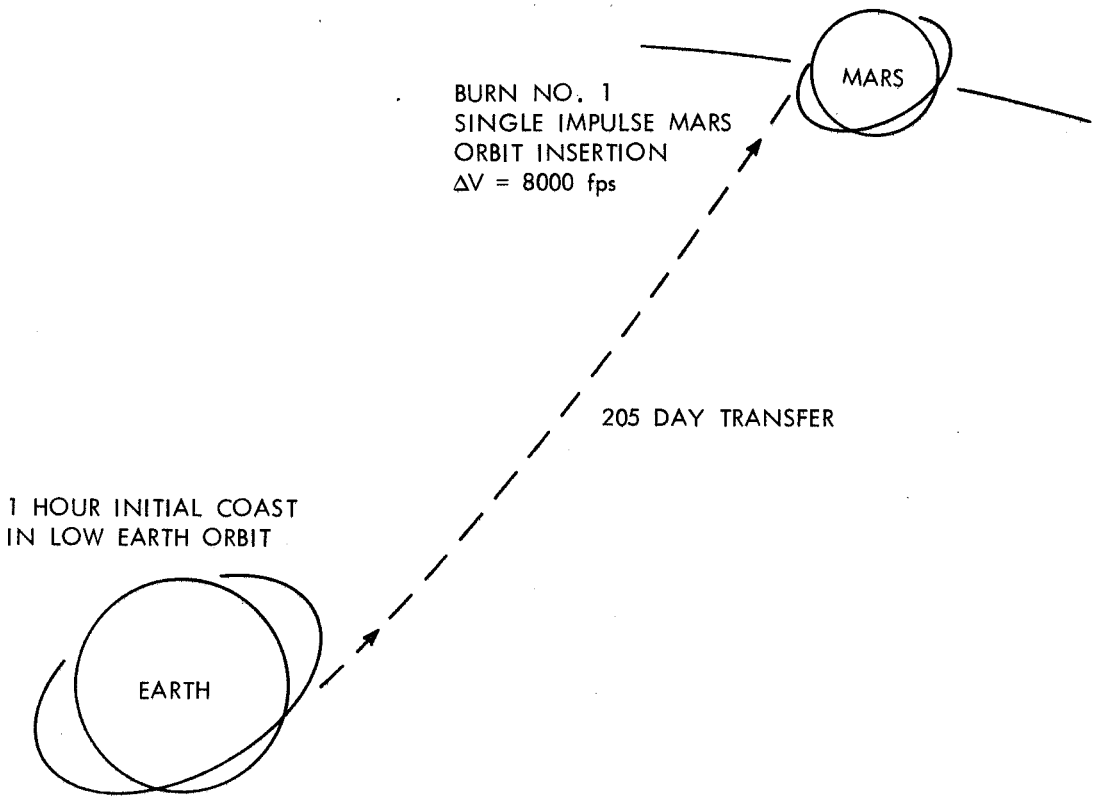

Figure 3-42 Mission Profile for a Single-Burn Mars Stage

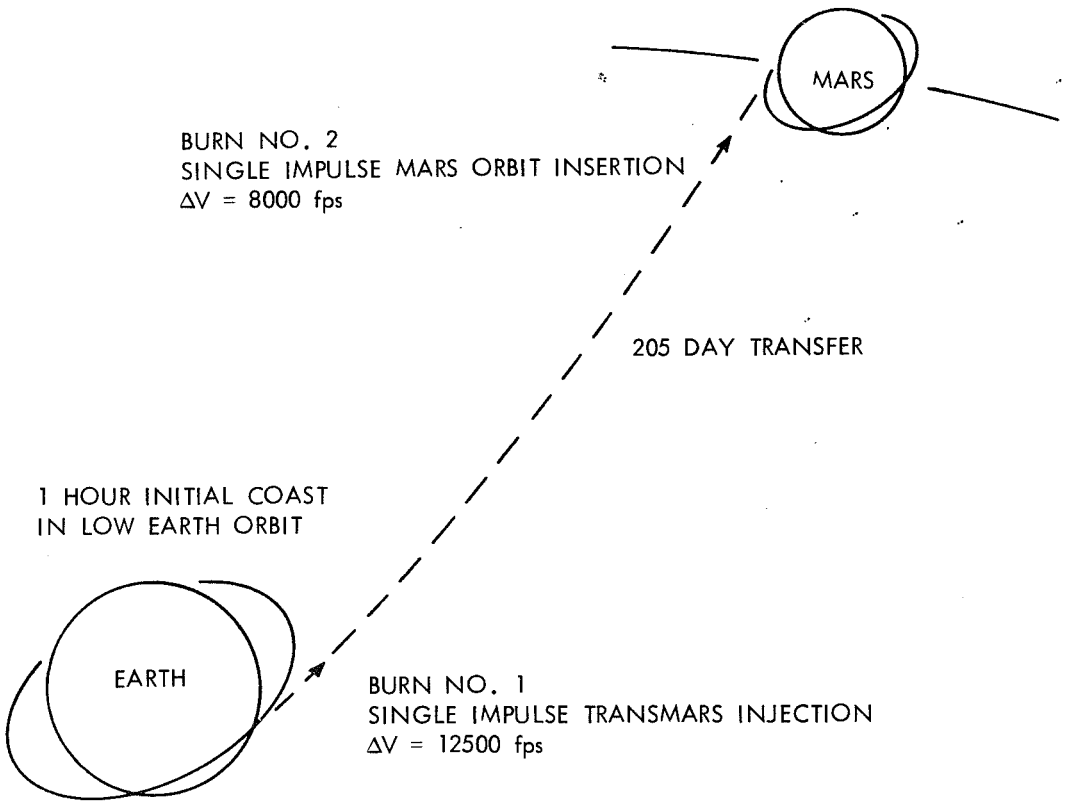

Figure 3-43 Mission Profile for a Two-Burn Mars Stage

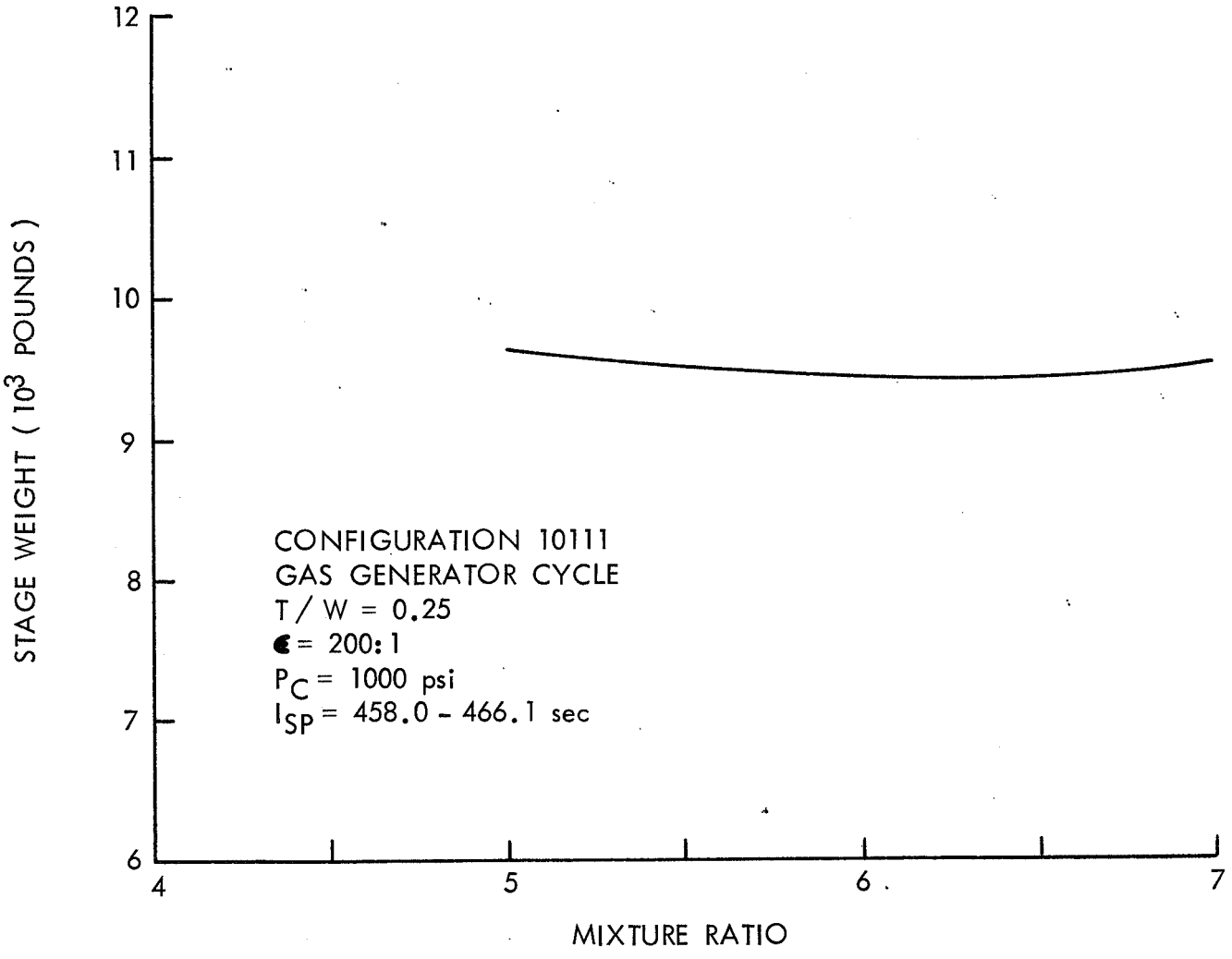

Figure 3-44 Mixture Ratio Optimization of the Single Burn Mars Stage

in figures 3-45 through 3-48. The optimum chamber pressure and area ratio for the two-burn Mars stage, were found to be 3,000 psi and 400:1, respectively. As shown in figure 3-48, the mixture ratio optimized at greater than 7.0:1.

The optimum mixture ratio of the two-burn stage is higher than that of the single-burn Mars stage, because the two-burn stage has a much more severe thermal problem, even though both stages have approximately the same mission duration. This results from the fact that during the interplanetary coast, the two-burn stage has a relatively larger tank surface area through which heat is entering, and only a fraction of the original propellant remaining is available to absorb this heat.

3.6.3 Sample Stage Weights and Design Charts

Weight statements and design characteristics for both Mars stages are given in tables 3-20 to 3-23. A significant difference between these two stages and those studied for the other missions was the meteoroid shielding. For these two stages the prime structure was assumed to be an open truss to permit the tanks to radiate heat to space and hence could not be used for meteoroid shielding. Instead, a separate bumper, in addition to the backup wall, was required to protect the tanks.

Since a non-vented stage would have some operational advantages over a vented stage for interplanetary missions, an analysis was conducted to determine the effect such a requirement would have on a one-burn Mars stage. The results are presented in table 3-24. Although for the non-vented case, the optimum insulation thicknesses and the tank design pressures both increased, there was only a small increase in overall stage weight.

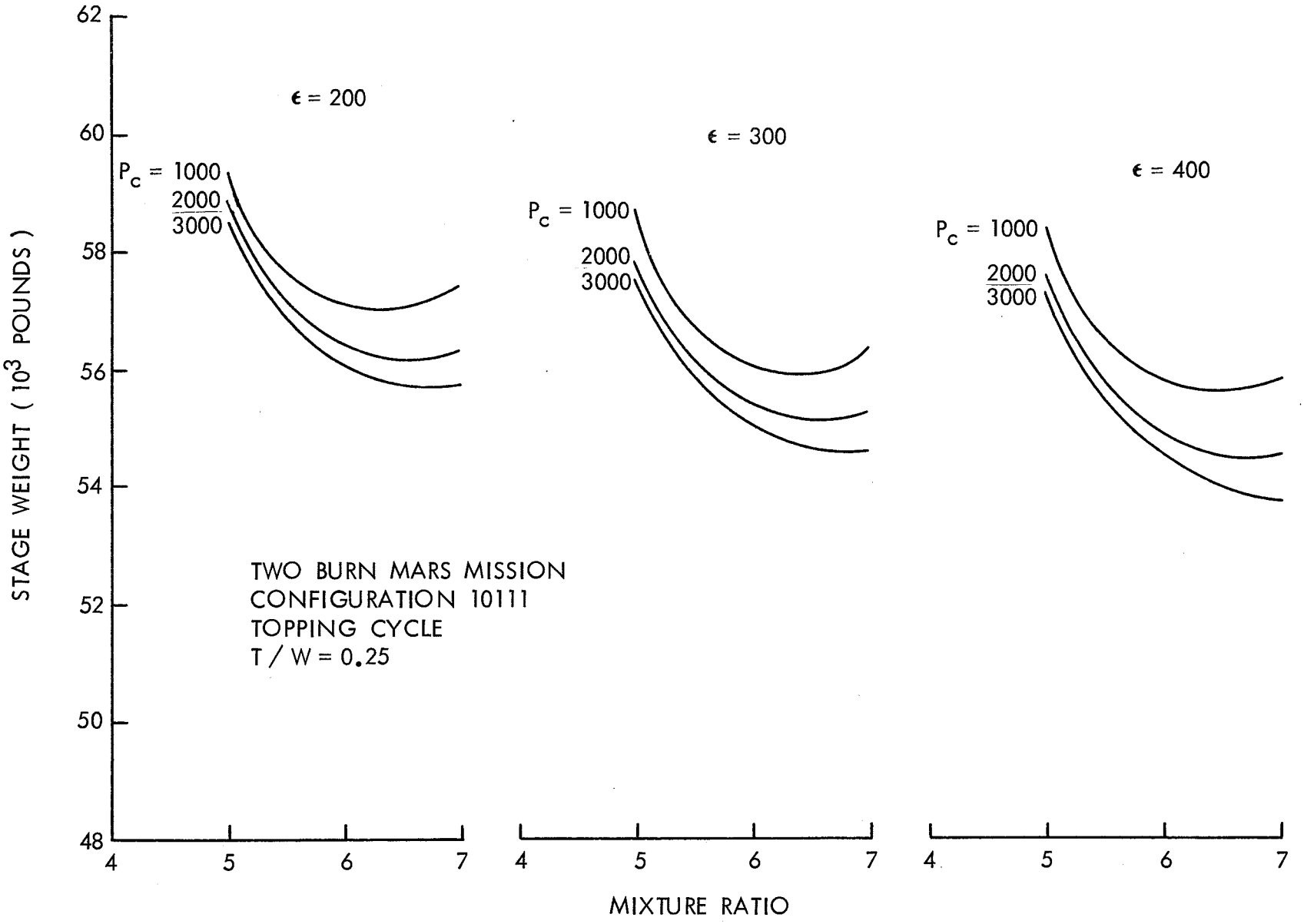

Figure 3-45 Engine Parameter Optimization for a Two Burn Mars Stage

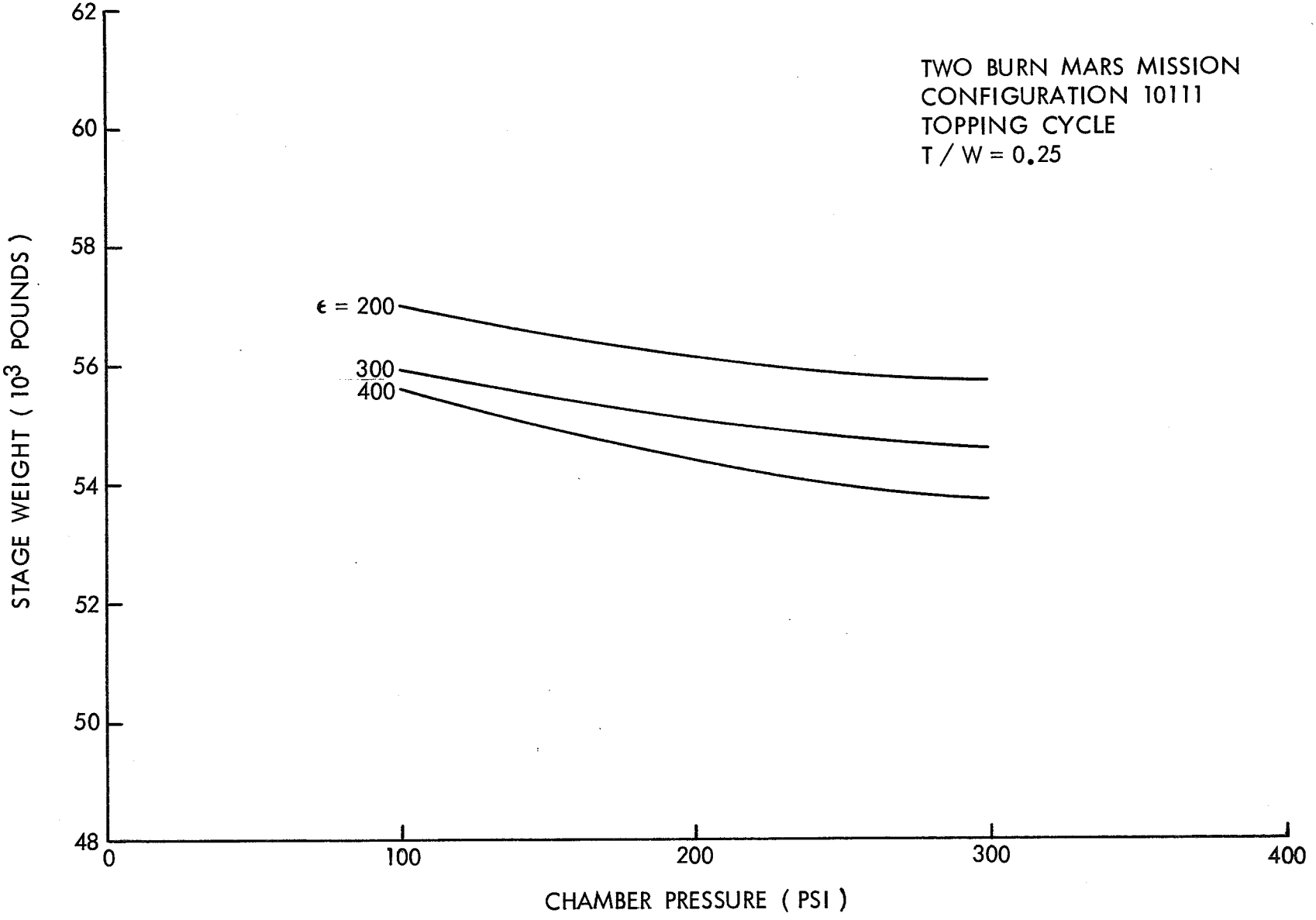

Figure 3-46 Chamber Pressure Optimization for a Two Burn Mars Stage

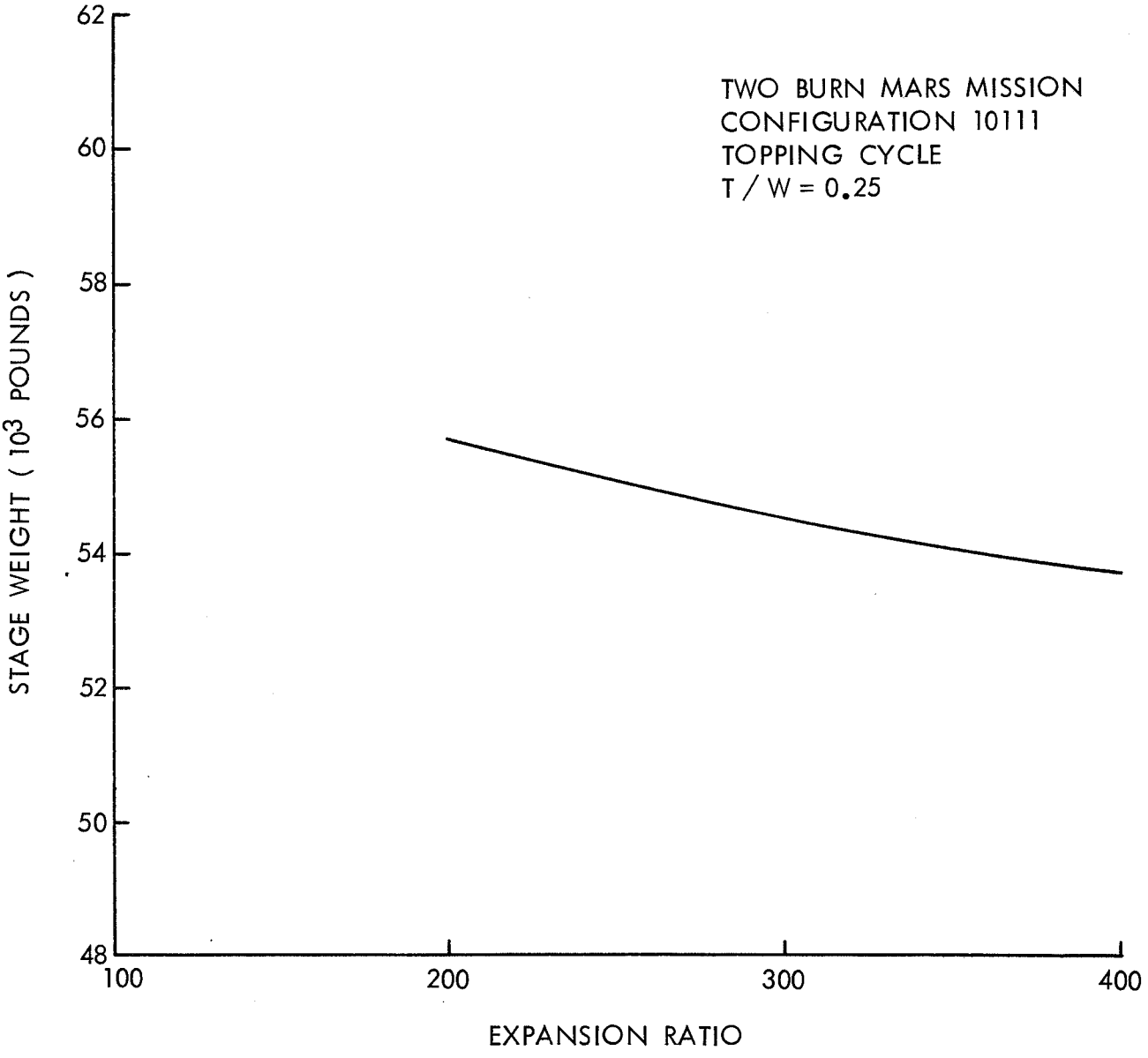

Figure 3-47 Expansion Ratio Optimization for a Two Burn Mars Stage

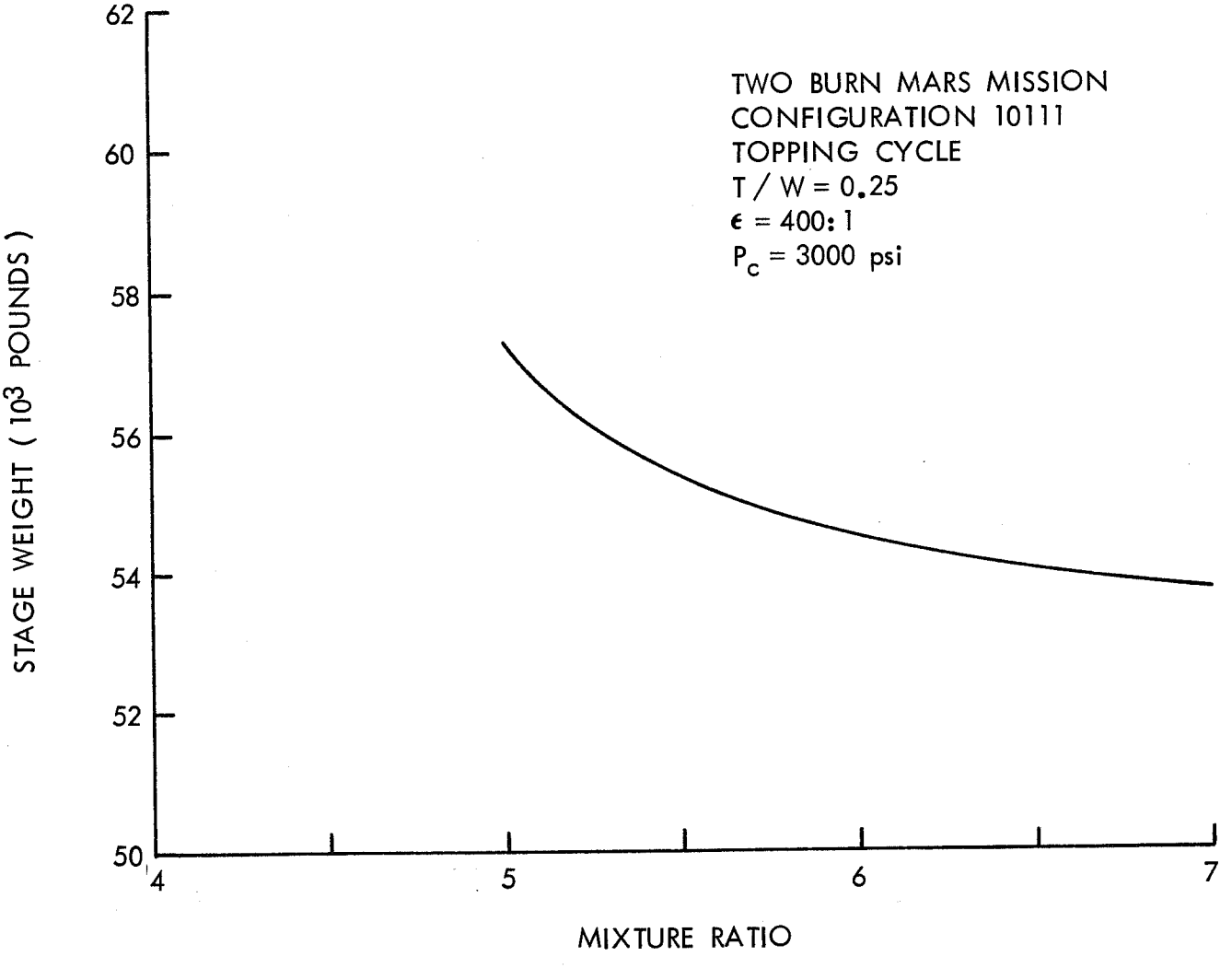

Figure 3-48 Mixture Ratio Optimization for a Two Burn Mars Stage

Table 3-20 Weight Summary of a Single Burn Mars Stage

STRUCTURE			539
TANKAGE		162	
Hydrogen	120		
Oxygen	42		
INTERSTAGE		0	
LANDING SYSTEMS		0	
SHELL		181	
THRUST STRUCTURE		44	
OTHER(TANK SUPPORTS, FEED SYSTEMS)		152	
METEOROID SHIELD			208
INSULATION			402
FUEL TANK		358	
OXIDIZER TANK		44	
PROPULSION			258
ENGINE		128	
OTHER INERT(RCS, PRESS)		130	
ASTRIONICS			550
MISCELLANEOUS FIXED WEIGHTS			130
CONTINGENCY(@ 7.5 %)			156

PROPELLANT INVENTORY			7100
TOTAL FUEL LOAD		1169	
Useable	965		
Residual	23		
Vented	166		
Final Ullage	12		
Startup/Shutdown	3		
TOTAL OXIDIZER LOAD		5931	
Useable	5793		
Residual	119		
Vented	0		
Final Ullage	4		
Startup/Shutdown	15		
PRESSURIZATION & INERT GASES			6
TOTAL LOAD		6	
Vented	1		
Residual	5		
RCS PROPELLANT			131
TOTAL FLUIDS			7237
CONSUMED		6907	
VENTED		167	
RESIDUAL		163	

BURN OUT WEIGHT	2406
TOTAL STAGE WEIGHT	9480
PROPELLANT FRACTION	0.713

Table 3-21 Design Data Summary of a Single Burn Mars Stage

COAST AND BURN NUMBER		1	
COAST TIME		4921	
PAYLOAD		7000	
VELOCITY INCREMENT(TOTAL- 8,000 fps)		8000	
PROPELLANT BURNED		6758	
FUEL VENT(incl. Press/Inert Gases)		13	
OXID. VENT(incl. Press/Inert Gases)		0	
ENGINE CHARACTERISTICS			
Thrust		4123	
Specific Impulse		465.2	
Area Ratio		200:1	
Mixture Ratio		6.0:1	
Chamber Pressure		1000	
TANKAGE	FUEL		OXIDIZER
Vent Pressure	61.0		59.0
Design Pressure	71.3		71.0
Insulation Thickness	4.04		1.14
Additional Meteoroid Shield Thickness			
Bumper	0.015		0.015
Backup Wall	0.021		0.019
Volume	303.1		93.3
STAGE GEOMETRY			
Overall Length		291.8	
Maximum Diameter		125.9	
Stage L/D		2.32	

Table 3-22 Weight Summary of a Two Burn Mars Stage

STRUCTURE			2461
TANKAGE		656	
Hydrogen	467		
Oxygen	189		
INTERSTAGE		0	
LANDING SYSTEMS		0	
SHELL		714	
THRUST STRUCTURE		232	
OTHER(TANK SUPPORTS, FEED SYSTEMS)		859	
METEOROID SHIELD			700
INSULATION			1506
FUEL TANK		1140	
OXIDIZER TANK		366	
PROPULSION			679
ENGINE		275	
OTHER INERT(RCS, PRESS)		404	
ASTRIONICS			550
MISCELLANEOUS FIXED WEIGHTS			130
CONTINGENCY(@ 7.5 %)			452

PROPELLANT INVENTORY			47441
TOTAL FUEL LOAD		7454	
Useable	6465		
Residual	149		
Vented	595		
Final Ullage	226		
Startup/Shutdown	19		
TOTAL OXIDIZER LOAD		39987	
Useable	38792		
Residual	800		
Vented	0		
Final Ullage	284		
Startup/Shutdown	111		
PRESSURIZATION & INERT GASES			18
TOTAL LOAD		18	
Vented	1		
Residual	17		
RCS PROPELLANT			614
TOTAL FLUIDS			48073
CONSUMED		46001	
VENTED		596	
RESIDUAL		1476	

BURN OUT WEIGHT	7954
TOTAL STAGE WEIGHT	54551
PROPELLANT FRACTION	0.830

Table 3-23 Design Data Summary of a Two Burn Mars Stage

COAST AND BURN NUMBER	1	2
COAST TIME	1	4920
PAYLOAD	7000	7000
VELOCITY INCREMENT(TOTAL 20,500 fps)	12500	8000
PROPELLANT BURNED	34460	10797
FUEL VENT(incl. Press/Inert Gases)	0	596
OXID. VENT(incl. Press/Inert Gases)	0	0

ENGINE CHARACTERISTICS	
Thrust	15389
Specific Impulse	473.3
Area Ratio	400:1
Mixture Ratio	6.0:1
Chamber Pressure	3000

TANKAGE	FUEL	OXIDIZER
Vent Pressure	39.0	49.0
Design Pressure	47.6	53.9
Insulation Thickness	4.12	2.74
Additional Meteoroid Shield Thickness		
Bumper	0.015	0.015
Backup Wall	0.024	0.022
Volume	1759.3	591.2

STAGE GEOMETRY	
Overall Length	454.7
Maximum Diameter	211.2
Stage L/D	2.15

Table 3-24 A Comparison of Vented and Non-Vented Stages

ITEM	VENTED	NONVENTED
STAGE WEIGHT (LB)	9480	9784
TOTAL PROPELLANT WEIGHT (LB)	7100	7151
TANKAGE WEIGHT (LB)		
HYDROGEN	120	268
OXYGEN	42	43
INSULATION WEIGHT (LB)		
HYDROGEN	358	396
OXYGEN	44	42
VAPOR VENTED (LB)		
HYDROGEN TANK	167	0
OXYGEN TANK	0	0
TANK DESIGN PRESSURE (PSI)		
HYDROGEN	71.32	145.86
OXYGEN	71.04	72.83
TANK VENT PRESSURE (PSI)		
HYDROGEN	61.00	130.50
OXYGEN	59.00	55.25
INSULATION THICKNESS (IN.)		
HYDROGEN	4.04	4.20
OXYGEN	1.14	1.08

Section 4

CONCLUSIONS AND RECOMMENDATIONS

The objective of this study was to provide NASA with data which could be used in assessing technology requirements for future NASA missions and to serve as an aid in allocating future resources. Conclusions as to "what is best" are therefore, not per se, a pertinent result of this study. However, some general comments and observations can be made which are discussed in the remaining paragraphs.

4.1 ENGINE CHARACTERISTICS

It was found that stage design was not greatly sensitive to the selection of engine chamber pressure, mixture ratio, area ratio or cycle. While optimums do exist, it is believed that the final selection of operating characteristics should be predicated on practicabilities such as availability, development risks, etc. Considering these qualifying remarks, the following generalities can be made with respect to future paper studies of stages using hydrogen and oxygen as propellants:

1. Chamber pressure and area ratio should be as high as practical;

2. Mixture ratio should be about 6.0:1 for relatively short duration missions and higher, if possible, for long duration missions;

3. Engine cycle should be selected according to the previous two recommendations but minimum thrust requirements should be considered for certain cycles. For example, the topping cycle engines have a thrust level below which they cannot be designed;

4. For stages weighing 50,000 lbs. or more, the number of engines may be selected on the basis of operational mission requirements since performance penalties for multiple engines are small. For smaller stages, the performance penalties associated with multiple engines must be considered;

5. Thrust-to-weight ratio optimizations should be considered, since a poorly selected thrust-to-weight ratio can result in significantly over-designed stages.

4.2 STAGE CONFIGURATION AND DIAMETER

The implications of stage characteristics such as configuration selection and diameter constraint vary according to stage size and mission requirement, therefore, generalizations are dangerous. In fact, these results show that it is best to consider interfaces such as the cargo hole diameter of the Earth Orbital Shuttle, EOS, from a total transportation

systems standpoint, i.e., how a diameter constraint affects the EOS and the Orbit-to-Orbit shuttle.

4.3 THERMAL AND METEOROID PROTECTION

In the area of thermal protection, this study suggests that the research and development of low density, low thermal conductivity insulation and effective heat blocks for tank supports will eventually pay off significantly in reducing the sizing requirements of stages designed for long duration missions. Similarly,meteoroid shielding can represent a very large fraction of the total inert weight of the stage. Thus, continued research into developing a better understanding of meteoroid shielding requirements and design techniques should prove to be an effective way of allocating available funds.

4.4 GENERAL OBSERVATIONS

The sizing requirements of stages used in a recoverable mode are extremely sensitive to assumed operational requirements such as coast time, initial orbit inclination, Isp's efficiencies and fixed inert weight (e.g., astrionics and similar systems). In some cases, as much as a 100% increase in stage size can be attendant with changing study groundrules. Thus, it would seem that trade-offs to develop optimum design criteria in these areas can be far more important in conceptual design studies than subsystem design trade-offs.

Appendix A

REFERENCES

REFERENCES

1. Cour-Palais, B. G., et al, "Meteoroid Environment Model - 1969 (Near Earth to Lunar Surface) NASA Space Vehicle Design Criteria Environment", Report NASA SP-8013, National Aeronautics and Space Administration, Washington, D. C., March 1969, page 18.

2. Ibid, page 19.

3. Ibid, page 21.

4. Cour-Palais, B. G., "Meteoroid Protection by Multiwall Structures", AIAA Paper No. 69-372, AIAA Hypervelocity Impact Conference, Cincinnati, Ohio, April 30 - May 2, 1969, American Institute of Aeronautics, New York.

5. Telecon - P. D. Thompson and Cour-Palais (MSC/NASA), March 11, 1971.

6. Schneider, E. J., "A Parametric Study of Attitude Control Systems (ACS) Design for a Space Vehicle", Report TB-EE-65-67, Chrysler Corporation, Space Division, New Orleans, Louisiana, March 2, 1966.

7. Letter from E. A. Lamont to G. M. Joseph, 70RC10270, Rocketdyne Division, North American Rockwell, Canoga Park, California, dated September 17, 1970, 6 enclosures.

8. Telecon - P. D. Thompson and E. A. Lamont (Rocketdyne), February 16, 1971.

9. Telecon - P. D. Thompson and F. Stephenson (OART/NASA), February 17, 1971.

10. "Nuclear Flight Systems Definition Study, Final Briefing," LMSC-A968323, Lockheed Missile & Space Company, Sunnyvale, California, May 19, 1970, page 2-5.

11. Meyer, H. J. and Minich, J. J., "Mission Definition, Performance Capability, and Operations Analysis of Chemical Orbit-to-Orbit Shuttle," Aerospace Report No. TOR-0059(6758-01)-17, Systems Engineering Operations, The Aerospace Corporation, El Segundo, California, December 18, 1970.

Appendix B

ENGINE DATA

ADVANCED TECHNOLOGY
30000 POUND THRUST
HIGH AREA RATIO
O_2/H_2 BELL ENGINE DESIGN

Rocketdyne
North American Rockwell

ADVANCED TECHNOLOGY 30000 POUND THRUST HIGH AREA RATIO O_2/H_2 ENGINE DESIGN

The high area ratio O_2/H_2 engine design is a 30000 pound thrust, 750 psia chamber pressure, mixture ratio 5, 150 area ratio, 80 percent length bell engine having an expander drive cycle. The design makes maximum use of technology resulting from Air Force and NASA contracts and company funded efforts. The basic engine concept is illustrated in Fig. 1.

Major engine parameters are shwon in Fig. 1. The engine delivers a specific impulse of 462.7 lb_f-sec/lb_m and weighs 375 pounds. The engine has throttling capability and can have, if required, a low thrust idle mode operation for propellant settling or small maneuvers.

ENGINE OPERATION

The engine requires no preconditioning and has a rapid start after liquid reaches the valve inlets. The engine is capable of an unlimited number of restarts and can be restarted immediately after shutdown. Mixture ratio excursions for propellant utilization can be made from 4.5:1 to 6:1.

Start time is approximately 2.5 seconds after liquid propellants are available at the valve inlets.

BELL EXPANDER CYCLE CONFIGURATION

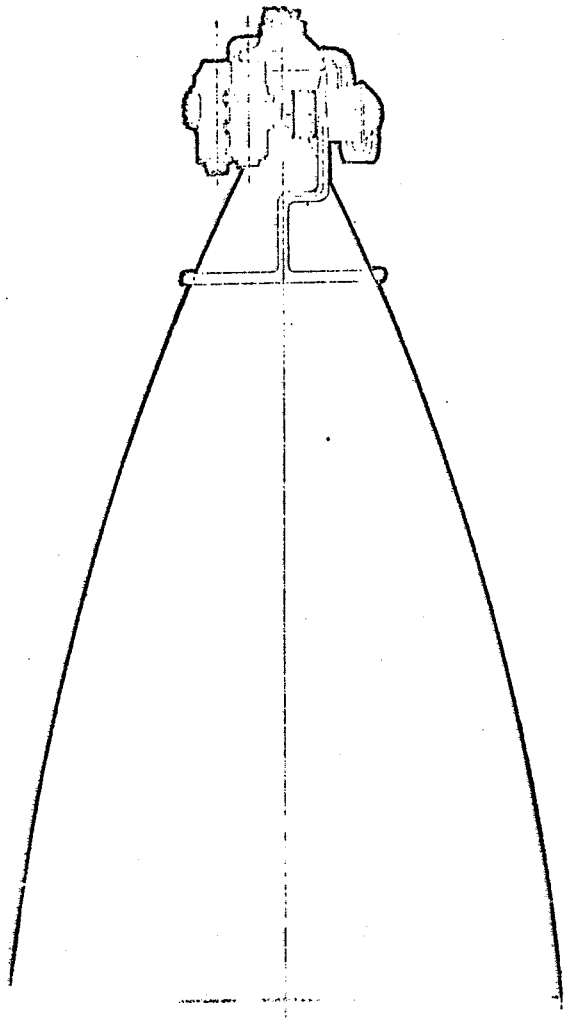

◎ THRUST, POUNDS	30,000
◎ CHAMBER PRESSURE, PSIA	750
◎ AREA RATIO	150:1
◎ ENGINE MIXTURE RATIO	5:1
◎ SPECIFIC IMPULSE, SEC	462.7
◎ LENGTH, IN.	97.0
◎ DIAMETER, INCHES	61.0
◎ WEIGHT, POUNDS	375.0

Figure 1

Approximate full thrust start and cutoff propellant requirements are:

	Propellant	Amount (lbs)	Impulse
Start (achieving full thrust and ±.5 nominal MR)	H_2	13	
	O_2	40	15000 lb-sec
Cutoff	H_2	10	
	O_2	33	20000 lb-sec

The engine can be started at any thrust with proportionately reduced propellant usage.

ENGINE DRIVE CYCLE

The power cycle as shown in Fig. 2 is an expander cycle using 95 percent of the hydrogen flow to power the turbines. The 5 percent margin is intended for control purposes. Individual turbines powered in a parallel flow arrangement are provided for each pump. The trubines are single row velocity compounded and provide 1561 horsepower for the two stage centrifugal fuel pump and 228 horsepower for the one stage centrifugal oxidizer pump. After experiencing a 40°R temperature drop through the turbines, the hydrogen enters the injector with a temperature of 250°R.

THRUST CHAMBER DESIGN

The thrust chamber uses a seven inch combustion chamber and an optimum bell expansion nozzle. The combustion chamber is of channel construction while the nozzle, starting at a low area ratio, is of tubular construction.

ADVANCED O_2/H_2 BELL ENGINE

FLOW SCHEMATIC EXPANDER CYCLE

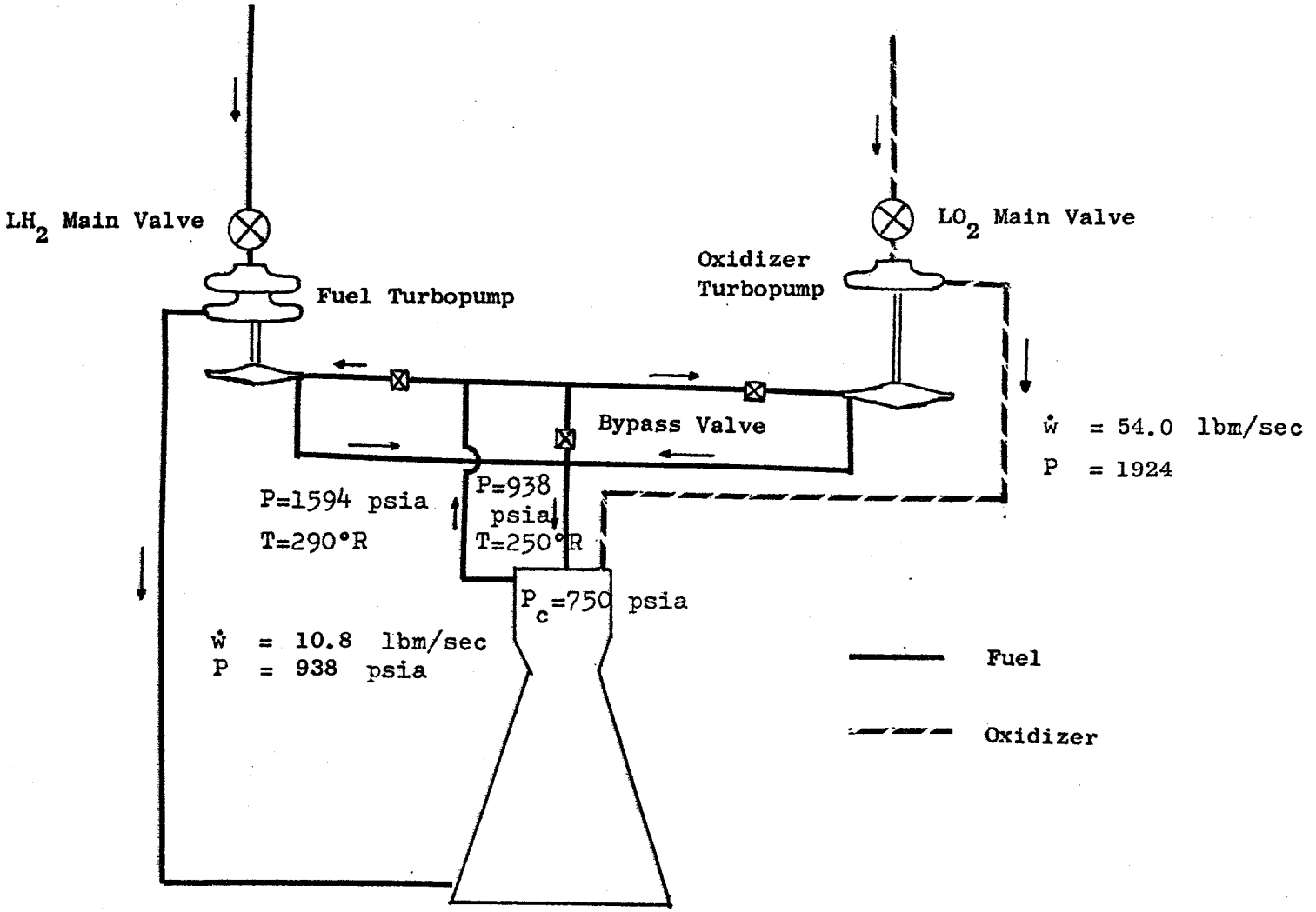

Figure 2

A concentric element injector is used. This injector surrounds a central core of oxygen with high velocity hydrogen to provide both high combustion efficiency and acceptable heat transfer to the chamber wall.

TURBOMACHINERY DESIGN

The oxidizer pump is a one stage centrifugal design producing a pressure rise of 908 psia at a speed of 24000 rpm with an efficiency of 0.79. The required NPSH is 21.0 feet (10.0 psia NPSP).

The fuel pump is a two stage centrifugal design producing a pressure rise of 1864 psia at a speed of 69,500 rpm with an efficiency of 0.76. The required NPSH is 96 feet (3.0 psia NPSP).

Both the oxidizer and fuel pumps are coupled with inducers. If preinducers are also used, the oxidizer and fuel NPSH requirements can be lowered to 8.4 feet and 38.4 feet, respectively. Preinducer drive would be either hydraulic or hot gas.

Both fuel and oxidizer turbines are single row velocity compounded designs allowing speeds compatible with those dictated by the pump designs since the pumps and turbines are directly coupled. The oxidizer turbine is 20 percent admission. Both turbines operate at the same pressure ratio and have a turbine inlet temperature of 290°R. The oxidizer turbine efficiency is 0.56 while the fuel turbine efficiency is 0.77. Turbomachinery parameters are given in Table 1.

IGNITION SYSTEM

Ignition is achieved using a platinum wire resistance element. Before propellants begin to flow, a heating pulse is sent through the platinum wire coil. Low mixture ratio propellants are then introduced to the igniter. After ignition in the igniter, main injector propellant flow is started. Upon main chamber ignition,

TABLE 1

ADVANCED TECHNOLOGY O_2/H_2 BELL

FUEL PUMP TYPE - 2 STAGE CENTRIFUGAL
OXIDIZER PUMP TYPE - 1 STAGE CENTRIFUGAL
TURBINES - 1 ROW VELOCITY COMPOUNDED, PARALLEL ARRANGEMENT

	OXIDIZER	FUEL
PUMP		
PRESSURE RISE, PSIA	908	1864
SPEED, RPM	24000	69500
EFFICIENCY	0.79	0.76
TURBINE		
INLET TEMPERATURE, °R	290	290
SPEED, RPM	24000	69500
PRESSURE RATIO	1.7	1.7
EFFICIENCY	0.56	0.77
PERCENT ADMISSION	20	100

the oxidizer flow to the igniter is cut off and hydrogen only is allowed to flow through the igniter during mainstage.

If a more rapid restart is required, a controlled power, low radio frequency interference, spark plug igniter could be used to reduce the ignition time to 1 millisecond from 0.8 seconds.

ENGINE - VEHICLE INTERFACE REQUIREMENTS

Connections required between the engine and vehicle are mechanical, fluid, and electrical. The locations of the principle interface mechanical connections are shown in Figure 3.

The mechanical connection for thrust transmission is at the forward face of the gimbal block. Thrust alignment is maintained within 30 minutes annular and 1/8" lateral of the engine axial centerline. Two electromechanical gimbal actuators, located 90° apart are capable of a thrust vector angle of at least 10 degrees with a steady-state control of 1/2° at 2.5 HZ. The actuators can gimbal the engine at velocities up to 27 degree/sec. Approximate gimbal torque requirements are 1,400 ft-lb.

Fluid connections are required for the propellant supply lines, tank pressurant lines, and purge supply lines. These lines have flexibility to withstand the forces of gimbaling, thermal expansion, and manufacturing misalignment.

The vehicle main propellant supply lines interface with the engine at the main valve inlets. The oxidizer and fuel inlets positions are shown in Figure 3. They are below the gimbal point to allow leeway in propellant line positioning. Both valve inlets are fitted with standard flange attachments.

Tank pressurants in the form of heated propellants and/or helium are provided by the engine. The pressurant and purge lines interface with the vehicle at the fluid panel.

ENGINE-VEHICLE INTERFACE POSITIONS

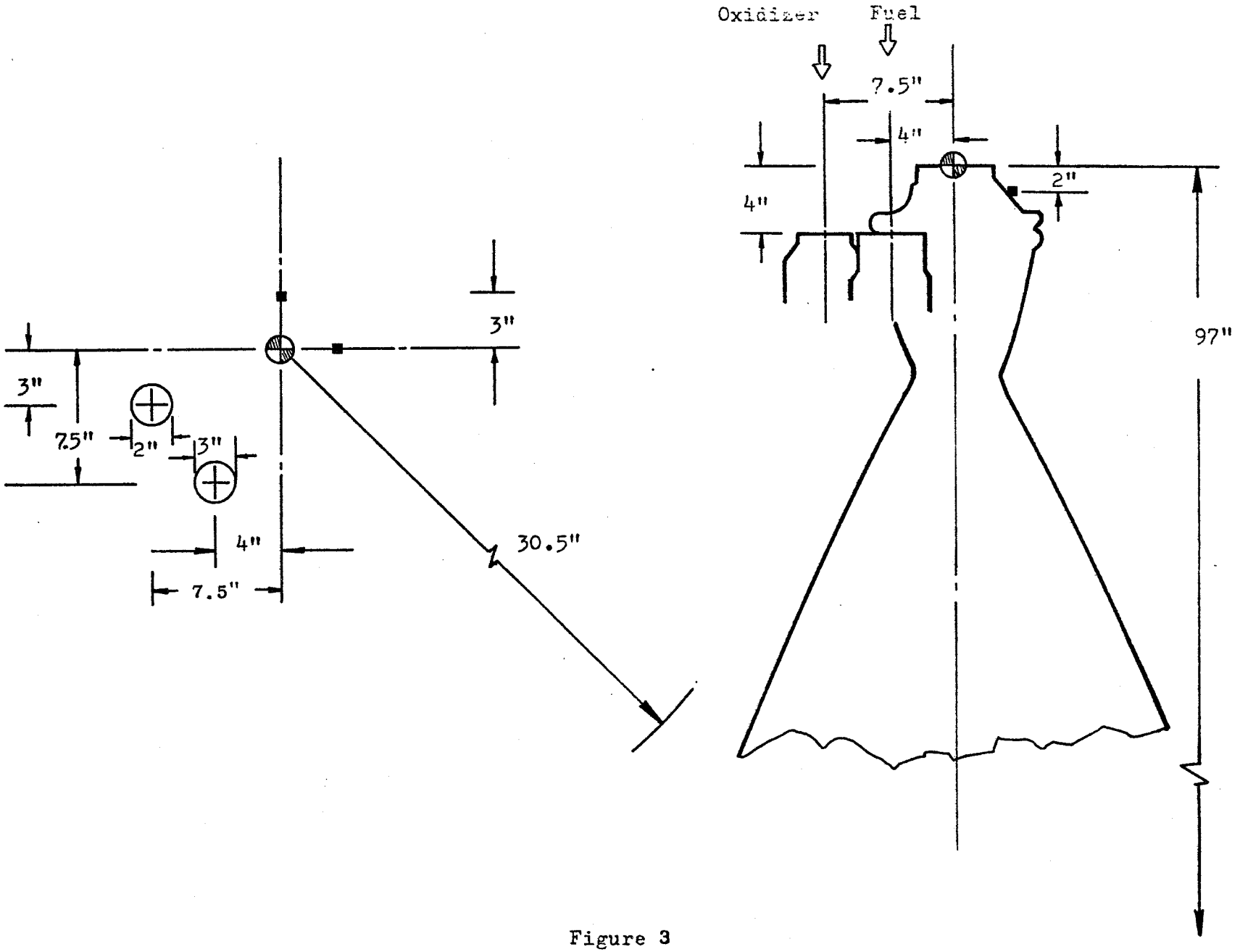

Figure 3

A single interface panel is required to provide electrical power to the engine and to transmit control signals between the engine and vehicle.

Propellant Supply Requirements

The required NPSH values for the pumps are:

	Fuel Pump	Oxidizer Pump
Without Preinducer	96 ft	21 ft
With Preinducer	38.4 ft	8.4 ft

Assuming oxidizer and fuel valve losses of 10 and 5 psia respectively, the required net positive pressure, at the engine inlet before the main valves are:

	Fuel Inlet	Oxidizer Inlet
Without Preinducer	8.0 psia	20 psia
With Preinducer	6.2 psia	14 psia

Pneumatic Requirements

Pneumatics are required for engine and seal purges. Purge requirements for each engine operating cycle are:

		Regulated Purge Press. (psia)	Purge Flowrate (scfm)	Required Purge Temp °F
Oxidizer System	Helium	750	75	180
Fuel System	Helium	750	100	180
Oxidizer Pump Seal	Helium	750	4.4	180

The oxidizer pump seal purge is used throughout engine operation. The oxidizer system purge operates for approximately 1 second at start. The oxidizer system purge operates for approximately 4 seconds and the fuel system purge for 2 seconds at cutoff.

The pneumatic requirement for main valve actuation assuming a 3000 psi helium supply pressure regulated at 750 psi (- 200°R) is 2600 standard cubic inches for each firing.

Electrical Requirements

The electrical power requirements for each engine operating cycle including gimbal actuation, valve actuation, engine controller package ignition system and engine instrumentation are:

Voltage	Total Power Requirement, Watts
26-30 DC	170 - 260*
26-30 DC	80 - 120**
110 AC	25*
2 DC	36***

* Continuous power during engine operation

** Power only during purge operation

*** Power only during 0.8 second ignition sequence. Can be provided from other DC sources by stepdown transformer.

The 110 AC source is preferred but other power sources may be acceptable.

PARAMETRIC ENGINE PERFORMANCE

Parametric engine performance, weight and size date for optimization studies are presented in Fig. 4 to 20. The data are for engines similar to the detailed design presented.

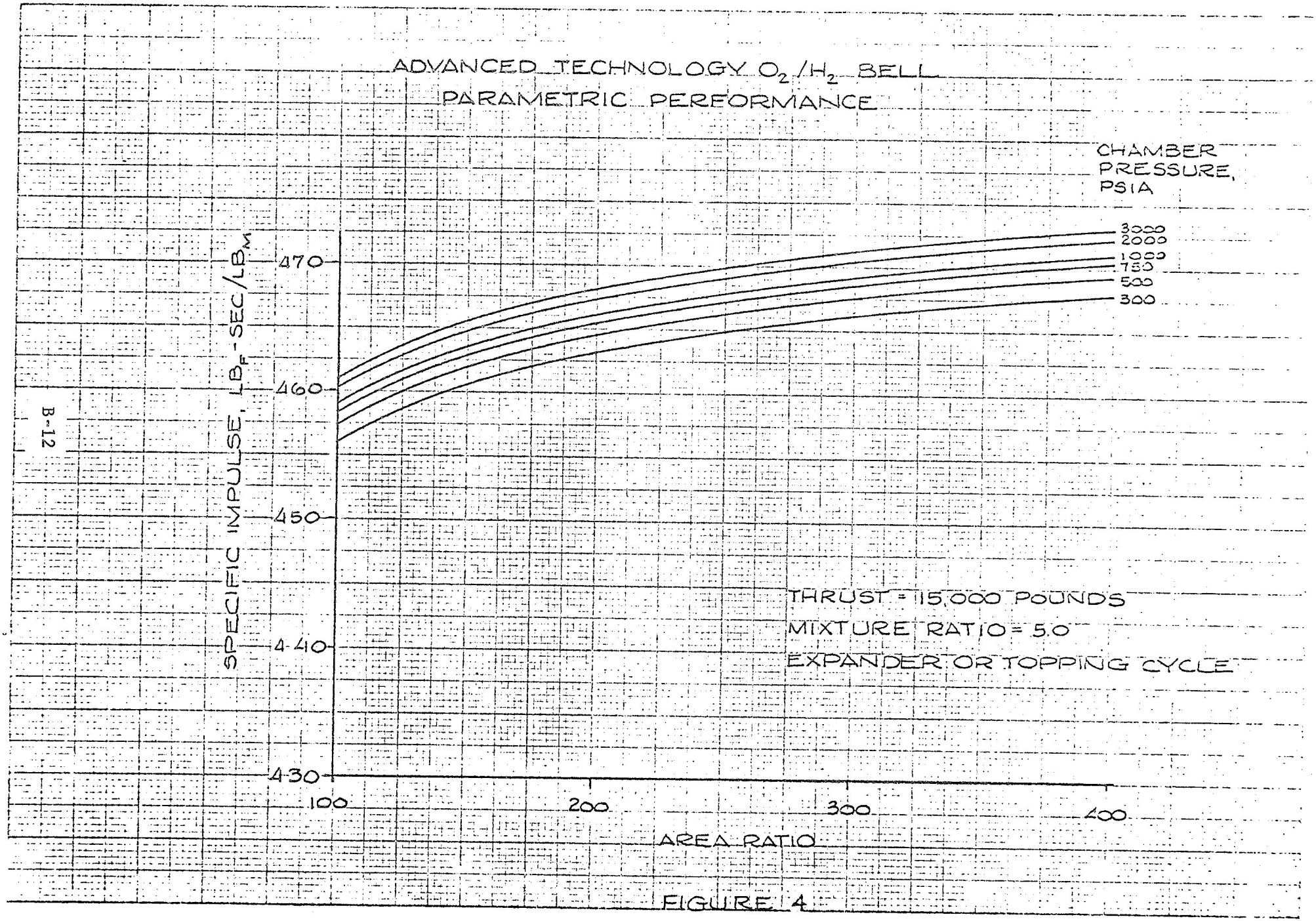
ADVANCED TECHNOLOGY O_2/H_2 BELL
PARAMETRIC PERFORMANCE
CHAMBER PRESSURE, PSIA
3000
2000
1000
750
500
300
SPECIFIC IMPULSE, LB_F-SEC/LB_M
470
460
450
440
430
100
200
300
400
AREA RATIO
THRUST = 15,000 POUNDS
MIXTURE RATIO = 5.0
EXPANDER OR TOPPING CYCLE

FIGURE 4

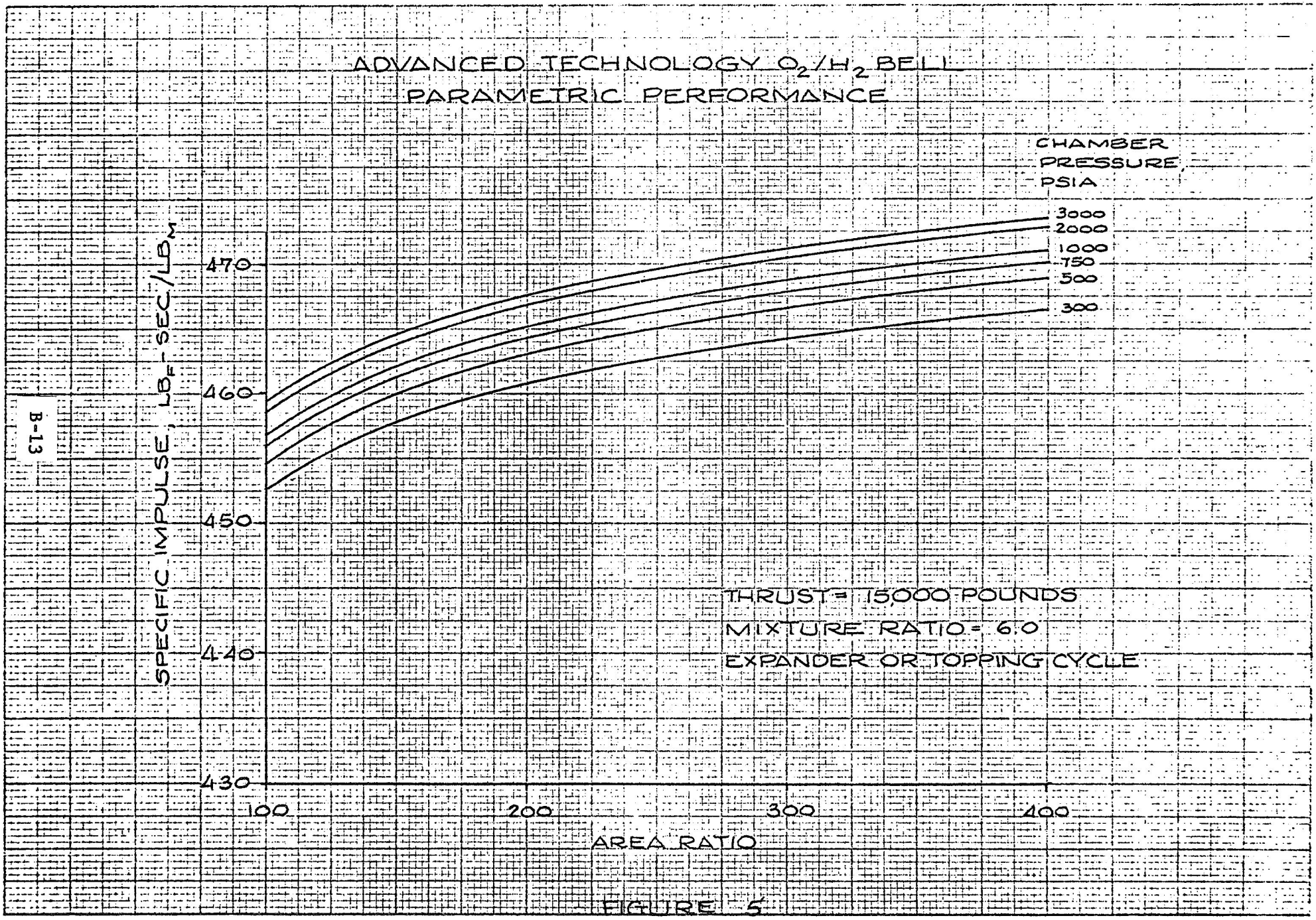
ADVANCED TECHNOLOGY O_2/H_2 BELL
PARAMETRIC PERFORMANCE
CHAMBER PRESSURE, PSIA
3000
2000
1000
750
500
300
SPECIFIC IMPULSE, LB_F-SEC/LB_M
470
460
450
440
430
THRUST = 15,000 POUNDS
MIXTURE RATIO = 6.0
EXPANDER OR TOPPING CYCLE
100
200
300
400
AREA RATIO

FIGURE 5

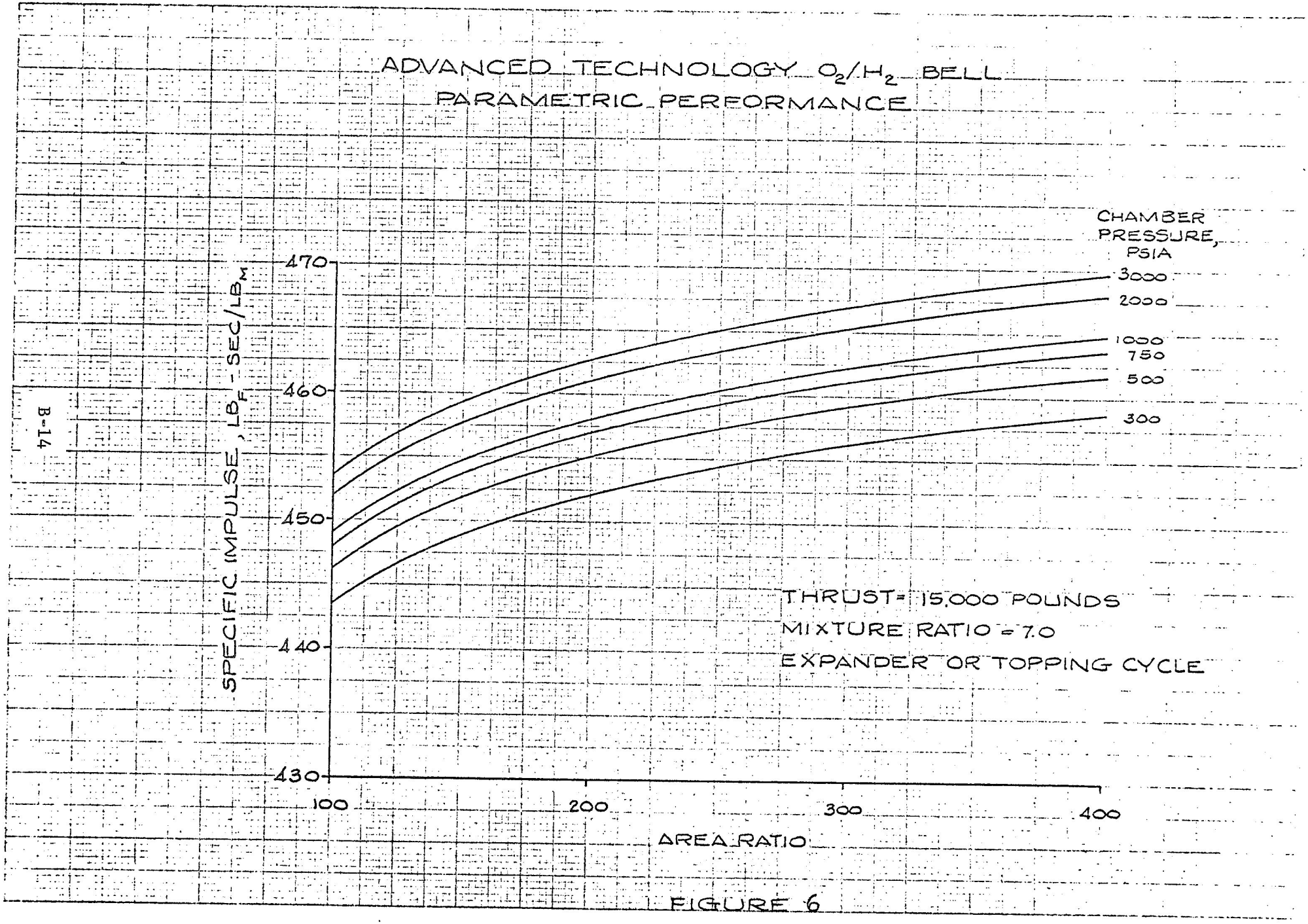
ADVANCED TECHNOLOGY O_2/H_2 BELL
PARAMETRIC PERFORMANCE
CHAMBER PRESSURE, PSIA
3000
2000
1000
750
500
300
SPECIFIC IMPULSE, LB_F - SEC/LB_M
470
460
450
440
430
100
200
300
400
AREA RATIO
THRUST = 15,000 POUNDS
MIXTURE RATIO = 7.0
EXPANDER OR TOPPING CYCLE

FIGURE 6

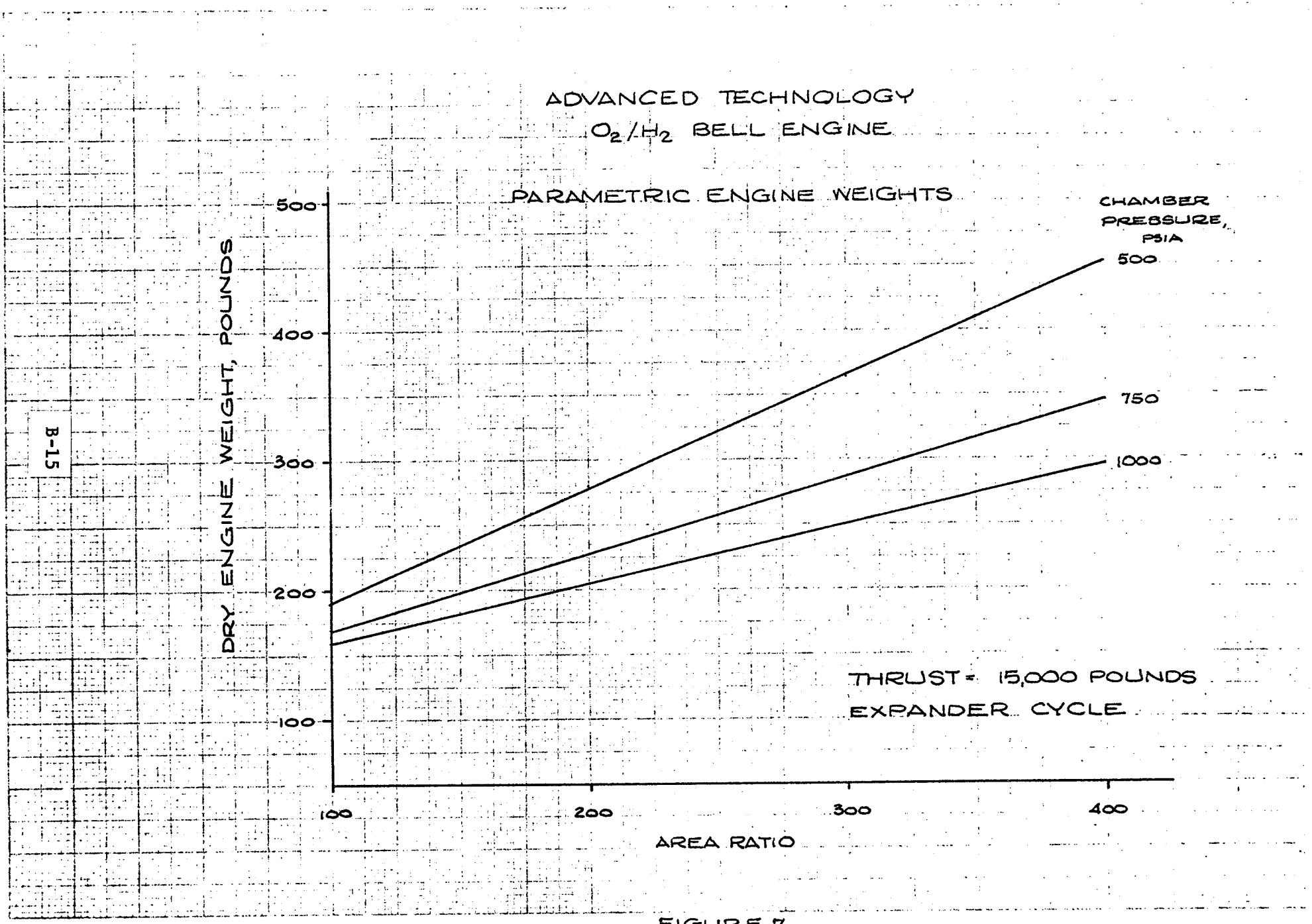
ADVANCED TECHNOLOGY
O_2/H_2 BELL ENGINE
PARAMETRIC ENGINE WEIGHTS
CHAMBER PRESSURE, PSIA
500
750
1000
DRY ENGINE WEIGHT, POUNDS
500
400
300
200
100
100
200
300
400
AREA RATIO
THRUST = 15,000 POUNDS
EXPANDER CYCLE

FIGURE 7

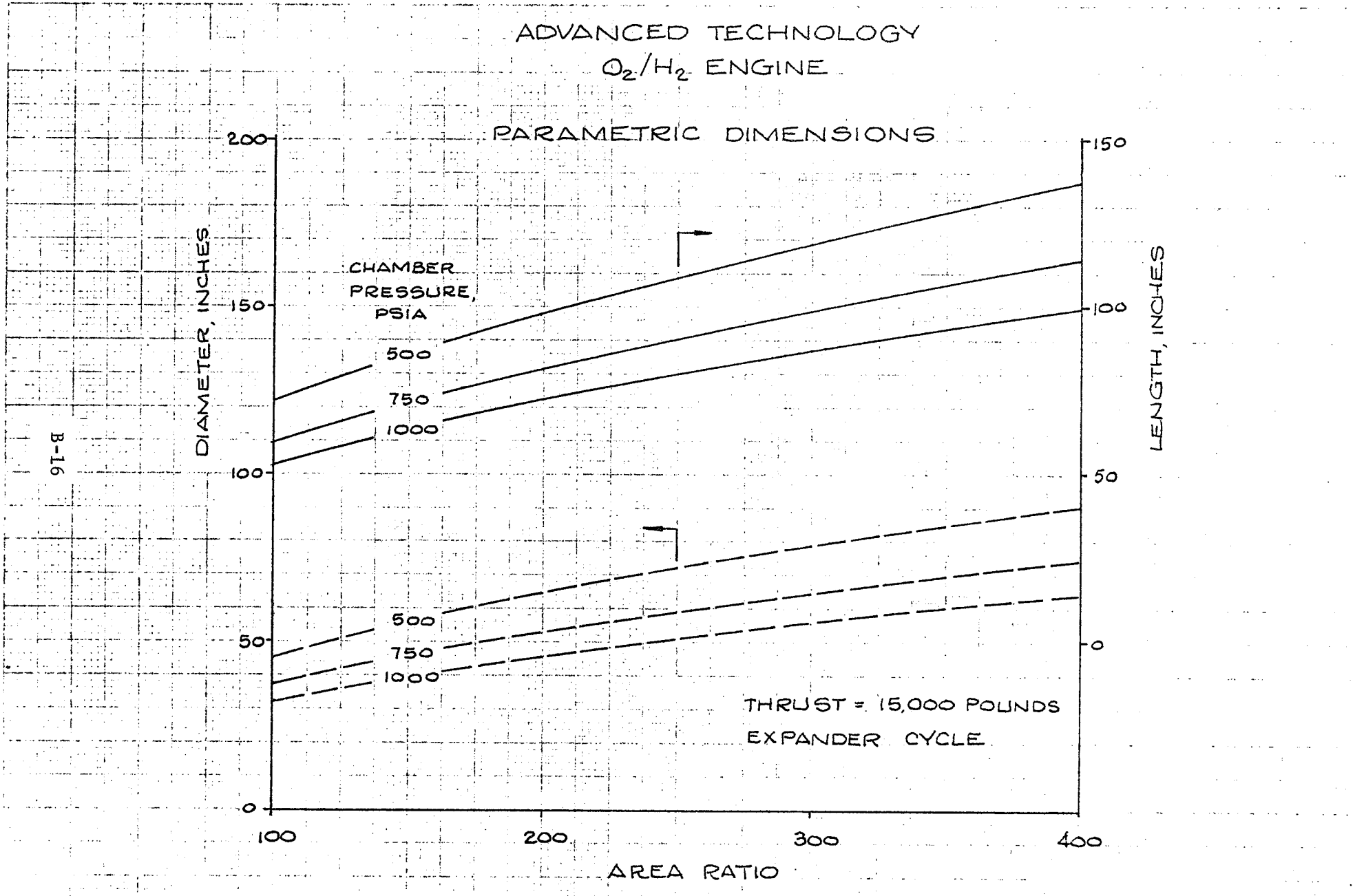
ADVANCED TECHNOLOGY
O_2/H_2 ENGINE
PARAMETRIC DIMENSIONS
DIAMETER, INCHES
LENGTH, INCHES
CHAMBER PRESSURE, PSIA
500
750
1000
500
750
1000
THRUST = 15,000 POUNDS
EXPANDER CYCLE
AREA RATIO
200
150
100
50
0
150
100
50
0
100
200
300
400

FIGURE 8

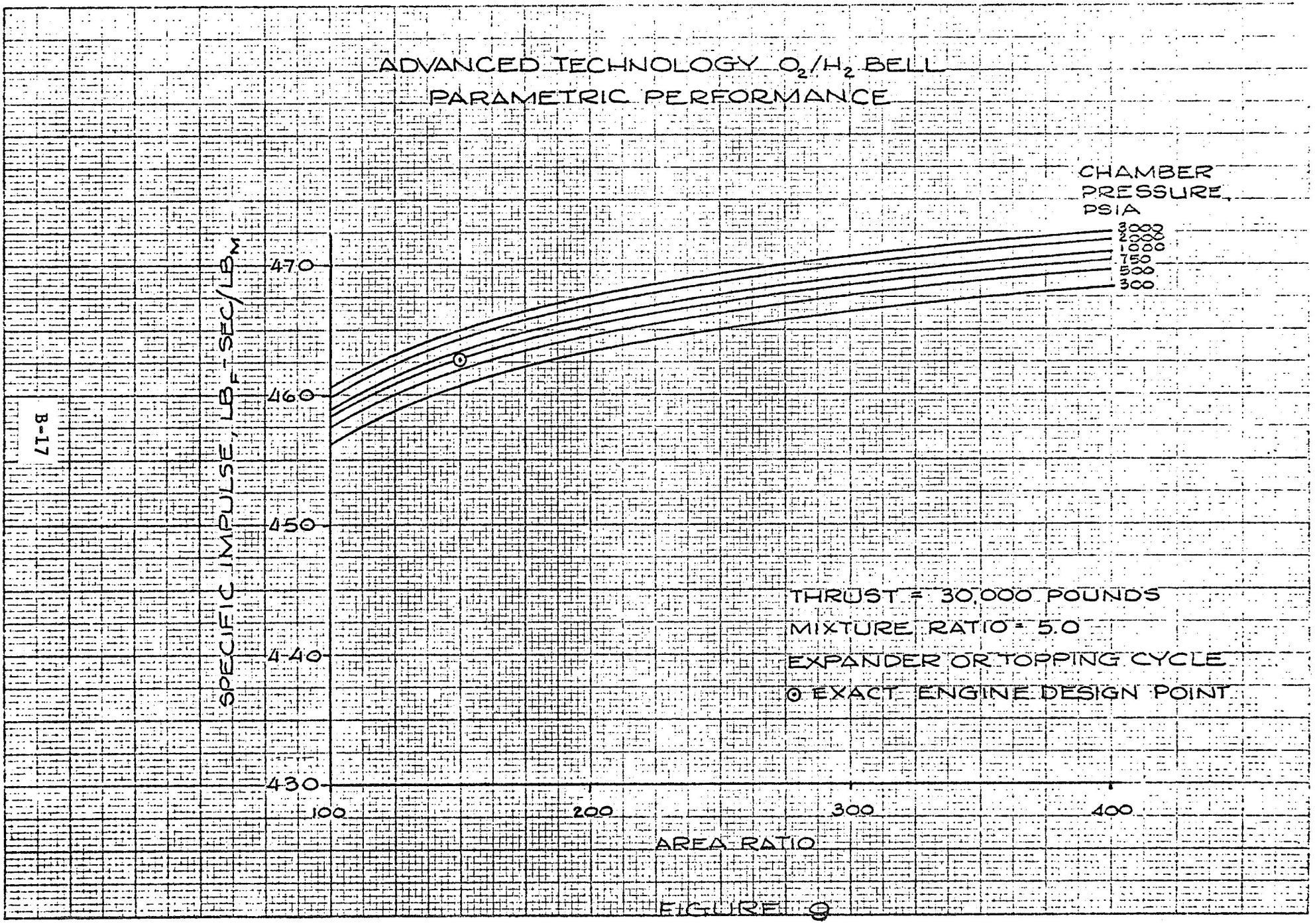
ADVANCED TECHNOLOGY O_2/H_2 BELL
PARAMETRIC PERFORMANCE
CHAMBER PRESSURE, PSIA
3000
2000
1000
750
500
300
SPECIFIC IMPULSE, LB_F-SEC/LB_M
470
460
450
440
430
100
200
300
400
AREA RATIO
THRUST = 30,000 POUNDS
MIXTURE RATIO = 5.0
EXPANDER OR TOPPING CYCLE
⊙ EXACT ENGINE DESIGN POINT

FIGURE 9

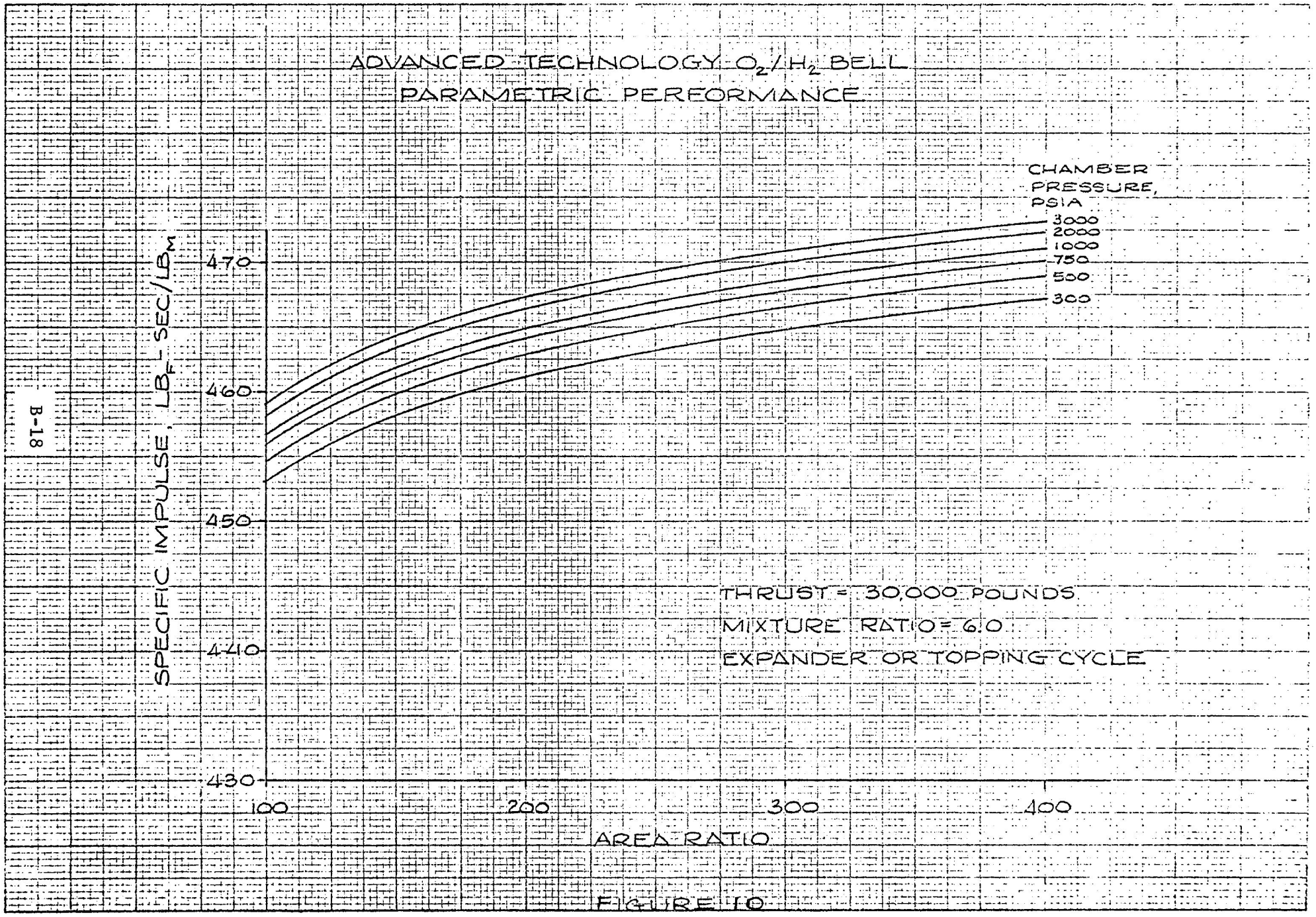
ADVANCED TECHNOLOGY O_2/H_2 BELL
PARAMETRIC PERFORMANCE
CHAMBER PRESSURE, PSIA
3000
2000
1000
750
500
300
SPECIFIC IMPULSE, LB_F-SEC/LB_M
470
460
450
440
430
100
200
300
400
AREA RATIO
THRUST = 30,000 POUNDS
MIXTURE RATIO = 6.0
EXPANDER OR TOPPING CYCLE

FIGURE 10

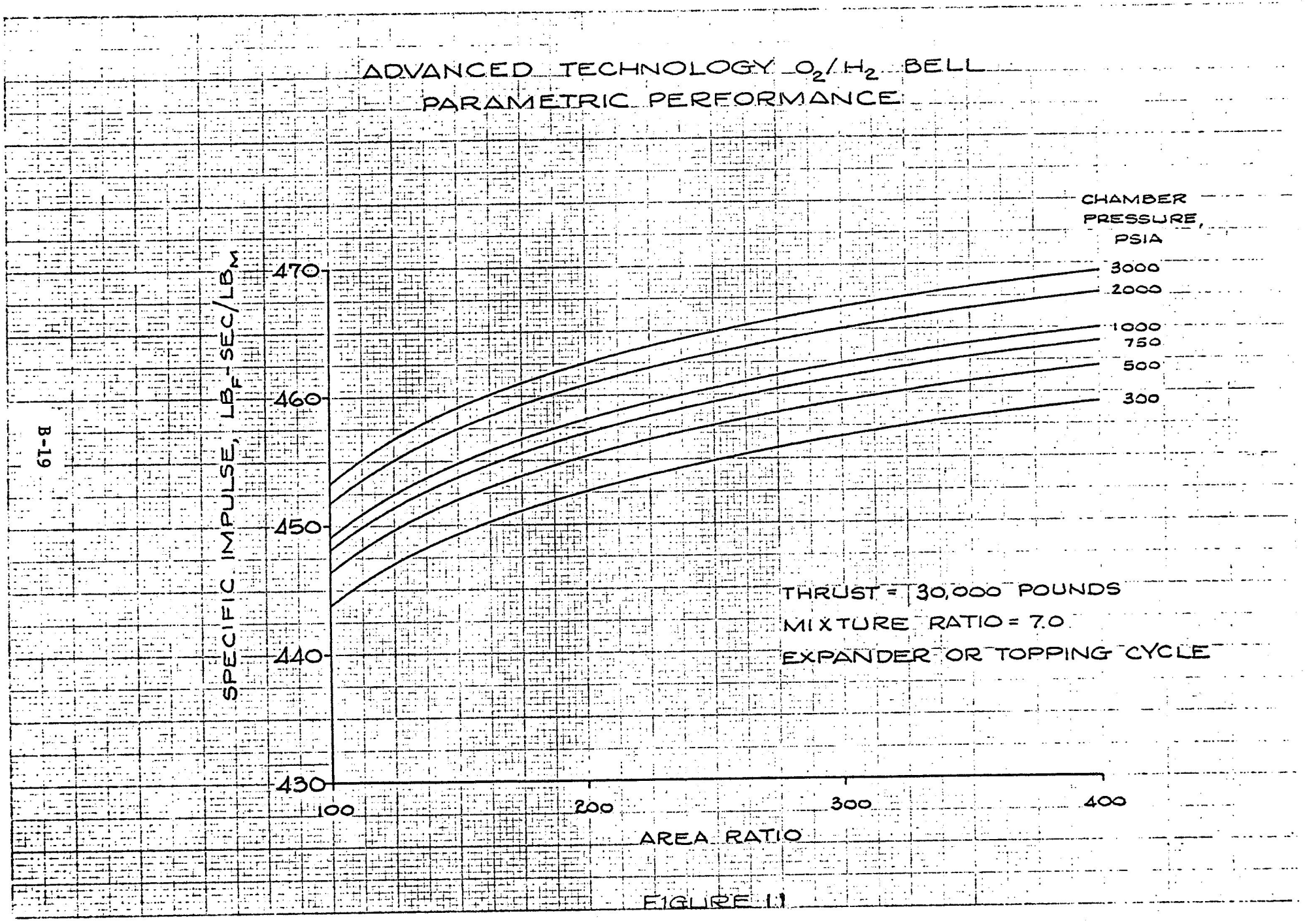
ADVANCED TECHNOLOGY O_2/H_2 BELL
PARAMETRIC PERFORMANCE
CHAMBER PRESSURE, PSIA
3000
2000
1000
750
500
300
SPECIFIC IMPULSE, LB_F-SEC/LB_M
470
460
450
440
430
100
200
300
400
AREA RATIO
THRUST = 30,000 POUNDS
MIXTURE RATIO = 7.0
EXPANDER OR TOPPING CYCLE

FIGURE 11

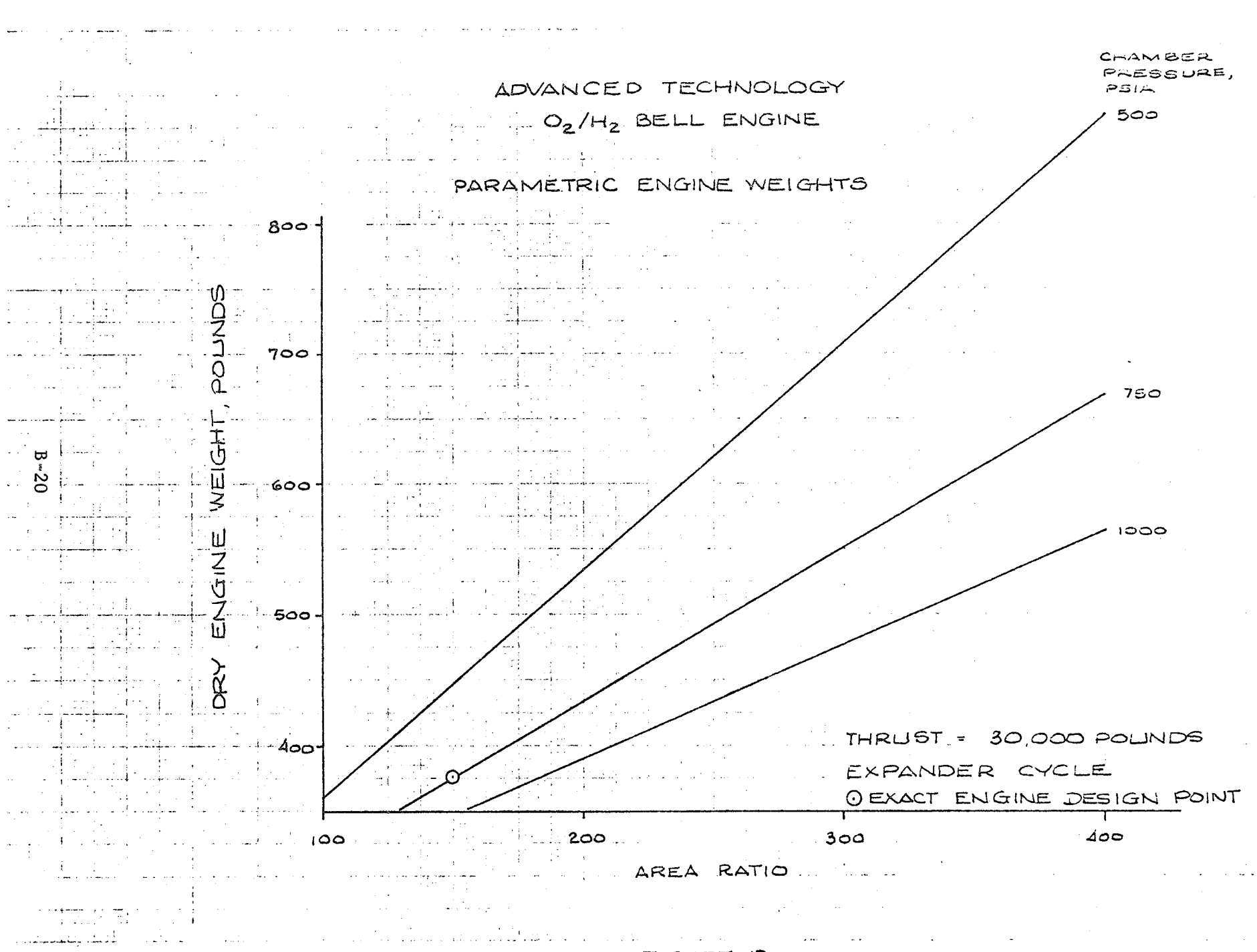
ADVANCED TECHNOLOGY
O_2/H_2 BELL ENGINE
PARAMETRIC ENGINE WEIGHTS
CHAMBER PRESSURE, PSIA
500
750
1000
DRY ENGINE WEIGHT, POUNDS
800
700
600
500
400
100
200
300
400
AREA RATIO
THRUST = 30,000 POUNDS
EXPANDER CYCLE
⊙ EXACT ENGINE DESIGN POINT

FIGURE 12

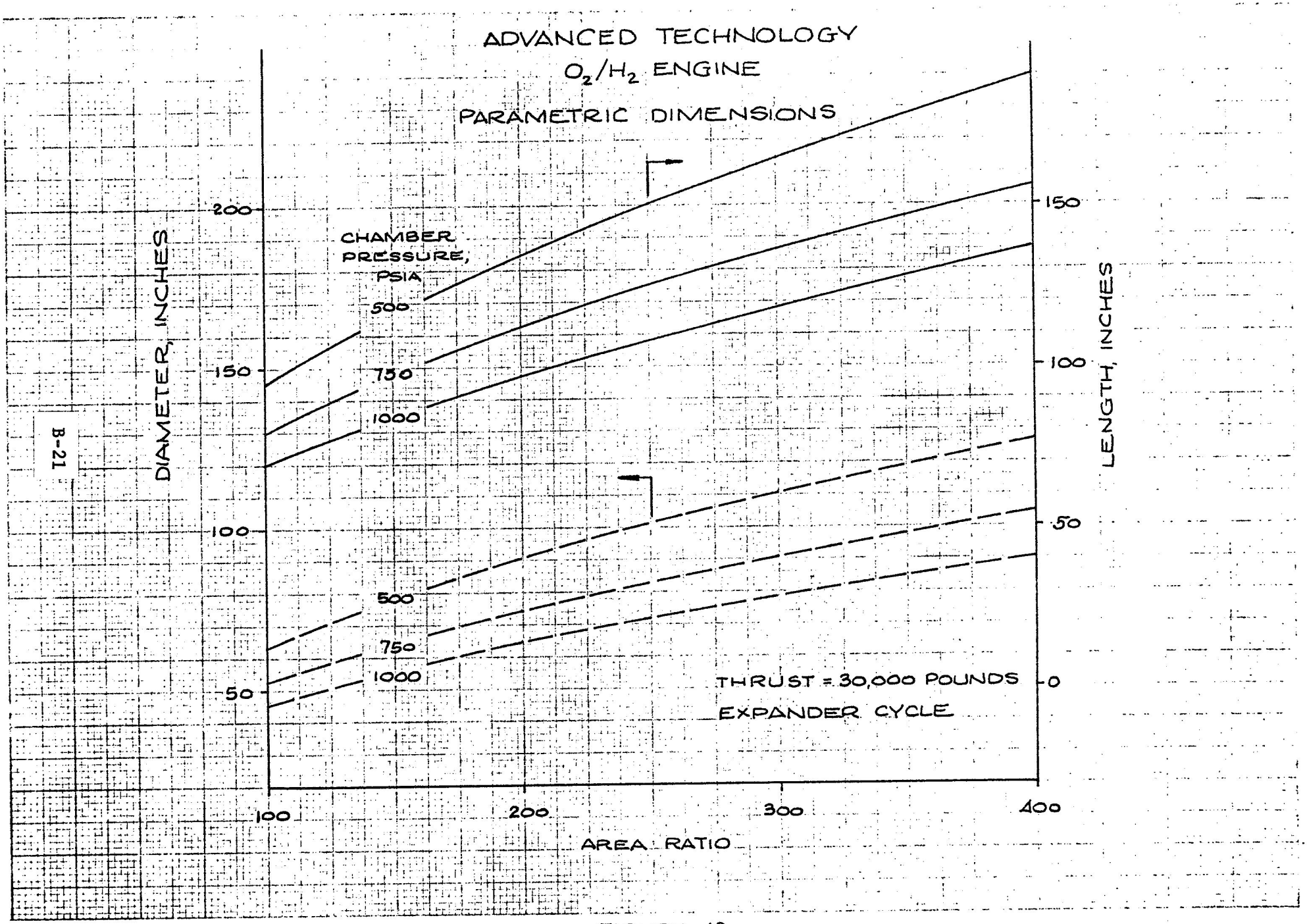
ADVANCED TECHNOLOGY
O_2/H_2 ENGINE
PARAMETRIC DIMENSIONS
DIAMETER, INCHES
LENGTH, INCHES
CHAMBER PRESSURE, PSIA
500
750
1000
200
150
100
50
150
100
50
0
100
200
300
400
AREA RATIO
THRUST = 30,000 POUNDS
EXPANDER CYCLE

FIGURE 13

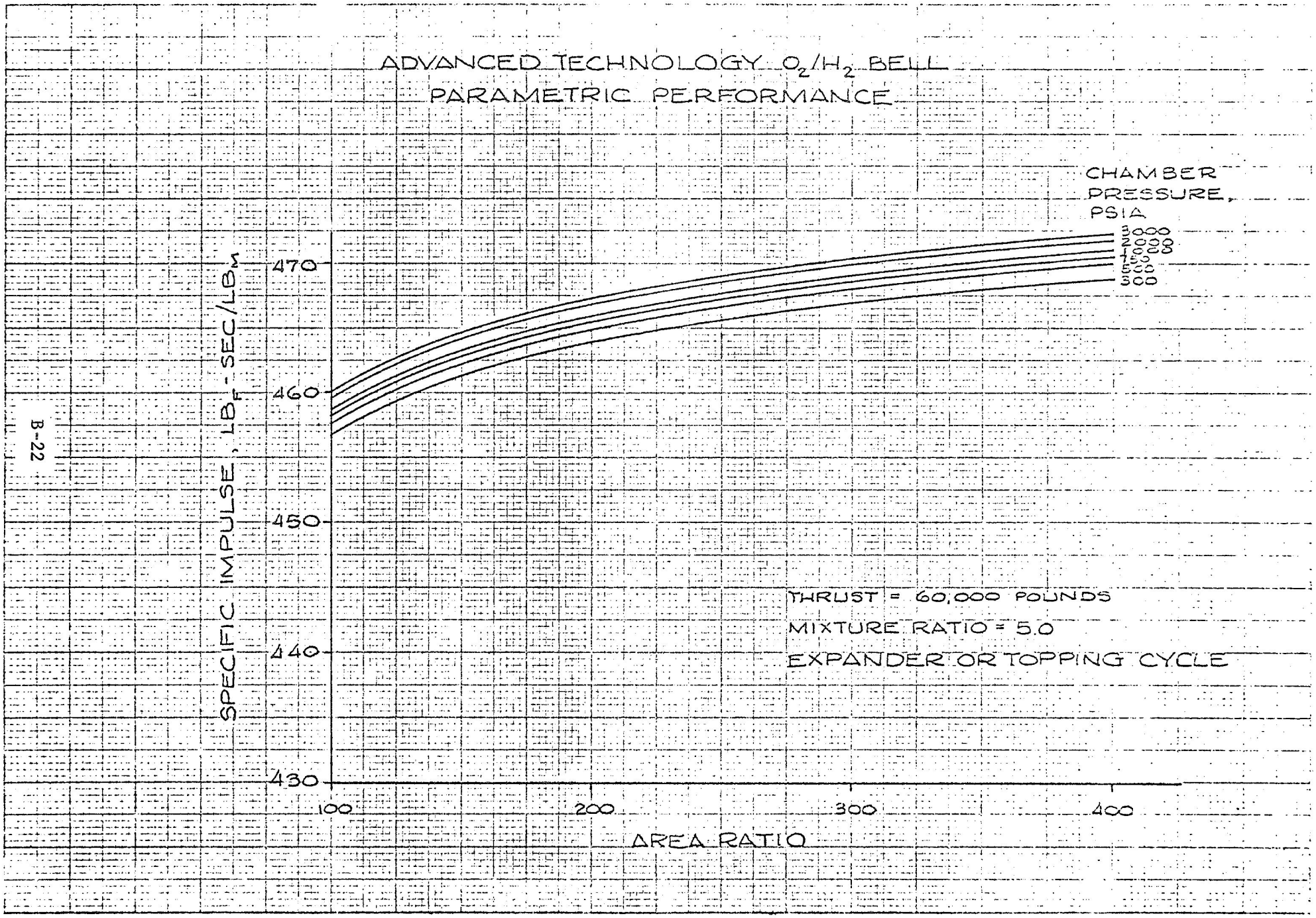
ADVANCED TECHNOLOGY O_2/H_2 BELL
PARAMETRIC PERFORMANCE
CHAMBER PRESSURE, PSIA
3000
2000
1500
1000
500
300
SPECIFIC IMPULSE, LB_F-SEC/LB_M
470
460
450
440
430
100
200
300
400
AREA RATIO
THRUST = 60,000 POUNDS
MIXTURE RATIO = 5.0
EXPANDER OR TOPPING CYCLE

FIGURE 14

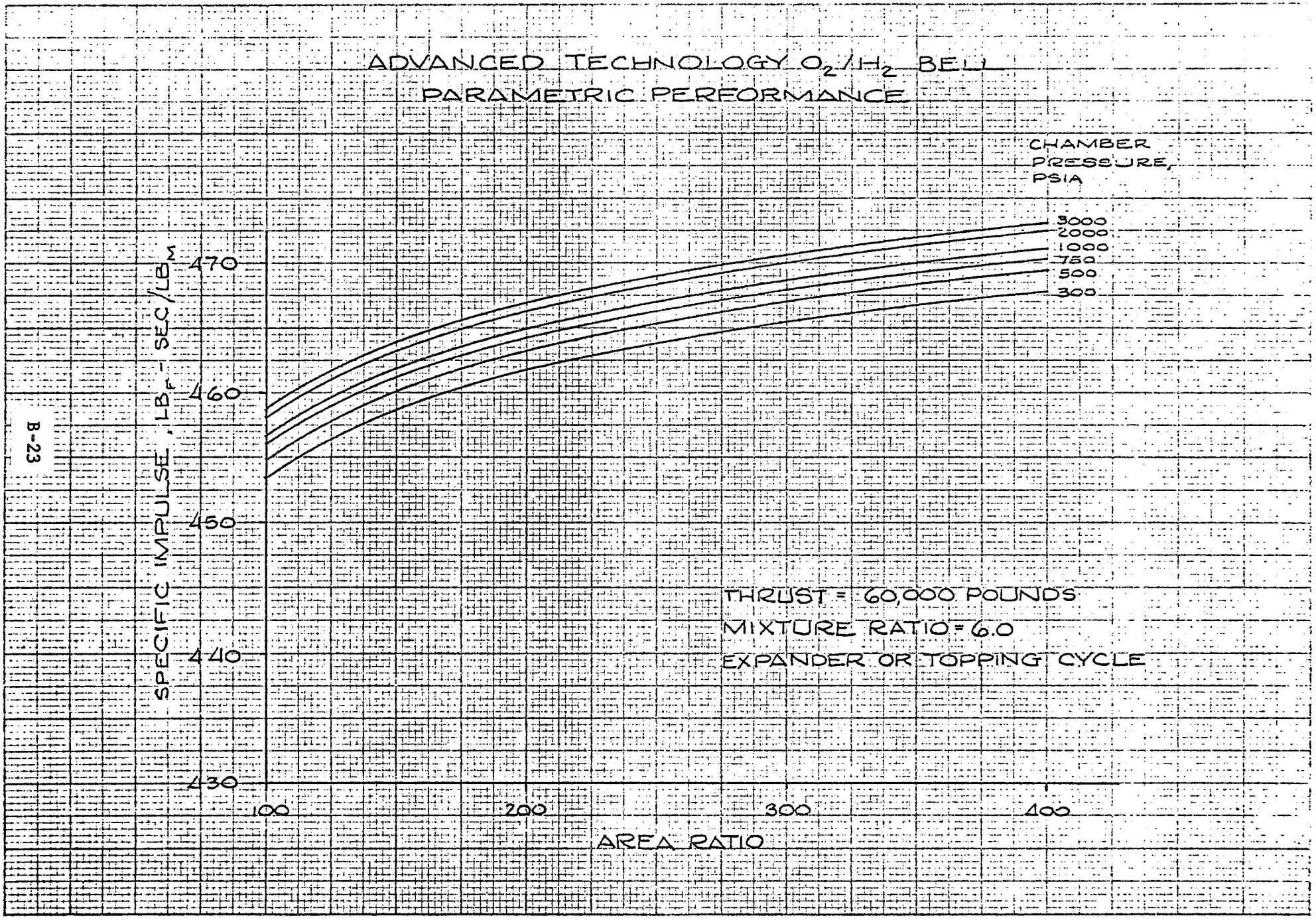
ADVANCED TECHNOLOGY O_2/H_2 BELL
PARAMETRIC PERFORMANCE
CHAMBER PRESSURE, PSIA
3000
2000
1000
750
500
300
SPECIFIC IMPULSE, LB_F - SEC/LB_M
470
460
450
440
430
100
200
300
400
AREA RATIO
THRUST = 60,000 POUNDS
MIXTURE RATIO = 6.0
EXPANDER OR TOPPING CYCLE

FIGURE 15

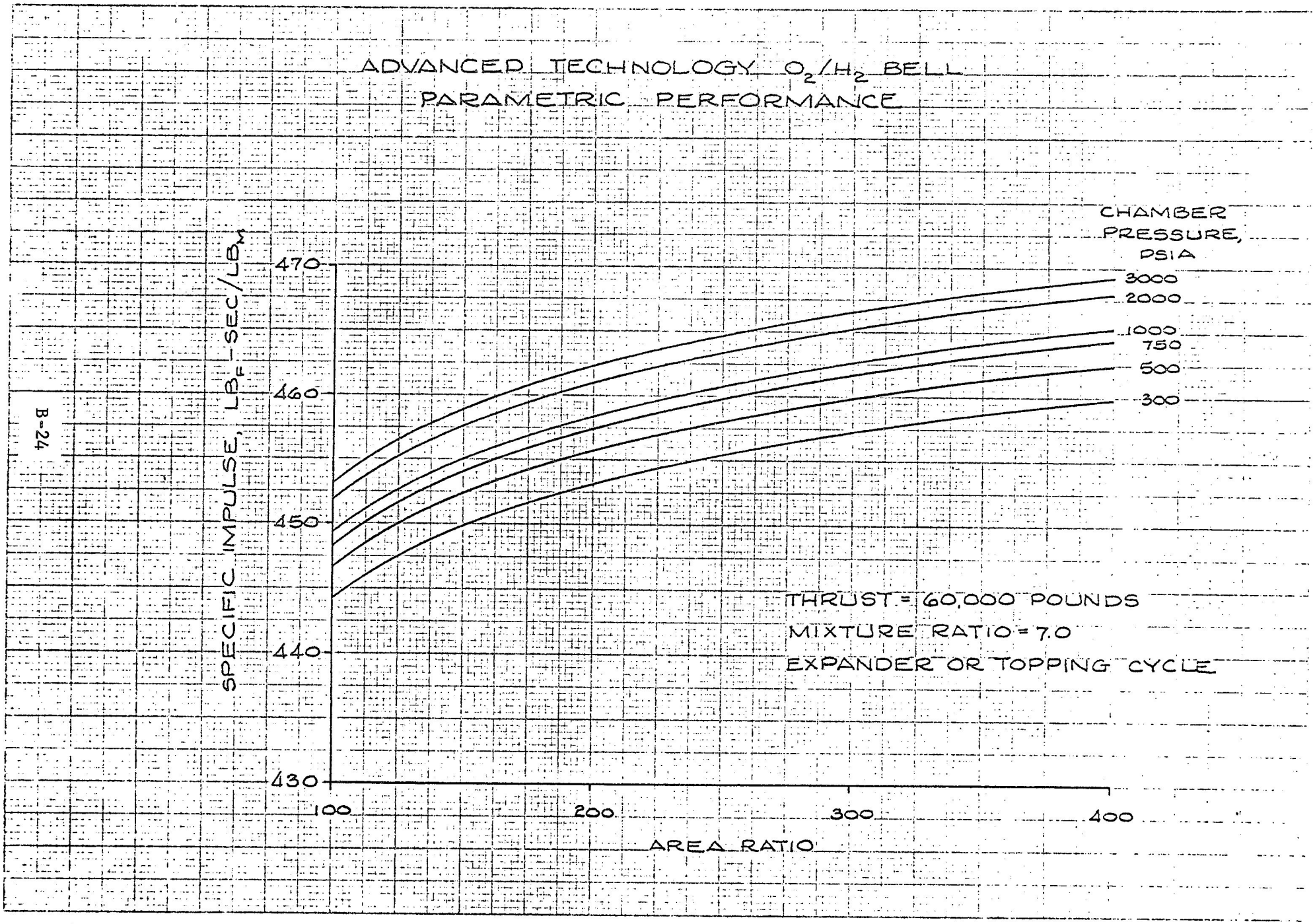
ADVANCED TECHNOLOGY O_2/H_2 BELL
PARAMETRIC PERFORMANCE
CHAMBER PRESSURE, PSIA
3000
2000
1000
750
500
300
SPECIFIC IMPULSE, LB_F-SEC/LB_M
470
460
450
440
430
100
200
300
400
AREA RATIO
THRUST = 60,000 POUNDS
MIXTURE RATIO = 7.0
EXPANDER OR TOPPING CYCLE

FIGURE 16

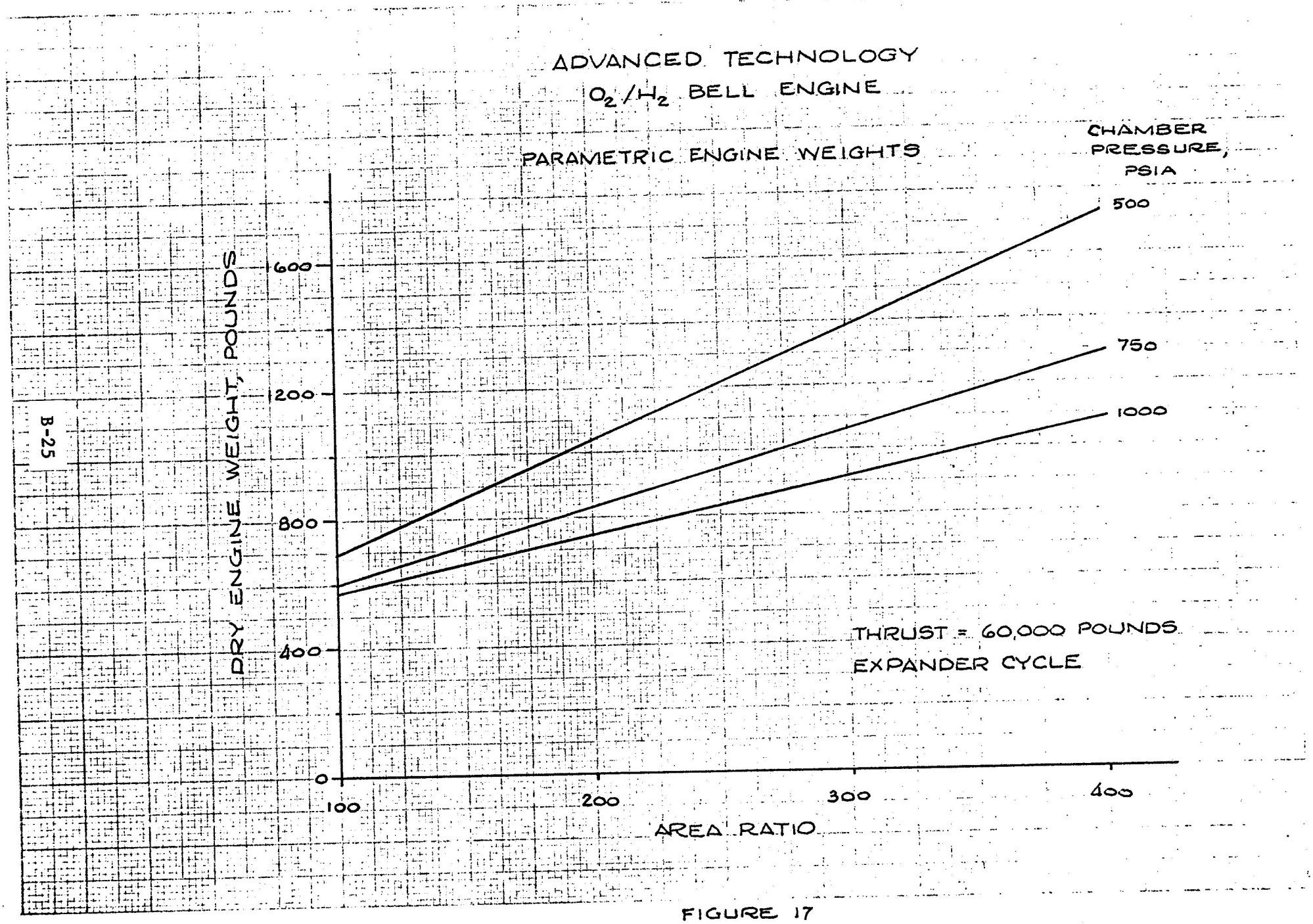
ADVANCED TECHNOLOGY
O_2/H_2 BELL ENGINE
PARAMETRIC ENGINE WEIGHTS
CHAMBER PRESSURE, PSIA
500
750
1000
DRY ENGINE WEIGHT, POUNDS
600
200
800
400
0
100
200
300
400
AREA RATIO
THRUST = 60,000 POUNDS
EXPANDER CYCLE
B-25

FIGURE 17

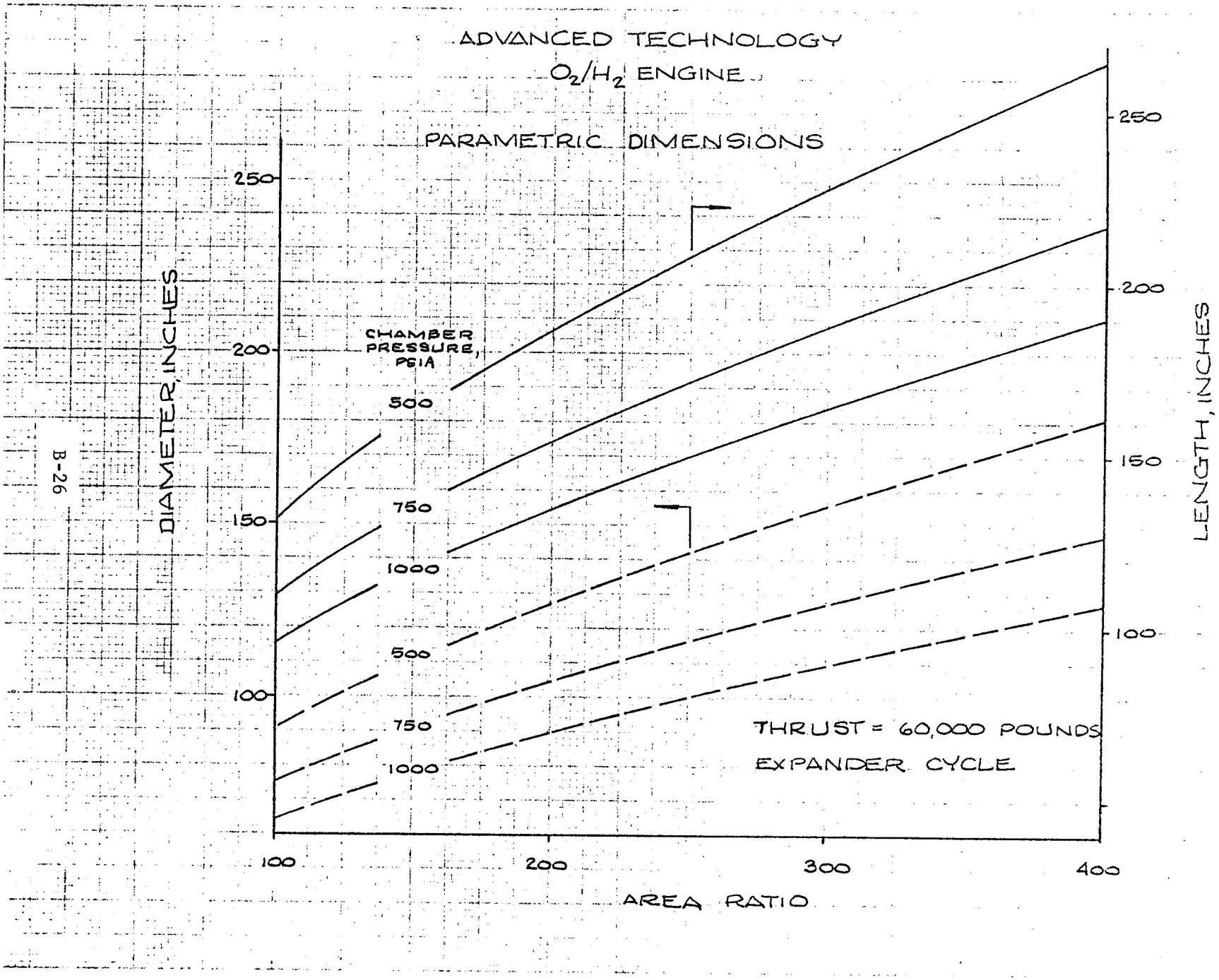
ADVANCED TECHNOLOGY
O_2/H_2 ENGINE
PARAMETRIC DIMENSIONS
DIAMETER, INCHES
LENGTH, INCHES
CHAMBER PRESSURE, PSIA
500
750
1000
500
750
1000
250
200
150
100
250
200
150
100
100
200
300
400
AREA RATIO
THRUST = 60,000 POUNDS
EXPANDER CYCLE

FIGURE 18

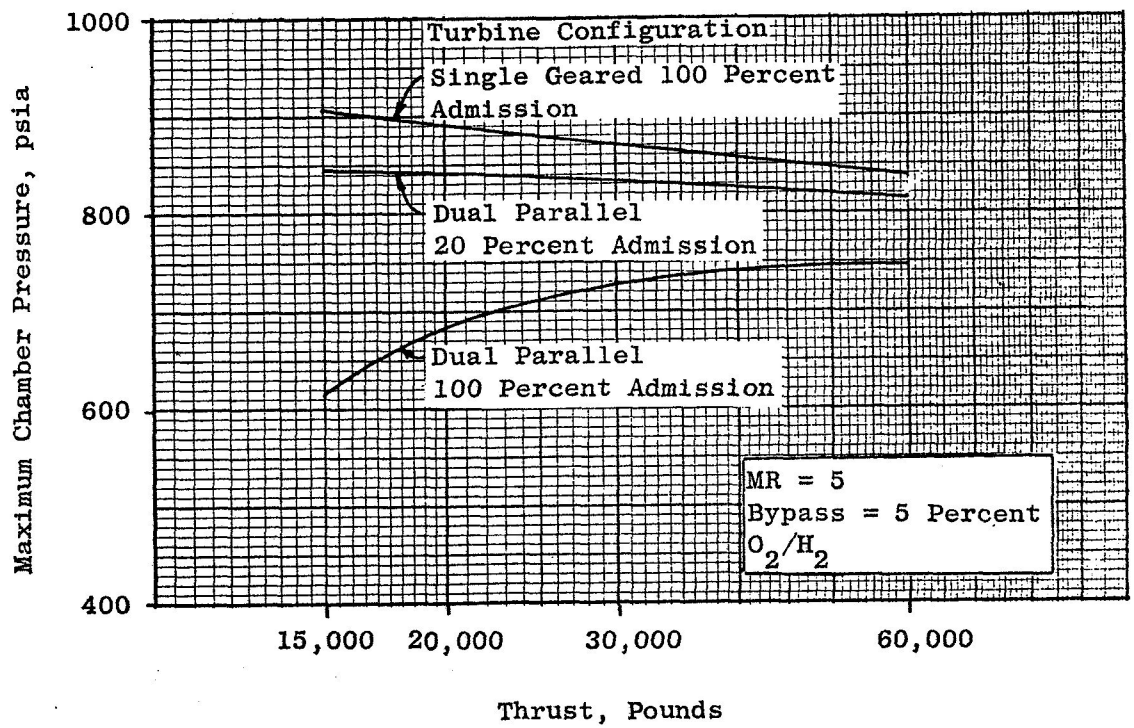

Figure 19. Expander Cycle Chamber Pressure Limits

Expander Cycle

Single Geared Turbine - 100 percent Admission

Thrust = 30,000 pounds

O_2/H_2

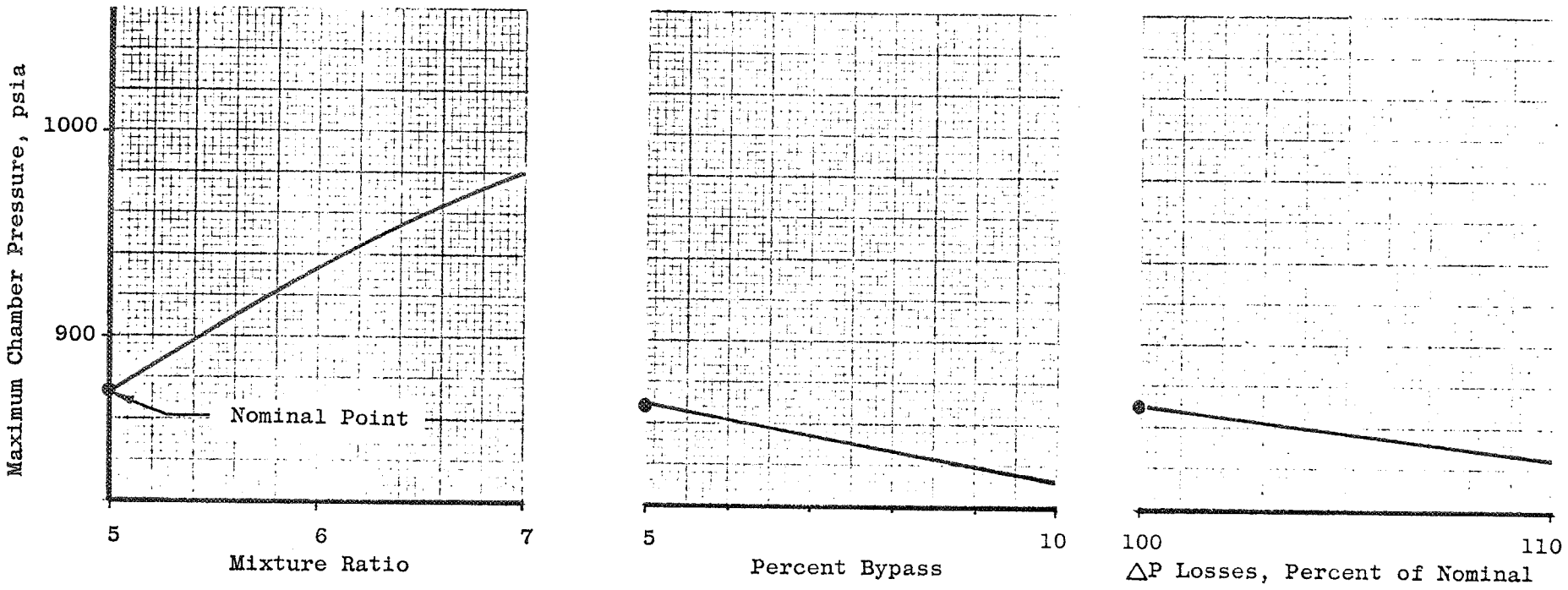

Figure 20. Chamber Pressure Limit Sensitivity

ADVANCED TECHNOLOGY
30000 POUND THRUST
HIGH AREA RATIO
HIGH CHAMBER PRESSURE
O_2/H_2 BELL ENGINE DESIGN

Rocketdyne
North American Rockwell

ADVANCED TECHNOLOGY HIGH AREA RATIO O_2/H_2 ENGINE DESIGN

The high area ratio O_2/H_2 engine design is a 30000 pound thrust, 2500 psia chamber pressure, mixture ratio 6, 400 area ratio, 80 percent length bell engine having topping drive cycle. The design makes maximum use of technology resulting from Air Force and NASA contracts and company funded efforts. The basic engine concept is illustrated in Fig. 1.

Major engine parameters are shown in Fig. 1. The engine delivers a specific impulse of 472.9 lb_f-sec/lb_m and weighs 500 pounds. The engine has throttling capability and can have, if required, a low thrust idle mode operation for propellant settling or small maneuvers.

ENGINE OPERATION

The engine requires no preconditioning and has a rapid start after liquid reaches the valve inlets. The engine is capable of an unlimited number of restarts and can be restarted 0.8 seconds after shutdown. Mixture ratio excursions for propellant utilization can be made from 5:1 to 7:1.

Start time is approximately 2.5 seconds after liquid propellants are available at the valve inlets.

BELL TOPPING CYCLE CONFIGURATION

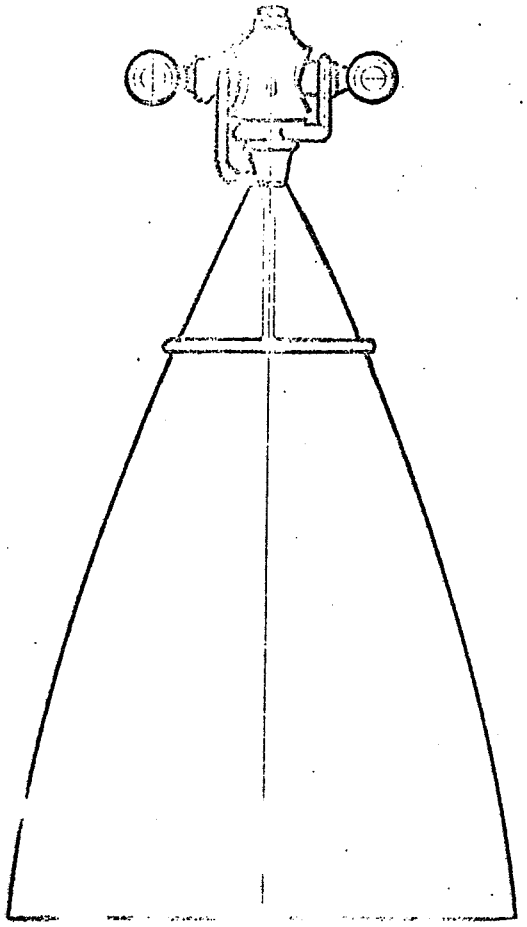

- THRUST, POUNDS 30,000
- CHAMBER PRESSURE, PSIA 2,500
- AREA RATIO 400:1
- ENGINE MIXTURE RATIO 6:1
- SPECIFIC IMPULSE, SECONDS 472.9
- LENGTH, INCHES 98.0
- DIAMETER, INCHES 58.0
- WEIGHTS, POUNDS 500

Figure 1

ADVANCED HIGH CHAMBER PRESSURE

O_2/H_2 BELL ENGINE FLOW SCHEMATIC

TOPPING CYCLE

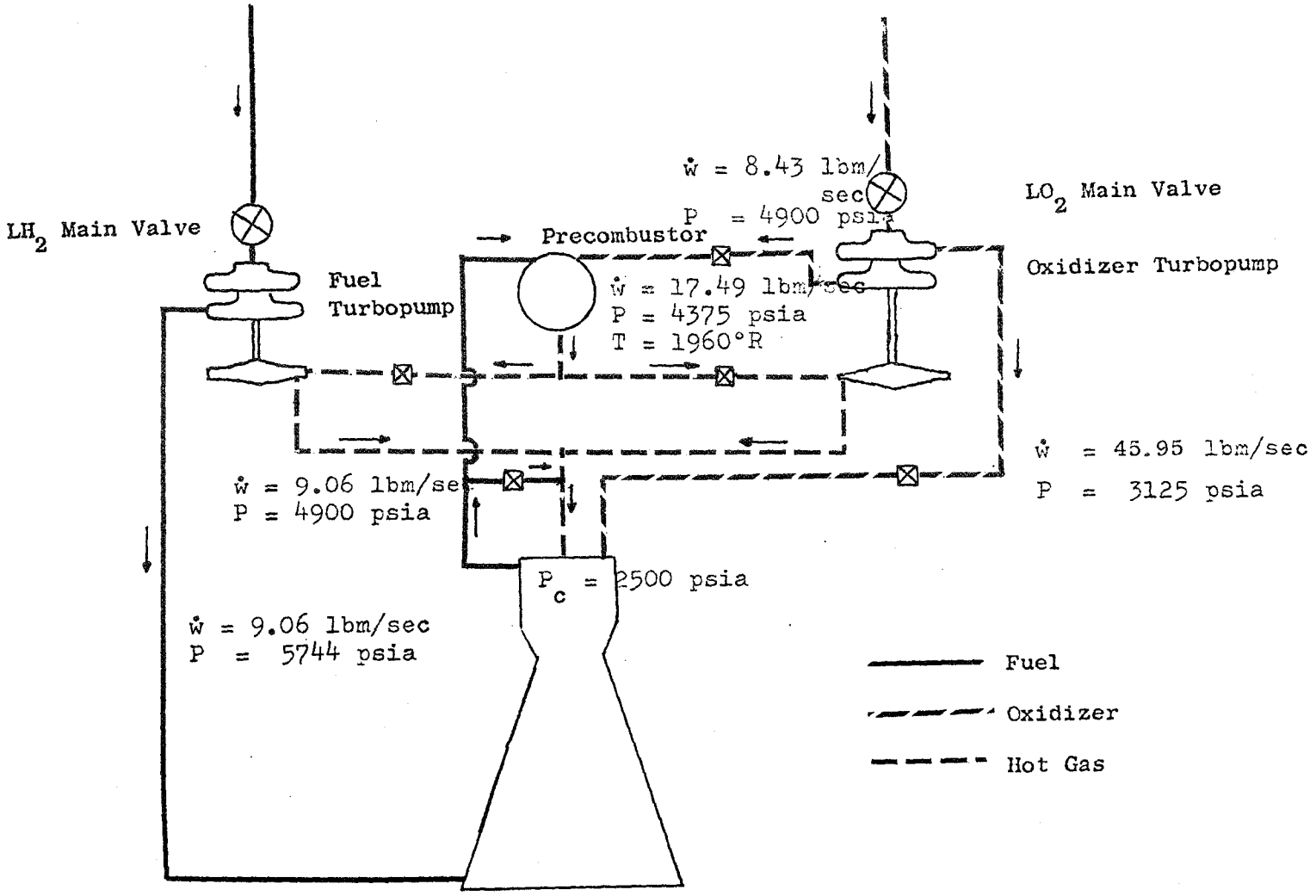

Figure 2

Approximate full thrust start and cutoff propellant requirements are:

	Propellant	Amount (lbs)	Impulse
Start (achieving full thrust and ±.5 nominal MR)	H_2	13	15000 lb-sec
	O_2	40	
Cutoff	H_2	12	20000 lb-sec
	O_2	33	

The engine can be started at any thrust with proportionately reduced propellant usage.

ENGINE DRIVE CYCLE

The power cycle as shown in Fig. 2 is a topping cycle using 95 percent of the precombustor flow to power the turbines. The 5 percent margin is intended for control purposes. Individual turbines powered in a parallel flow arrangement are provided for each pump. The turbines are single row velocity compounded and provide 4150 horsepower for the two stage centrifugal fuel pump and 897 horsepower for the two stage centrifugal fuel pump and 897 horsepower for the one stage centrifugal oxidizer pump.

THRUST CHAMBER DESIGN

The thrust chamber design makes use of a load carrying cylinder from the top of the injector with a separate spherical turbine exhaust plenum inside. The hot plenum, into which both turbines exhaust, carries no structural loading other than internal pressure. The turbine exhaust is ducted by the plenum directly to the injector. The injector has concentric elements with the oxidizer flowing through central posts surrounded by the hot turbine exhaust.

The chamber below the injector is of milled channel construction to a low area ratio at which point the tubular walled expansion nozzle skirt begins. The expansion nozzle is an optimum thrust contour having a length equal to 80-percent of an equivalent 15-degree cone.

TABLE 1

ADVANCED TECHNOLOGY HIGH CHAMBER PRESSURE O_2/H_2 BELL

FUEL PUMP TYPE - 2 STAGE CENTRIFUGAL
OXIDIZER PUMP TYPE - 1 STAGE CENTRIFUGAL
TURBINES - 1 ROW VELOCITY COMPOUNDED, PARALLEL ARRANGEMENT

		OXIDIZER	FUEL
PUMP			
	PRESSURE RISE, PSIA	3095	5714
	SPEED, RPM	50000	95000
	EFFICIENCY	0.76	0.66
TURBINE			
	INLET TEMPERATURE, °R	1960	1960
	SPEED, RPM	50000	95000
	PRESSURE RATIO	1.4	1.4
	EFFICIENCY	0.41	0.72

TURBOMACHINERY DESIGN

The oxidizer pump is a one stage centrifugal design producing a pressure rise of 3095 psia at a speed of 50000 rpm with an efficiency of 0.76. The required NPSH is 55.3 feet (26.5 psia NPSP). There is an additional stage providing a boost P of 1775 psia for the 17 percent of the oxidizer flow used by the precombustor. This stage requires only 78 horsepower.

The fuel pump is a two stage centrifugal design producing a pressure rise of 5714 psia at a speed of 95000 rpm with an efficiency of 0.66 The required NPSH is 144.5 feet (4.4 psia NPSP).

Both the oxidizer and fuel pumps are coupled with inducers. If preinducers are also used, the oxidizer and fuel NPSH requirements can be lowered to 22 feet and 58 feet, respectively. Preinducer drive would be either hydraulic or hot gas.

Both fuel and oxidizer turbines are single row velocity compounded designs allowing speeds compatible with those dictated by the pump designs since the pumps and turbines are directly coupled. Both turbines operate at the same pressure ratio and have a turbine inlet temperature of 1960°R. The oxidizer turbine efficiency is 0.41 while the fuel turbine efficiency if 0.72. Turbomachinery parameters are given in Table 1.

PRECOMBUSTOR

The precombustor takes all of the fuel flow and approximately an equal oxidizer flow. The design is cylindrical 10 inches long and 4 inches in diameter. The injector design is concentric with gaseous oxygen tubes surrounded by gaseous fuel annuli. The precombustor exhausts into three hot gas lines - one for each turbine and a bypass. Precombustor temperature control is provided by a valve in the oxidizer line.

IGNITION SYSTEM

Ignition is achieved using a platinum wire resistance element. Before propellants begin to flow, a heating pulse is sent through the platinum wire coil. Low mixture ratio propellants are then introduced to the igniter. After ignition in the igniter, main injector propellant flow is started. Upon main chamber ignition, the oxidizer flow to the igniter is cut off and hydrogen only is allowed to flow through the igniter during mainstage.

One ignition system is required for the precombustor. Ignition of the main chamber can be achieved with either the hot precombustor gases or with a separate main chamber ignition system depending upon the start requirements.

If a more rapid restart is required, a controlled power, low radio frequency interference, spark plug igniter could be used to reduce the ignition time to 1 millisecond from 0.8 seconds.

ENGINE - VEHICLE INTERFACE REQUIREMENTS

Connections required between the engine and vehicle are mechanical, fluid, and electrical. The locations of the principle interface mechanical connections are shown in Figure 4.

The mechanical connection for thrust transmission is at the forward face of the gimbal block. Thrust alignment is maintained within 30 minutes annular and 1/8" lateral of the engine axial centerline. Two electromechanical gimbal actuators, located 90° apart are capable of a thrust vector angle of at least 10 degrees with a steady-state control of 1/2° at 2.5HZ. The actuators can gimbal the engine at velocities up to degree/sec. Approximate gimbal torque requirements are 1400 ft-lb.

Fluid connections are required for the propellant supply lines, tank pressurant lines, and purge supply lines. These lines have flexibility to withstand the forces of gimbaling, thermal expansion, and manufacturing misalignment.

ENGINE-VEHICLE INTERFACE POSITIONS

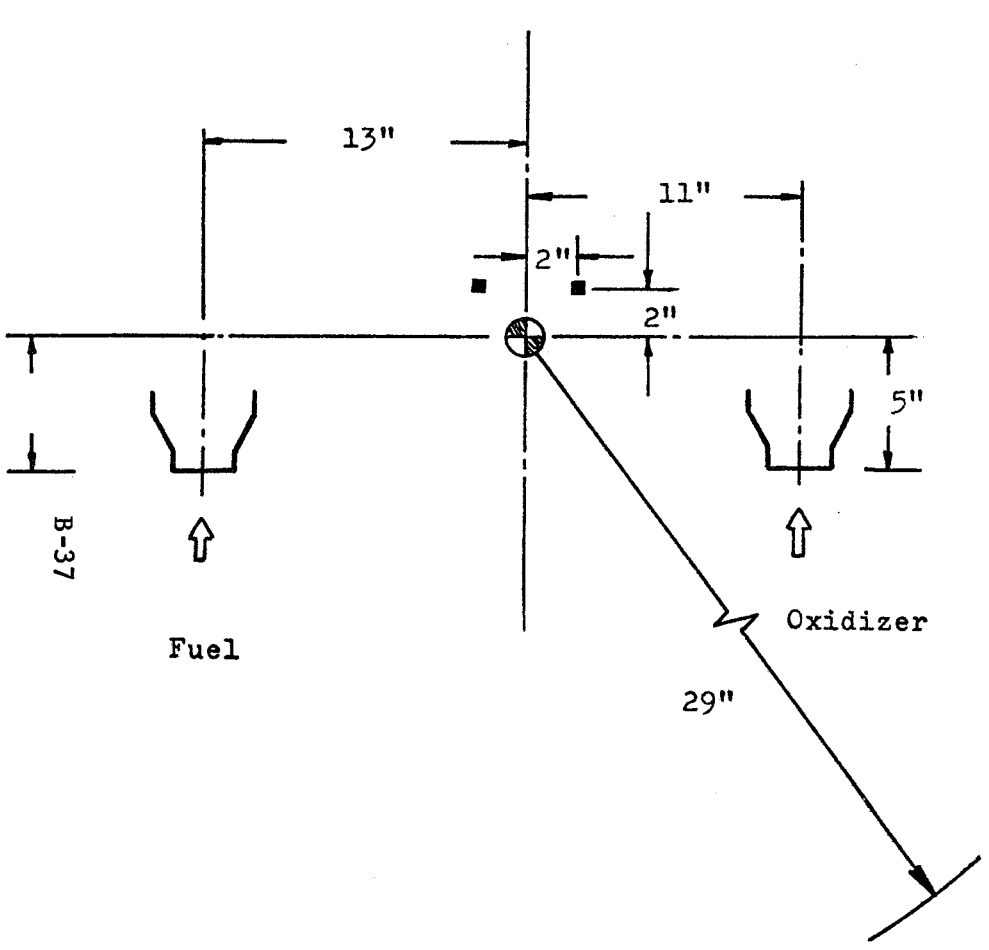

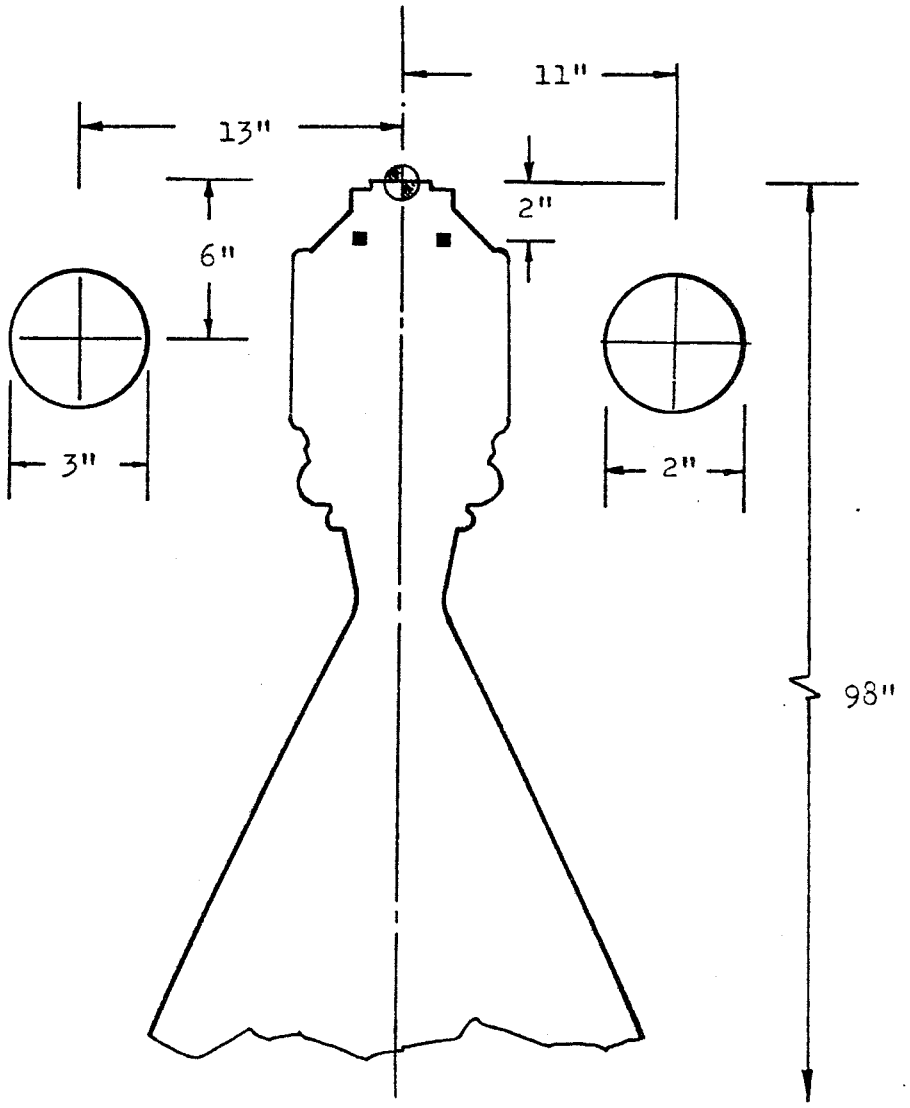

Figure 3

The vehicle main propellant supply lines interface with the engine at the main valve inlets. The oxidizer and fuel inlet locations are shown in Figure 4. The inlets are below the gimbal point to allow leeway in propellant line positioning. The oxidizer valve inlet is 2 inches in diameter and the fuel valve inlet is 3 inches in diameter. Both are fitted with standard flange attachments.

Tank pressurants in the form of heated propellants and/or helium are provided by the engine. The pressurant and purge lines interface with the vehicle at the fluid panel.

A single interface panel is required to provide electrical power to the engine and to transmit control signals between the engine and vehicle.

Propellant Supply Requirements

The required NPSH values for the pumps are:

	Fuel Pump	Oxidizer Pump
Without Preinducer	144.5 ft	55.3 ft
With Preinducer	58 ft	22 ft

Assuming oxidizer and fuel valve losses of 10 and 5 psia respectively, the required net positive pressure, at the engine inlet before the main valves are:

	Fuel Inlet	Oxidizer Inlet
Without Preinducer	9.4 psia	36.5 psia
With Preinducer	6.8 psia	20.6 psia

Pneumatic Requirements

Pneumatics are required for engine and seal purges. Purge requirements for each engine operating cycle are:

	Purge Medium	Regulated Purge Press. (psia)	Purge Flowrate (scfm)	Required Purge Temp °R
Oxidizer System	Helium	750	75	180
Fuel System	Helium	750	100	180
Oxidizer Pump Seal	Helium	750	4.4	180

The oxidizer pump seal purge is used throughout engine operation. The oxidizer system purge operates for approximately 1 second at start. The oxidizer system purge operates for approximately 4 seconds and the fuel system purge for 2 seconds at cutoff.

The pneumatic requirements for main valve actuation assuming a 3000 psi helium supply pressure regulated at 750 psi (- 200°R) is 2600 standard cubic inches for each engine firing.

Electrical Requirements

The electrical power requirements for each engine operating cycle including gimbal actuation, valve actuation, engine controller package and engine instrumentation are:

Voltage	Total Power Requirements, Watts
26-30 DC	170 - 260*
26-30 DC	80 - 120**
110 AC	25*
2 DC	36 or 72***

* Continuous power during engine operation

** Power only during purge operation

*** Power only during 0.8 second ignition sequence. Can be provided from other DC sources by step down transformer.

The 110 AC source is preferred but other power sources may be acceptable.

PARAMETRIC ENGINE PERFORMANCE

Parametric engine performance, weight and size data for optimization studies are presented in Fig. 4 to 20. The data are for engines similar to the detailed design presented.

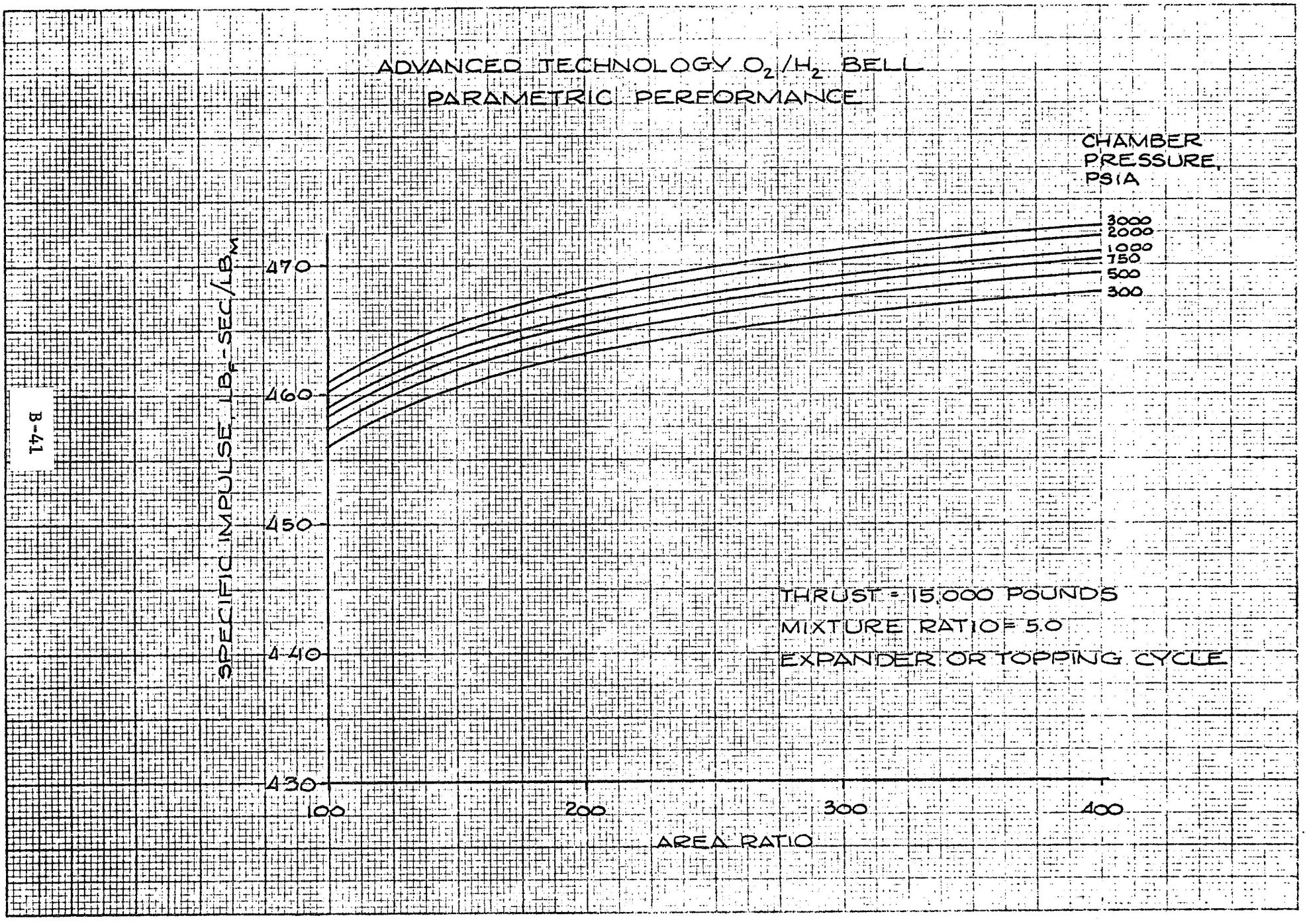
ADVANCED TECHNOLOGY O_2/H_2 BELL
PARAMETRIC PERFORMANCE
CHAMBER PRESSURE, PSIA
3000
2000
1000
750
500
300
SPECIFIC IMPULSE, LB_F-SEC/LB_M
470
460
450
440
430
100
200
300
400
AREA RATIO
THRUST = 15,000 POUNDS
MIXTURE RATIO = 5.0
EXPANDER OR TOPPING CYCLE

Figure 4

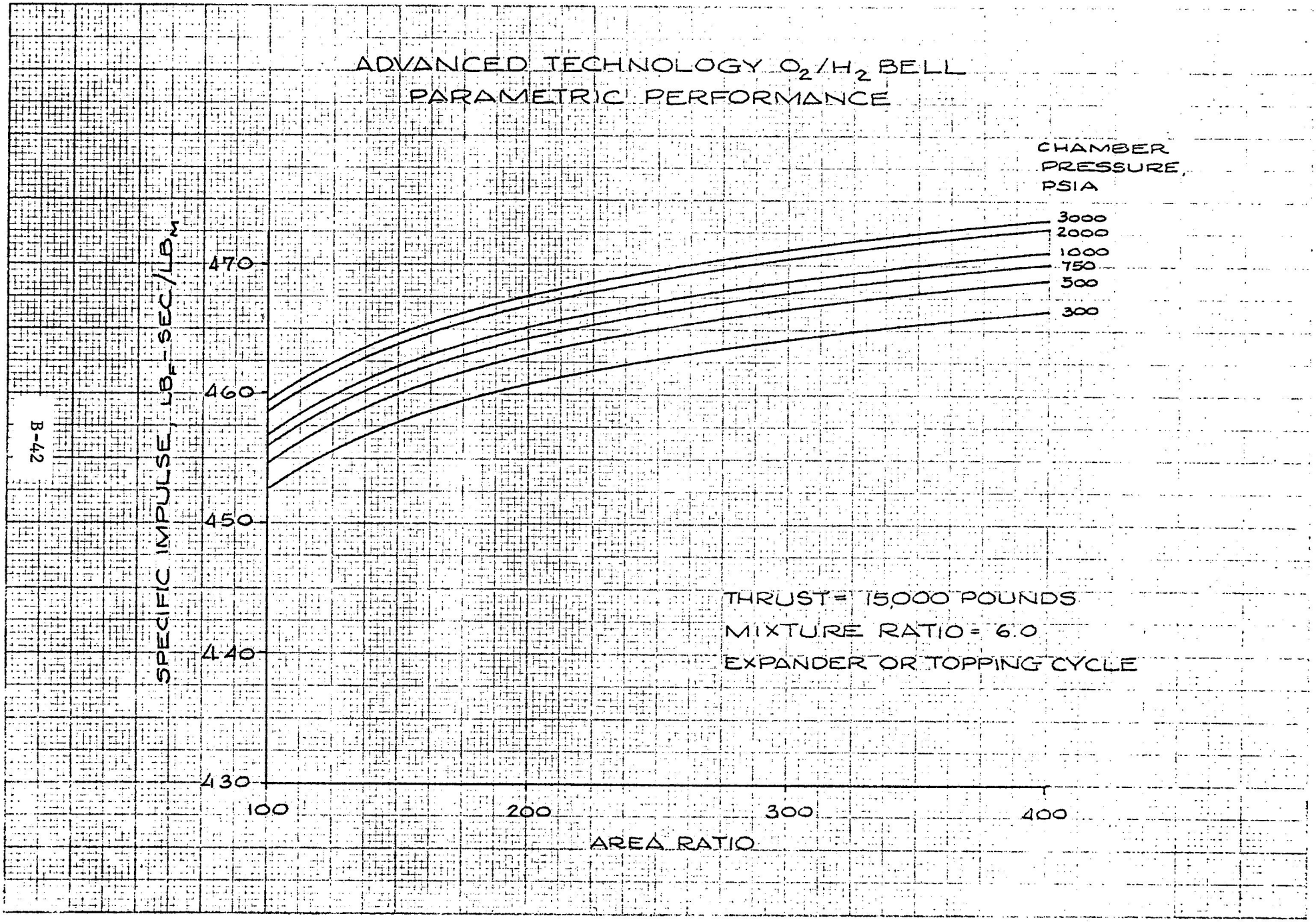
ADVANCED TECHNOLOGY O_2/H_2 BELL
PARAMETRIC PERFORMANCE
CHAMBER PRESSURE, PSIA
3000
2000
1000
750
500
300
SPECIFIC IMPULSE, LB_F-SEC/LB_M
470
460
450
440
430
100
200
300
400
AREA RATIO
THRUST = 15,000 POUNDS
MIXTURE RATIO = 6.0
EXPANDER OR TOPPING CYCLE
B-42

Figure 5

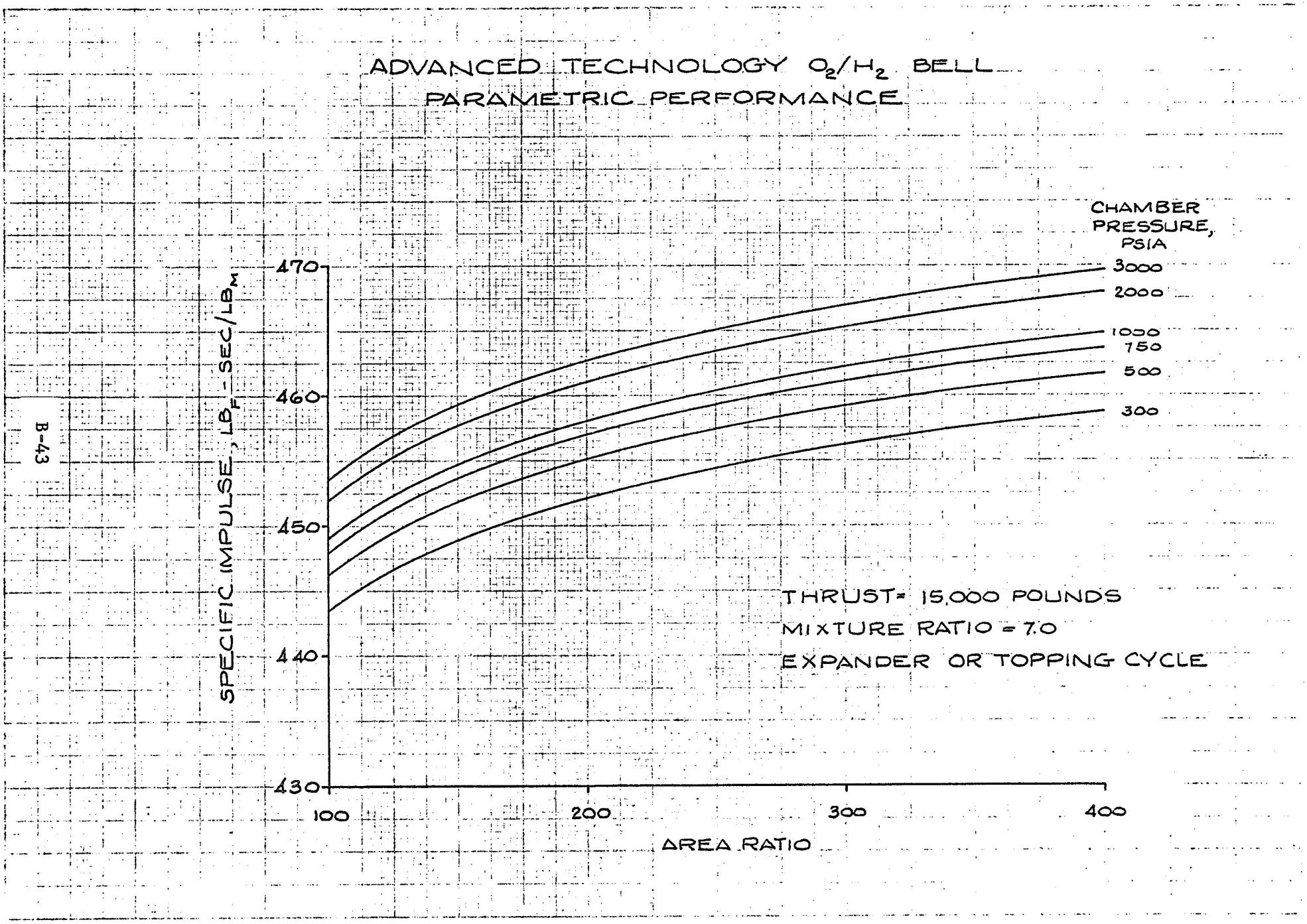
ADVANCED TECHNOLOGY O_2/H_2 BELL
PARAMETRIC PERFORMANCE
CHAMBER PRESSURE, PSIA
3000
2000
1000
750
500
300
SPECIFIC IMPULSE, LB_F-SEC/LB_M
470
460
450
440
430
100
200
300
400
AREA RATIO
THRUST= 15,000 POUNDS
MIXTURE RATIO = 7.0
EXPANDER OR TOPPING CYCLE

Figure 6

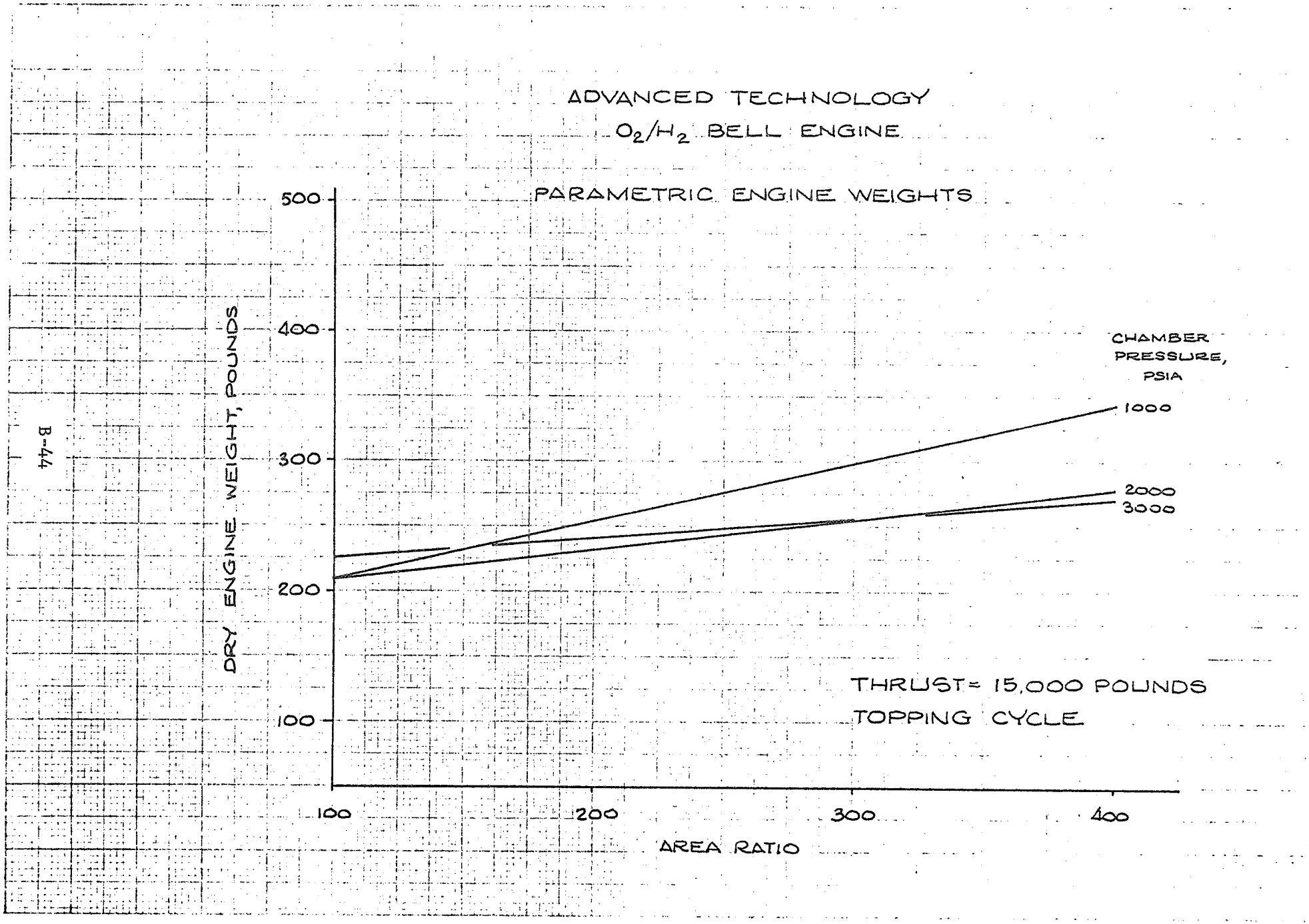
ADVANCED TECHNOLOGY
O_2/H_2 BELL ENGINE
PARAMETRIC ENGINE WEIGHTS
DRY ENGINE WEIGHT, POUNDS
500
400
300
200
100
CHAMBER PRESSURE, PSIA
1000
2000
3000
THRUST = 15,000 POUNDS
TOPPING CYCLE
100
200
300
400
AREA RATIO

Figure 7

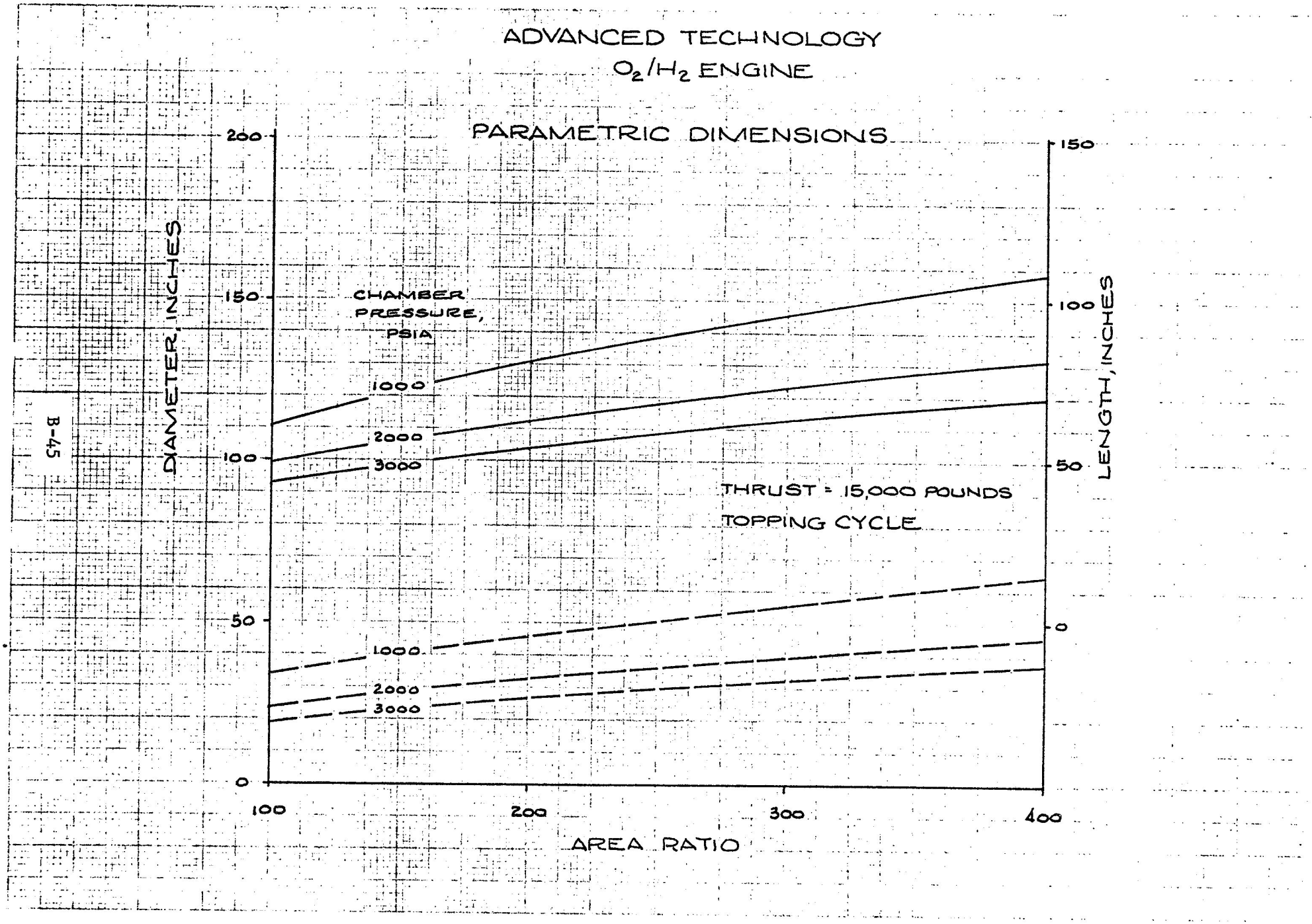
ADVANCED TECHNOLOGY
O_2/H_2 ENGINE
PARAMETRIC DIMENSIONS
DIAMETER, INCHES
LENGTH, INCHES
CHAMBER PRESSURE, PSIA
1000
2000
3000
THRUST = 15,000 POUNDS
TOPPING CYCLE
AREA RATIO
200
150
100
50
0
100
200
300
400
B-45

Figure 8

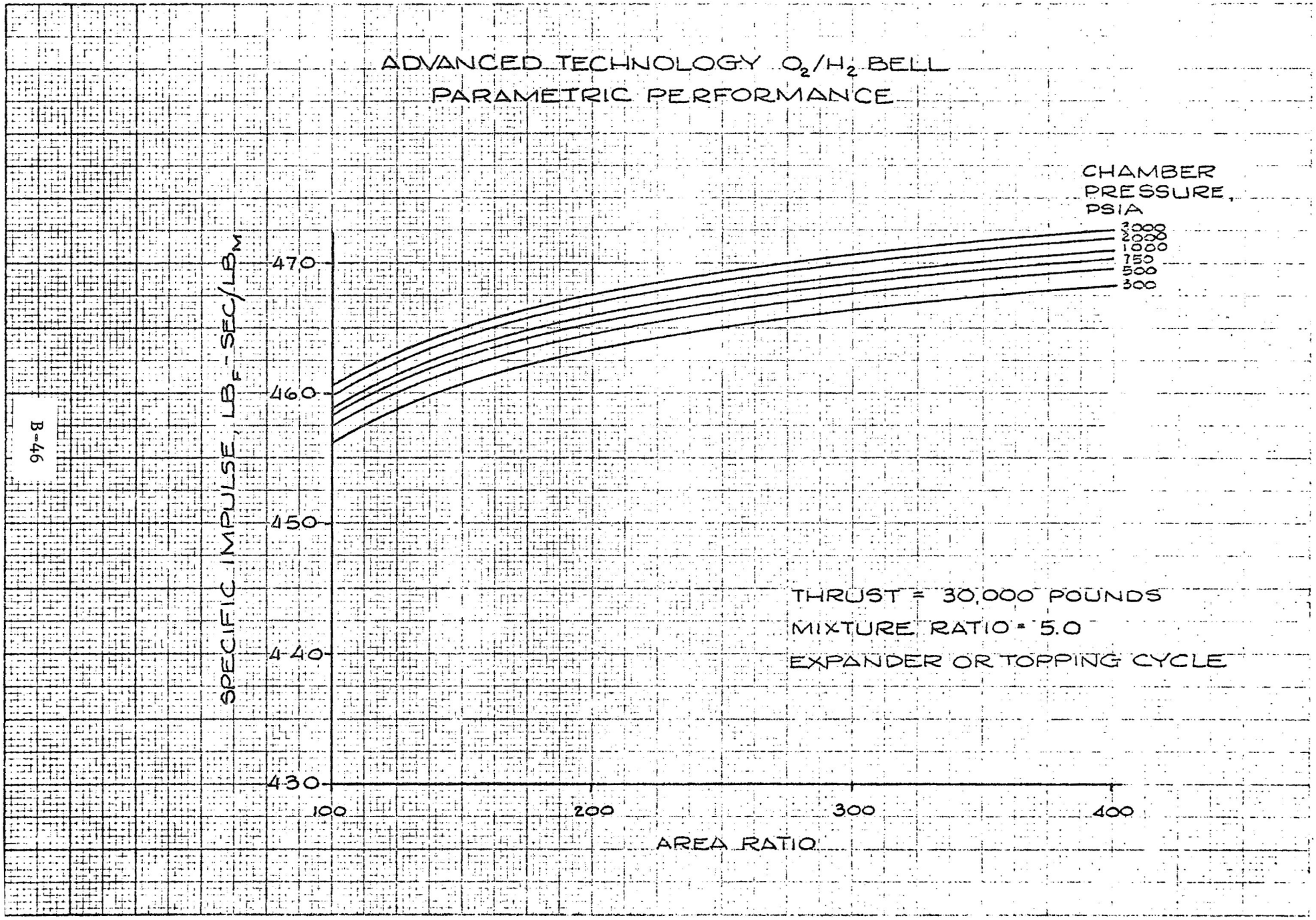
ADVANCED TECHNOLOGY O_2/H_2 BELL
PARAMETRIC PERFORMANCE
CHAMBER PRESSURE, PSIA
3000
2000
1000
750
500
300
SPECIFIC IMPULSE, LB_F-SEC/LB_M
470
460
450
440
430
100
200
300
400
AREA RATIO
THRUST = 30,000 POUNDS
MIXTURE RATIO = 5.0
EXPANDER OR TOPPING CYCLE

Figure 9

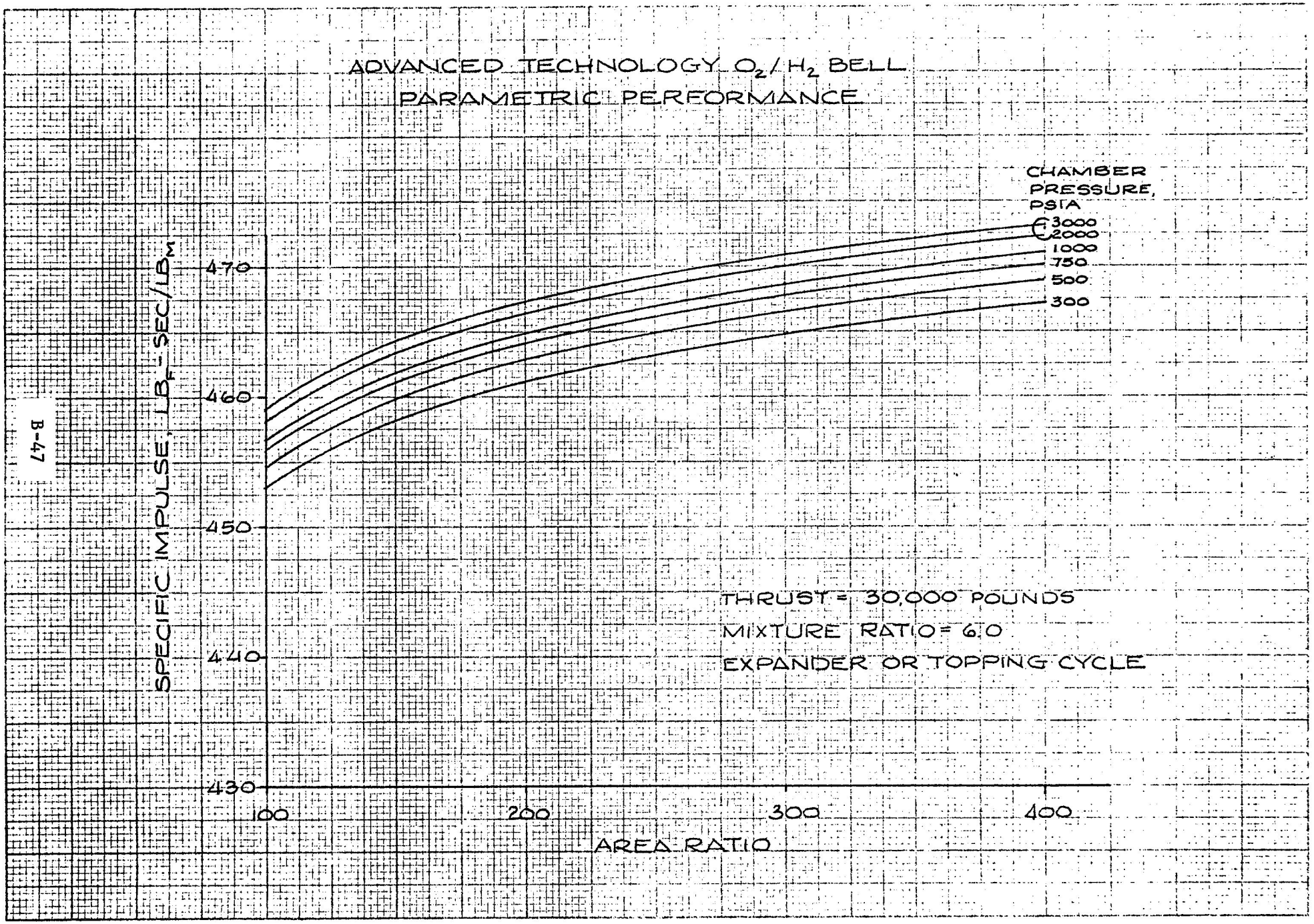
ADVANCED TECHNOLOGY O_2/H_2 BELL
PARAMETRIC PERFORMANCE
CHAMBER PRESSURE, PSIA
3000
2000
1000
750
500
300
SPECIFIC IMPULSE, LB_F-SEC/LB_M
470
460
450
440
430
100
200
300
400
AREA RATIO
THRUST = 30,000 POUNDS
MIXTURE RATIO = 6.0
EXPANDER OR TOPPING CYCLE

Figure 10

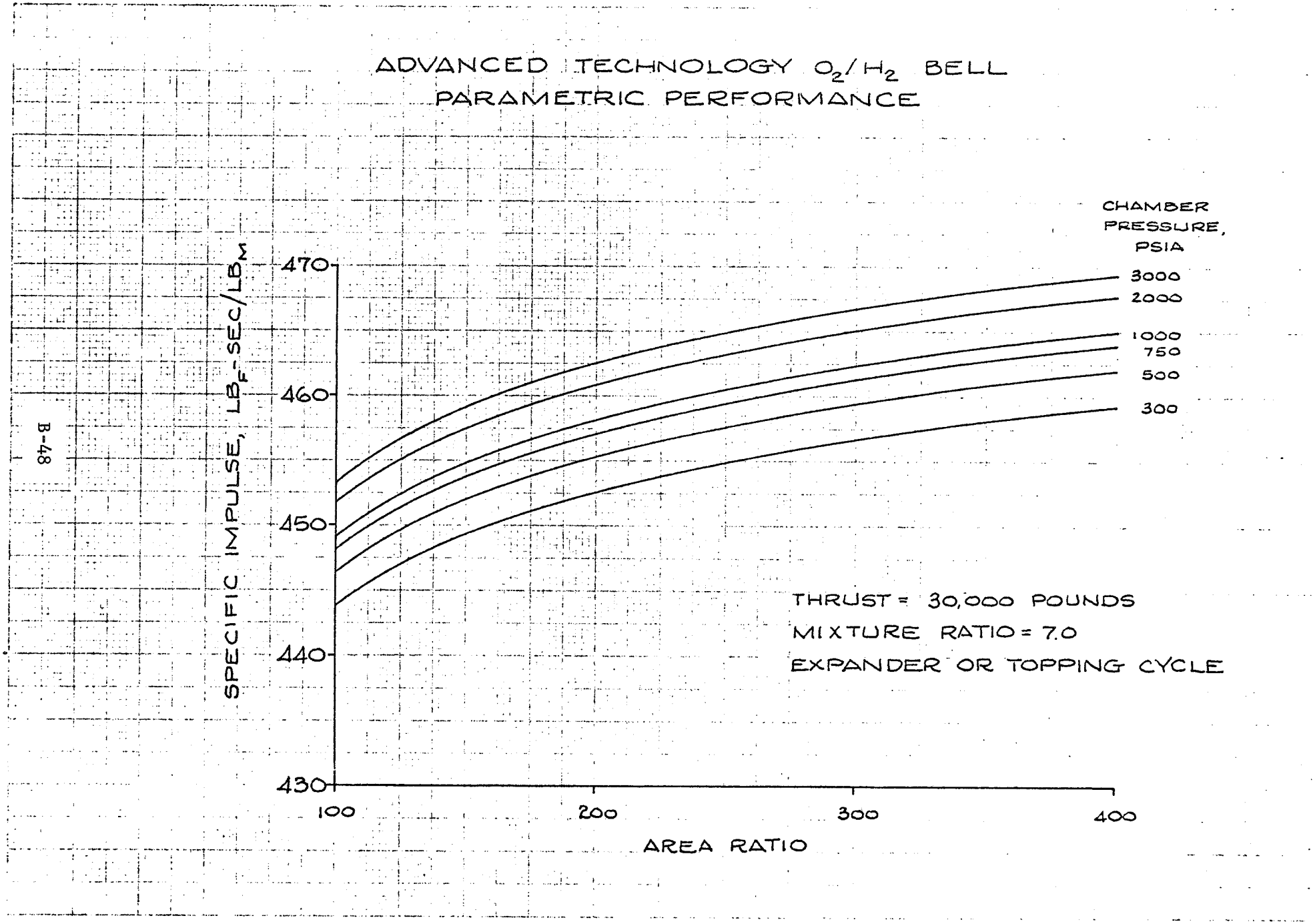
ADVANCED TECHNOLOGY O_2/H_2 BELL
PARAMETRIC PERFORMANCE
CHAMBER PRESSURE, PSIA
3000
2000
1000
750
500
300
SPECIFIC IMPULSE, LB_F-SEC/LB_M
470
460
450
440
430
100
200
300
400
AREA RATIO
THRUST = 30,000 POUNDS
MIXTURE RATIO = 7.0
EXPANDER OR TOPPING CYCLE

Figure 11

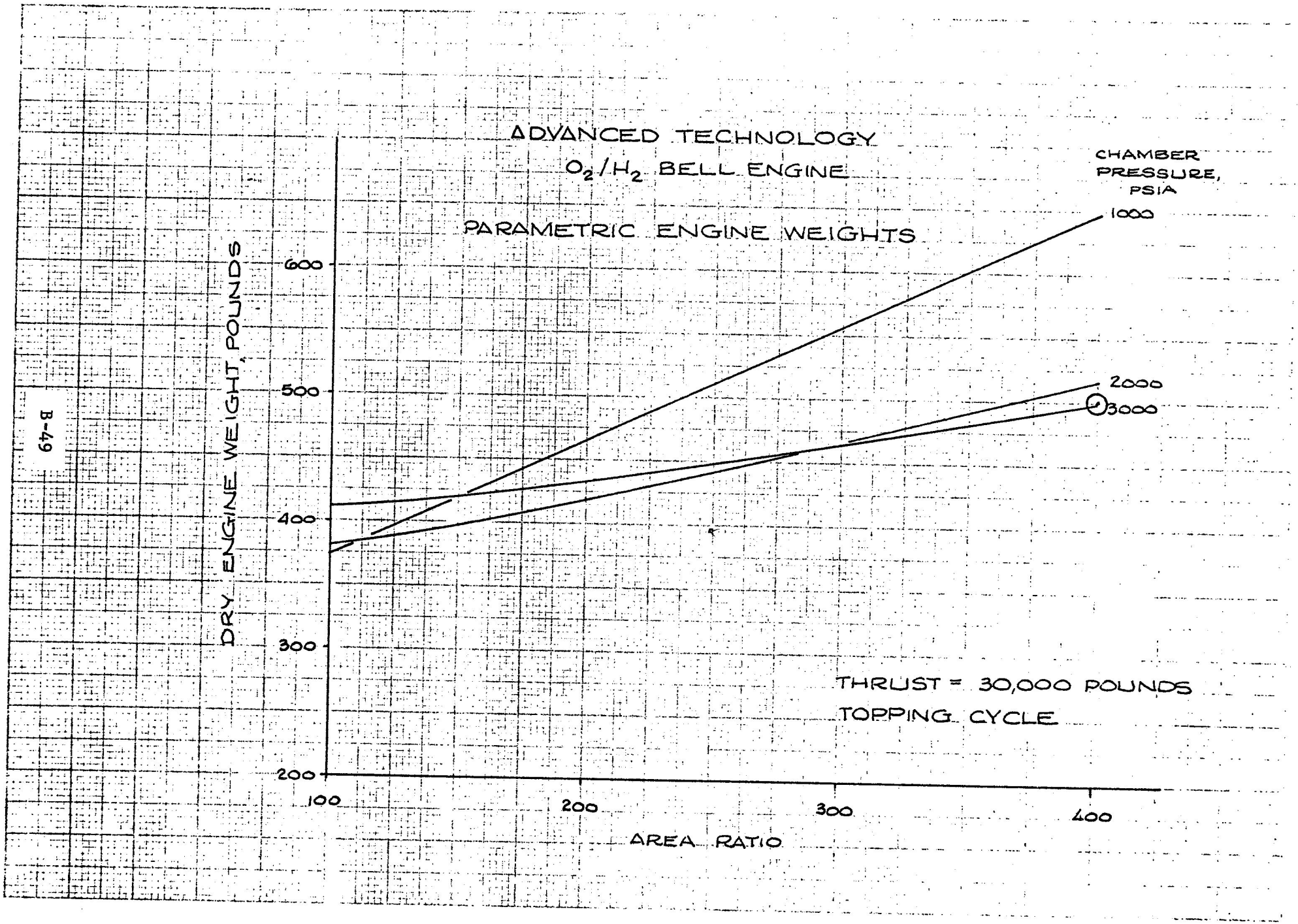
ADVANCED TECHNOLOGY
O_2/H_2 BELL ENGINE
PARAMETRIC ENGINE WEIGHTS
CHAMBER PRESSURE, PSIA
1000
2000
3000
DRY ENGINE WEIGHT, POUNDS
600
500
400
300
200
100
200
300
400
AREA RATIO
THRUST = 30,000 POUNDS
TOPPING CYCLE

Figure 12

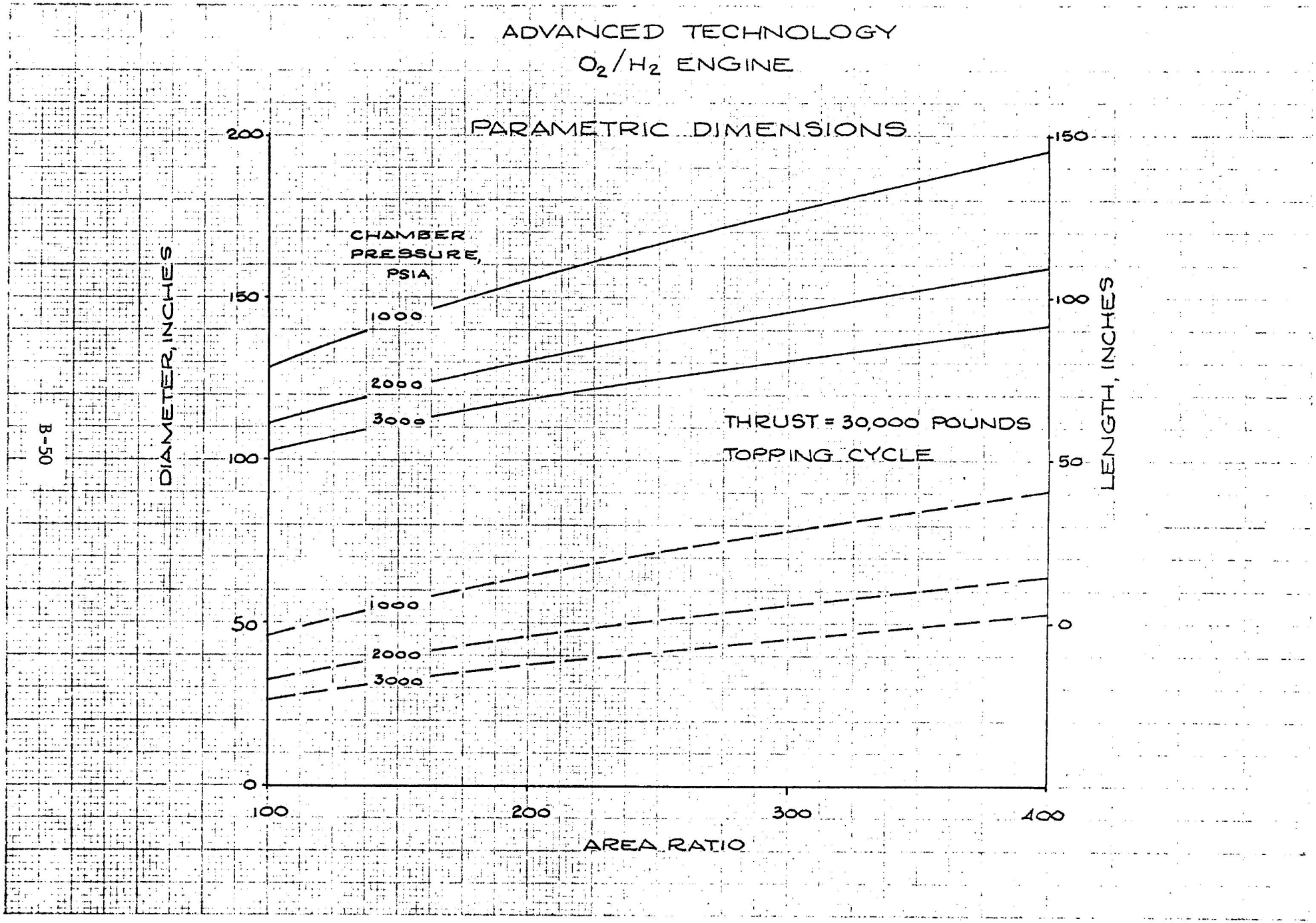
ADVANCED TECHNOLOGY
O_2/H_2 ENGINE
PARAMETRIC DIMENSIONS
CHAMBER PRESSURE, PSIA
1000
2000
3000
THRUST = 30,000 POUNDS
TOPPING CYCLE
DIAMETER, INCHES
LENGTH, INCHES
AREA RATIO
200
150
100
50
0
100
200
300
400
B-50

Figure 13

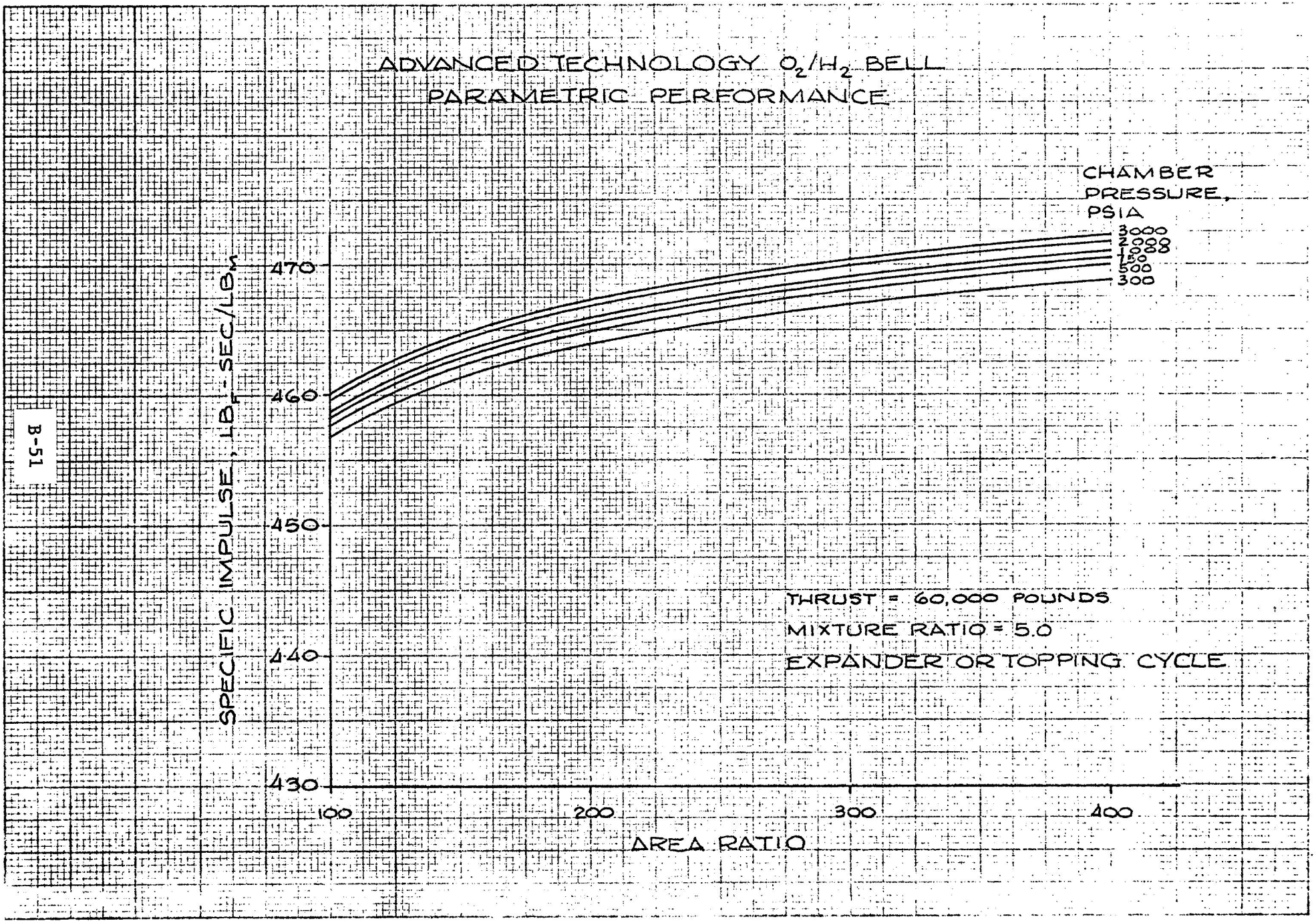
ADVANCED TECHNOLOGY O_2/H_2 BELL
PARAMETRIC PERFORMANCE
CHAMBER PRESSURE, PSIA
3000
2000
1000
750
500
300
SPECIFIC IMPULSE, LBF-SEC/LBM
470
460
450
440
430
THRUST = 60,000 POUNDS
MIXTURE RATIO = 5.0
EXPANDER OR TOPPING CYCLE
100
200
300
400
AREA RATIO
B-51

Figure 14

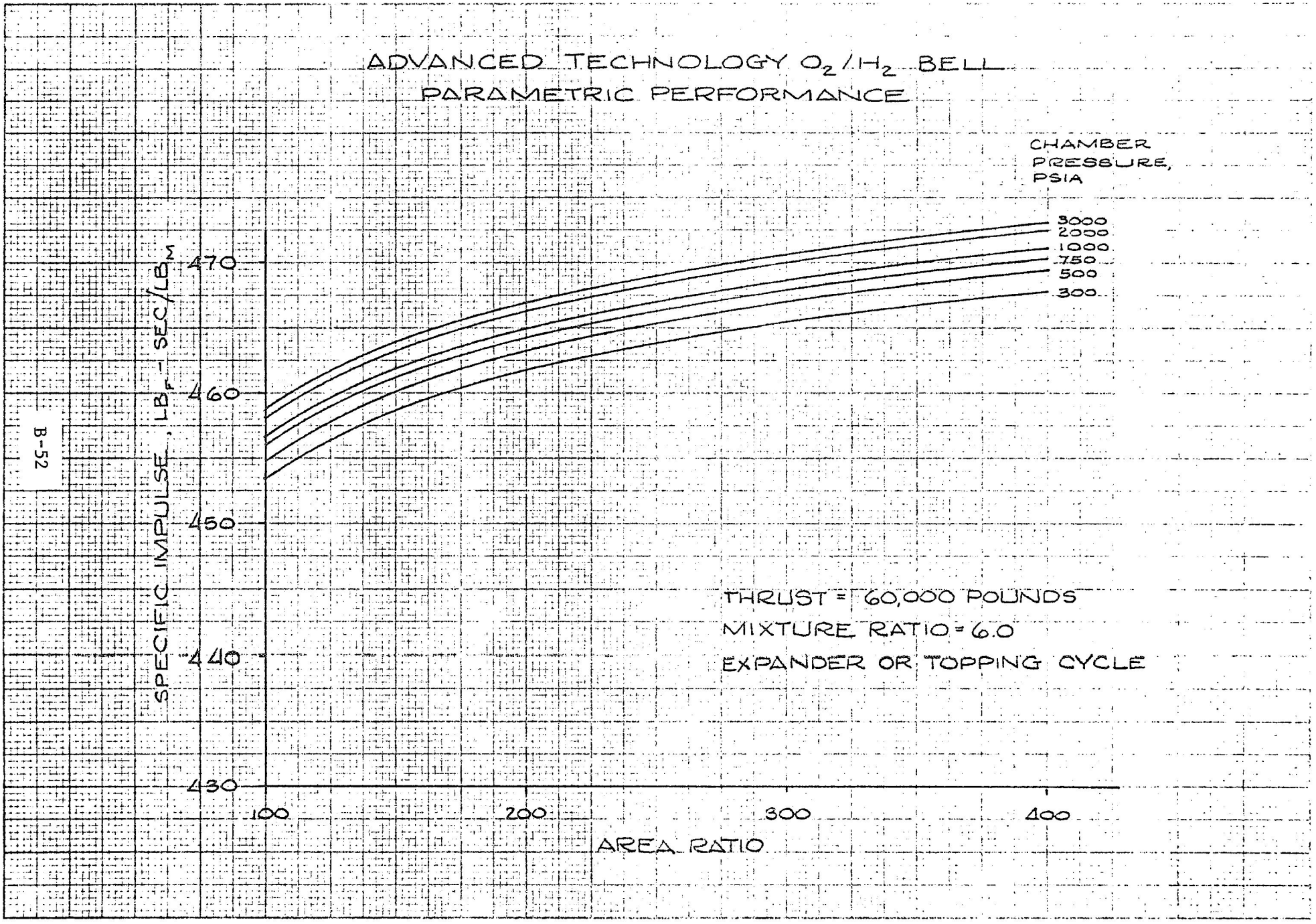
ADVANCED TECHNOLOGY O_2/H_2 BELL
PARAMETRIC PERFORMANCE
CHAMBER PRESSURE, PSIA
3000
2000
1000
750
500
300
SPECIFIC IMPULSE, LB_F - SEC/LB_M
470
460
450
440
430
100
200
300
400
AREA RATIO
THRUST = 60,000 POUNDS
MIXTURE RATIO = 6.0
EXPANDER OR TOPPING CYCLE

Figure 15

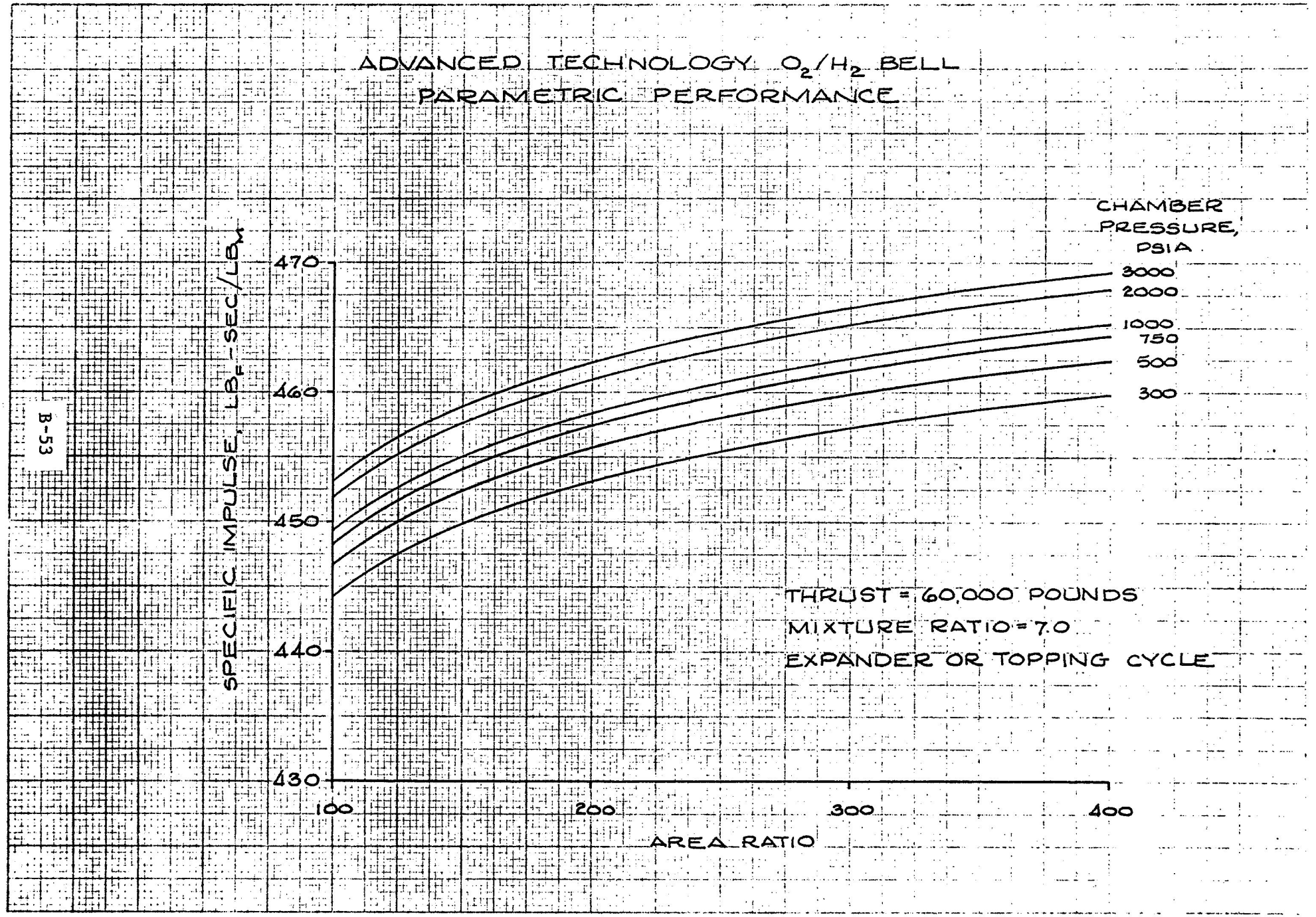
ADVANCED TECHNOLOGY O_2/H_2 BELL
PARAMETRIC PERFORMANCE
CHAMBER PRESSURE, PSIA
3000
2000
1000
750
500
300
SPECIFIC IMPULSE, LB_F-SEC/LB_M
470
460
450
440
430
100
200
300
400
AREA RATIO
THRUST = 60,000 POUNDS
MIXTURE RATIO = 7.0
EXPANDER OR TOPPING CYCLE

Figure 16

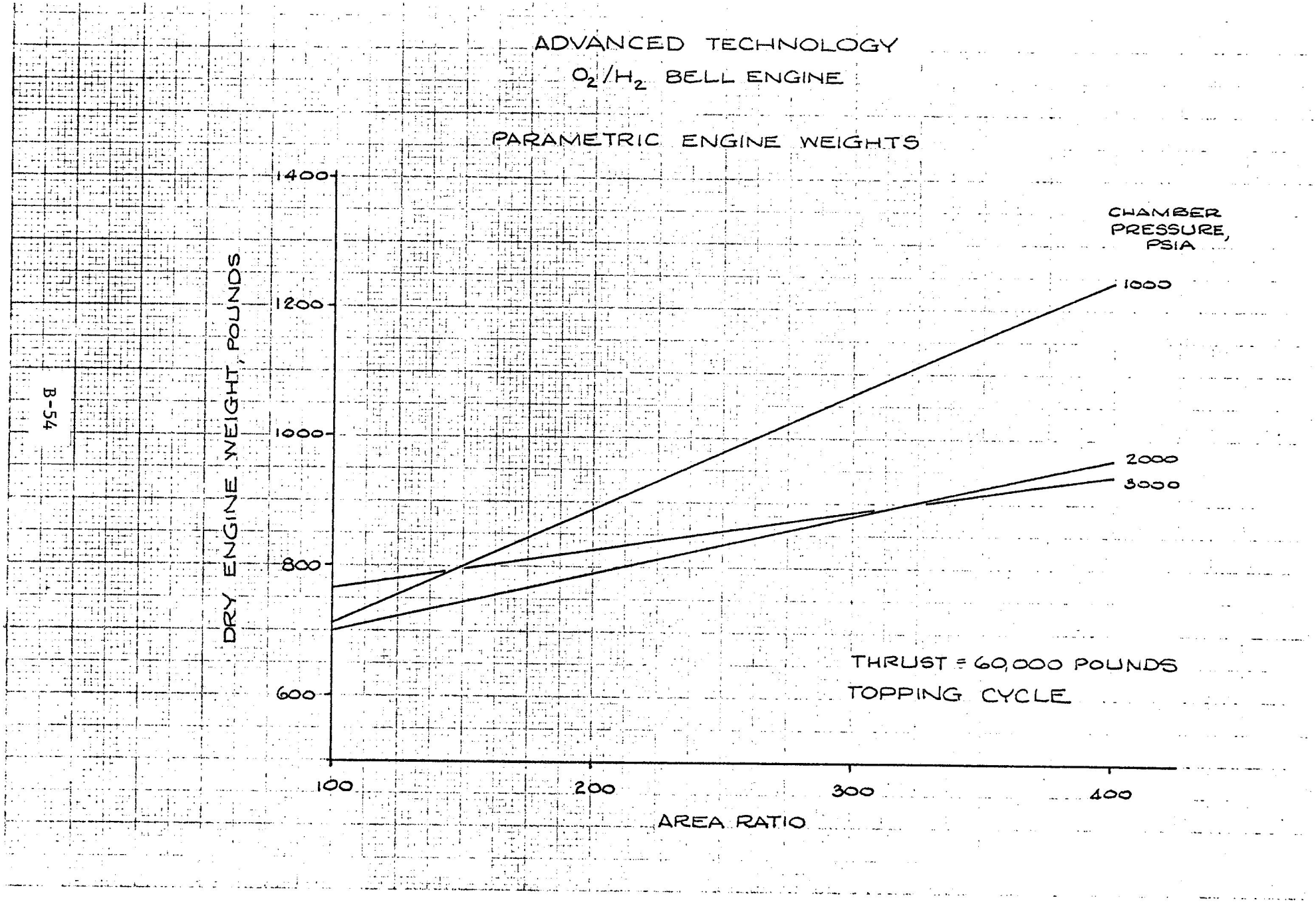
ADVANCED TECHNOLOGY
O_2/H_2 BELL ENGINE
PARAMETRIC ENGINE WEIGHTS
DRY ENGINE WEIGHT, POUNDS
1400
1200
1000
800
600
CHAMBER PRESSURE, PSIA
1000
2000
3000
THRUST = 60,000 POUNDS
TOPPING CYCLE
100
200
300
400
AREA RATIO
B-54

Figure 17

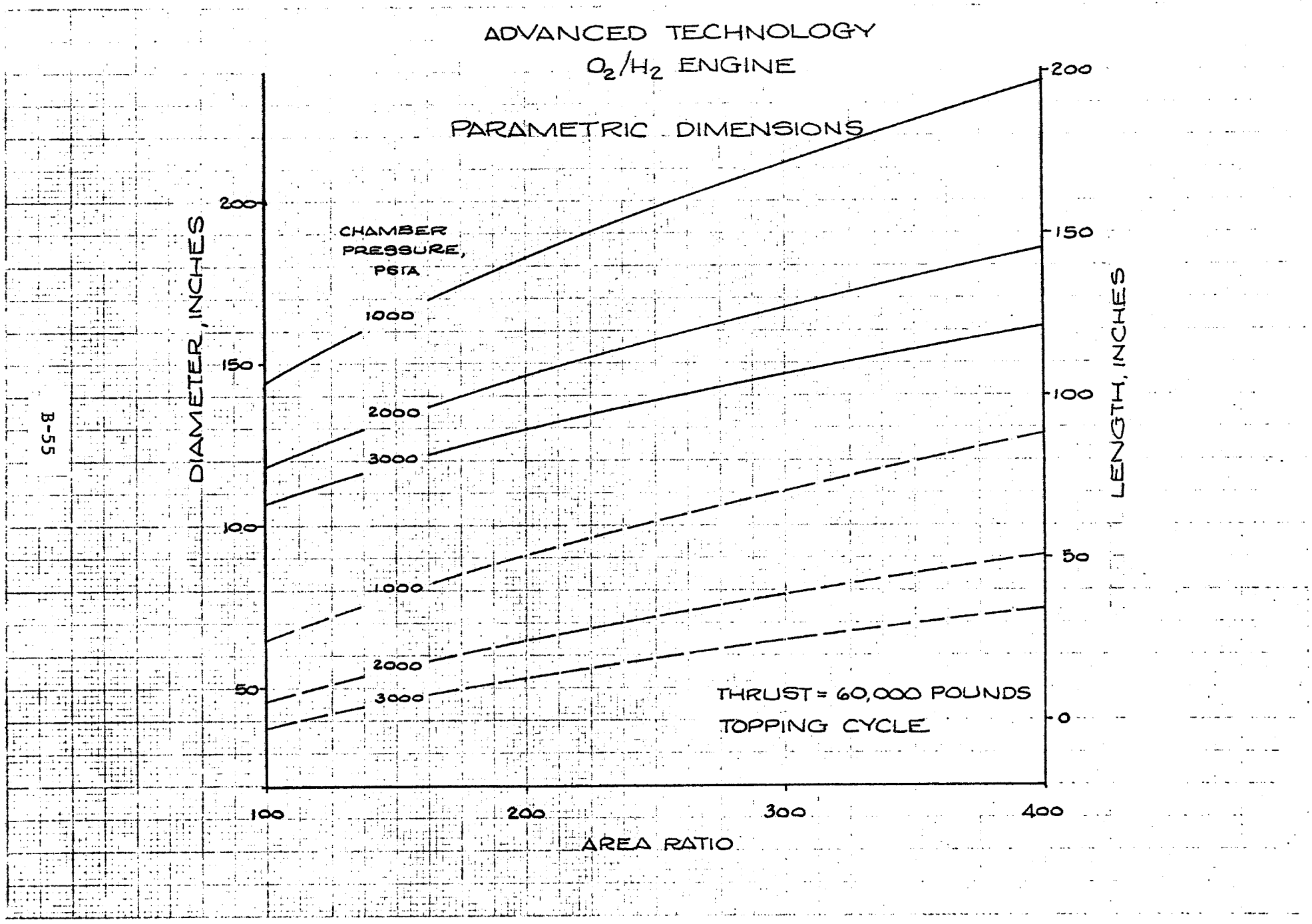
ADVANCED TECHNOLOGY
O_2/H_2 ENGINE
PARAMETRIC DIMENSIONS
CHAMBER PRESSURE, PSIA
1000
2000
3000
1000
2000
3000
DIAMETER, INCHES
LENGTH, INCHES
AREA RATIO
THRUST = 60,000 POUNDS
TOPPING CYCLE
B-55

Figure 18

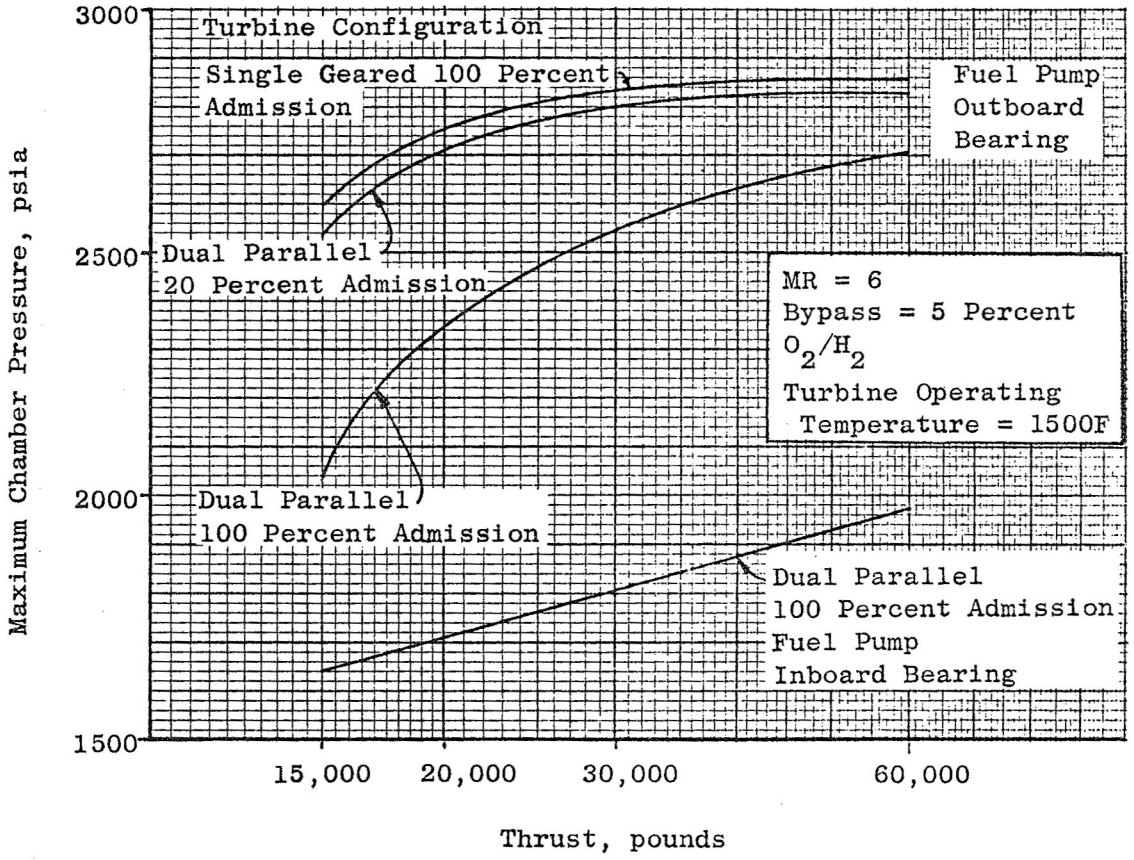

Figure 19. Staged Combustion Cycle Chamber Pressure Limits

Precombustor Topping Cycle

Geared Turbine - 100 Percent Admission

Thrust = 30,000 pounds

O_2/H_2

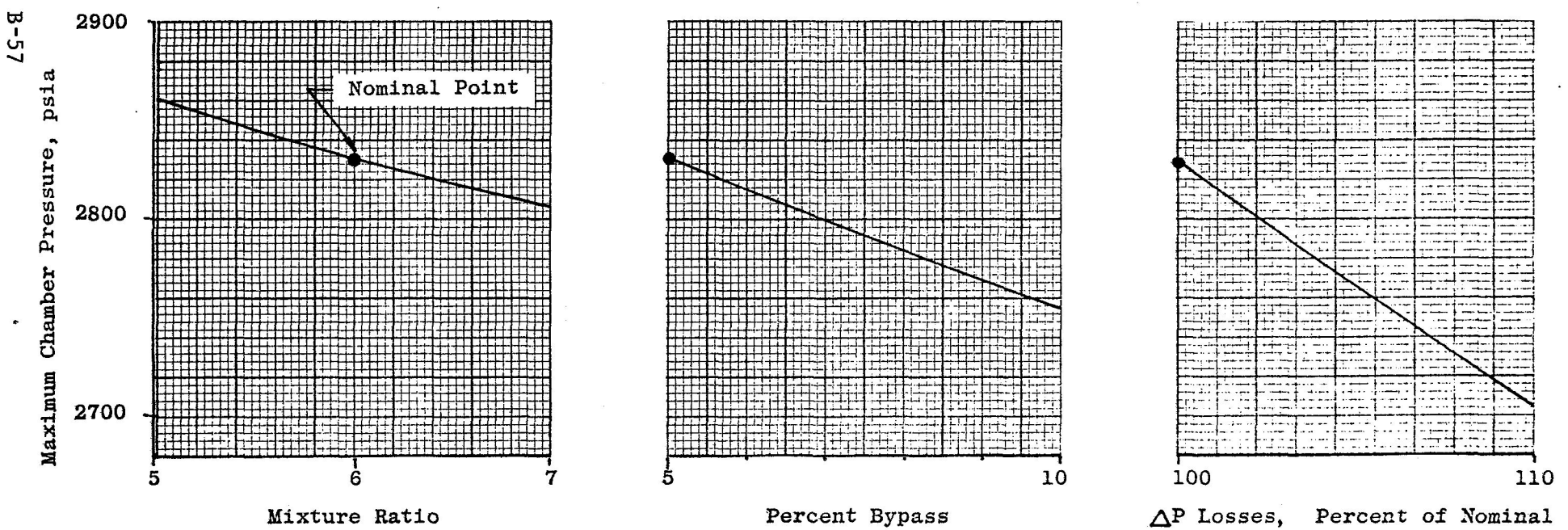

Figure 20. Chamber Pressure Limit Sensitivity

TABLE

ADVANCED TECHNOLOGY O_2/H_2 BELL

PARAMETRIC PERFORMANCE

THRUST = 80,000 LB

MR = 5

P_C	ϵ	I_S
500	100	457.0
	200	464.0
	300	467.2
	400	469.0
750	100	457.7
	200	464.7
	300	467.9
	400	469.7
1000	100	458.2
	200	465.1
	300	468.3
	400	470.1
2000	100	459.1
	200	466.1
	300	469.3
	400	471.1
3000	100	459.6
	200	466.6
	300	469.8
	400	471.6

TABLE

ADVANCED TECHNOLOGY O_2/H_2 BELL
PARAMETRIC PERFORMANCE

THRUST = 80,000 LB

MR = 6

P_C	ε	I_S
500	100	454.4
	200	462.5
	300	466.3
	400	468.5
750	100	455.4
	200	463.6
	300	467.4
	400	469.6
1000	100	456.1
	200	464.3
	300	468.1
	400	470.3
2000	100	457.5
	200	465.7
	300	469.6
	400	471.8
3000	100	458.3
	200	466.4
	300	470.3
	400	472.5

TABLE

ADVANCED TECHNOLOGY O_2/H_2 BELL

PARAMETRIC PERFORMANCE

THRUST = 80,000 LB

MR = 7

P_C	ϵ	I_S
500	100	446.0
	200	454.9
	300	459.1
	400	461.6
750	100	447.8
	200	456.8
	300	461.1
	400	463.6
1000	100	448.8
	200	457.8
	300	462.1
	400	464.6
2000	100	451.3
	200	460.4
	300	464.7
	400	467.3
3000	100	452.7
	200	461.8
	300	466.2
	400	468.8

TABLE

ADVANCED TECHNOLOGY O_2/H_2 BELL

PARAMETRIC PERFORMANCE

Thrust = 120,000 lb
MR = 5

Pc	ϵ	I_s
500	100	457.2
	200	464.2
	300	467.4
	400	469.2
750	100	457.8
	200	464.8
	300	468.0
	400	469.8
1000	100	458.2
	200	465.2
	300	468.4
	400	470.2
2000	100	459.0
	200	466.1
	300	469.3
	400	471.1
3000	100	459.5
	200	466.5
	300	469.7
	400	471.6

TABLE

ADVANCED TECHNOLOGY $O_2/$ [illegible]

PARAMETRIC [illegible]

Thrust = 120,000 Lb
MR = 6

Pc	$\frac{A}{A^*}$	I_s
500	100	454.5
	200	462.7
	300	466.5
	400	468.7
750	100	455.5
	200	463.7
	300	467.5
	400	469.7
1000	100	456.1
	200	464.3
	300	468.3
	400	470.4
2000	100	457.5
	200	465.7
	300	469.6
	400	471.8
3000	100	458.2
	200	466.4
	300	470.2
	400	472.5

TABLE

ADVANCED TECHNOLOGY O_2/H_2 BELL

PARAMETRIC PERFORMANCE

Thrust = 120,000 lb
MR = 7

Pc	ϵ	I_s
500	100	446.2
	200	455.2
	300	459.4
	400	461.9
750	100	448.0
	200	457.0
	300	461.3
	400	463.8
1000	100	448.9
	200	458.0
	300	462.3
	400	464.9
2000	100	451.3
	200	460.4
	300	464.8
	400	467.4
3000	100	452.7
	200	461.8
	300	466.2
	4000	468.8

PARAMETRIC WEIGHTS

BELL ENGINES, EXPANDER CYCLE

P_C	AREA RATIO	THRUST = 80	
500	100	900	1300
	200	1380	2000
	300	1845	2690
	400	2380	3350
750	100	785	1120
	200	1090	1550
	300	1400	2040
	400	1700	2480
1000	100	740	1070
	200	960	1370
	300	1190	1810
	400	1420	2100

PARAMETRIC WEIGHTS

BELL ENGINES, STAGE COMBUSTION TOPPING CYCLE

P_C	AREA RATIO	THRUST = 80,000	
1000	100	915	1310
	200	1155	1660
	300	1400	2040
	400	1600	2400
2000	100	900	1390
	200	1020	1460
	300	1145	1650
	400	1250	1810
3000	100	985	1400
	200	1060	1500
	300	1145	1640
	400	1220	1800

TABLE

BELL ENGINE DIMENSIONS, STAGED COMBUSTION TOPPING CYCLE

THRUST	P_C	ϵ	DIAMETER	LENGTH
80,000	1000	100	74.2	115.4
80,000	1000	200	104.5	160.6
80,000	1000	300	127.8	195.4
80,000	1000	400	147.4	224.6
80,000	2000	100	52.8	86.5
80,000	2000	200	74.2	118.6
80,000	2000	300	90.7	143.1
80,000	2000	400	104.5	163.8
80,000	3000	100	43.3	73.8
80,000	3000	200	60.8	99.9
80,000	3000	300	74.2	120.0
80,000	3000	400	85.5	136.9
120,000	1000	100	90.7	137.5
120,000	1000	200	127.8	192.9
120,000	1000	300	156.3	235.4
120,000	1000	400	180,3	271.3
120,000	2000	100	64.4	102.2
120,000	2000	200	90.7	141.4
120,000	2000	300	110.8	171.5
120,000	2000	400	127.8	196.8
120,000	3000	100	52.8	86.5
120,000	3000	200	74.2	118.6
120,000	3000	300	90.7	143.1
120,000	3000	400	104.5	163.8

TABLE

BELL ENGINE DIMENSIONS, EXPANDER CYCLE

THRUST	P_C	ϵ	DIAMETER	LENGTH
80,000	1000	100	74.2	108.4
80,000	1000	200	104.5	153.6
80,000	1000	300	127.8	188.4
80,000	1000	400	147.4	217.6
80,000	2000	100	52.8	79.5
80,000	2000	200	74.2	111.6
80,000	2000	300	90.7	136.1
80,000	2000	400	104.5	156.8
80,000	3000	100	43.3	66.8
80,000	3000	200	60.8	92.9
80,000	3000	300	74.2	113.0
80,000	3000	400	85.5	129.9
120,000	1000	100	90.7	130.5
120,000	1000	200	127.8	185.9
120,000	1000	300	156.3	228.4
120,000	1000	400	180.3	264.3
120,000	2000	100	64.4	95.2
120,000	2000	200	90.7	134.4
120,000	2000	300	0.8	164.5
120,000	2000	400	127.8	189.8
120,000	3000	100	52.8	79.5
120,000	3000	200	74.2	111.6
120,000	3000	300	90.7	136.1
120,000	3000	400	104.5	156.8

J-2S ENGINE CHARACTERISTICS

THRUST, POUNDS	265,000
CHAMBER PRESSURE, PSIA	1214
OXIDIZER FLOWRATE, LB/SEC	515.44
FUEL FLOWRATE, LB/SEC	93.72
ENGINE MIXTURE RATIO	5.5
THRUST CHAMBER MIXTURE RATIO	5.84
SPECIFIC IMPULSE, LB-SEC/LBm	436.0
AREA RATIO	39.68:1
WEIGHT, POUNDS	4040
LENGTH, INCHES	116
DIAMETER, INCHES	80

GAS GENERATOR CYCLE ENGINE DATA

THRUST (LB)	8,000
CHAMBER PRESSURE (PSI)	800
MIXTURE RATIO	5.0:1
EXPANSION RATIO	200:1
SPECIFIC IMPULSE (SEC)	460.7
WEIGHT (LB)	151
LENGTH (IN.)	62.7
DIAMETER (IN.)	36.4

THRUST (LB)	ENGINE WEIGHT (LB)	
	P_c = 800 PSI	P_c = 1000 PSI
5,000	130	135
8,000	151	162
10,000	175	180
15,000	220	228

Appendix C

STAGE DESIGN DATA

Table C - 1. Monocoque to Complex Structure Weight Ratio for Shell and Interstage

DIAMETER (IN.) / LIMIT LOAD (LB/IN.)	120	260
0.0	0.6700	0.5575
753.5	0.6325	0.4900
1435.0	0.6000	0.4333
1671.4	0.5875	0.4100
5175.0	0.4200	0.1050
6000.0	0.3800	0.0325

Table C - 2. Tank Support Weight Factors

CONFIGURATION	FACTOR FOR LARGE TANK	FACTOR FOR SMALL TANK
TANDEM TANK	0.0150	0.0150
2 MULTIPLE TANKS	0.0150	0.0100
3 MULTIPLE TANKS	0.0150	0.0100
4 MULTIPLE TANKS	0.0150	0.0100
TRANSTAGE	0.0100	0.0100

Table C - 3. Monocoque to Complex Structure Weight Ratio for Thrust Cone Type Thrust Structure

DIAMETER (IN.) / LIMIT LOAD (LB/IN.)	120	260
0	0.7500	0.7500
200,000	0.7500	0.7500

Table C - 4. Monocoque to Complex Structure Weight Ratio for Spider Beam Type Thrust Structure

DIAMETER (IN.) / LIMIT LOAD (LB/IN.)	120	260
14,999	0.4050	0.4520
21,000	0.4210	0.4700
47,000	0.4950	0.5500
84,000	0.5990	0.6625
110,000	0.6700	0.7410
120,000	0.7000	0.7710

Table C - 5. Thermal Conductivity of Insulation (Btu / Hr - Ft - $^{\circ}$R)

THICKNESS (IN.) / AVERAGE TEMPERATURE (R)	0.01	9.00
40	2.10×10^{-5}	4.20×10^{-5}
100	2.29×10^{-5}	4.60×10^{-5}
150	2.50×10^{-5}	5.00×10^{-5}
250	4.60×10^{-5}	9.00×10^{-5}

GOVERNMENT FIELD PRINTING PLANT
(UNDER CONTRACT NAS 8-14017)
NASA - MICHOUD ASSEMBLY FACILITY 1971
NEW ORLEANS, LOUISIANA 70129

DISTRIBUTION LIST FOR FINAL REPORT ON

LOX/HYDROGEN ENGINE TECHNOLOGY

TR-AP-71-3 - CONTRACT NAS7-790

COPIES	RECIPIENT	DESIGNEE
1	NASA Headquarters, Washington, D.C. 20546 Patent Office	
	NASA Lewis Research Center 21000 Brookpark Road, Cleveland, Ohio 44135	
1	Office of Technical Information	
1	Contracting Officer	
1	Patent Office	
	NASA Marshall Space Flight Center Huntsville, Alabama 35812	
2	Office of Technical Information, MS-IP	
1	Technical Library	
1	Purchasing Office, PR-EC	
1	Patent Office, M-PAT	
1	Keith Chandler, R-P&VE-PA	
1	Technology Utilization Office MS-T	
	NASA Pasadena Office 4800 Oak Grove Drive Pasadena, California 91103	
1	Patents and Contracts Management	
NASA FIELD CENTERS		
2	Ames Research Center Moffett Field, California 94035	H. J. Allen Mission Anal. Div.
2	Goddard Space Flight Center Greenbelt, Maryland 20771	Merland L. Moseson Code: 620
2	Jet Propulsion Laboratory California Institute of Tech. 4800 Oak Grove Drive Pasadena, California 91103	Henry Burlage, Jr. J. H. Rupe
2	Langley Research Center Langley Station Hampton, Virginia 23365	Dr. Floyd Thompson Director

NASA FIELD CENTERS - Contd.

COPIES	RECIPIENT	DESIGNEE
2	Lewis Research Center 21000 Brookpart Road Cleveland, Ohio 44135	Dr. A. Silverstein Director R. J. Priem E. W. Conrad
2	Marshall Space Flight Center Huntsville, Alabama 35812	Hans G. Paul R. J. Richmond
2	Manned Spacecraft Center Houston, Texas 77058	Dr. Robert R. Gilruth Director J. G. Thibodaux
2	John F. Kennedy Space Center, NASA Kennedy Space Center, Florida 32899	Dr. Kurt H. Debus, Director

GOVERNMENT INSTALLATIONS

1	Aeronautical System Division Air Force Systems Command Wright-Patterson Air Force Base Dayton, Ohio 45433	D. L. Schmidt Code: ASRCNC-2
1	Air Force Missile Development Center Hollomen Air Force Base New Mexico	Maj. R. E. Bracken Code: MDGRT
1	Air Force Missile Test Center Patrick Air Force Base, Florida	L. J. Ullian
1	Air Force Systems Division Air Force Unit Post Office Los Angeles 45, California	Col. Clark Technical Data Center
1	Arnold Engineering Development Center Arnold Air Force Station Tullahoma, Tennessee	Dr H. K. Doetsch
1	Bureau of Naval Weapons Department of the Navy Washington, D. C.	J. Kay RTMS-41
1	Chemistry Research Laboratory Building 450 Wright-Patterson Air Force Base Dayton, Ohio 45433	K. Scheller ARL (ARC)

GOVERNMENT INSTALLATIONS - Contd.

COPIES	RECIPIENT	DESIGNEE
1	Department of the Navy Office of Naval Research Washington, D.C. 20360	R. O. Jackel Code: 429
1	Headquarters U.S. Air Force Washington, D.C.	Col. C.K. Stambaugh AFRST
1	Picatinny Arsenal Dover, New Jersey 07801	I. Forsten, Chief Liquid Propulsion
1	Air Force Rocket Propulsion Lab Research and Technology Division Air Force Systems Command Edwards, California 93523	RPRR
1	U.S. Atomic Energy Commission Technical Information Services Box 62 Oak Ridge, Tennessee	A.P. Huber Oak Ridge, Gaseous Diffusion Plant
1	U.S. Army Missile Command Redstone Arsenal Huntsville, Alabama 35808	W.W. Wharton AMSMI-RRK
2	U.S. Naval Ordnance Test Station China Lake, California 93555	E.W. Price D. Couch
1	Air Force Office of Scientific Research Propulsion Division 1400 Wilson Blvd. Arlington, Va. 22209	B. T. Wolfson
CPIA		
2	Chemical Propulsion Information Agency Applied Physics Laboratory 8621 Georgia Avenue Silver Spring, Maryland 20910	Neil Safeer T. W. Christian W. G. Berl

INDUSTRY CONTRACTORS (Contd.)

COPIES	RECIPIENT	DESIGNEE
1	Aerojet-General Corporation P. O. Box 296 Azusa, California 91703	L. F. Kohrs
1	Aerojet-General Corporation P. O. Box 15847, Sacramento, Calif. 95809	R. Stiff
1	Aerospace Corporation 2400 East El Segundo Blvd. P.O. Box 95085 Los Angeles, California	O. W. Dykema W. C. Strahle
1	Atlantic Research Corporation Edsall Road & Shirley Highway Alexandria, Virginia 23314	R. Friedman
1	Beech Aircraft Corporation Boulder Division Box 631 Boulder, Colorado	J. H. Rodgers
1	Bell Aerosystems Company P. O. Box 1 Buffalo, New York 14205	Dr. Kurt Berman
1	Bendix Corporation Bendix Systems Division 3300 Plymouth Road Ann Arbor, Michigan	John M. Brueger
1	Martin Marietta Corporation Baltimore Division Baltimore, Maryland 21203	John Calathes Code: 3214
1	Martin Marietta Corporation Denver Division P. O. Box 179 Denver, Colorado 80201	J. D. Goodlette Code: A-241
1	Massachusetts Institute of Tech. Dept. of Mechanical Engineering Cambridge, Mass. 02139	T. Y. Toong
1	McDonald-Douglas Aircraft Company Astropower Division 2121 Paularino Newport Beach, California 92663	Dr. George Moc Director, Research

INDUSTRY CONTRACTORS (Contd.)

COPIES	RECIPIENT	DESIGNEE
1	McDonnell Aircraft Corporation P.O. Box 516 Municipal Airport St. Louis, Missouri 63166	R. A. Herzmark
1	Multi-Tech, Inc. 601 Glenoaks Blvd. San Fernando, California	F. B. Cramer
1	North American Aviation, Inc. Space & Information Systems Div. 12214 Lakewood Blvd. Downey, California 90241	D. Simkin
1	ROCKETDYNE 6633 Canoga Avenue Canoga Park, Calif. 91304	R. B. Lawhead
1	Northrop Space Laboratories 3401 West Broadway Hawthorne, California	Dr. William Howard
1	Pennsylvania State University Mechanical Engineering Dept. 207 Mechanical Engineering Blvd. University Park, Pa. 16802	G. M. Faeth
1	Polytechnic Institute of Brooklyn Graduate Center Route 110 Farmingdale, New York	V. D. Agosta
1	Pratt & Whitney Aircraft (United Aircraft Corp.) Florida Research & Development P.O. Box 2691 West Palm Beach, Florida 33402	G. D. Lewis
1	Princeton University Forrestal Research Center Guggenheim Laboratories Princeton, New Jersey 08540	I. Glassman D. T. Harrje
1	Purdue University School of Mechanical Engineering Lafayette, Indiana 47907	J. R. Osborn

INDUSTRY CONTRACTORS (Contd.)

COPIES	RECIPIENT	DESIGNEE
1	Ohio State University Dept. of Aeronautical & Astronautical Engineering Columbus, Ohio 43210	R. Edse
1	Republic Aviation Corporation Farmingdale, Long Island New York	Dr. Wm. O'Donnell
1	Sacramento State College Engineering Division 60000 J. Street Sacramento, California 95819	F. H. Reardon
1	Space General Corporation 9200 East Flair Avenue El Monte, California 91734	C. E. Roth